Set-Up of a Process-based Model to Investigate the Outer Weser Estuary Development

Long-term morphological modeling with Delft 3D to hindcast the genesis and development of channel - shoal patterns in the Outer Weser estuary

Jannek Gundlach

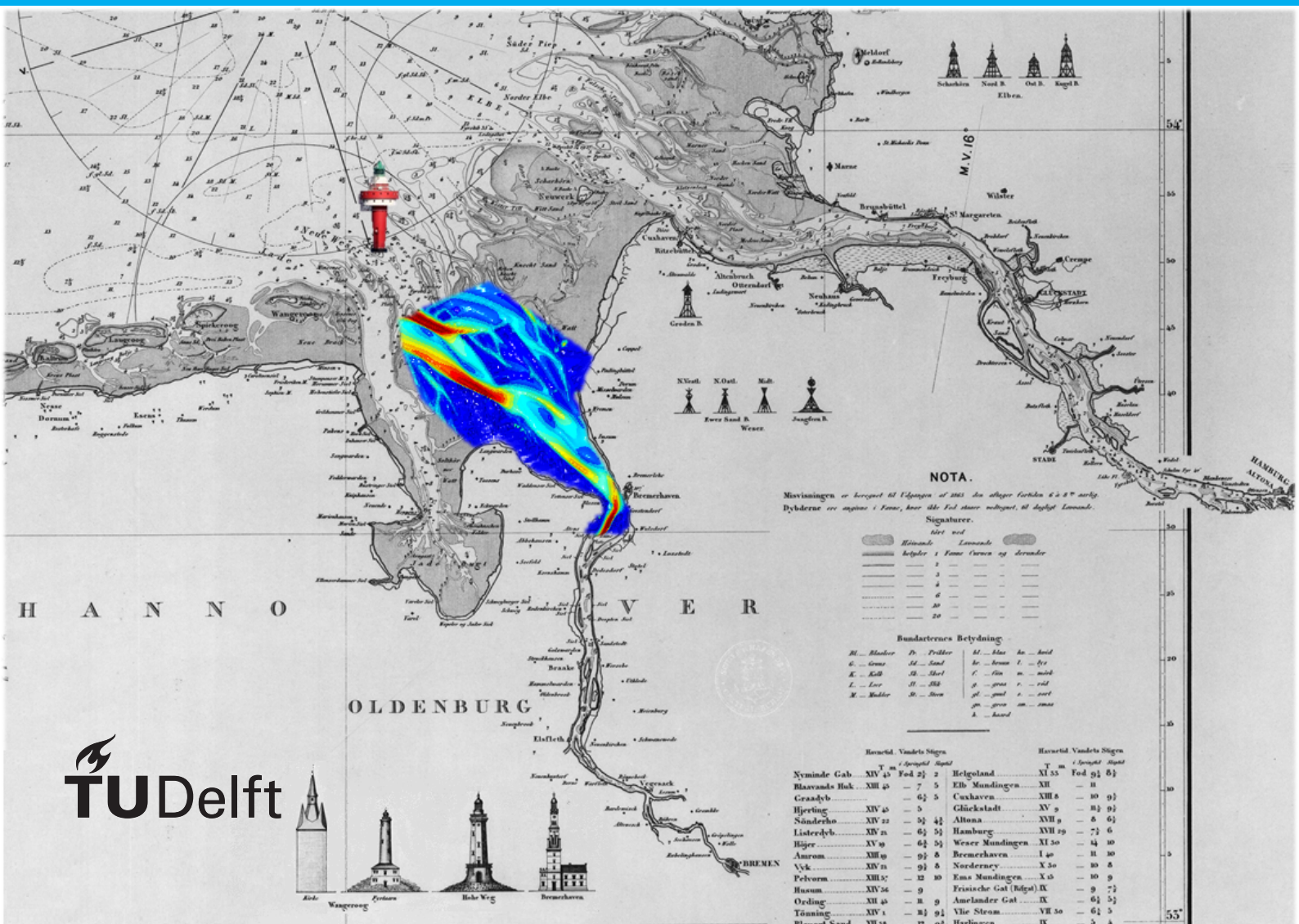

TU Delft

Set-Up of a Process-based Model to Investigate the Outer Weser Estuary Development

Long-term morphological modeling with Delft 3D to hindcast the genesis and development of channel - shoal patterns in the Outer Weser estuary

by

Jannek Gundlach

to obtain the degree of Master of Science
at the Delft University of Technology,
to be defended publicly on Wednesday April 18, 2018 at 11:00 AM.

Student number:	4450426	
Project duration:	August 1, 2017 – March 29, 2018	
Thesis committee:	Prof. dr. Z. B. Wang,	TU Delft, head
	Dr. B. C. Van Prooijen,	TU Delft, supervisor
	Dr. S. de Vries,	TU Delft, supervisor

An electronic version of this thesis is available at `http://repository.tudelft.nl/`.

Preface

This graduation project concludes the Master of Science program in the track Hydraulic Engineering of Civil Engineering at the Delft University of Technology in Delft, The Netherlands. It has been carried out together with the Federal Waterways Engineering and Research Institute (BAW), section Coastal Engineering in Hamburg, Germany.

Since this thesis marks the end of my master studies, I would like to take the opportunity to thank a couple of people, who made this graduation possible and supported me on my way to and through it:

First of all, I would like to thank my daily supervisor Anna Zorndt, who came up with the idea of this graduation project and gave me competent guidance in all challenging moments that appeared within this thesis. I am very grateful for her effort, her personal and professional support that made this graduation project possible.

Secondly, I would like to thank my graduation committee, namely Prof. ZB. Wang, Bram van Prooijen and Sierd de Vries, for their continuous contribution, their commitment and their constructive support in the meetings held. I appreciate their way of adding their expertise and technical suggestions to this project, especially at the beginning, where challenges were faced frequently. Thanks to their straightforward supervision, doing this graduation project in Germany has been comfortably uncomplicated.

Apart from my supervisors, I would like to thank Frank Kösters, Andreas Plüß and all other colleges, students and friends from BAW-Hamburg for providing me such a supportive and professional environment during this graduation project. Their dedication made me being a part of BAW-Hamburg in this last year.

It is a good opportunity also to thank my former professor, lecturers and mentors from the University of Hanover: Prof. Schlurmann, Christian Jordan and Knut Krämer. They awoke and supported my enthusiasm for Coastal Engineering and encouraged my plans to do my master studies at TU Delft.

This also includes Lea, who in Hanover emboldened the idea of my / our journey to Delft, joined me in this adventure and went through a number of challenges in Delft with me, as a colleague, roommate and friend.

During my time in Delft, I had the chance to meet people from all over the world and get in touch with their cultures. This impressed me and substantially enriched my personality. Apart from all the students and employees of TU Delft that I got to know, I especially would like to thank the Chilean community in Delft, namely Carlos, Daniel, Paula, Susan and the Spanish contributor Maricarmen who were my partners in many projects and became good friends on a professional and personal level. Furthermore, I want to take the chance to thank my old neighbors Angelo and Katarina who literally fed me with fantastic menus and atmosphere during tough periods.

I deeply want to thank my parents and family who made this whole study experience possible. They always had faith in my capabilities and supported my ideas and plans. They empowered me to go my way which contributes the successful conclusion of this master program significantly.

Finally, but highly important, I want to thank Kathrin who gave me constant strength and perseverance, even when I decided to leave the country to do my master degree in Delft. Without your love and support I would not be where I am today.

Jannek Gundlach
Hamburg, March 2018

Abstract

This graduation project investigates the main processes that are influencing the morphological development of the Outer Weser estuary by setting up a process-based model (Delft 3D) and applying it by means of simulating multiple scenarios, each driven by a different forcing. The aim of this project is to gain insight into the causes for the development of a two channel system in the Outer Weser and into the origin of the related alternation pattern of a dominant channel. Due to the construction of training walls and groynes at the end of the 19th century, the described characteristics disappeared and thus, they are a historical phenomenon but yet today not fully understood. However, to gain insight into the natural development in the Outer Weser estuary is beneficial for current and future engineering projects.
For the investigation a schematic model is generated in which only essential processes are considered and simplified. By applying a flat bed as initial bathymetry, using simplified boundary conditions, multiplying the morphological changes with a morphological factor and using relatively coarse grid, the model is able to predict long term morphodynamics. In the next step scenarios are composed by considering the most relevant processes that could be responsible for the generation of two channels and for the alternation, leading to six scenarios. These scenarios are compared to a base case.
In order to investigate the morphologic equilibrium, the development of two channels and their cyclic behavior, a number of methods are applied. These include time depended hypsometries, cumulative bed load transport, visual inspection and a special method for characterization of channel forms / geometries in a cross-section.
The six scenarios cover the influences of the Kelvin wave, the Coriolis effect, wind waves, extreme river discharge, the absence of river discharge and an increased tidal range. All simulations have a period of ten years of hydromechanics which in combination with the applied morphological factor of 400 results in 4000 years of morphodynamics. The scenarios as well as the reference simulation reach a morphologic equilibrium within the first fourth of the simulation time. Afterwards, all simulations reveal the development of two channels with different dimensions and locations with respect to the reference simulation: While the scenarios excluding the Kelvin wave and river discharge result in a stronger development of the western channel, the scenario excluding Coriolis and the scenario including wave action lead to a more dominant eastern channel. The simulation with extreme discharge and the simulation with an increased tidal range do not favor one of the two channels. For the alternation, the developed evaluation method indicates an alternation between western dominance and equal dominance for the no Kelvin wave and no river discharge scenarios. For the no Coriolis scenario the alternation is observed between eastern dominance and equal dominance. No alternation is found for the extreme river discharge and wave scenarios, while the only scenario indicating an alternation between eastern and western dominance is the scenario with an increased tidal range. For the scenarios in which an alternation is indicated the alternation period is determined and compared to the reference case. This shows a shorter alternation period for the no river discharge scenario and a similar alternation period for the no Kelvin wave and no Coriolis simulation, while the alternation period is raised in the increased tidal range scenario.
The conclusions are that the development of the two channel system is mainly caused by the tides and the basin geometry, since it evolves even when the Kelvin wave, Coriolis, the river discharge and waves are excluded. Furthermore, it is reasoned that the alternation pattern and period are dependent on the dominance of the tides and the depth of the two channels, due to a shortening of the alternation period in the scenario without river discharge (stronger domination of the tides) and an increased alternation period in the scenario containing an amplified tidal range (deeper channels). Additionally, it has been reasoned that the alternation might be introduced by the shape and geometry of the Weser estuary.

Contents

List of Figures

List of Tables

Abbreviations

BAW Bundesanstalt für Wasserbau - Federal Waterways Engineering and Research Institute

D3D Delft 3D

EM2 evaluation method 2

MY morphological years

DTM digital terrain model

SLR sea-level-rise

JWE Jade Weser Elbe

AOI area of interest

MSE mean square error

RMSE root mean square error

BSS Brier Skill Score

GIS geographical information system

1 Motivation

1.1. Introduction to the Weser Estuary

The German Bight is influenced by four large estuaries: Eider-, Elbe-, Weser- and Ems-Estuary.
They are part of a sensible and protected nature, which was claimed UNESCO World Heritage in 2009 due to its special ecological importance. However, all of these estuaries are also economically important shipping routes for container, bulk and liquid-bulk transport.
The Weser river (figure 1.1) in is divided into [22]: Upper Weser, Middle Weser, Lower Weser and Outer Weser.
The Lower Weser and the Outer Weser form the estuarine part of the Weser as a weir in the city of Bremen limits the influence of the tide. Thus, the lower limit of the Weser estuary is Bremen where the Lower Weser starts (km 0) and flows up to Bremerhaven (km 65). This section includes the access to the harbors of Bremen, Brake and Nordenham. The outer Weser part starts at the city of Bremerhaven (km 65) and includes the adjacent area of the North Sea (~km 120). Here the seaward access to the container terminal Bremerhaven is located, which a decade ago has been mentioned as one of the most important container terminals worldwide [22]. Therefore, the Weser estuary plays an important role for Germany in the international trade market and is maintained intensively. In this project the focus lies on the Outer Weser, but also considers the influence of the Lower Weser.

Figure 1.1: Spatial definition of the sectional separation of the Weser. Hereby, the German names translated are: Oberweser = Upper Weser, Mittelweser = Middle Weser, Unterweser = Lower Weser and Außenweser = Outer Weser

The bed material in the Lower Weser is mainly composed of fine and medium sand. From Bremen (km 0) to Nordenham (km 55) tidal currents, river discharge and variation in depth form typical estuarine bed forms like ripples and dunes. Whereas the turbidity maximum zone is located from Nordenham (km 55) to Bremerhaven (km 65), which leads to an accumulation of fine and very fine sediments [31].
The Outer Weser part is funnel shaped with the open end north west oriented towards the North Sea. This estuary part is dominated by extensive tidal flats, two main channels and a number of smaller side channels. North of the two main channels the Robbensbalje is a tidal channel with a typical branch formation simmilar to the ones described by Van Veen (2005) [44]. West of the two main channels there is the Hohe Weg shoal, a large sandy tidal flat, which is not flooded each tidal cycle. The Hohe Weg divides the Outer Weser estuary from the Jade bay, a relatively large tidal basin that is in the same order of magnitude as the Outer

Weser estuary. The wadden areas in the Outer Weser estuary are morphodynamically highly active. Historical maps show shifts of channel and shoals within decades and even nowadays changes in the position of side channels are not of rare occurence. Tidal gullies and sand banks even move with approximetely 100 m/a [22]. Tidal channels in the Outer Weser often show mostly flat reaches partly with large dunes (5m height, several 100 m length) and local scoured spots [22].

1.2. Knowledge and Science Gap

In the past centuries, the Weser estuary, has shown characteristic morphological changes in the development of channels and tidal flats [29], [11], [31]. Apart from the historical development, one of the main observed and documented phenomenon is the alternation of the dominant and non-dominant channel in the two channel system in the Outer Weser estuary. The constant morphological changes and the confusion about the location of the dominant channel in the future led to the construction of training walls and groynes at the end of the 19th Century. Yet, today, it is not fully understood how the two channel system has evolved and which process is dominant. With modern computer models, it is possible to investigate the natural situation (before the structural measures forced the estuarine behavior) and understand the underlying mechanisms which formed the Weser estuary. The advantage of using a process-based model is that simulations can be run with different processes included. With this approach multiple scenarios can test the influence of forces and natural factors and thus an improved understanding of causes and reasons for morphological development can be gained. In 2012, Van der Wegen et al. [39] reproduced the bathymetry of the Western Scheldt (Netherlands) by means of a flat bed model and investigated the governing processes that are responsible for the main morphological features. This has initiated the motivation to examine whether this approach could be used in the Weser estuary to provide new insights. Inspired by the flat bed modeling in the Western Scheldt, the possible research options that would arise for the Weser, in case this modeling approach can be validly applied there, are multifarious.
The first application of the flat bed modeling method is to reproduce the natural channel and shoal pattern of the Weser estuary. Historically seen, this would be before large scale human interventions like structural measures have been taken place in the Weser. With such a model Weser specific phenomena can now be investigated and described that have been observed in the past, but could not be investigated scientifically at that time, due to a lack of data and technical resources available. This project focuses on two research question:

> The first one investigates the causes for the development of two channels in the Outer Weser estuary.
>
> The second research question aims to gain some insight in the forces affecting the alternation of the dominant channel, a phenomenon that has not been fully understand yet and will be described in its historical documentation later on.

The two research questions are examined by comparing evolving morphologies under different external influences. Together with developed analyzing methods, conclusions can be drawn about influences and their effects on first, the generation of two channels and second, an alternation pattern.
The results of these investigations will contribute to further understanding of these phenomena. The idea is to provide investigative studies that are motivated from a more scientific side rather than driven by a current practical need or project. Nevertheless, since the structures in the Weser have been constructed more than a century ago, it could at some point be beneficial to have some ideas for optional investigation approaches, in case the training walls and groynes need to be renewed one day.

2

Theoretical Background

2.1. Macroscale Morphodynamics

Classification of the Weser Estuary Coastal systems and coastal features can be divided based on plate tectonic setting and the respective substancial sea-level changes [4] [17]. Additionally, on a smaller scale, Boyd et al. [5] categorized coastal environments based on the dominant processes that they are governed by. Boyd et al. defined three categories including their transitions: River, Wave and Tide.

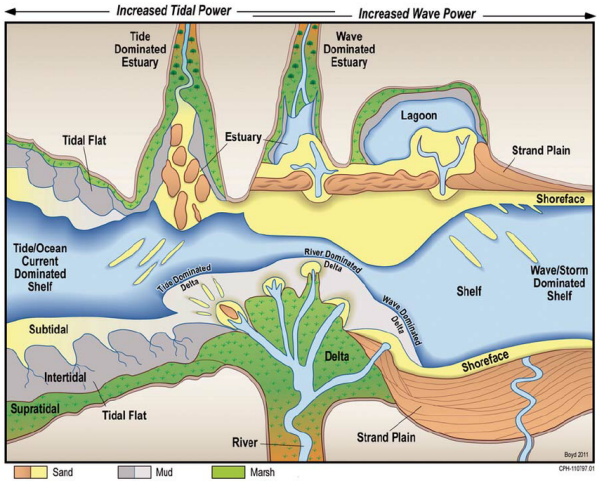

Figure 2.1: Classification of coastal environments based on Boyd

In their research they analyzed several coastal systems with respect to the dominant forces. Figure 2.1 gives an overview about the main drivers and the resulting coastal systems. They concluded that dependent on the relative sea-level rise there are characteristic features that are formed according to wave action, tidal currents, river discharge or a combination of these. As part of their investigation the German bight has been analyzed and marked as a tide dominant system with low to moderate influence of wave action and river discharge. The Weser estuary itself shows conspicuous resemblance with the sketches made by Dronkers [7] for the typical tide dominated transgressive coastal system which are based on the categorization of Boyd et al. An earlier study of William Galloway [10] forms the basis of the studies made by Boyd and Dronkers, where relations of river flow and sediment supply on the one hand with the river sediment distributing forces namely waves and tides on the other hand are sketched. Ramacher [31] describes the Outer Weser as a funnel shaped estuary that consists of a vast number of tidal flats, tidal channels and tidal creeks. According to the classifications that have been published later on this description corresponds to the characteristics of a tidal driven estuary.

2.2. Historical Background

2.2.1. History of the Outer Weser Estuary

According to geological time scales [4] (Chapter 2, Figure 2-1) the German Bight and its estuaries are relatively young [46]. During the Holocene the valleys and low lying areas, formed during the last glacial stage and the thus resulting fluvial erosion, were drowned due to significant sea-level-rise (SLR) (see Bosboom [4] in Coastal Dynamics I, Appendix A and Wienberg [46]). Within several millennia under the influence of hydrodynamics and morphodynamics an estuary was formed. At the end of the 6th century the city of Bremen built its first quay wall. From there conventional sea trade started, already using parts of the Outer Weser estuary as navigational routes. During a storm surge (between 500 to 1000 years ago) a large part of the western mainland was flooded and became the Jade bay [12]. The Jade bay is the adjacent tidal prism that has an influence on the development and the hydrodynamics of the Outer Weser estuary. At the beginning of the 19th century (1827) the port of Bremerhaven was constructed at the southern end of the Outer Weser part, due to problems in maintaining the navigational depths in the Lower Weser. Since 1830 ships approached Bremerhaven by using the natural tidal channels of the Outer Weser estuary. During the last decades of the 19th century the first large scale artificial measures were introduced to the Outer Weser estuary. A detailed description of the constructions and their historical development can be found in the article of Ramacher [31]: At that time the first ships who needed a higher navigational depth than the natural morphodynamically active channel provide were build. Over centuries and decades the position, depth and channel structure changed continuously. At the end of the 19th century the main navigational channel started at the southern end of the Outer Weser estuary as one wide channel that is divided by a large tidal flat. Around ten kilometers further north the channel system splits up again into an ebb and a flood channel with a tidal shoal in between them (see figure 2.2). When a critical point regarding the navigational depth was reached at that time, the first training

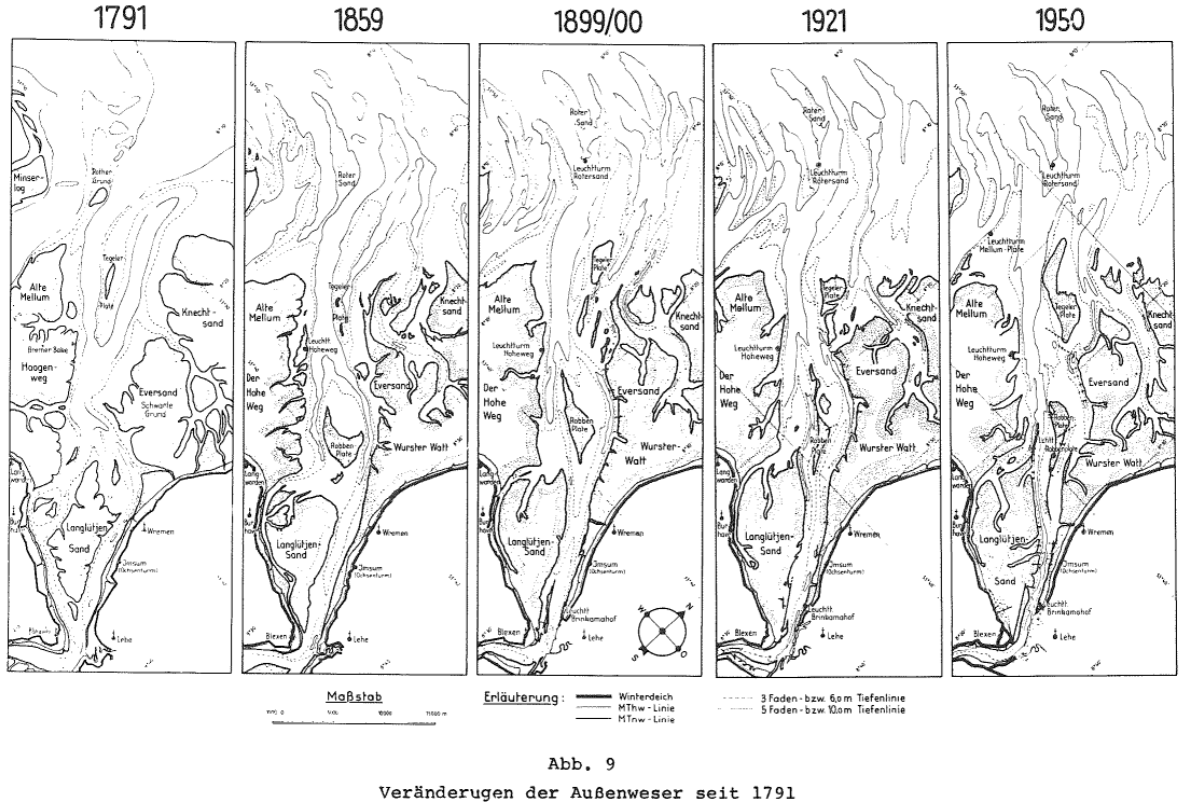

Figure 2.2: Development of the historical state of the outer Weser from 1791 to 1950 (Ramacher 1974 [31])

walls were build in the eastern (ebb) channel of the divided two channel system even though the western (flood) channel was gaining dominance in that period. In the years before the first world war there were intensive discussions between the different authorities, whether the western or the eastern channel should be supported by structures. The young engineer Ludwig Plate observed the natural behavior of the Outer Weser and took measurements on behalf of the Bremer authorities. He could prove sufficiently that for fu-

ture developments the western channel (the Fedderwarder Arm) should be chosen due to its development tendencies. Thus, even though millions of Goldmark (an enormous amount of the former German currency) had been spent on the construction of the eastern channel it was dismissed and instead intensive dredging and construction processes were started in the western channel. It was an exceptional line of action for that time. The training walls and groynes that were planned and designed by Plate were built until the second world war. In the decades of the 20th century the work started by Plate has been continued by other engineers and the anthropogenic influence on the Outer Weser estuary has been intensified due to the need of higher navigational depths and maintenance dredging. Still today, the Outer Weser estuary is dominated by the constructions introduced over a century ago.

2.2.2. Historical Documentation on Recurrent Pattern

At the beginning of the 20th century two German engineers Krüger [20] and Poppen [30] were the first to describe a recurrent migration of sand bars in the offshore part of the Outer Weser estuary. Krüger describes a detachment of sand bars from the island Minsener Oog (number 1 in figure 2.3) recurrently every 20 years, whereas the migration of these bars to the location Roter Grund (number 2 in figure 2.3) takes around 100 years and the migration further towards Roter Sand (number 3 in figure 2.3)is indicated with 70 years. Poppen around the same time looked at the periodic morphological behavior of the area Roter Grund and states that the lifespan of the morphological development in this area is 60 years. Additionally, Poppen observed a movement of inner shoals within 30 years.

Both, Krüger and Poppen indicated the tides as the driving mechanism while morphology and waves are

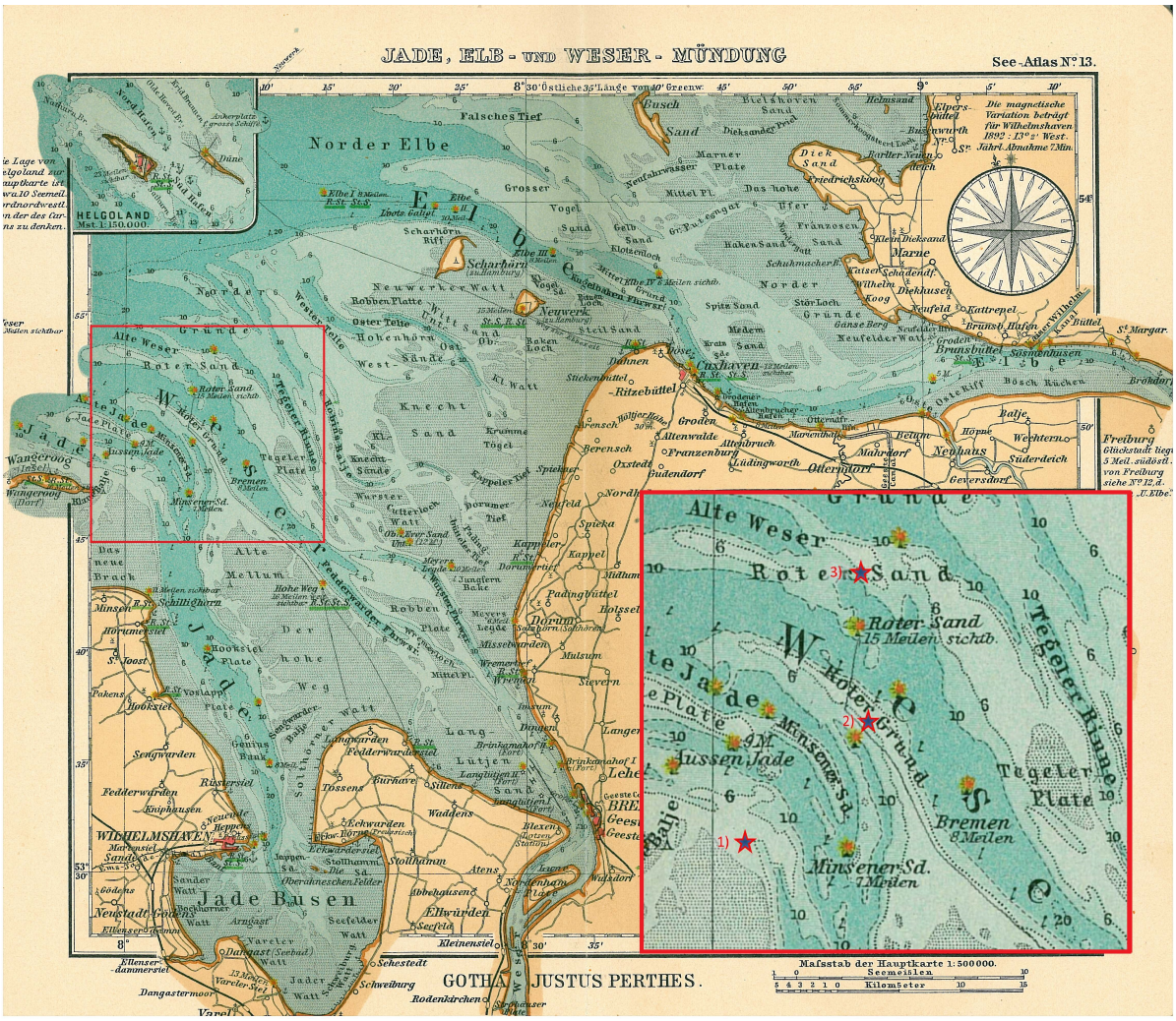

Figure 2.3: Historical locations of Minsener Oog, Roter Grund and Roter Sand on a map of the outer Weser estuary from 1906

playing a secondary role [35].
Plate [29], who has been introduced in the latter subsection as the responsible engineer for the large constructions in the Outer Weser estuary (end of 19th century), is the main author found in literature, who described a recurrent pattern in the Outer Weser estuary. Apart from other studies, he compared several historical maps starting at the year 1588 [28]. Plate wrote: "... Und ein solcher Vorgang wiederholt sich nun alle 60-70 Jahre. [...] Es handelt sich also um eine periodische Wiederkehr gleichartiger Gestaltungen im Mündungsgebiet der Jade und Weser" [29]. A free translation would be: '... And this process repeats every 60-70 years. [...] Therefore, it is a matter of periodic resurgence of identical formation in the estuarine area of the Jade and Weser.' Plate does not only state the cyclic period for the development of morphological features but he does also include the time period which corresponds to the shift of the navigational channel. From historical maps and documentations he found out that every 60-70 years the navigational channel has been moved. Plate commented his observations as being unambiguous [28].
Later, Göhren [11] looked at different publications which dealt with the recurrent morphological pattern in the Outer Weser estuary. He summarized that all authors (Krüger 1911, Poppen 1912, Jesse 1922, Plate 1935, Hensen 1939 and Simon 1960) are describing the period sandbars need to propagate once the distance equivalent to their wavelength. According to Göhren only Plate [29] [28] is describing the recurrent formation of large scale morphological features. In contrast, the analysis Göhren made revealed that the period of 60-70 years for the propagation of sand bars could not be confirmed. Instead his studies indicate a recurrent period of 110-120 years for the formation of similar morphological features in the Outer Weser estuary which is almost twice as much compared to the other authors [11]. The explanation Göhren gives for this significantly different result is found in the analyzing method. Plate and the other authors investigated the recurrent occurrence of morphological features and pattern without considering their exact position, whereas Göhren looked additionally at the geographic location of these features and pattern. Furthermore, the method applied by Göhren does not take the changes in the navigational channel position into consideration, which is an elementary aspect in the research done by the other authors. In his conclusion Göhren states that the methods applied so far are not suitable in order to describe realistic developments comprehensively. As a result, Göhren questions that a period can be assigned to the morphological development where the initial bathymetry and the bathymetry after each period are matching or are similar.
Barthel [2] was looking into the propagation of sand bars in the Outer Weser estuary in the second half of the 20th century and when recapitulating the historical studies he states that it is likely that the return period of similar morphological pattern has been 110-120 years.

2.3. Hydrodynamics in the Weser Estuary

The development of the tidal wave in the Weser estuary differs when looking at the state before and after the construction of the training walls and groynes. In the historical state for example at 1884 measurements show that the tidal wave has a decreasing pattern when propagating through the estuary. According to figure B.1 by Ramacher [31] a few things can be stated about the tidal wave propagation: Coming from the North Sea, the tidal wave develops a tidal range of around 3.80 m until it passes Bremerhaven. While propagating through the relatively shallow Lower Weser it loses tidal energy until the tidal range decreases to an amount of less than 0.4 m around the location of Bremen-Vegesack and 0.3 m at the city of Bremen [31]. After the installation of structures and the deepening of the navigational channels, the tidal range starts with 2.80 m at the northern part of the Outer Weser estuary [22] and increased to 3.80 m at Bremerhaven. Consequently, the tidal range has not changed significantly at Bremerhaven, whereas it has changed enormously further upstream at Bremen. Here in the present days a tidal range of around 4.10 m is measured [22] which is an increase of 3.80 meters within a hundred years. It is observed, that the high water has not been increased much, but the low water has been lowered due to the dredging and maintaining processes [22].
Another characteristic of estuaries is the flood-ebb-dominance. Since there are no measurements of velocities from the 19th century and there is no digital terrain model (DTM) available that would allow the determination of the historical tidal volumes or surfaces, Herrling et. al. [14] simulated the hydrodynamics of the Lower Weser with the bathymetries of 1887. From their simulations, where they plotted the ebb- and flood-duration, it can be seen that around Bremerhaven the flow has been flood-dominant in 1887. However, the Outer Weser estuary has not been modeled by Herrling et. al. in its historical state so that no conclusions can be drawn about that section.
For the present day ebb-flood-dominance, the situation in the Outer Weser estuary is studied and revealed to be not homogeneous. Zorndt [48] summarized the ebb-flood-dominaton in the Weser estuary as follows: The tidal wave that approaches the Outer Weser estuary from the North Sea has a very slight flood-dominant properties. While traveling through the estuary, the extensive tidal flats cause the average depth to be lower during high water than during low water which consequently results in ebb-dominant currents (as a process described by Bosboom [4] and stated for the Outer Weser estuary by Wetzel [45] and Schrottke [36]). Due to the slow down of the tidal wave crest by the present tidal flats, the rising tide does elongate, although it does not get longer than the falling tide. Thus, more inside the Outer Weser estuary, the tide is almost symmetric with similar rising and falling duration. South of Bremerhaven, where the Lower Weser starts the narrow channel with hardly any tidal flats reverses the former development, since here the averaged depth during high water is significantly larger than during low water, which introduces a flood-dominant behavior. Contrary, the asymmetry in the current velocities remains slightly ebb-dominant which at some point upstream can also be linked to the river runoff.

2.4. Method Examples to Determine Current-Dominance

There are several methods to measure the flood-ebb-dominance: Flood- and ebb-dominance can be related to the net sediment transport direction [4]. If the net transport is directed towards a tidal basin, it is considered flood-dominant. Since sediment transport is related to the flow velocities, this indicates that the flood currents are higher than the ebb currents. Thus, looking at the tidal currents or else at the tidal range per flood- or ebb-period can give an indication about the prevailing dominance. Additionally, two ratios can determine, if a system is flood- or ebb-dominant. The first one is the ratio of tidal amplitude over depth a/h with a the tidal amplitude and h the water depth [4]. If this ratio is large enough, the system can be expected to be flood-dominant, since the water depth, which mainly determines the average flow velocity, is large enough to overcome a domination of friction. If the ratio is not large enough, it can happen that during flood flow tidal flats are covered by water with low water depth. Thus the propagation speed of the flood on the tidal flats is relatively small by definition $\sqrt{gh}$ and friction plays a dominant role. Furthermore, during ebb flow the tidal flats might not be covered with water and the whole tidal flow is propagating through the tidal channels, resulting in a on average higher water depth and thus higher flow velocities. In this case the ebb flow dominates over the flood flow. But in order to decrease the flood flow in a significant way it needs an extensive area of tidal flats. The presence of large tidal flats is indicated by the relation of V_s/V_c where V_s is the intertidal storage volume and V_c is the channel volume [9] or via S_{HW}/S_{LW} where S_{HW} is the wet surface during high water and S_{LW} the wet surface during low water [7].

2.5. Morphodynamic Modeling in the Weser Estuary

In 2016 Herrling et al. [13] from MARUM have modeled the Outer Weser estuary within the project MORPHOWESER, which aimed to analyze the estuarine morphodynamics in cooperation with the Bundesanstalt für Wasserbau - Federal Waterways Engineering and Research Institute (BAW). Within this project the outer channel and shoal evolution in dependency on different forcing conditions have been investigated.
The first project phase covers the set-up of a morphodynamic model and its validation. For the simulations a depth-averaged curvilinear grid has been generated that covers the Outer Weser estuary and the Jade Bay. Herrling et al. have chosen to apply a higher grid resolution in the area of the Outer Weser and the Fedderwarder Priel, a tidal channel that has been of special research interest in this project. The numerical grid has been used by Delft 3D FLOW in combination with the spectral wave model SWAN. As an initial bathymetry bathymetric data have been interpolated onto a DTM with a resolution of 25 m (except the island Neuwerk) according to the method of Milbradt (2015) [24]. The training walls and groynes that have been introduced in section 2.2 are represented by the Delft 3D function 2D dams. The model is driven by 31 boundary sections on the open boundary at the North Sea side and one boundary section on the river side. The real time boundary conditions of tides, wind, waves, river discharge, salinity and temperature are imposed based on the BAW North Sea model [19] and measurements of discharge, wind and waves data. For the sediment composition and interaction a stratified bed layer model is applied considering four non cohesive sediment fractions ($95\mu m$, $151\mu m$, $233\mu m$ and $571\mu m$). Furthermore, a bed roughness height predictor has been applied according to van Rijn 2007 [42] implemented in Delft 3D FLOW.
The validation of the hydrodynamics is done by means of a root mean square error (RMSE) analysis for water levels, velocities and waves in the Outer Weser. The validation revealed a RMSE of 0.06 m to 0.11 m in the Outer Weser for the water level, a RMSE of 0.09 m/s to 0.11 m/s for the currents and a RMSE of 0.19 m and 1.63 sec for the (significant) waves.
The validation of the morphology has been done by means of a correlation analysis of observed and simulated the bed elevation range next to the visual comparison of simulated and measured maps. The direct correlation reveals a value of less than 0.19 for the bed elevation range, whereas the visual comparison indicates a qualitative agreement of channel migration trends.
The second phase aims to investigate the influence of initial conditions and applied parameters. Next to a further calibration of the roughness predictor in the first part of the second project phase, the second part deals with the effect of the initial model bathymetry on the simulated morphodynamics.
For the investigation a comparison is worked out, where two different measurements of a specific area of the Outer Weser (namely the Fedderwarder Priel) have been implemented as the initial bathymetry, while the rest of the model domain originates from the same data source. The two measured DTM applied, are from the years 2011 and 2012. The predicted morphological differences of both simulation have been extrapolated linearly in order to allow a qualitative comparison with the observations of the one year later. The qualitative comparison reveals a good agreement between both simulations, although some local differences in magnitude and spatial extend have been noticed. It has been concluded that the influence of the initial bathymetry on the results is not significant.
Additionally, the effect of Coriolis on the residual sediment transport has been analyzed. In order to determine the influence of Coriolis on the residual transport, three scenarios were selected:

- The exclusion of the Coriolis effect inside the model, by setting the latitude to 0
- The application of an equal phase along the open boundary in order to disregard the Kelvin wave
- A combination of the first two points, where neither Coriolis nor the Kelvin wave is included

The simulation results indicated a smaller influence of Coriolis on the mean transport magnitudes than the progressive Kelvin wave. It has been indicated that partly, both effects are balancing out each other in the net response, which leads to a reduced cross-sectional variability of residual transport. As a conclusion it is stated that the progressive Kelvin wave dominates over the Coriolis effect which is in alignment with the conclusions of Van Leeuwen and De Swart [40].
As the final report of the project MORPHOWESER is not published yet, further studies will deal with a further calibration of the roughness height predictor, the morphodynamic response to variable river discharge and the effect of extreme events like storm conditions.

2.6. Flat Bed Modeling Approach

The flat bed modeling approach describes the application of an initial bathymetry, that has a constant depth or depth gradient without any morphological features (ripples, channels, etc.). Thus, it allows a free development of the morphology since it is only forced externally (wind, waves, tides, etc.). In this way, the influence of forces on the morphology can be examined individually, based on the option to exclude influences even in the bathymetry.

In their book Roelvink and Reniers [34] question how much morphology of an estuary is forced by its boundaries. Approaching this question, they indicate that for very schematic cases similar depth patterns develop as seen in nature. Additionally, different channel and shoal pattern evolve when a short and wide basin is applied, rather than a long and narrow one. The same counts for the closed boundaries: If they are defined erodible, channels tend to get less deep and wider. These observations raise the question if the morphological development of an estuary can be predicted when looking at an satellite image of an estuary together with the according tidal amplitudes outside it. If such predictions would be feasible it would have two major advantages: Firstly, it would be an optimal method to investigate morphological questions when data and measurements are scarce. Secondly, it could be an excellent test for the model in order to check its ability of predicting morphology rather than morphology change. Roelvink and Reniers mention two examples for a practical application where the prediction of morphology would be an appreciated tool: The prediction of a scour hole and the reopening of a closed estuary.

Van der Wegen et al. have modeled the Western Scheldt estuary by applying the flat bed approach in order to investigate the processes that are governing the development of the channel and shoal pattern in an estuary. They have been specifically interested in the role that the basin geometry has on the evolution and allocation of tidal channels and tidal flats. The idea is to exclude as many processes as possible from the simulations and keep the model simple.
For the simulation the process based model Delft 3D has been applied and model results have been valued by means of a various analysis, i.a. the Brier Skill Score (BSS). In order to speed-up the mophological development, the hydrodynamics have been multiplied with a MORFAC (as applied by [33]). The MORFAC is a constant factor that is multiplying the calculated morphological response to the hydrodynamics in each time step.
The model grid covers the Western Scheldt and extends about 20 km further offshore and has a grid resolution of around 100 m times 200 m in the central area. With a time step of 1 minute, simulations have been done being 2D and some being 3D. A water level boundary condition has been set at the open boundary on the North Sea side, where the tidal components M2, M4, M6 and C1 (a combination of K1 and O1) are generating the water level changes. The tidal components have been gained from nesting the Western Scheldt model into a larger and coarser Model of the North Sea. Moreover, a Neumann boundary condition has been applied to the two smaller side open boundaries at the North Sea part of the model. The boundary condition at the open boundary on the landward side is prescribed by constant river discharge without sediment supply.
As the basis of the initial bathymetry, measurements from 1998 have been taken and processed to an averaged depth. Additionally, non erodible areas that have been indicated in former studies have been included in some simulations as well as the process of intensive dredging activities in the Western Scheldt estuary.
The transport formulations that have been used are van Rijn [41] and Engelund Hansen [8]. It has been noted, that the bed slope factor α_{Bn} has a significant influence on the morphological simulation results and is an order of magnitude larger for the transport equation of van Rijn.
Generally, when comparing the simulations to the measured bathymetry, a remarkable resemblance can be achieved, even when only applying the Engelund Hansen transport formula (only bed load) in a 2D simulation. A difference that has been seen is the development of rather straight channels in the 2D simulations whereas more bended channel have been found in the 3D case, due to the consideration of secondary flow. Additionally, the 3D simulation are resulting in a better fit to the measured bathymetry when analyzing it visually. A remarkable observation has been the fairly good representation of the estuary, when only applying the M2 tidal component as external forcing.
By means of calculating the hypsometry for all cases it has been indicated that representation of the simulations is increasing over time. Furthermore, it has been investigated that the hypsometry analysis suggests a significant role of the basin geometry in the evolution of channel and shoal pattern.
For the simulations the BSS has relatively high values that can be considered to indicate reasonable to good results according to Sutherland [38]. However, it is stated that the BSS values should be questioned since the

base line prediction taken by van der Wegen is not a measured bathymetry but a flat bed, which introduces high volumetric differences to the measured bathymetry which automatically results in higher skill scores. Moreover, van der Wegen et al. have investigated the effect of the initial bathymetry on the development of channel and shoal patterns. They have seen that the morphological features developing are dependent on the availability of sediments, which leads to less extensively developed morphological features in case a comparable deep initial bathymetry is implied. Furthermore, it has been indicated that the simulation results suggest a dependency of the geometry impact on the development and the averaged depth of the basin: The deeper a basin, the higher the impact of the geometry on the development of morphodynamic features [39]. Simulation results with the best resemblance to the measured bathymetry is gained when applying a flat bed depth that is equal to the averaged real depth of the model domain.

2.7. Delft 3D

Delft 3D is process based model developed by Deltares [16] and [23]. It is one of the most commonly applied modeling suitesthat can simulated hydrodynamics, morphodynamics and waves in fluvial, estuarine and coastal environments [16]. Since 2011 Delft 3D is available open source. The Delft 3D modeling system in hydro- and morphodynamics is described by Lesser [23]. The equations of the hydrodynamics are based on the Navier-Stokes-Equation under the assumption of the incompressible fluids, shallow water and Boussinesq approximation [16]. For the calculation of sediment transport various transport formulas can be applied, where in this project the transport equations after van Rijn [41] and Engelund Hansen [8] are used. For long-term morphodynamic modeling, an amplification factor can be applied in order to accelarate the morphodynamic changes resulting from the hydrodynamics. This factor is called MORFAC [33] and [32] and does multiply the calculated morphodynamic changes per timestep with a constant factor. The underlying assumption in order to make this factor applicable is that the hydrodynamics will not change considerably during the resulting accelerated time (time step + MORFAC). Additionally, Delft 3D is coupled with Swan, a third generation that computes the full spectrum including various processes [16]. In this project the latest Delft version 4.03.01 is used.

2.8. Model Evaluation

2.8.1. Evaluation Criteria for Morphodynamic Models

The evaluation of a numerical model is always dependant on the purpose it has to serve. Even though the past has shown that the following parameters and scores have proven to show a good overview over the overall fit of simulated data with measured data. Generally, all parts of the model are tuned based on measured data or common sense [34]. The choice of the tuning basis depends on the intentional use of the model. While in most cases a model is built in order to represent reality up to a certain degree of accuracy, there can also be scenarios where a physical phenomenon is investigated by means of a more schematic model, which also applies for this project. As mentioned in the introduction the model of this project aims to simulate the historical situation. But it differs from a hind-cast since the main focus is the investigation of causes and reasons for the formation and alternation of the two channel system in the Weser estuary rather than the complete physical representation of the Weser estuary. In order to compare simulation results to measurements or the other way round there are a number of coefficients and parameters that can value the representation. As a relatively simple method, analysis of the tidal characteristics can be performed, as well as the determination of mathematical parameter. The mean square error (MSE) or the RMSE of water levels, tidal ranges or velocities between measurements and simulations are examples of these. A more advanced strategy of calibrating a model is the use of Skill Scores. Skill scores are widely applied in meteorology (Sutherland, 2004) and can be converted into evaluation criteria for morphodynamic modeling applications. A skill score that is often applied is the BSS.

2.8.2. Brier Skill Score

In other experimental modeling projects with a flat bed approach like the Western Scheldt [39]; [6] the Brier Skill Score has been applied. The BSS values the model performance of bed level changes by comparing a base case prediction to modeling results. A base case prediction can be grounded on measurements, or a reference scenario. A simplified version of the BSS for the application in the field of coastal engineering (equation 2.1 has been published by [43] based on the derivations of [26]. The formula reads

$$BSS_{vanRijn} = 1 - \left[\frac{\langle (|z_{bc} - z_{bm}| - \Delta z_{bm})^2 \rangle}{\langle z_{b0} - z_{bm} \rangle^2} \right]^2 \tag{2.1}$$

where z_{bm} is the measured depth, z_{b0} is the initial depth of the model, z_{bc} is the computed depth at the end of the simulation and Δz_{bm} is the consideration of measurement errors. The disadvantage of this skill score is that it includes a double penalty by underestimating the variability of the morphodynamic changes [3].The double penalty is the reason why a slight in the channel location can kill a skill score [34]. In the case of the channel position shift, the depth at the real channel location is overestimated by the model and at the simulated location of the channel the model is underestimating the depth. Although, the channel shoal patterns are correctly presented the shift of the channel introduces a negative influence of the overall skill of the model.

2.8.3. Selective Skill Score

To overcome this double penalty phenomenon Bosboom recommended the application of a scale selective validation [3]. In the scale selective validation method areal maps of the structural similarity, the amplitude similarity and the pattern skill are generated for different spatial scales. According to the spatial scale that needs to be met by the model, a good indication of representation can be given through this method. A disadvantage of these coefficients is that they require a number of calculations and interpolations of results. Furthermore, due to the circumstances that the model aims to represent the bathymetry of the late 19th century there are no digital terrain models from this time available which would be needed for the use of a skill score. A skill score can still be used when comparing simulations with each other. Nevertheless, the benefits of applying a skill score are relatively small when the limitations of a skill score of schematic representations are considered. Additionally, the implementation for an automatic evaluation with the given data and output volume (quantitatively and qualitatively) can be quite time consuming and rather complex. Apart from the problematic implementation, the lack of digital information about the historic state (except historical maps from former German marine administrations) is limiting the evaluative options. This deficit of available information is another reason why a skill score will not be used in this case. Digitizing the available maps is, due to time limitations, not an option. Thus, other criteria might need to be defined in order to evaluate the model results.

2.8.4. Flat Bed Evaluation Criteria Applied in the Western Scheldt

As stated above, other scientists have applied the approach of flat bed modeling. Van der Wegen [39] has used several methods to analyze the evolution and development of the Western Scheldt:

- Bed level development (visual)
- Hypsometry
- RMSE
- The BSS
- Depth (averaged over model domain)
- Width-averaged depth (along the estuary axis)

From these criteria some inspiration can be gained for the evaluation of the scenario analysis. Apart the BSS, including other Skill Scores that have been found inapplicable (see subsection 2.8.3), there are measures that might be useful for further applications.

3

Investigation Concept

3.1. A Flat Bed Model

The concept applied in this project is, as introduced in chapter 1 and described in chapter 2, the flat bed modeling. The research question that reasons this project aims for an improved comprehension of the Outer Weser estuary in order to understand the processes that represent today and are highly influencing the navigational and maintenance endeavors. Since the Outer Weser estuary has been significantly influenced by human interaction (see section 2.2) it is not clear which causes are responsible for the observed morphodynamic changes. Distinguishing the different influences on morphodynamics and their resulting effects is a challenge.
By running simulations in a computational model, where different conditions are applied, a relation can be generated between the individually simulated conditions and the resulting impact that these have on the channel and shoal pattern. In order to investigate the evolution of channels and shoals the relevant processes need to be represented by the computational model.
The main process that should be covered by the model is the sediment transport in order to model morphodynamic activities. Sediment transport is proportional to the current velocity to:

- The power of 3 for bed load transport [4]

$$\langle S_b \rangle \propto \langle u|u|^2 \rangle \tag{3.1}$$

- The power of 4 for suspended sediment transport [4]

$$\langle S_s \rangle \propto \langle u|u|^3 \rangle \tag{3.2}$$

Consequently, the computational model applied needs to compute the velocity in the model domain considering the influences of tide, discharge and wave induced currents. Computational models offer the possibility to show an overall morphodynamic behavior are process based models [34]. A process based model can predict the sediment transport by solving the hydrodynamic equations based on the Raynolds-Averaged-Navier-Stokes-Equations under the assumption of incompressible fluids, shallow water and Boussinesq (the effect of variable density is only taken into consideration in the pressure term) approximation [16].
It is desired that the morphodynamics develop freely without being influenced by former conditions. Therefore a real bathymetry cannot be applied. Disregarding the constructions that have been made in the Weser estuary, applying a real bathymetry would already pre-define channels and thus areas where higher velocities can be found. In a way, any morphological feature would artificially affect the results. Consequently, the idea of using a flat bathymetry arises, where free development is possible. As a result, the boundary conditions applied to the model (external *tides, discharges, waves* and internal *land boundary, estuarine shape*) will shape the channels and shoals.

Using a flat bed as the initial bathymetry includes trade-offs:
First of all, it is a highly schematized approach which cannot be seen as a reproduction of reality, where estuaries are shaped in time spans of millennia with various processes included. By simplifying the genesis

of the estuary the investigation will focus on the macro scale morphodynamics by definition. It means that channel and shoal features will be considered in a broad sense or vice versa the simulations do not aim for the reproduction of small details.
Another trade-off is that the complete development of tidal flats and channels requires long term morphodynamic modeling. Thus, the extensive simulated time span is resulting in computationally intensive calculations. Additionally, in order not to overload the investigation with endless parameter studies, it is necessary to only include parameters that are essential for the processes taken into account.

Processes, which are not as relevant as the previously described ones, should not be included, for example wind stresses on the sea surface. Furthermore, it is assumed, that simplified processes will yield an order of accuracy good enough in the scope of this project, such that it is valid to apply simplified conditions, rather than physically exact and accurate conditions. Consequently, and in order to limit the computational time to an acceptable amount, processes included are generally simplified and only included if necessary.
Apart from the initial depth the simplification includes the grid, the boundary conditions and processes incorporated. The grid needs to be coarse with a resolution that conforms the macro scale. It covers the Outer Weser estuary and extends further offshore and upstream in order to assure results that are not influenced by numerical effects of the boundary condition. Furthermore, the boundary conditions are chosen such, that they resemble the governing processes in the simplest way possible. Processes that could be included by the model like wind, waves, secondary flow, the concentration of salt and distribution of temperature are not included, neither 3D effects nor the multi-fractional modeling approach in order to have a feasible computational time. Combining the ideas and features of a flat bed model into a model set-up, a base case is formed that will be calibrated and validated.

The calibrated base case simulation is the benchmark for this project and mainly fulfills two duties: It represents first of all the historical situation of the macro scale morphodynamics. The base case aims for reproduction of a two channel system where the depth of the channels varies in time. Ideally, a situation can be modeled, where the behavior of the depth alternation between the two channels is in such a way, that explains why intensive measures were needed at that time as described in chapter 2 under 2.2.
Secondly, the base case builds the foundation for the comparisons that are made between the scenarios. Since it cannot be expected that a comparison between the scenario simulations with one another will clearly indicate the influence of the different mechanisms applied, it needs a common case that the scenario simulations can refer to.

3.2. Scenario Composition

As introduced in chapter 1 there are two basic research questions that are treated in this project:

1. What influences the formation of two channels in the Weser estuary?
2. Why do the two channels alternate in the natural case?

The following approach will be performed:
When thinking about influences leading to a two channel system in the Outer Weser estuary, the investigation should start with a theoretical analysis (chapter 2). There, the Weser estuary has been classified as a mainly tidal influenced estuary within the three categories tides, waves and river. The idea behind the theory developed and applied by Boyd et al. [5] is that the combination of the three forces is shaping an estuary. Consequently, all three forces could have an influence on the development of two channels in the area. Starting with the influence of the tides, it is not questioned if tides are responsible for the development of two channels. The question is, which factor of the tides is relevant with respect to the research questions. As seen in the base case validation simulation (see subsection 5.3) where M2 is the only tidal component shaping the estuary, the main tidal component is creating a two channel system. Based on this observation, it is expected that tidal asymmetry introduced by the other tidal components will result in a two channel system as well. Thus, it needs to be investigated if other aspects that are included in the M2 simulation contribute to the development of two channels apart from the tidal components. One feature that is not covered by the tidal components itself is the influence of Coriolis namely the Kelvin wave. The Kelvin wave results from the tidal propagation through the oceans under the influence of Coriolis. It causes a phase difference of the tidal wave along the German Bight. This phase difference may result in the development of other channel patterns. Either due to the different tidal propagation based on the Kelvin wave or due to the influence of Coriolis during ebb and flood even though it is questionable if that forcing is strong enough. Furthermore, waves which are not included in the base case simulations could influence the presence of a second channel. Even though two channels can be observed in the scenarios disregarding waves it is interesting to see the influencing component. It is expected that waves might cause a shift of the channel(s) location towards the direction opposite of the wind direction.
Additionally, according to Boyd [5], the river discharge is the third category that acts on the morphodynamics of an estuary. Thus, it may prove favorable for the development of two channels or at least influence their shape and location.
In order to investigate the reasons for the alternation of the dominant channel within the two channel system, it has to be checked which external processes have an influence. The alternation appears within decades (every 60-70 years) to centuries (110-120 years) according to several authors (see section 2.2). The forcing causing this alternating pattern thus must be varying as well and in the same order of magnitude. Again, the three external forces which are the categories for Boyd's classification [5] are in question here. The Kelvin wave and Coriolis force should not be the cause since they are constant in time. Although, as a matter of fact, the nodal tide component has a return period of 18.6 years [47]. The nodal tide is considered neither in the base case simulation nor in the scenarios since just ten years of hydrodynamics are simulated. Instead, among others the nodal tide is covered by a scenario which is simulating a general rise of the tidal range. It covers the effect of sea level rise, seasonal differences and components like the nodal tide. The nodal tide could also have been considered as a factor [4], but it seems a more straight forward process to include the nodal tide within the scenario of an increased tidal range. An increased tidal range is supposed to be representative for variations within the tides which might be the cause for alternating channels. Next to the increased tidal range, another external force that varies over time and thus may influence the development of tidal channels are wind waves and storm events. Therefore, the wave scenario is investigating the first two research questions all together. The same holds for the river discharge. Since the river discharge depends on season, precipitation and other factors, it is not constant in time as simplified in the base case scenario. It is relatively error-prone to create a time series of river discharges that is representative for ten years of river discharge in the 19th century. Hence, the discharge scenarios that are defined in order to answer research question one, will also be used in a way to indicate how different river discharges affect the location of channels and thus may be responsible for changes in the channel depth.

Summarized, the following scenarios are chosen in order to answer the research questions:

- Two tidal channels
  1. Kelvin wave
  2. Coriolis
  3. Waves
  4. River discharge
- Alternation of the two channels
  1. Waves
  2. River discharge
  3. Tidal range

Each of the listed influences is assigned to one scenario simulation. It is not the idea to answer the research question on top comprehensively with this selection of scenarios. Instead, it is the goal of the scenarios to investigate if and to which degree the different forces or phenomena have an influence on the research questions.

To judge if a scenario simulation is of any use for further analyses, three questions are specified:

1. Does the simulation reach any kind of equilibrium?
2. If so, is there an alternation pattern visible?
3. If yes, can a period be assigned to the alternation?

The questions are investigated for the base case and each scenario in chapter 6, while the combination and interpretation of all results proceeds in chapter 7.
In the following a conceptual description can be found for each scenario:

3.3. Scenario Concepts

3.3.1. Kelvin Wave

The Kelvin wave scenario is looking at the influence of the tidal wave propagation in the North Sea on the Outer Weser estuary. A Kelvin wave is a tidal wave that moves with shallow water speed along the coast line as a coastally trapped wave [4]. In the North Sea it starts at the northern side of the North Sea basin and propagates counterclockwise along the coasts of England, Netherlands, Germany, Denmark and Norway. Since the Kelvin wave travels counterclockwise it approaches the model domain from the north-west, propagation towards north-east. Within the open boundary condition of the base case the Kelvin wave is considered by the phase shift of the open boundary sections. As mentioned above, in the base case, the North Sea side open boundary is divided into three pieces in order to get an accurate representation of the tidal wave in that sector. An easy method to investigate the development of shoals and channels without the influence of the Kelvin wave is to introduce the same tidal amplitude and phases at all open boundary points. This way the tidal wave propagates straight into the model domain from the whole open boundary section (compare figure B.2 in appendix B).

3.3.2. Coriolis

Similar to the Kelvin wave scenario the Coriolis scenario investigates the influence of the Coriolis force on the development of channel and shoal pattern. As a matter of fact the Coriolis force is a fictitious or pseudo force since it does not appear as a natural force caused by physical interaction but originates from the choice of a reference frame [4]. Since most observations are done from the earth's surface or the earth's atmosphere everything is seen from a reference frame that spins with the earth's rotation. Consequently, the centripetal acceleration of the earth is hidden in this rotating reference frame but still influences every propagation on earth (if not exactly located on the equator). In order to account for this phenomenon the Coriolis "force" has been introduced, named after Gaspard-Gustave de Coriolis who first described it at the beginning of the 19th century. The effect of Coriolis is that moving particles in the northern hemisphere are deflected to the right and moving particles in the southern hemisphere are deflected to the left. The influence of Coriolis becomes stronger the further away from the equator. The reason for this is, that Coriolis acts in a direction perpendicular to the rotation axis of the earth, which is normal to the earth's surface at the equator. On mid-latitudes the Coriolis acceleration is around ten-millionth of the gravitational acceleration [37], whereby water particles are affected significantly on long distance. To find out, if the distances that water and sediment particles are covering is long enough to get significantly influenced by Coriolis is the main goal of this scenario. If so, the Coriolis acceleration could be an explanation for the forming of two tidal channels since Coriolis deflects moving particles to the right in the northern hemisphere. If for example the flood transports the water into the estuary, water particles are tendentially deflected to the western side, while the out-flowing water during ebb would be deflected to the right resulting in an eastern channel. This theory at least does not object the arrangement of flood and ebb channels as they were observed at the end of the 19th century. If that is correct, the simulations without the influence of Coriolis should show a different arrangement of tidal channels and shoals, for example only one tidal channel in the AOI.

3.3.3. Wave

When thinking about influences that may have shaped the Outer Weser estuary, waves are a factor as well. As already mentioned in chapter 2 waves can be a significant aspect in shaping an estuary. But as stated, the shape of the Weser estuary is mainly influenced by tidal forcing. Still, waves might be a reason for the existence of two channels in the Outer Weser estuary. Kösters [18] looked on the effects of tide, wind and wave on the bed shear stress intensity and the mean bed elevation range. According to his studies it can be concluded that waves mainly have an effect on the outer tidal flats which are exposed to wave attack. Consequently, in shaping the estuary, it would be expected that the biggest differences between the wave scenario and the base case will be found in the outer parts. Additionally, tidal flats on the inside of the Outer Weser estuary experience an influence through wave attack as well, even though it is not of the same intensity as it is in the areas at the outer part of the estuary. It is an interesting question, how different the estuary will shape in comparison to the base case, when waves are included as an external force within millennia of morphodynamic development. Theoretically, the constant influence of waves on the morphology should lead on the long term to a different estuarine system, as indicated in Boyd's analysis [5].
It has to be kept in mind, that the application of a MORFAC (see chapter 2) with a value of 400 might artificially overestimate the effects of waves, since wave induced currents will be multiplied unnaturally high. However,

due to the possible overestimation of wave impact, the schematic effects that waves have on the development of tidal channels and shoals in the Outer Weser estuary should be indicated very clearly in this scenario. In order to keep it simple, an averaged wave scenario is applied based on measurements made in the German Bight in 2012. Figure B.3 gives an overview of measurements taken by BAW for the open boundary generation of the Jade Weser Elbe (JWE) model. It shows a summary of the wind and wave data, covering a bit more than two months during late summer. From this data the average significant wave height, wave direction, wind speed and wind direction are extracted and applied for the wave scenario.

3.3.4. Extreme River Discharge

In the simplified representation of the historical reality (the base case) the model is influenced by two external forces only. One of them is the discharge as an open boundary condition at the south end of the model domain (at location Bremen-Vegesack). As one of the external impacts acting on the Weser estuary it can also be considered as a factor that is influencing the development of multiple channels in the Outer Weser estuary. In order to investigate the effect of the river discharge, two scenarios are created. This one is looking at the extreme discharges and the next one at no discharge at all. As stated in section 4.1.5, the river discharge applied in the base case is 325 m^3/s. The multi-annual mean extreme discharge of the Weser has been 1220 m^3/s published by the federal authorities in 2017 [1]. Nowadays, where rivers are controlled and artificially dammed, extreme river discharges are likely to be damped by weirs and reservoir dams. To account for this hindering of extreme discharge events and in order to have a schematically very clear result the discharge in this scenario is increased to 2000 m^3/s. It is evident that this high discharge might be overestimated, especially since it is applied constant over time. Nevertheless, this discharge rate is applied as an extreme case scenario and thus should yield an explicit result, how such extreme discharge events tendentially shape the estuary.

3.3.5. No River Discharge

In the Key-Note of the extreme river discharge scenario it has already been mentioned that a different discharge might lead to a dissimilar development of the tidal channels and shoals in the Outer Weser estuary. Additionally, the other way around it could also have an influence in case there is less discharge. If this idea is exaggerated the discharge set to zero should result in a different bathymetrical result than the base case or the extreme discharge scenario just mentioned. By disabling wind, waves and river discharge the Weser estuary is turned into a bay. The open boundary condition at the southern end of the model domain is kept, but since a discharge of zero is assigned, it is the same as closing off that part. Thus, the channel and shoal pattern that will develop should in theory be somehow similar to the ones observed in a tidal inlet/bay (i.e. the Jade bay).

3.3.6. Increased Tidal Range

The last scenario that is simulated is supposed to give some more insight in the question what may be the influences that affect the alternation of the channels in the Outer Weser. Since the alternation has a period that varies between 60 and 120 years, the external influence should be temporally somehow related. One of the external forces that underlies variation on small and large time scales is the tidal range. It can vary due to various effects:

- Seasonal Variation
- Nodal Tide
- Sea Level Rise

Seasonal variations of the tidal range occur on a small time scale but still they might influence the development of channel and shoals on a longer time scale. Müller [25] indicated the seasonal variation of the M2 tidal component among others for the German Bight. Additionally, as stated in the introduction of this chapter, the nodal tide as a long periodic tidal component cannot be added as a standard simulation case due to its period of 18.6 years. Instead, it is considered as an increasing factor in the tidal range, even though its amplitude is relatively small and it could have simply been added to the tides as a factor as mentioned in the introduction to this chapter. As the last influence that can cause changes in the tidal range SLR is taken into account as well. Studies have shown, that depending on the set-up of a model, sea level rise can lead to a locally increased tidal range within the European Shelf [27]. Thinking about a case, where SLR adds to the tidal range, three factors can cause variations over time. This scenario has the purpose to look at the effects that an increased tidal range would have on the development of the channel and shoal pattern.

4

Methods

4.1. Model Set-Up

Multiple aspects need to be taken into account when setting up a numerical model.

4.1.1. Area of Interest:

In chapter 1, the target of this project has been defined as the inner part of the Outer Weser estuary (see figure 4.1). This definition came up due to the location of the alternating channel system which is the elementary feature for this thesis. Additionally it needs to be discussed whether the Outer Weser part should also be considered as the AOI for the model evaluation. First of all, it would not be at a disadvantage to take the same spatial frame for the model AOI. Furthermore, since the red rectangle in figure 4.1 labels up to some degree of precision the extent of the two channels, it likely fulfills the most important criteria and has the advantage of simplicity. Another reason for taking this definition of the AOI is that it does not only cover the extent of the current positions of two main channels but also the positions of the historical state (see historical maps in the appendix A). Thus the pre-defined scope of this project can be taken as the area of interest for the evaluation procedure.

Figure 4.1: Indication of the AOI in the Weser estuary

It is important to define an AOI since the modeling approach chosen here does not aim for a 100 % representation of the reality/historical state for the whole model domain.
Thus, in order to have a feasible evaluation process for the simulations, all criteria mentioned in the following would need to be applied in the area defined by the red box of figure 4.1.

4.1.2. Model Domain

First of all, it needs to be defined which area should be modeled. Since the scope of the project lies on the Outer Weser estuary, it is clear that the area covered by the spatial definition of the Outer Weser estuary should be the minimum extent of the model. The land boundary is extracted from the available historical maps. Apart from that and in order to keep the computational effort minimal, the model should be spatially as small as possible but sufficiently large enough to guarantee a physically justifiable representation of the area. All adjacent hydrodynamic features (see figure 4.2) that might have an influence on the Outer Weser estuary (disregarding the North Sea) are:

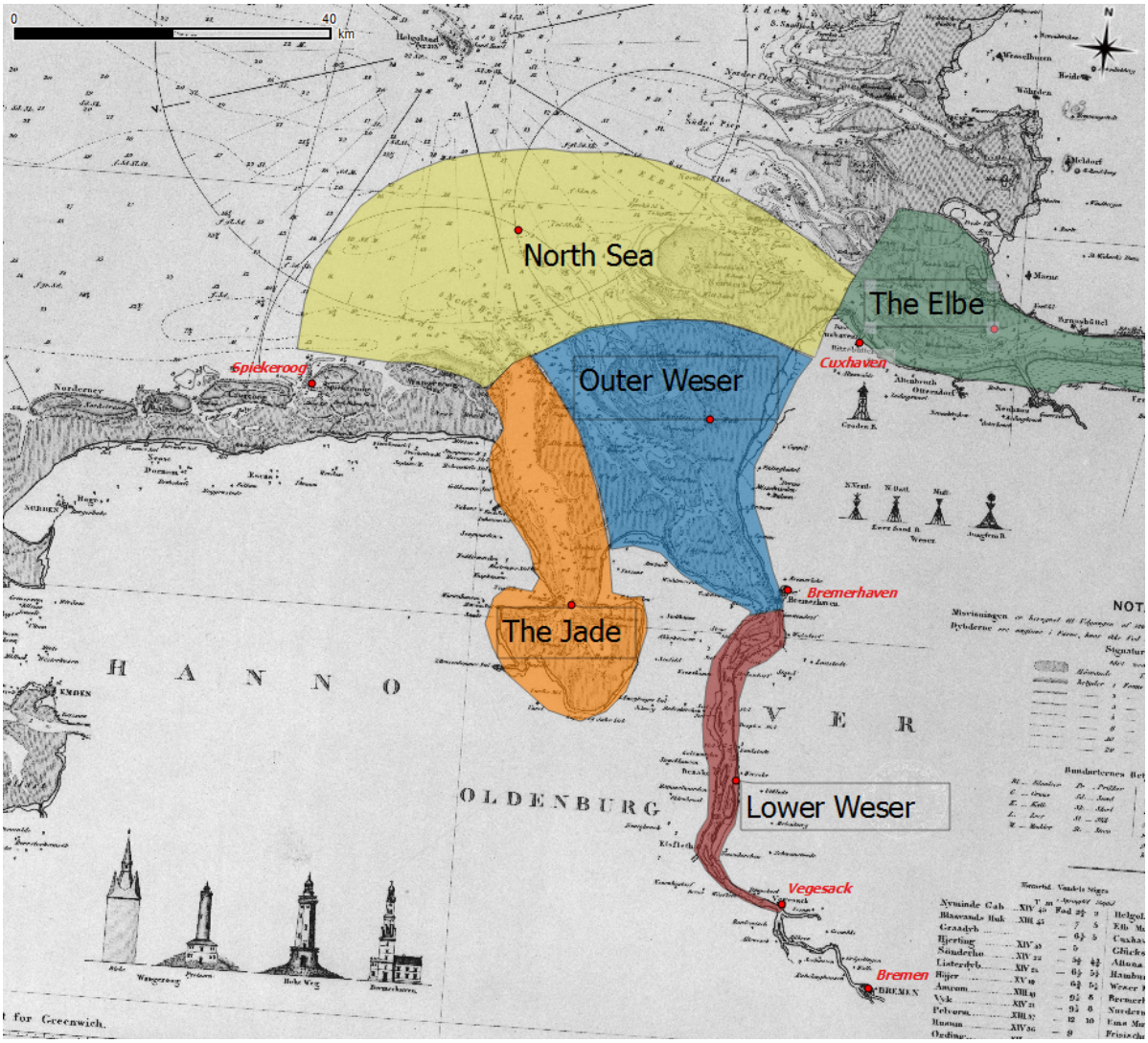

Figure 4.2: Sections within the model domain. Optional areas that could be taken into account for the model domain.

- The Jade bay
- The Lower Weser estuary
- The Elbe estuary

The Jade has a non-negligible influence on the hydrodynamics of the Weser estuary [21]. The Kelvin wave comes from the northwest and thus reaches the Jade bay first. During high tide (especially during the spring period) the extensive tidal shoal which divides the Jade and the Outer Weser estuary gets flooded and thus water flows from the Jade into the Weser. Consequently, it is necessary for a valuable model to include the Jade as a boundary condition or as the whole bay.
The second hydrodynamic influence on the Outer Weser estuary is logically the Lower Weser estuary. Its effect on the Outer Weser estuary is obvious: As the adjacent upstream section of the Weser estuary it introduced the river discharge from upstream of the Weser to the Outer Weser part and additionally functions as a tidal prism.
Furthermore, the Elbe estuary is located north east of the Outer Weser estuary. Both in the historical situation and today the two estuaries are divided by large tidal flats and a couple of small islands. The Kelvin wave first arrives in the Weser estuary and then progresses towards the Elbe estuary. Consequently, the water flows from the Weser estuary towards the Elbe estuary, but not vice versa. Thus it can be assumed that the large scale tidal flats that divide the Elbe estuary from the Weser are functioning as a closed end of the model where no flow enters the domain from the north east side.

Domain Extent and Borders The extent of the closed boundary is derived from the historical map of 1870 where the -2 m depth contour is taken as the limiting line in this sector. The influence of the remaining two features needs to be considered by the model.
The Lower Weser estuary needs to be attached, to take advantage of the following important aspects: First, not many grid cells are needed to represent the Lower Weser river, since it is a quite narrow channel. Furthermore, not the whole length of the Lower Weser needs to be considered, according to the historical tidal range from 1884 (see figure B.1 in appendix B). In figure B.1 the tidal range between 1884 and 1888 is in average very small from location Vegesack upstream. It is assumed that the influence of the tide is relatively small compared to the river discharge at Vegesack and thus only the discharge needs to be considered from this point upstream. Hence, it is seems justified to include the Lower Weser until Vegesack. The second advantage of including the Lower Weser estuary is that it is relatively easy to include it into the model domain while it would be much more complicated to get a well balanced boundary condition of tidal components and river discharge at the transition between the Outer and the Lower Weser part. Lastly, it is beneficial for an unrestricted free development of the morphodynamics when the open boundary and thus the end of depth changeable cells is further away. It could have become problematic if the southern open boundary condition was too close to the scope of the project. In a nutshell, the Lower Weser estuary will be included as part of the model domain.
The Jade bay could be considered as an open boundary or as part of the model domain. Including the Jade as an open boundary condition would have the advantage of less cells that would need to be computed. Comparing the whole model domain spatially with the Jade bay, the Jade has roughly a fraction of 1/4 to 1/3 - a considerable amount. However, using an open boundary condition for the Jade would introduce a number of problems that first would need to be solved before a boundary condition could be generated. First of all, the Jade and the Outer Weser estuary are divided by the Hohe Weg shoal that falls dry during low tide. It is challenging to get a tidal signal from the JWE model or other sources at that location that could be used as input for the boundary condition generation. The issue could be solved by taking adjacent locations into account and interpolate a representative set of tidal components or other types of boundary conditions from a number of tidal gauges. Another disadvantage would be that two open boundary conditions would be applied to the model domain from two different directions next to each other. In most model applications [34] this is a challenging situation that might cause instabilities or at least requires some fine tuning. Consequently, even though it will increase the computational time, it will be from the perspective of a numerical modeler easier to include the Jade bay in the model domain.
Furthermore, as mentioned in the conceptual description, the extent of the model domain towards the North Sea needs to be defined. Since it can cause instabilities if the northern boundary of the model is just the straight end of the Outer Weser estuary (see subsection 5.6), the model domain gets a more circular and further extended boundary, that goes from the German island Spiekeroog to Cuxhaven.

Grid Resolution As already described in this section, not all areas included in the model domain are equally important. Since some parts of the domain are there due to simplicity and completeness they do not need to have the same grid resolution as the scope of the project. Therefore, the grid resolution has been chosen to be lowered in the Jade, the Lower Weser and the outer part of the North Sea. The other way around, the grid resolution in the Outer Weser estuary has been chosen to be fine enough to cover the width of potential tidal channels with multiple cells. The resulting model domain and different grid resolution areas are presented in figure 4.3.

Figure 4.3: The modeling grid - model domain with a map of 1862 in the background

4.1.3. Inital Depth

The second feature of the model is the initial bathymetry. In a flat bed model it seems to be obvious how the initial bathymetry should look like. However, a few more aspects need to be considered in addition to the idea of an initial bathymetry with constant depth. The first and most intuitive approach would be calculating the average depth of the bathymetry that exists in reality. This project aims to reproduce a historical state, where it is not possible to take a DTM and do the necessary calculation via geographical information system (GIS). Since there is no DTM for the historical state it is assumed that the volume a century ago is equivalent to the nowadays/current tidal volume. It seems to be a qualitatively justified assumption since the bathymetric changes in the last century have been quite limited due to the constructions build at the end of the 19th century (see section 2.2). From the tidal volume and the surface area the average depth can be calculated. For a correct representation all grid points that are located on the landward side of the historical land boundary are set to one meter above sea level and are made non-erodible. For the rest of the area perturbations are added to the calculated mean depth value (see figure 4.4). They are spread randomized and with an elevation of plus or minus two centimeters. The perturbations are included for a faster spin up of the morphodynamics. Additionally, it could be an idea to already include an inclination of the width average depth according to the present depth gradient from the Lower Weser estuary towards the Outer Weser estuary. Eventually, the inclination is not included in the initial bathymetry in order to not artificially influence model tendencies of bathymetric changes.

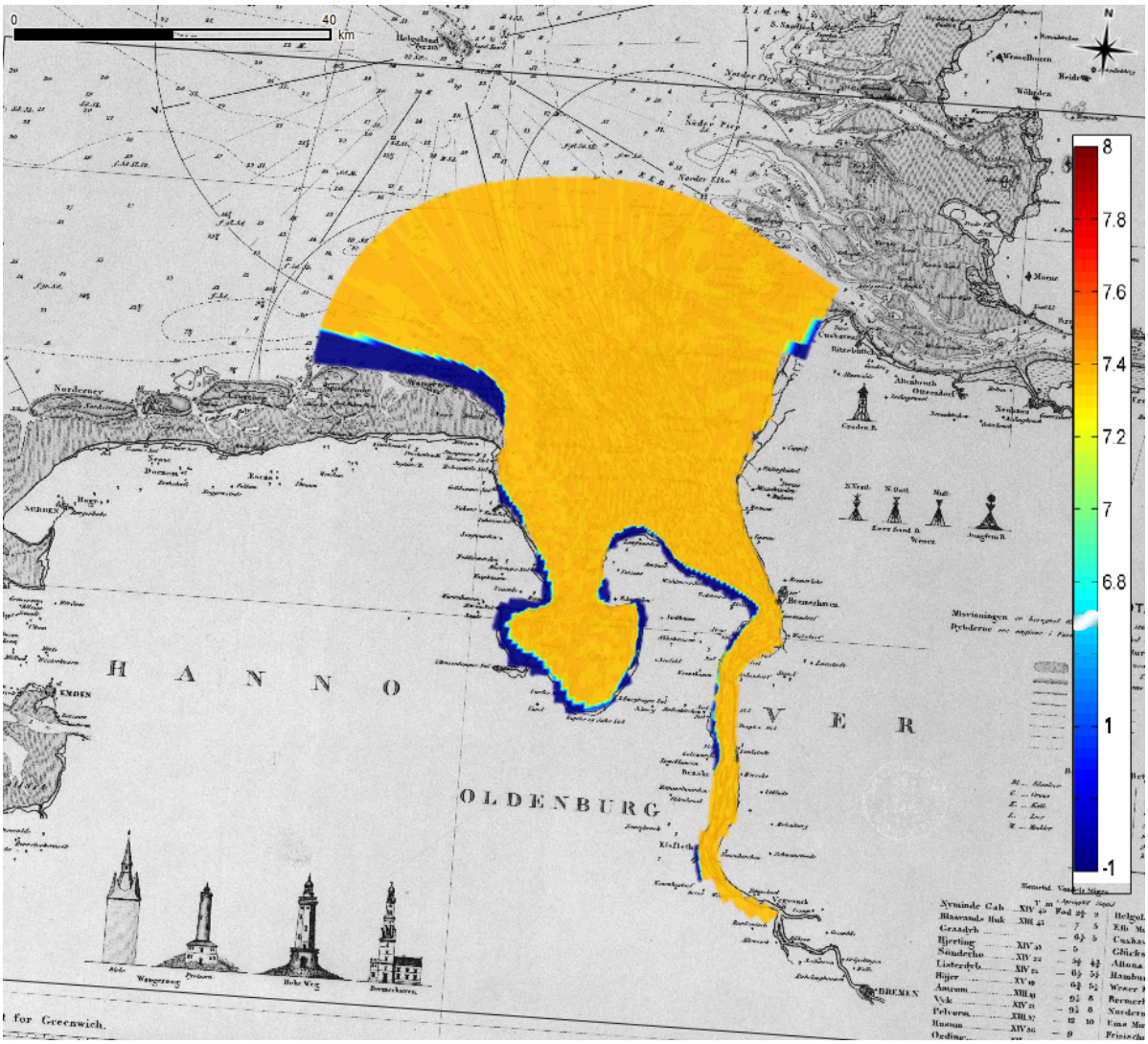

Figure 4.4: Initial depth for the model domain, including perturbation pattern randomly spread with a few centimeter of amplitude.

4.1.4. Sediment Composition

In order to perform morphodynamic simulations next to the initial bathymetry the sediment fractions and bed composition needs to be defined for the model domain. Figure 4.5 shows the sediment distribution in the Jade and Outer Weser based on measurements that have been taken by the German authorities. The visualization (BAW, 2016, unpublished) gives an overview of the main sediment types that are deposited on surface. The three main sediment fractions are medium sand ($\sim 325\mu m$), fine sand ($\sim 200\mu m$) and very fine sand ($\sim 90\mu m$), where the fine sand fraction is the most common sediment class in the area. To keep the model as simple as possible, only one fraction is taken for the set-up with a constant availability of 35 m in the model domain. An exception are the non erodible areas that are defined on the landward side of the historical land boundary (see dark blue areas in figure 4.4). They do mainly affect the model domain in the northwest where barrier islands are covered by the model domain. Due to the single sediment fraction there is no need to define a bed composition. The sediment grain diameter applied is chosen to be 200 μm according to figure 4.5.

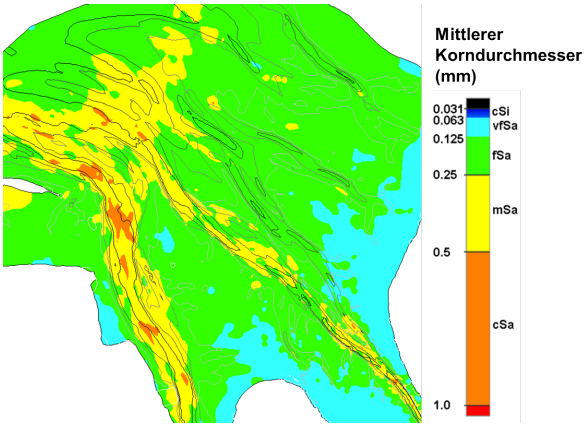

Figure 4.5: Sediment distribution in the Jade and outer Weser estuary - according to the mean sediment diameter

4.1.5. Open Boundary Conditions

There are two open boundaries that need to be specified. The first is located at the North Sea side whereas the second is specified at the southern part of the Lower Weser. Since both boundary conditions need to be defined for a timescale of multiple years and should be representative for the situation more than one century ago some ideas need to be developed. For both boundary conditions an individual solution needs to be found:

The boundary condition for the open boundary at the North Sea should be to specify a water level boundary condition, since the main effect that wants to be included from the North Sea is the tide. In order to consider the tidal wave in the German Bight accurately, there is a need to split up the open boundary into a few parts due to the presence of the Kelvin wave in the North Sea and the resulting phase differences along the open boundary. It is assumed that a division into three sections is accurate enough for the purposes of this model. Using multiple time series from measurements is not possible: Firstly, because there are no measurements for such a long timescale that are post-processed well enough to be applied. Secondly, measurements would include storms, surges and other effects which are part of the conditions found in the North Sea but not wanted as an influence on the open boundary. The reason not to include storms or surges is that a plain movement of the tides will make it easier to distinguish the effects that tides have on the development of channel and shoal pattern. Additionally, a smooth and steady tidal signal will help detecting the changes that will be introduced by the scenario simulations. Thus, a solution needs to be found that can provide a tidal signal which does not include unwanted side effects. Furthermore, measurements are just taken at one specific location and it might be difficult to find enough measurements that are taken along the open boundary in order to generate a boundary condition that accurately represents the tidal propagation.

To overcome the mentioned challenges, it was decided to extract the needed time series from a well calibrated model in order to have the option to gain input at the necessary positions. After the time series have been extracted they get processed by means of a tidal component analysis. Analysis tools, such as *ttide* for matlab or equivalents, can give the according tidal components for each tidal signal. An example of all tidal components with an amplitude of more than 5 cm can be found in table 4.1. From these tidal components a boundary condition is generated that forces the model through water level variations which are introduced by the astronomical components. In order to simplify the boundary condition and just take the most important components into account, a set of tidal components is chosen to represent the tides. As stated in chapter 2, van der Wegen [39] used the components:

- M2
- M4
- M6
- C1

With, C1 being an artificial tidal component that is combining the effects of O1 and K1. Using van der Wegens choice as a starting point, the components M2, M4, M6, O1 and K1 were applied as well, but adding the S2 due to its amplitude being the second largest in the Outer Weser. Furthermore, the MS4 is included in the boundary condition as well, in order not to underestimate the tidal asymmetry during spring tide which would be introduced by considering the M4. As a result, the following tidal components are included:

- O1
- K1
- M2
- S2
- M4
- MS4
- M6

Tidal Component	Frequency [Hz]	Amplitude [m]	Phase [deg]
O1	0.038731	0.092857	249.751672
K1	0.041781	0.069416	33.209244
MU2	0.077689	0.127143	69.570479
N2	0.078999	0.207398	316.900349
NU2	0.079202	0.062276	309.783985
M2	0.080511	1.332152	340.624045
L2	0.082024	0.085741	353.782060
S2	0.083333	0.341235	49.930215
K2	0.083561	0.104435	46.100060
M4	0.161023	0.089852	204.134606
MS4	0.163845	0.051653	265.834301
M6	0.241534	0.051714	54.426212

Table 4.1: Tidal components with an amplitude of more than 5 cm

The river discharge applied is 325 m^3/s which is equivalent to the multiannual mean river discharge (324 m^3/s) specified by the federal authorities in 2012. Ramacher [31] stated that the average discharge at the second half of the 20th century has been 330 m^3/s. Since both discharge values are in the same order of magnitude it seems justified to assume 325 as a constant discharge value over time.

4.2. Scenario Set-Up

4.2.1. Kelvin Wave

The model set-up for the scenario Kelvin wave only differs from the base case settings by the northern open boundary condition. With the Engelund-Hansen transport formula and an alpha Bn of 7.5 the model uses bed load transport only. For the open boundary condition on the North Sea side one boundary point (BP 3) is applied at each of the boundary points. Thus, the same phase and tidal amplitude will be introduced to the model. The reflection coefficient remains the same in order to produce comparable results. The simulation period is ten years of hydrodynamics with a MORFAC of 400.

4.2.2. Coriolis

The model set-up for the scenario Coriolis does not differ from the base case settings except that the latitude is set to zero. By changing the latitude to zero, the horizontal component of the Coriolis force is zero as well, since it is normal to the earths surface. As for the base case, the transport formula is chosen according to Engelund-Hansen, and an alpha Bn of 7.5 is applied. At the open boundary the Kelvin wave is included in order to determine the effect of Coriolis in the model domain and in order to have a clear distinction about the influences regarding Coriolis and the Kelvin wave, as seen in the previous part. Again, the simulation period is ten years of hydrodynamics accelerated with a MORFAC of 400.

4.2.3. Wave

For the wave scenario Delft 3D (D3D) is coupled with Swan [15] within the D3D-FLOW interface. The wave scenario uses the same computational grid and the according bathymetry without nesting. For the spectral resolution the directional space is defined circular with 36 directional sections. The frequency space ranges from 0.05 Hz till 1 Hz with 24 frequency bins in between. The hydrodynamic simulation results are considered in the wave calculation as well: Water level, current and bathymetry are used and extended. The wind gained from D3D-Flow is used but not extended. The wave boundary condition is applied for the same open boundary location on the North Sea side as in the base case. Along the open boundary, which is defined by the orientation from northwest, uniform parametric wave conditions are specified with:

Significant wave height	1.2 [m]
Peak period	7 [s]
Nautical direction	300 [deg]
Directional spreading	4 [-]

Table 4.2: Wave conditions along the open boundary

Furthermore, physical parameters are defined for the wave scenario: The constants are mainly set according to default values, a 3rd generation mode for the physics is applied, considering depth-induced breaking (with alpha = 1 and gamma = 0.73) and bottom friction according to JONSWAP with a coefficient of 0.067. Further processes that are included in the calculations are wind growth and whitecapping (according to Komen et al.). For the wave propagation in the spectral space refraction and frequency shift are enabled. Additionally, for numerical parameters the D3D-Swan default values are used and the wave output for the computational grid of D3D-Flow is generated with an interval of 60 min.

4.2.4. Extreme River Discharge

The differences in the model settings are trivial in comparison to the base case. Since the amount of river discharge is the only difference, only the .bct file needs to be adapted. Instead of 325 m^3/s constant over time now 2000 m^3/s are defined as the steady discharge. All other model settings are kept as indicated at the base case: The transport formula according to Engelund-Hansen, an alpha Bn of 7.5, a simulation period of ten years of hydrodynamics and an acceleration for the morphodynamics with a MORFAC of 400.

4.2.5. No River Discharge

The set-up for the scenario no river discharge is the same as for the extreme river discharge scenario, except that in this case there is a river discharge of zero assigned to the southern boundary condition. As the other scenarios presented before this scenario uses the Engelund-Hansen transport formula and an alpha Bn of

7.5. The simulation period is ten years of hydrodynamics as well and the morphodynamics are accelerated with a MORFAC of 400.

4.2.6. Increased Tidal Range

For this model set-up the amplitude of the tidal components at the open boundary on the North Sea side needs to be adapted to the scenario conditions. Since the open boundary condition is composed of multiple tidal components, a solid factor cannot just be added to a time series or an individual tidal component, because that would manipulate the result in a too artificial way. Additionally, the increased tidal range should be somehow realistic in order to get schematic but realistic results. Here, inspiration is gained from the determination of the significant wave height in order to develop a way to meet the previously described criteria for an increased tidal range. The idea is to look at the time series from the JWE model that has been taken to perform the analysis of the tidal components. From the time series the mean tidal range (TR_{mean}) is calculated. Afterwards, the tidal range of each tidal cycle in that time series is taken and analyzed. The tidal ranges are sorted descendant and the highest third is extracted and averaged. As mentioned, the procedure is comparable to the determination of the significant wave height. Hence, the mean highest third of the tidal range is referred to as significant tidal range (TR_{sig}). The TR_{sig} can be set in a relation with the TR_{mean} which results in a coefficient (c_{TRsig}) that can realistically represent an increase in the tidal range: $TR_{sig}/TR_{mean} \approx 1.1$. The relation can be applied in order to increase the amplitude of the tidal components by multiplying the amplitude of each tidal component individually with the coefficient c_{TRsig}. The increased amplitudes obtained are replacing the tidal amplitudes from the base case scenario in the .bca file. The phase (Kelvin wave) and arrangement of the tidal components themselves remain the same. Also all other settings like the correction coefficient of zero, the reflection coefficient of 10 000 and the sediment transport formulation according to Engelund and Hansen with an alpha Bn of 7.5 stay the same. The scenario is simulating ten years of hydrodynamics multiplied with a MORFAC of 400 as in the other scenarios as well.

4.2.7. Summary of the Scenario Introduced Changes

Scenario	Changes
Kelvin Wave	Equal phase at the open boundary
Coriolis	No Coriolis effect inside the model domain
Wave	Influence of waves added
Extreme River Discharge	Constant discharge of 2000 m³/s
No River Discharge	Constant discharge of 0 m³/s
Increased Tidal Range	Tidal range at the open boundary increased by 10 %

Table 4.3: Overview of all scenarios

4.3. Model Evaluation

As introduced in section 2.8.1 there is a need for evaluation criteria for this flat bed model of the Weser estuary, but with a distinction between the calibration and the scenario simulations. Since the scenario simulations are not aiming for a better representation, their evaluation criteria needs to be defined different from the model calibration.

4.3.1. Calibration Criteria

The calibration evaluation criteria should indicate, if a simulation is improving the representation of the historical natural state. The first and obvious choice is a visual comparison of the main features, where the two characteristic channels of the Outer Weser estuary are the most conspicuous and striking ones. Accordingly, the following criteria rise up, in order of priority:

1. Number of main tidal channels
2. Alternation Yes/No
3. Exact location
4. Depth of the channels

Firstly, the numeric comparison of the main channels in the AOI is the main criteria for evaluating the calibration simulations. Secondly, it would be a great achievement, if in general the alternation of the two main channels can be reproduced with the model. The third point would be a comparison of the location of the two channels. Taking this point into account a few uncertainties rise up due to the modeling approach chosen. As introduced in chapter 2 the Weser estuary is a highly active system. If available data (marine charts, historical maps) are compared to the simulated bathymetry results after a certain time, just two states would be compared. The disadvantage is that the areal channel location indicated on a map gives the position at one moment in time within the development of millennia. This circumstance makes it difficult to find the right moment in time of the simulation result, that represents this specific state in time. Instead of comparing the final (last time step) simulation result with the historical state, the complete simulation (all time steps) would need to be compared, in order to check if the specific state of the map is well represented at some point of the simulation. It would be a more efficient way approaching this issue the other way around: Multiple historical charts are taken and combined. From this combined maps multiple spatial locations of the two channels in time are provided for a comparison with one or a few simulation results in time. From the historical maps available three charts are selected for the processing. The maps have been selected by the criteria whether the characteristic channel pattern is clearly visible. Resulting in the maps of the years:

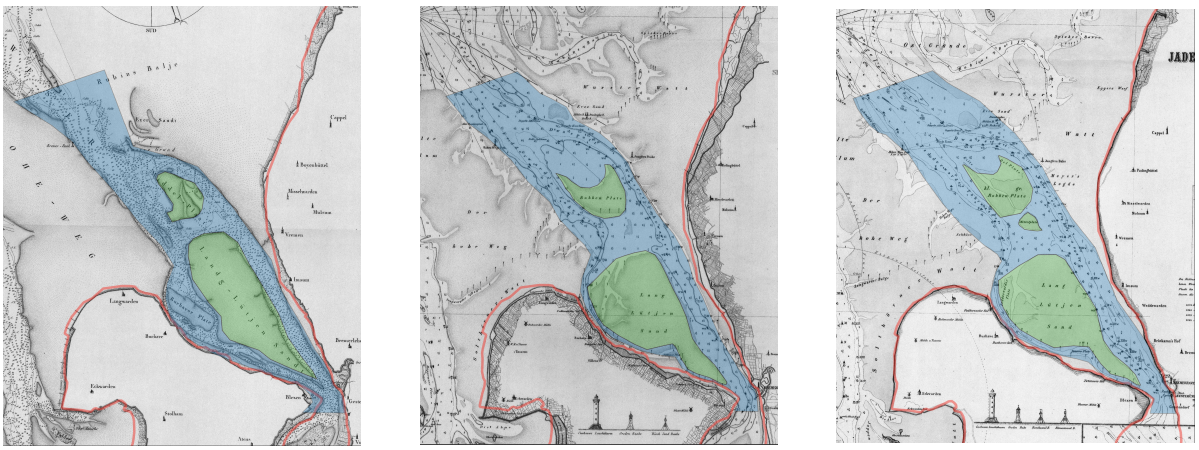

(a) 1812 (b) 1859 (c) 1870

Figure 4.6: Tidal channels (blue) and tidal flats (green) on the historical maps of 1812, 1859 and 1870

All three historical charts are imported in a GIS for further processing. The area of interest defined in 4.1 is abstracted to the historical state for each of the three maps. Within the defined historical AOI the two channels of the Weser estuary are detected and extracted. The extracted spatial channel location are then

intersected with each other. The intersectional area shows possible locations where the channels have been at the certain points in time based on the maps of 1812 (see figure A.1 appendix A), 1859 (see figure A.2 appendix A) and 1870 (see figure A.3 appendix A). This can result in a better comparability between one or a few simulation results in time with the historic reality. In order to improve the comparability, data of several centuries would be the ideal case. But available and applicable marine charts are limited to the extent of around one century. It is not seen as a main task of this project to intensively investigate alternative historical documentations which makes it necessary to find a different approach.
Another possibility is the use of other features from the AOI and from the surrounding area. Features that are represented in geographical position and size are:

- Features inside the area of interest
  - Tidal shoals between the two main channels
  - Small channel features
- Features outside the area of interest
  - The Jade bay
  - The Hohe Weg (shoal)
  - Robbensbalje (channel)

The tidal flats that are surrounded by the two main channels can be considered as a recognizable part of the outer Weser estuary. Additionally, they can be clearly recognized on all three chosen historical charts. The second item contained in the AOI features are the small channel features originating at the two main channels. Below, two of the three selected historical charts contain details about side channels that can be followed. It is a less strong representation for the area and its development in time, but it might be an additional, less important evaluation criterion in the AOI.
Furthermore, there are three other remarkable features that could be taken into account. The first and most intuitive one is the Jade bay that is included in the model domain and functions as the closest large scale tidal inlet without significant freshwater discharge [12].
Due to its clear dimensions and its constant natural state (same tidal volume for centuries and thus a sta-

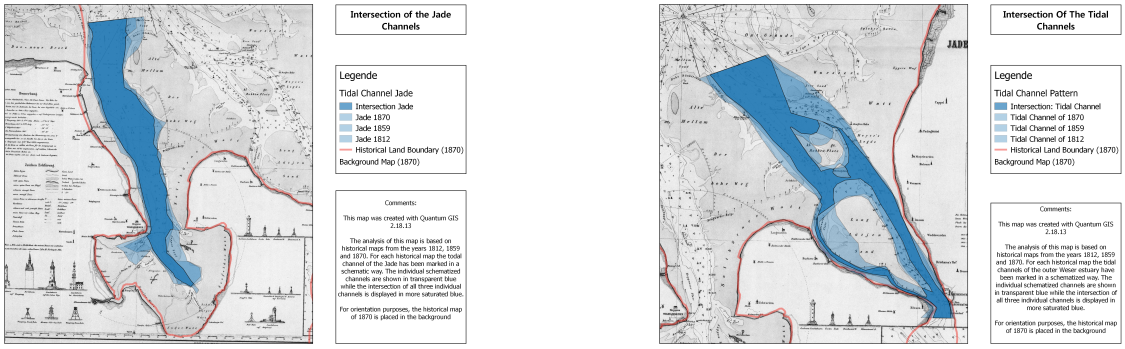

(a) Intersection of the Jade channel

(b) Intersection of the two main channels

Figure 4.7: Intersection of the Jade and the two main channels of the outer Weser from the years 1812, 1859 and 1870

ble deep tidal channel [21]) it is a feature that should be appropriately described by a representative model. As a consequence the Jade bay is added to the evaluation criteria for the calibration phase. The Hohe Weg wadden area is a tidal flat, which is surrounded by the channels of the Outer Weser estuary, the Jade bay and its channel. It is a quite highly elevated and large territory which falls dry during most of the low tides. The Hohe Weg is included in all charts and could thus be used for GIS operations. A reason for not including the Hohe Weg is that hardly any information would be added for the spatial analysis, since the two surrounding channels are already included in the evaluation process. Information beyond that were to be gained if the sediment volume of the Hohe Weg in the historical state would be compared with the volume at the end of the simulation. But here the same argumentation as in section 2.8.3 is valid. There are no digitized maps available out of which raster data could be extracted which would be needed for the necessary GIS operations. Furthermore, the Robbensbalje could be included as a calibration criterion. The set up of the model

(see section 4.1) though is unfavorable to include this root patterned tidal channel as a criterion due to the fact that the Elbe estuary has been excluded from the model. Since the Robbensbalje is located between the Elbe and the Weser estuary both have an influence on its shape and root pattern. Thus, it can not be expected that a flat bed model including only the Weser estuary could reproduce these channels up to an extent that is fulfilling the requirements of an evaluation criterion.
Lastly, the depth of the two channels can be taken as a measure of representation in the calibration process. The same disadvantages as in point three apply for this point as well: The historical charts are showing only a short moment in time. Due to the constant variations in position and depth, it is not trivial to combine the depth pattern of the three historical charts through GIS operations into a quantitative criterion. Ergo, depth will be valuably used by taking the depth patterns qualitatively. A clear distinction between channels and shoals (with respect to the depth) should be seen and the channel depth should be in the order of magnitude as indicated by the maps, around ~ 10 m.

Based on the historical charts available, the evaluation criteria for the calibration phase can be summarized into the following points, arranged according to importance:

1. Number of channels
2. Alternation visible
3. Location of features
   (a) Two main tidal channels
   (b) Small channel features
   (c) Tidal shoals between the main channels
   (d) The Jade bay (incl. dimensions)
4. Depth of the main channels (qualitatively)

4.3.2. Scenario Criteria

As stated in subsection 2.8.4 there are evaluation criteria that can be applied for the Weser estuary as well.

Obviously, the visual comparison of the result files at different points in time is a necessary criterion in order to get a feeling for the differences between the various scenarios. Since visual inspection and getting a feeling for differences are not easily quantified, other methods should be included as well.

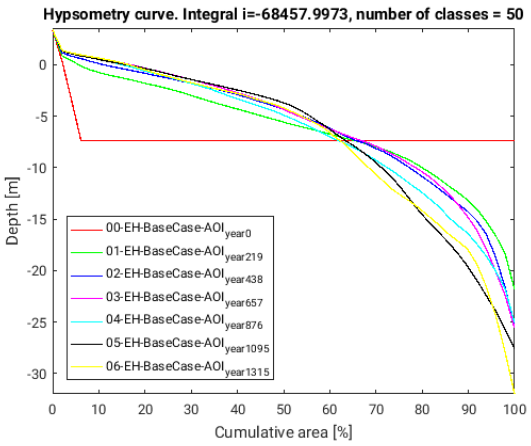

Figure 4.8: Example of a hypsometric graph for different points in time, plotted in one figure to see the development over time.

The Hypsometry The hypsometry is nothing to include in the calibration process due to the incompatibility of the simplified calibration runs with reality (either historical or present). But for the scenario analysis the hypsometry can indicate firstly, when the simulation has reached any kind of equilibrium and secondly, how the configurations made in the dedicated scenario influenced the development of the overall depth patterns. It can be applied to the whole model domain and additionally for a user defined area where the hypsometry could show more sensitive analysis of local results. More insight can be gained when looking at the hypsometry development over time. As an example the hypsometry of one case can be plotted at different stages in time into one plot. By the changes of the lines in the graph it can be investigated how the distribution of depth contours developed over time (see figure 4.8). However, as soon as there are more than five or six lines the graph starts to get less intuitive regarding readability. Consequently, a clearer graph should show the hypsometry development in time. Here, the same idea as used in the Hovmöller diagram or a so called Heat Map is adapted. It shows matrix data where the individual values of the matrix are represented by colors. Time can be seen on the x-axis, the percentage of cumulative area on the y-axis and with the depth values itself represented by colors. An example for this representation can be found in figure 4.9.

Standard Morphodynamic Evaluation Methods The RMSE and the BSS are two measures which are not easy applicable nor of major significance for the analysis of the simulations done in this project. Using the RMSE as a scenario evaluation criterion would result in one value that represents the root-mean-square of topographic differences between a scenario and the base case scenario. It is questionable whether in such simplified and abstract case studies a RMSE adds extra information in a qualitative better way then the hypsometry. As discussed in subsection 2.8.2 the BSS would not result in useful outcomes due to its double penalty (see subsection 2.8.2). Furthermore, applying the scale selective skill score as proposed by Bosboom [3] would overcome the problematic double penalty, but would not be useful. Skill scores, as they are discussed here, describe the similarities between two different outputs and set them in relation to the initial stage. Usually, measurements are compared with simulation results. In the Scenario evaluations basic simulations are compared with the scenario simulations and it is not the principal goal to make the simulations as resembling to each other as possible. The main information that could be attained through a skill score would be how much the scenarios differ from the base case in the sense of bathymetric changes. Taking into account the significant morphological activities in the Outer Weser estuary, it is expected that it will be unlikely to get valuable results by comparing two stages in time of two different simulations by means of a skill score. Consequently, no skill scores will be applied at the scenario evaluation.
Two more methods were used by van der Wegen [39] to show the modeling results for his case study: A figure indicating the depth (averaged over the complete model domain) over time and the width averaged depth along the estuary axis. The latter does not seem to be useful for this project since the focus does not take the whole estuary into account but the AOI. The width average plot could be adapted for the AOI but in order to not overshoot the scope of the project with various figures which do not add significant value to the analysis, it has been decided to disregard this method. Furthermore, the average depth over time is somehow repre-

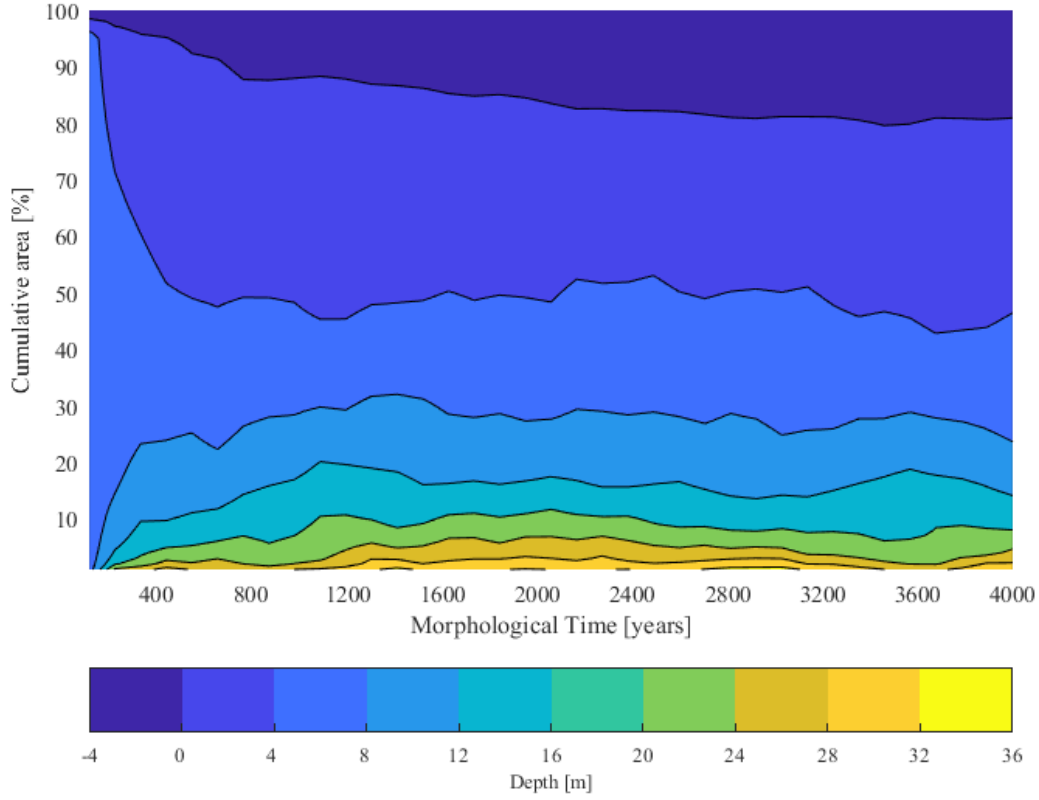

Figure 4.9: Example of the hypsometry over time (here for the AOI in the base case)

sented by the hypsometric plots, but it might be a good measure to compare the different scenarios with each other. In that case, the method would be applied to the AOI with all cases at the same time to get a valuable comparison.

Developed Evaluation Methods Additionally, a measure needs to be found that can give some clear analysis about the existence of two channels (when they are present) and about the alternation pattern. The idea is to extract a specific cross-section ($CS_{X(s)}$; $s = [1, m]$, where m is the spatial extent of the cross-sectional axis) in the AOI and analyze its development in time (CS_X^t; $t = [0, n]$, where n is the simulated time span). The cross-section chosen should be located inside the AOI and should be, as far as possible, representative for all cross-sections that show the two channel system pattern. Two mentionable analysis tools are developed, one scientifically intuitive and one working with user introduced definitions.

Evaluation Method 1 The user defined tool (called Method 1 in the following) analyzes the development of the cross-section CS_X in time for each time step individually $CS_X^{t=1}$, $CS_X^{t=2}$, ..., $CS_X^{t=n}$ by user induced criteria. The aim is to get the following results for each cross-section in time CS_X^t: The number of main tidal channels, their depth and location and the identification of the dominant channel in depth and position. However, besides the determination of minima and maxima which is a straight forward process, it is a relatively complicated process to distinguish the main channels from artifacts that are part of a channel rather than a channel itself and thus should not be considered. It needs a number of user introduced definitions for the dimensions and characteristics of channels, shoals or channel dividing elements that can be converted into conditional statement in order to be applicable in the analysis. Still, when criteria and conditions are included in the analysis there are data gaps that are resulting from the criteria fulfilled in time step $CS_X^{t_1}$ and

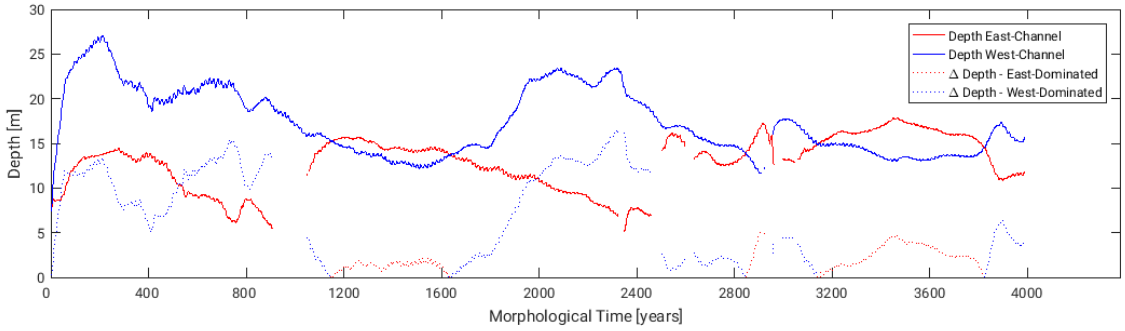

Figure 4.10: Example of an output graph from Method 1, where the user defines conditions for the analysis

not fulfilled in $CS_X^{t_2}$ as can be seen in figure 4.10 ($CS_X^{t=950}$ to $CS_X^{t=1000}$).

Evaluation Method 2 A clearer and relatively simple method (see figure 4.11 for a schematic explanation) is to plot the chosen cross-section CS_X (figure B.4) over time (called Method 2 in the following). In the resulting figure the development of channels and shoals can be spotted. Due to the chronological order of the cross-section (from $CS_X^{t=1}$ to $CS_X^{t=n}$) spatial shifts of the deepest point and the general depth contours along the cross-sectional axis ($CS_{X(s=1)}$ to $CS_{X(s=m)}$) can easily be determined (see example figure 4.11 and point 2 on the schematic example of figure 4.11). This breakdown enables the extraction of a set of remarkable cross-section cases (point 3 in figure 4.11) from different points in time (i.e. $CS_X^{t=300}$(base case), $CS_X^{t=2200}$(base case), ...). Each case describes a cross-section situation that in its characteristics is representative for a typical channel and shoal pattern of that area in time (point 4 in figure 4.11). By correlating the set of cases (i.e. for Cross-Section 75 shown in table 4.4) with the cross-section at each individual temporal state ($CS_X^{t=1}$, $CS_X^{t=2}$, ..., $CS_X^{t=n}$) the cross-sectional development in time can be related to the different main cross-sectional depth contours that can be expected to occur (point 5 in figure 4.11). This figure can be used to define the recurrent pattern, which can be extracted and converted into a time sample. The temporal centers of a recurrent patterns can be taken as the temporal samples for the patterns for example. The samples then can function as the input values (more specifically as y-input together with x-input that ranges from 1 until the number of samples) for a linear regression. By means of the linear regression, that is calculated from the temporal sampling a initiation value and a slope factor can be gained. The initiation value is not of interest, whereas the slope factor indicates the period of sample occurrence and thus can be taken as the period that is assigned to the alternation pattern observed.

Case	Cross-Section	Time Step	Source Run	Description		
				No. of Channels	Dominance	Extend
1	75	300	Base Case	2	West	Narrow
2	75	2200	Base Case	1	West	Narrow
3	75	1000	Base Case	1	West	Wide
4	75	920	Incr. Tidal Range	2	Equal	Wide
5	75	1600	Base Case	2	Equal	Small Hump
6	75	2100	No Coriolis	3	Equal	Wide
7	75	350	Wave	2	East	Narrow
8	75	2250	Incr. Tidal Range	1	East	Narrow
9	75	3400	Base Case	1	East	Wide

Table 4.4: Cases and their sources for cross-section 75

The correlation coefficients resulting from the correlation analysis are compared with each other for each temporal state of the cross-section. A higher correlation coefficient represents a higher match with the according standard case, where a value of one is a match of 100 % (the two compared cross-sections would be

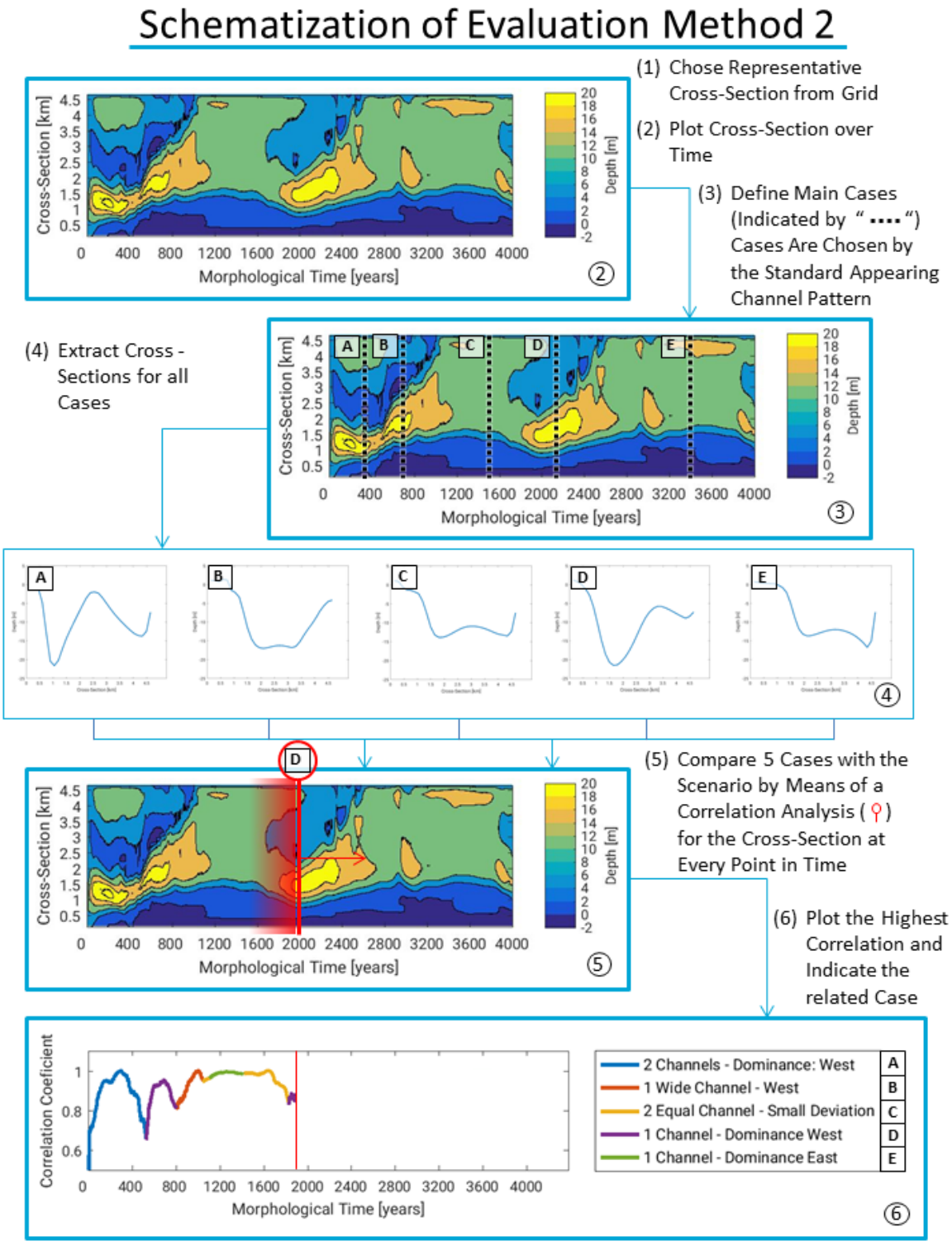

Figure 4.11: schematic explanation of EM2

equal). Thus, the best representation is reached when the correlation coefficient is close to one. This way, by taking the maximum correlation coefficient of the set of comparisons, the best matching case is determined for the given cross-section CS_X at one point in time. Continuing this process for each time step including the extraction of the best matching case respectively, results in the final figure where for each temporal state of the cross-section the best fitting case is indicated, including the correlation coefficient. Consequently, the figure shows at which temporal periods which channels are present, which are dominant and which spatial properties they have. The correlation coefficient itself indicates how close the cross-section at a certain time step is to the best matching case regarding depth contours.
Combined with the other evaluation criteria mentioned in this paragraph the scenario simulations can be analyzed and compared to the base case which will be shown in chapter 6.

Conceptual Figure Combining Activity and Dominance So far evaluation methods have been defined and described that can be used in order to analyze the different scenarios individually and to compare the results at the end. But what is not developed, yet, is an evaluation method that combines the previously gained results in a simple and compact way so that a comparison of the result can be made more intuitively. By combining the results new relations might be revealed that could be beneficial for the understanding and interpretation of the results.
Based on the two previously defined research questions, the channel dominance within the two channel system and the alternation of this dominance are two criteria which could be applied when creating a summarizing figure. The idea is to have a channel dominance indication on the x-axis and an alternation indication on the y-axis. Since it can be expected that not all cases will show a variation between eastern and western dominance, a method needs to be developed that can track the alternation activities, even when a "complete" (eastern - western - eastern) alternation cycle might be absent. The alternation period which is assigned to each scenario according to EM2 could be a parameter that is representing the recurrent patterns. But, due to the fact, that the alternation period does not indicate, if there is for example an alternation between eastern and western dominance or between eastern and equal dominance, the assigned alternation period does not seem to give enough information about the different kinds of variations. Consequently, the y-axis parameter should be linked to the alternation, but should not be the alternation itself. In order to overcome these difficulties advantage can be taken of the correlation analysis within EM2. It is the idea to use the number of changes between the highest correlation cases over time. The underlying assumption is that the number of changes is higher, when the channel dominance is shifting from eastern to western, compared to a case, where equal dominance is turned in western dominance for example. Thus, the y-axis shows the channel activity from *stable* (no changes) with no change of the highest correlation case until *active* (high number of changes) with an user defined value of 40, which is chosen according to the maximum number of changes observed. The upper limit 40 also represents a change of the most correlated case in less than every 100 morphodynamic years (1/4 hydrodynamic year). To keep the scenarios comparable, the counting of changes starts after the morphological equilibrium is reached. For the x-axis the overall dominance is taken, gained from the determination analysis. Hereby, the x-axis has three states (western dominance, equal dominance and eastern dominance) and ranges from -1 to 1. Here, -1 represents 100 % of western domination whereas a value of 1 stands for 100 % eastern domination and a value of 0 means 100 % of equal domination. The according dominance for each scenario is calculated the following way:

$$Dominance_{relative,overall} = \Sigma[R^2_7(rel), R^2_8(rel), R^2_9(rel)] - \Sigma[R^2_1(rel), R^2_2(rel), R^2_3(rel)] \tag{4.1}$$

with

$$R^2_n(rel) = \frac{R^2_n}{\Sigma(R^2_1, R^2_2, ..., R^2_9)} \tag{4.2}$$

By summing up the relative determination coefficients 4.3.2 of case 7, 8 and 9 for a given scenario, the relative value of western domination is gained, since these three cases are representing different states of western dominance. Performing the same addition for the cases 1, 2 and 3 of the same scenario, leads to the relative value for the eastern dominance. Subtracting the relative eastern dominance value from the relative western dominance value 4.3.2 results in the overall domination value for the given scenario and can be plotted together.

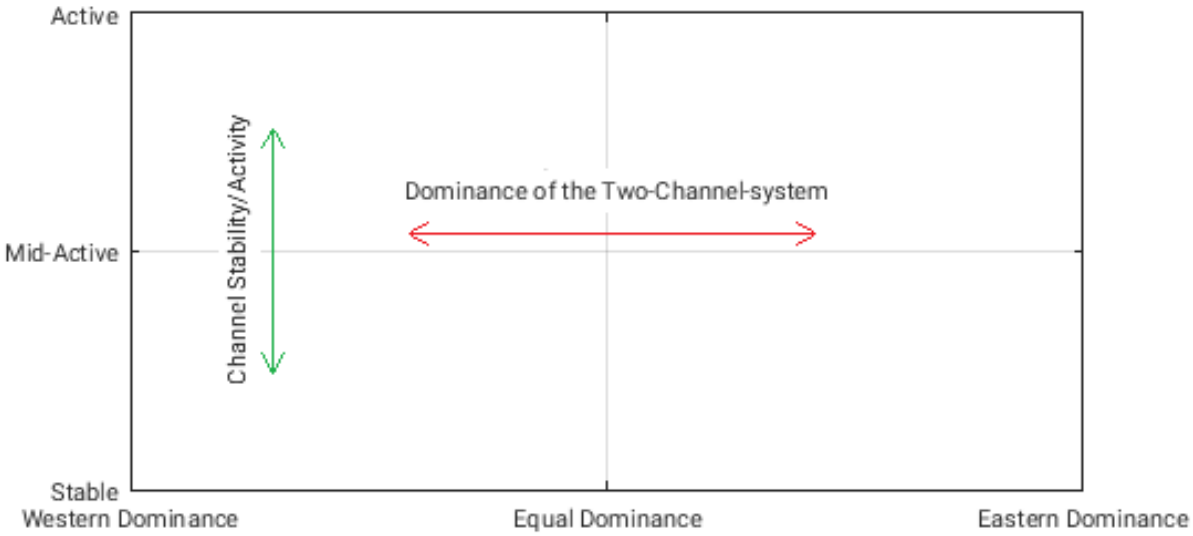

Figure 4.12: Idea of the conceptual figure for the comparison of all simulations

4.4. Data and Sources

Data No.	Description	Source
D1	Sediment data and spatial distribution of sediments	WSA Bremerhaven and BSH, Postprocessing method based on Milbradt 2015
D2	Bathymetrical data	Functional Geoinformation Model Smile Consult, processing method based on Milbradt 2015, meta data: German authorities
D3	Wind and wave data of the German Bight	Publications BAW 2012
D4	Tidal data	JWE-Model BAW

Table 4.5: Data sources that have been applied

5

Calibration

In order to gain a a model that is representative for the historical state during the calibration more than 150 simulations (see run table in the digital appendix) have been performed. The result is the base case simulation, which is presented in the next chapter.

5.1. Application of Calibration Criteria

In chapter 4 the model evaluation criteria were derived for the calibration. Four criteria were defined:

1. Number of channels
2. Alternation
3. Location of features
4. Depth inside the channels

Number of channels The most important criteria is that in the base case two channels should develop. As seen in section 2.2 the channels that are aimed to be modeled are morphologically very active and thus do not need to be stable in time, but they should be a feature that appears recurrently. During the calibration process multiple model set-ups led to the development of two channels, as indicated below in figure 5.1.

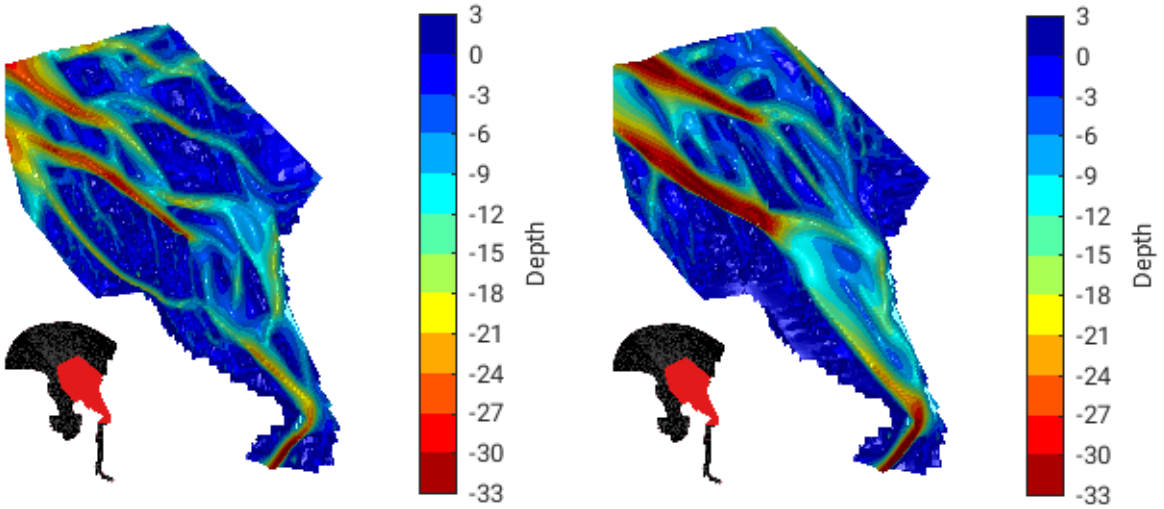

(a) Bathymetry at t = 650

(b) Bathymetry at t = 2150

Figure 5.1: Two examples of a two channel system developed in the AOI of the outer Weser

Alternation The second criterion that has been defined and that is essential for the investigation of this project is the alternation of the deepest / most dominant channel. The alternation can be shown by plotting a number of bathymetries at different points in time, where the western channel and the eastern channel are dominant recurrently. After the morphological equilibrium develops first a western dominance governs the

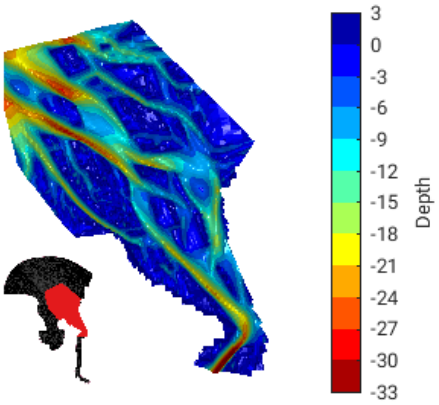

(a) Dominance of the western channel (after the spin-up time)

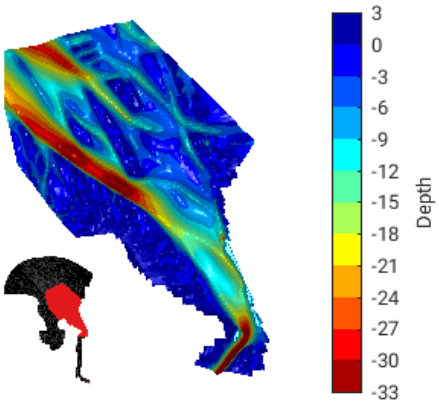

(b) Equal dominance with a tendency towards east (after almost 1500 morphological years (MY))

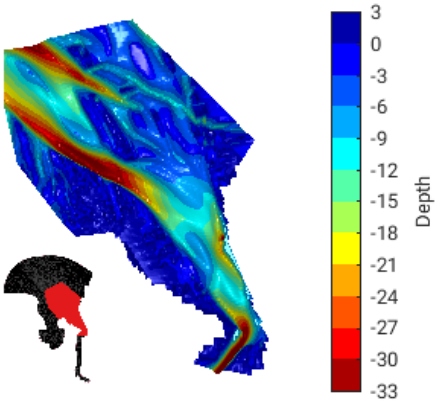

(c) Eastern dominance (after 1800 MY)

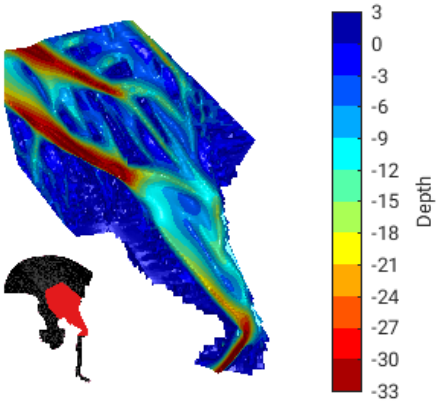

(d) Western dominance (after 2150 MY)

Figure 5.2: Four bathymetries that indicate the alternation as a calibration criterion

AOI for quite some time as indicated in plot (a) of figure 5.2. As revealed by plot (b) further in time the channel depths change in such a way, that the eastern channel gains depth, until it is generally deeper than the almost disappeared western channel (c). Lastly, after a relatively short time, the western channel gains depth again. This recurrent pattern can be observed multiple times, but will be shown and analyzed in chapter 6.

Location of features In chapter 4 two different morphological features have been defined that are aimed to be represented in dimension and location: The Jade Bay and the two channels of the Outer Weser. The following figures show the comparison of the historical channel location that have been processed with GIS and the best representation that has been achieved during the calibration process.

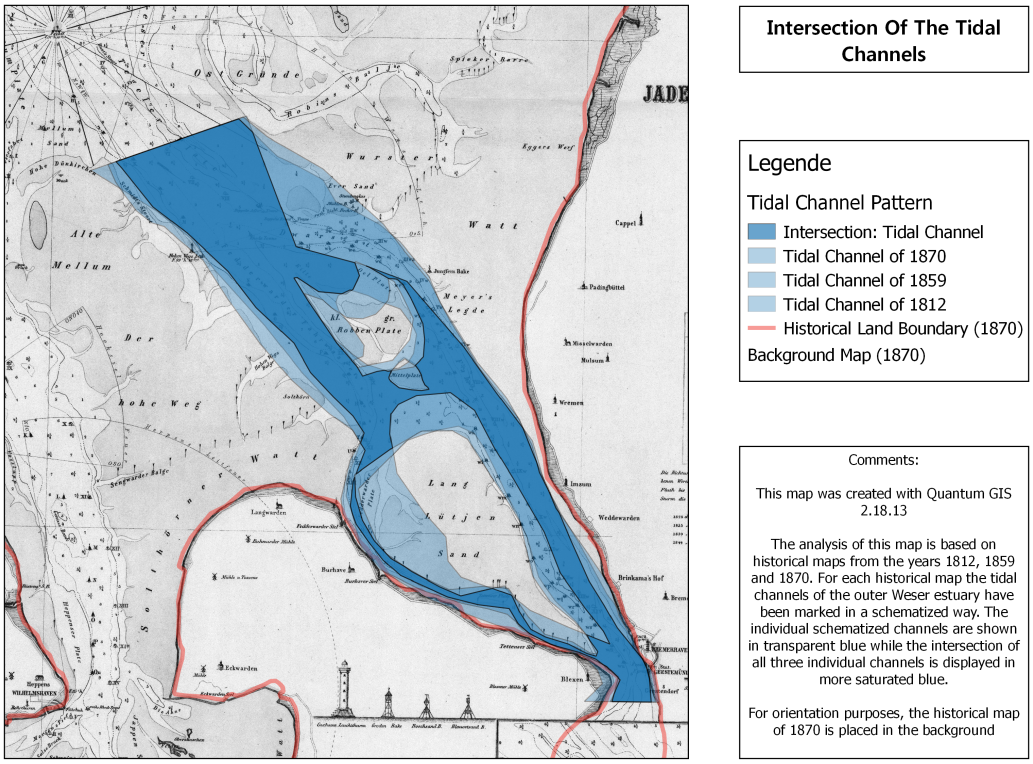

(a) Intersection of the historical channel locations in the outer Weser

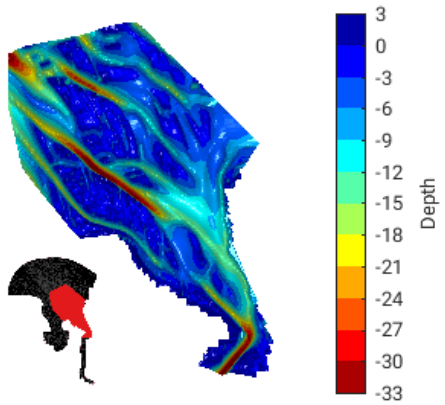

(b) Bathymetry at t = 365

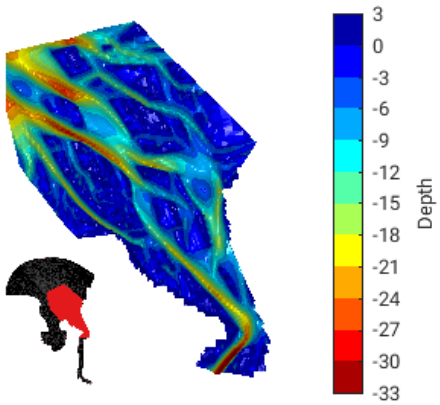

(c) Bathymetry at t = 695

Figure 5.3: Two examples of dimension and location in the AOI of the outer Weser

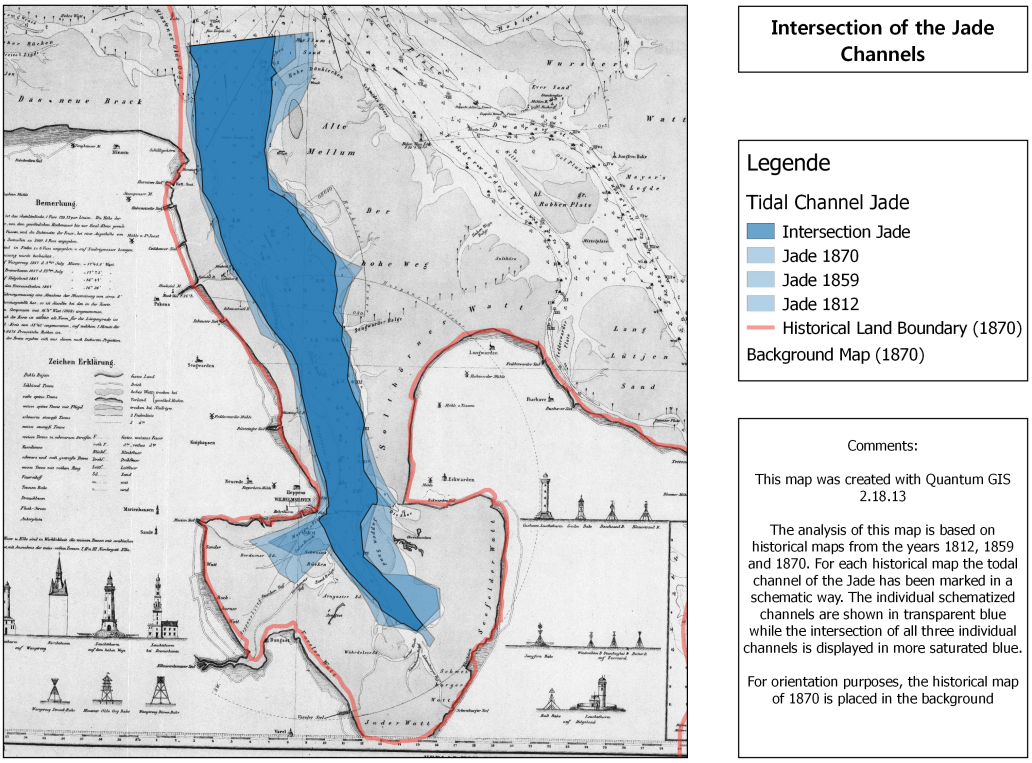

(a) Intersection of the historical channel location in the Jade Bay

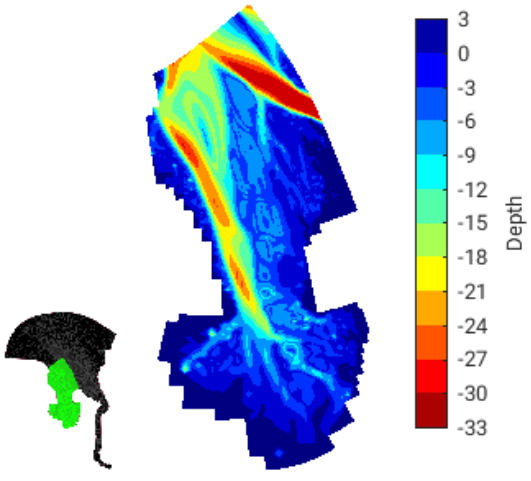

(b) Bathymetry at t = 2000

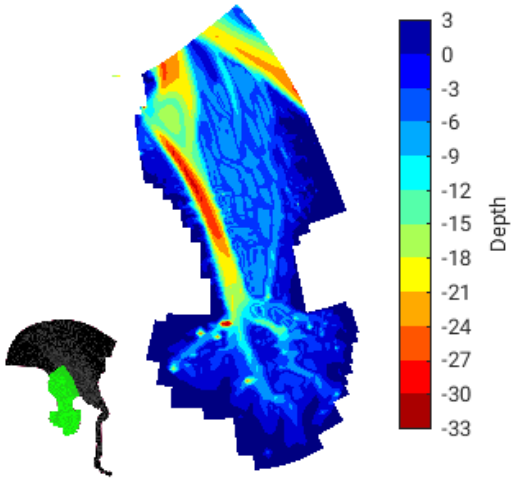

(c) Bathymetry at t = 3000

Figure 5.4: Two examples of dimension and location in the AOI of the Jade Bay

In the Outer Weser the channels that are indicated on the historical map are not matching comprehensively with the channels that can be seen in the simulation results. Especially, the channel that is surrounding the southern tidal flat of the Langlütjensand in the west and is relatively narrow is not represented by the model. Instead the model indicates two channels that are progressing north/northwestwards more parallel. Most of the time, the two channels are better represented in the north of the funnel shaped part of the AOI whereas in the southern part the western channel is less accurately represented. Generally, the eastern channel is matching well with the locations that are indicated by the historical maps. The presence of two tidal flats in

between the two channels that have been present in the natural historical state, can be found in most of the time in the model as well.
The Jade is represented very well by the model. In the theory part the Jade channel approaching the Jade Bay has been described as being a naturally deep channel and can be found in the simulation as well. Especially after more than 1000 MY a stable channel develops that is in location and dimension as indicated by the historical maps (see figure 5.4)

Depth Inside the Channels The depth representation is the last criterion of the calibration catalog. Generally, the depths in the channels that are forming in the simulations are overestimated by an order of magnitude. Due to the limited time in this project, this criterion (as it has been defined as the last important one) has not been included in the calibration process intensively.

5.2. Parameter Study

According to the modeling concept, as many processes as possible were excluded from the model. For the base case simulation only sediment transport has been enabled as a process that is included next to the hydrodynamics. Following the approach of simplification and schematization, next to the model simplifications that have been applied according to chapter 4, as many default settings as possible have been applied in the initial configurations. As an exception the roughness predictor after van Rijn 2007 is included for adjusting the roughness in the model domain. The roughness predictor parameters are taken from a well calibrated Outer Weser model that has been set up by MARUM [13] and can be found in the digital appendix. Additionally, as another simplification, due to the computational efficiency and reasonability of the results, the transport formula after Engelund and Hansen [8] has been applied, that is only considering bed load transport. Table 5.1 is giving an overview about the parameters that have been calibrated and about the values that have been found to be most representative.

Category	Calibration Parameter	Value	Unit
General Settings			
	Latitude	53	degrees
	Time Step	0.5	minutes
Hydrodynamics			
	Reflection Coefficient	10 000	[-]
Morphodynamics			
	Alpha Bn	7.5	[-]
	MORFAC	400	[-]
	wetslope	0.5	[-]
	avaltime	1440	minutes
Transport Formula			
	Calibration Coefficient	15	[-]
	bed roughness (dummy)	0.01	[-]
Sediment			
	Grain Size	200	μm
	Sediment depth	35	m
Roughness Predictor			
	Trtrou	# Y#	
	Trtdef	# vanrijn04.trt#	
	Trtu	# trtuv_ MP.inp#	
	Trtv	# trtuv_ MP.inp#	
	TrtDt	4	minutes
	Chezy	# Y#	
	Rough	# Y#	
	BdfRou	# vanrijn07#	
	BdfRpC	1	
	BdfRpR	0	

Table 5.1: Parameters of the Calibration

Courant Number The time step indicated in table 5.1 has been determined and validated by the courant criterion. It indicates a stable time step for a given numerical scheme under consideration of the flow velocities and the spatial grid cell resolution. For the standard implemented scheme in Delft 3D the courant number should not be above 10 in order to have a stable and reasonable simulation. Figure 5.5 indicates the courant number that has been calculated with QUICKIN in order to check the numerical stability of the generated grid in combination with the initial bathymetry.

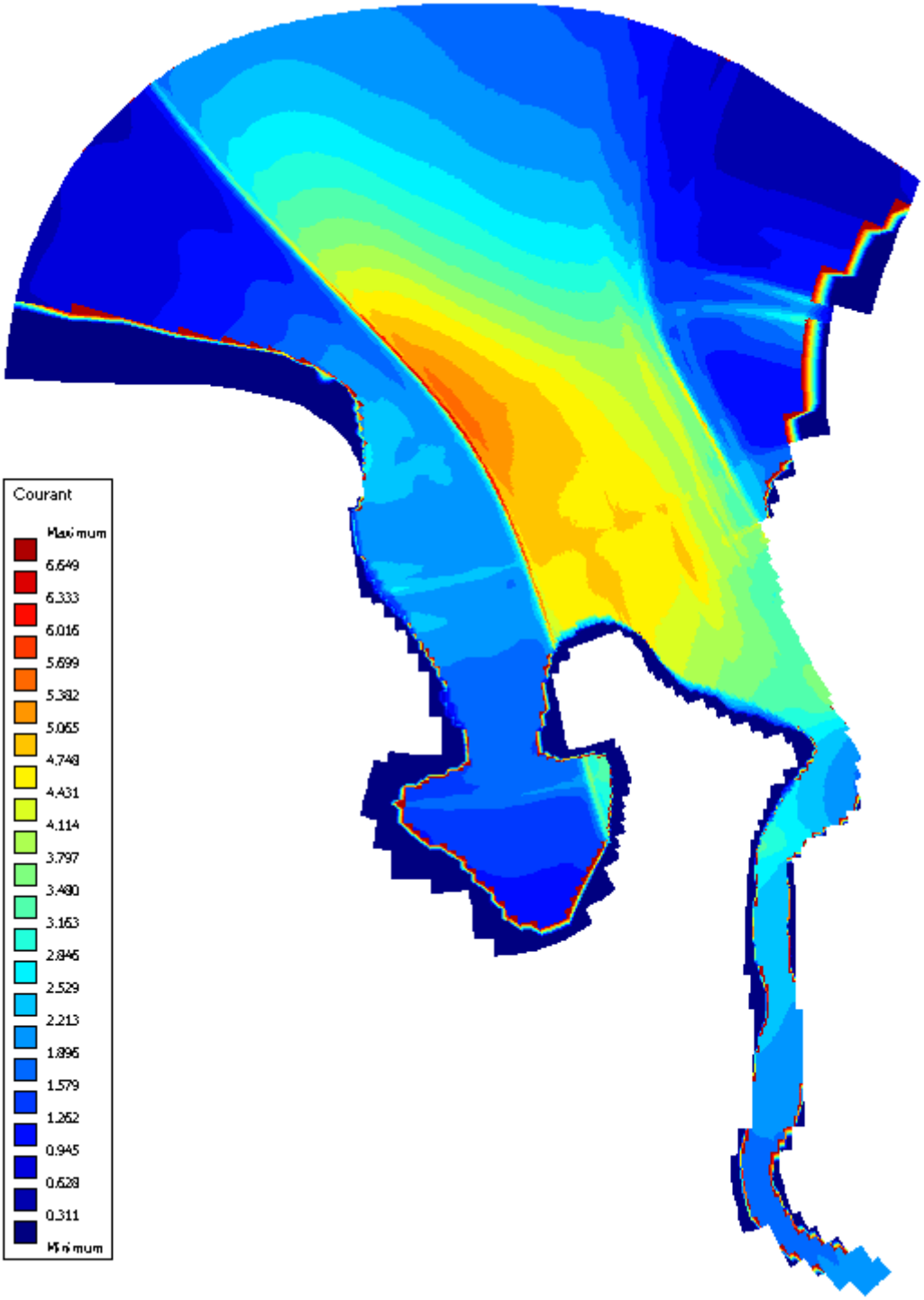

Figure 5.5: Courant number calculated with QUICKIN for a time step of 0.5 minutes

5.3. Simulation M2

M2: Line of Reasoning The aim of the calibration is to develop a model that represents the schematic morphological behavior of the Outer Weser estuary in its natural state as accurate and simple at the same time as possible. One of the most important aspects that should be represented is the alternation between the two channels that have been present in the historical natural state (see chapter 1). In case a model that takes several tidal components as external forcing is representing a cyclic behavior, there is the possibility that these cyclic motions are numerically induced by model induced overtides, which do not represent natural processes. An easy way of ensure that the cyclic behavior is due to the natural forcing of the tides the most significant tidal component can be taken as the only tidal component that is forcing the model. If the cyclic patterns are still visible, they are not artificially induced by the model. Consequently a simulation is started that has the identical set-up as the calibrated model with the exception that the M2 tidal component is the only tidal forcing.

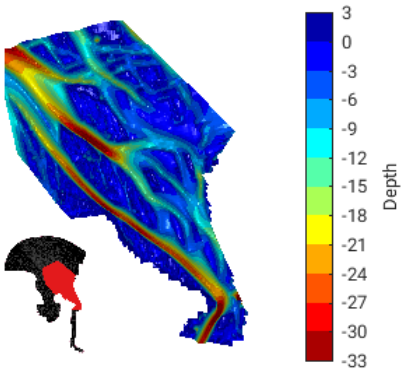

(a) Bathymetry at t = 700

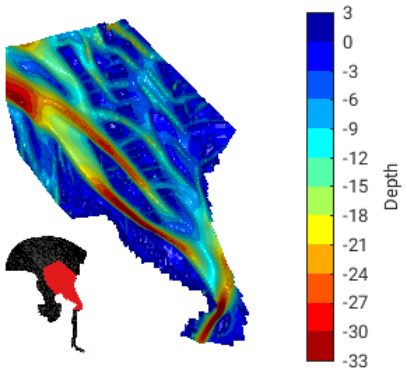

(b) Bathymetry at t = 1200

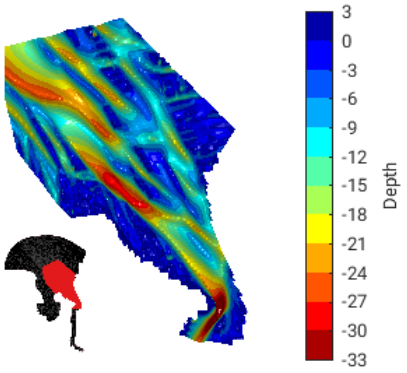

(c) Bathymetry at t = 2000

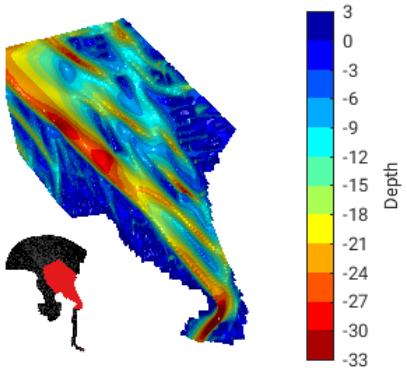

(d) Bathymetry at t = 2800

Figure 5.6: M2: Channel and shoal development over time. A two channel system develops including an alternation of the deepest channel (compare (a) - (b) - (c))

M2: Results When looking at the results of the M2 Simulation the focus lies on the alternation pattern as described in the latter subsection. Consequently the results and the simulation results will generally be discusses briefly and all analysis will focus on the detection of recurrent alternation pattern. Figure 5.6 shows the developed bathymetry at four different points in time. Without looking at the general development of the channels that are approaching the AOI from the North Sea side, a few observation can be made:

There are two channels for most of the cases

At plot (a) there is one deep western channel while the eastern channel has hardly developed yet

Plot (b) reveals an eastern channel that is deeper in the southern part of the funnel shaped area of the AOI than the western channel

In the northern part of the funnel shaped area of the AOI the western channel has a larger depth than the eastern channel

Plot (c) shows almost the opposite, since the western channel is deeper at the southern split, whereas the eastern channel is slightly deeper at the northern junction

In the last plot (d) there are two channels which are most of the time equally deep except for the southern part close to the bend into the Lower Weser where the western channel shows larger depths

The described channel development in the AOI over time indicates morphodynamic activities showing at least one alternation cycle during the simulation period. In order to ensure the alternation the first plot of EM2 is presented in figure 5.7. The plot of cross-section 75 over time reveals the development of two channels within the cross-section one on the western side (the yellow part more towards the bottom of the figure) and one on the eastern side (yellow-orange parts more at the top of the contour plot). During the spin-up phase a channel develops on the western side that after 800 MY migrates towards the middle of the cross-section. Around 1000 MY it splits into two channels where the eastern channel in the following centuries of morphodynamic development gains depth whereas the western channel remains at its depth of the morphological time point of 1000. At around 1600 MY the eastern channel decreases in depth, where the western channel gains depth significantly. This situation remains the same for more than a millennium until the eastern channel gains depth again until the end of the simulation period and the western channel remains at the former depth.
Summarizing the analysis of the figure 5.6 and 5.7 it can be concluded that the M2 simulation has an alternation pattern and consequently proves that these are not caused by model induced overtides.

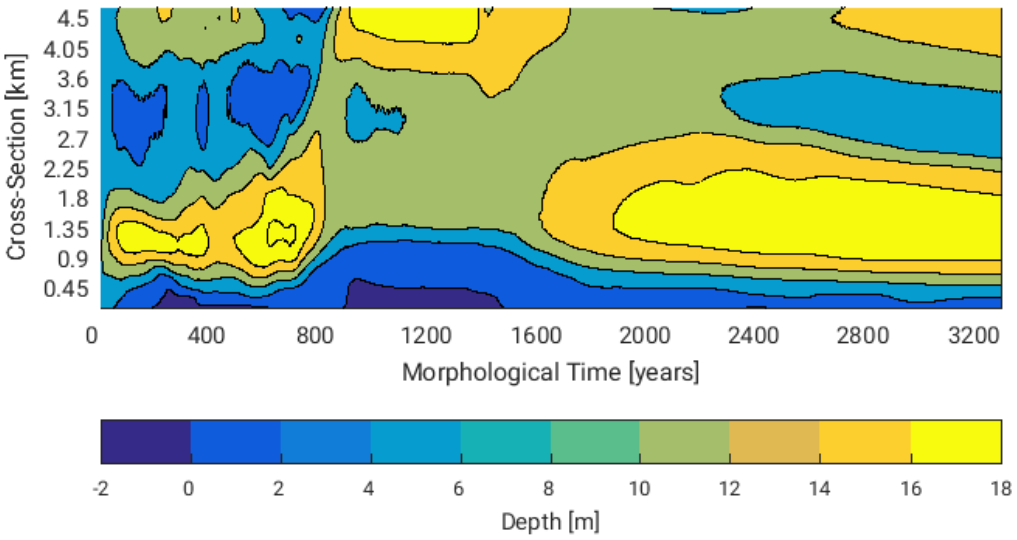

Figure 5.7: M2: Cross-Section 75 over time, revealing the development of the two channels over time and an alternation

5.4. Influence of the Initial Bathymetry

The influence of the initial bathymetry on the simulation results has been tested in order to ensure that the development of tidal channels and shoals is not induced by the predefined initial depth. Throughout the simulation various initial depth versions have been applied, aiming for a faster development of channel and a less damped propagation of the tidal wave through the model domain. Two exemplary results are shown in appendix C. All simulations revealed, that there is hardly any influence of the initial bathymetry visible on the long term morphodynamic result. In some cases the development of shoals and channels is enhanced, but the long term results remains the same. At the end, as indicated in section 4.1, it has been decided to apply the most reasonable depth distribution as an initial bathymetry, by applying the same depth pattern in the whole model domain, except at the land boundaries.

5.5. Modeling Recommendations

With a powerful process based model like Delft 3D it is possible to get an idea of the processes that area shaping an estuary, but a model cannot claim to represent reality in all its complexity [34]. However, every numerical model aim to create a virtual reality by trying to reproduce all processes included as detailed as possible [34]. This intention applies for this project as well.

Within this project the process based model has been calibrated up to a certain level. But, due to the limitation in time, there is still potential for improvements on the model itself, including the consideration of additional processes and the comprehensive calibration of model parameters. Apart from many other numerical parameters that could be calibrated more intensively, four suggestions will be given about aspects that have the highest potential to improve the model results.

Multi-Fraction The first and most important aspect is to include multi-fractional sediment. In the current simulation set-up just one sediment fraction has been considered. The presence and distribution of sediment in the Outer Weser estuary can have a significant influence on the development of channel and shoals: More coarse sediment located inside tidal channels could prevent further erosion in there, while more fine sediment could result in deeper channels and in the development of more extensive tidal flats in areas with low flow velocities. The latter case has been tested in order to determine the effect that a mixture of $\frac{1}{3}$ mud (50 μm) and $\frac{2}{3}$ fine sand (200 μm) would have on the development of channels and shoals:

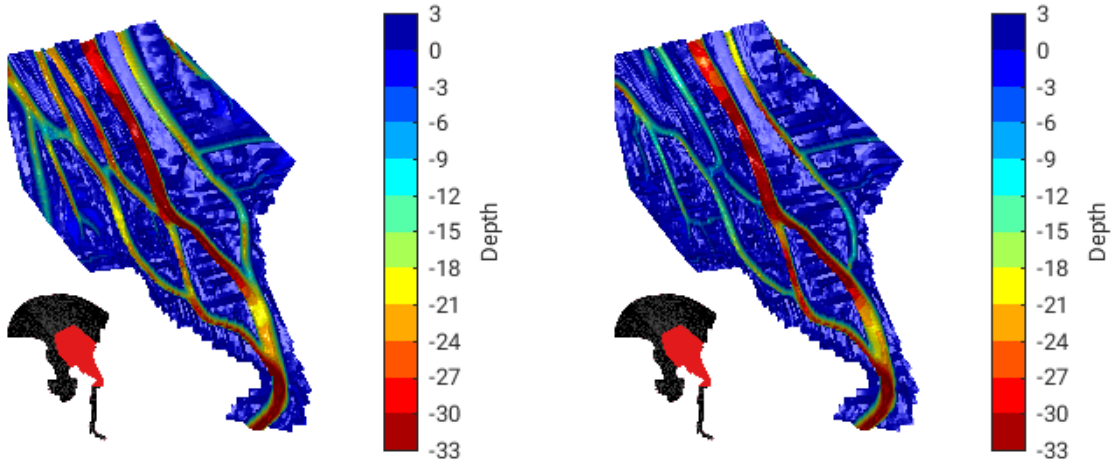

(a) Bathymetry at t = 800

(b) Bathymetry at t = 2000

Figure 5.8: Two examples of the bathymetrical result from a multi-fraction simulation - very stable, narrow and deep channels develop.

The conclusions, that might be derived from the multi-fraction simulation results shown above, should be treated with care, since this simulation has some salients that occur after a certain time are not necessarily numerically induced. It is assumed that the irregularities are related to the missing calibration and fine tuning of this set-up. Thus, only the first 2000 MY are presented, where the morphological development is reasonable. Within this first 200 MY a very clear development of channel and shoals can be seen. The arrangement of channels in the funnel shaped part of the Outer Weser shows some pattern that is missing in the current base case simulation so far. An example is the orientation and location of the western channel, that is surprisingly well represented in this simulation in comparison to the base case simulation. Another aspect is the distinct separation of channels and shoals that are developing fast and do not change much in time. As expected, the addition of mud deepens the channels significantly. An alternation is not visible in this uncalibrated multi-fraction simulation.

Hydrodynamics A second option that could increase the accuracy of the model results would be a more detailed calibration and a validation of the hydrodynamics. As indicated before, the overall channel depth is an order of magnitude larger than it is supposed to be according to the historical charts. Especially a calibration of the applied roughness predictor, and the thus resulting improved hydrodynamics could lead to an increased representation of the channels depth. So far the roughness predictor has been taken from the MARUM model without further adjustments.

Physics and 3D-Hydrodynamics Another very important aspect would be the consideration of processes that have been excluded so far. An example could be secondary flow that could compensate the absence of effects that are usually part of three dimensional flow pattern. Another example would be the consideration of wind and wind waves which are in this project considered as a scenario, but are influencing the estuary constantly in reality.

Lower MORFAC Lastly, the MORFAC of 400 that has been applied in this project is unrealistically high. Firstly, it is necessary to use such a high MORFAC in order to get long enough simulations for the investigation of an alternation period. Secondly, it is reasonable to chose a MORFAC of 400 when investigating schematic developments as also done by Van der Wegen (2012) [39], who applied the same high MORFAC. Nevertheless, amplifying the hydrodynamics with factor 400 introduces uncertainties, as the morphodynamic development indicates when comparing MORFAC 200 with MORFAC 400.
Therefore, it is recommended to apply a lower MORFAC, if possible in order to get more realistic results.

5.6. Troubles / Lessons learned

During the modeling phase, one major problem has been faced: At the beginning of this project, when the model domain had to be defined, the main goal has been to tighten the number of grid cells, in order to guarantee a fast computation time later on. The idea was to close the model domain off on each side, as close as possible, make the Jade Bay detachable and only allow a high grid resolution in the Outer Weser part. This settings resulted in the following grid definition, that is called "grid zero" in the following:

- Eastern boundary: The tidal flat Eversand
- Northern boundary: The end of the nowadays tidal flats
- Western boundary: Land boundary of the Jade Bay
- Southern boundary: Land boundary of the Lower Weser and Vegesack

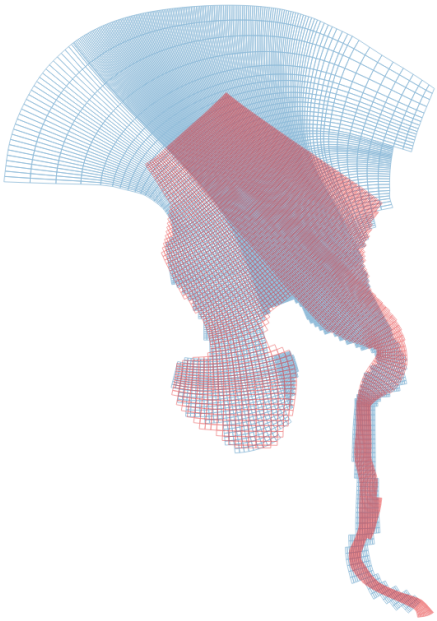

Figure 5.9: Comparison of the grid applied in this project and an instable grid that has been developed earlier

Figure 5.9 shows the grid that has been applied in this project (in blue) and that has been stable in comparison to grid zero (in red). The reason for naming and describing the extend of grid zero in detail is that this domain set-up has introduced severe numerical instabilities that have caused a considerable delay of this project in the order of months. The instabilities that have introduced the delay can be described as a local pile-up of sediment. From one time step to another large flow velocities developed and caused a local accumulation of sediment that would create depths (positively defined) of -120 m. In other words, an exposed mountain has formed in one grid knot, whereas the surrounding knots still had positive values (were below sea level). The numerical instabilities have been observed close to the northern open boundary

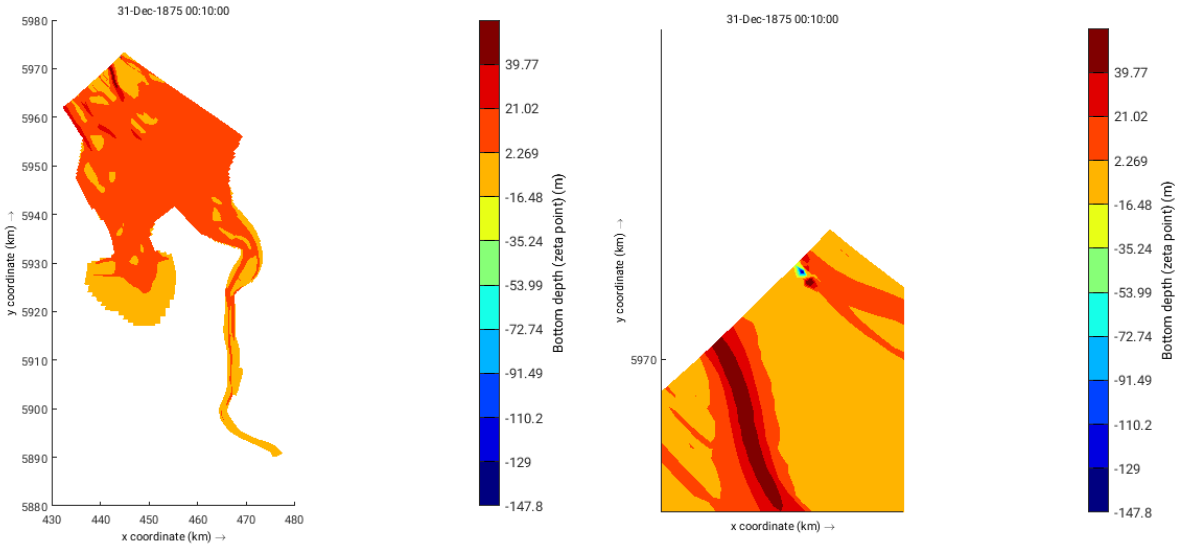

(a) Depth contours at the collapsing point

(b) Zoom into the depth contours at the collapsing point

Figure 5.10: Two examples of a collapsed simulation with grid zero

that has been defined on the straight northwestern side of the model and could not be linked to a fixed period or a spin-up time. Instead, at some point in the simulation the pile-up pattern that is indicated by figure 5.10

are found and in most of the cases no error has been reported by the log-file.
The explanation for this numerical instability is that locally the bathymetry can reveal an unevenness (i.e. a bump) that is resulting in local advection velocities which are opposed to the local flow velocity. Based on a fundamental problem of the implemented discretization scheme this inconsistency can lead to the pile up of sediment at one point. Even though this issue kept the project busy for quite some time, a further numerical investigation has not been done.
The problem has been solved by implementing a new grid. Here the area along the northern open boundary is firstly, not a straight line anymore, secondly, more space is provided for the hydrodynamics to settle and lastly, where a higher depth has been defined. With the new grid and the related benefits mentioned in the latter sentence, a number of other troubling aspects have been solved that will not be described in detail. Most of these troubles have been related to the northern boundary condition and local erosion patterns in the adjacent areas.
Modeling wise, the main lesson learned is to define the model domain carefully. It is worth to expand the model domain further in order to provide enough space for the hydro- and morphodynamics to develop. Furthermore, applying a flat bed bathymetry can cause issues due to the limited depth in the offshore part of the model domain. If the depth provided close to the open boundary is not large enough, it might happen that the tidal wave gets damped out relatively fast, which slows down the development of tidal channels and shoals. This has negative influences on the simulation period. This issue can be solved by defining a depth that is large enough and does not damp the tidal wave too much. As a last aspect to mention here, it has been experienced that the coupling of Swan with Delft 3D-Flow is computationally quite expensive.

6 Results

6.1. Base Case

The presentation and description of the base case results are divided into hydrodynamics and morphodynamics. The hydrodynamics represent ten years of hydrodynamic activities forced by the tidal components and the river discharge. Equivalently but multiplied with a MORFAC of 400, the morphodynamics indicate the development of shoal and channel patterns based on the forces of the hydrodynamics.

6.1.1. Hydrodynamics

Equilibrium Tide Due to the flat bed approach and the thus resulting limited depth during the spin-up phase of the model, the tidal wave is damped at the beginning. With the further morphodynamic development of shoals and channels, the tidal wave is expected to progress less damped through the model domain. When looking at water levels that are extracted every 60 minutes, the spin-up time for the tidal wave can be estimated as indicated in figure 6.1. At the beginning (June 2012), the tidal range during spring tide is less 2.5 m while it is around 4 m during spring tide for the fully developed morphodynamic state (2015). Despite the small data gap during low water at the end of the hydrodynamic year 2013 caused by the temporary formation of a tidal shoal at that location, the tidal wave signal indicates that the hydrodynamics are at their equilibrium state after 2.5 hydrodynamic years of development.

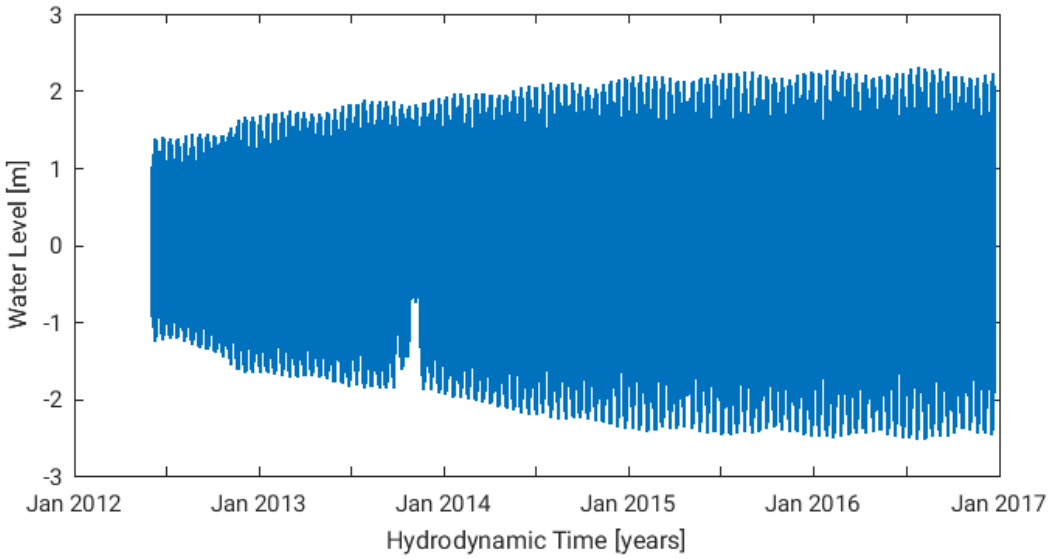

Figure 6.1: Base case: Spin-up time for the tidal wave in AOI

Tide Inside the Model When looking at the tidal propagation through the Weser estuary in reality, the tidal range gets amplified while propagating inland as indicated by [22] and figure B.1. One reason for the amplified tidal range can partly be found in the width convergence which can introduce a shoaling effect on the tidal wave [4] in conjunction with a decrease of depth. In the hydrodynamic equilibrium state of the model(as indicated in the latter paragraph), the tidal range is expected to increase as well when following the channel axis since the same influences (depth restriction and funnel shape) apply here. To check the representativity of the hydrodynamics, the development of the tidal wave is investigated at different locations along the channel axis. Figure 6.2 shows the water level over time for different locations that were extracted at random points along the Weser channel axis. After approximately seven years of hydrodynamics, they have been plotted for slightly more than a day. The increase of the tidal range from the most outside located extraction point towards the most southern located extraction point is clearly visible. It confirms the expectation that the tidal range increases when going further landwards in the Weser estuary.

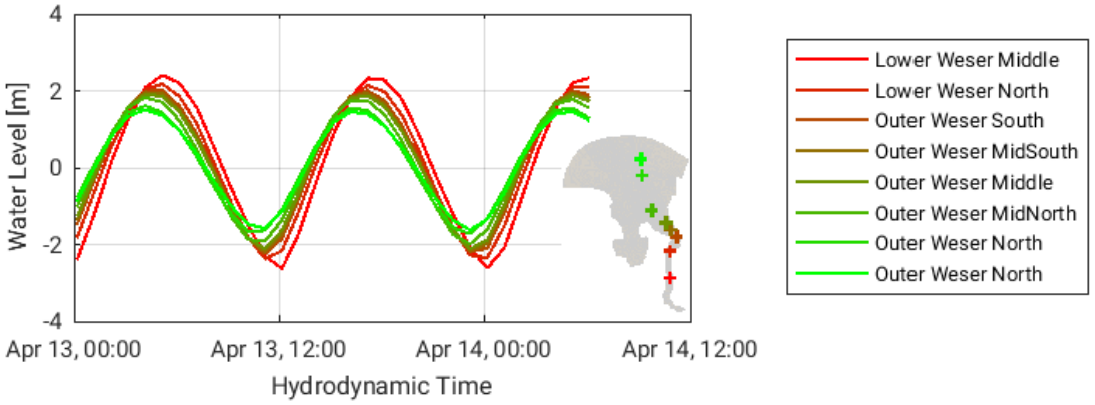

Figure 6.2: Base case: tidal wave in the model - Tidal range increases while the wave propagates inside the estuary.

Tidal Asymmetry Tidal asymmetry determines whether an estuary is flood- or ebb- dominant (see section 3.2). Ebb- or flood-dominance has a significant influence on the net-sediment-transport-direction whereby a prediction can be gained by analyzing the tidal asymmetry [4]. For the base case, a distinction is made between the tidal asymmetry during spring and during neap tide once inside the Outer Weser and once inside the Lower Weser (figure 6.3). Here, tidal asymmetry differs, when comparing the locations of the Outer and Lower Weser, but it is the same when comparing the asymmetry during spring and neap tide.
Figure **??** shows the tidal wave in the middle part of the Lower Weser (around the southern end of the present city and harbor Nordenhamm) after more than seven simulated years of hydrodynamics. For an easier location of the low water (LW) and high water (HW), they were automatically determined and indicated in the plot with the respective time. Unfortunately, the resolution is limited to one hour, but a trend in the tidal signal can be identified:

During neap tide 6.3c, the flood duration is around 6 hours, while the ebb duration is roughly 7 hours .

During spring tide 6.3d, the flood duration is around 6 hours, while the ebb duration is around 7 hours.

For both spring and neap tide, the flood duration is shorter than the ebb duration. Since the same tidal volume needs to be filled and/or emptied during flood and ebb flow a shorter duration means that the water masses need to flow faster in order to move the same volume of water. Consequently, higher flow velocities result in higher sediment transport rates so that the net-sediment transport direction is identical with the flood direction.

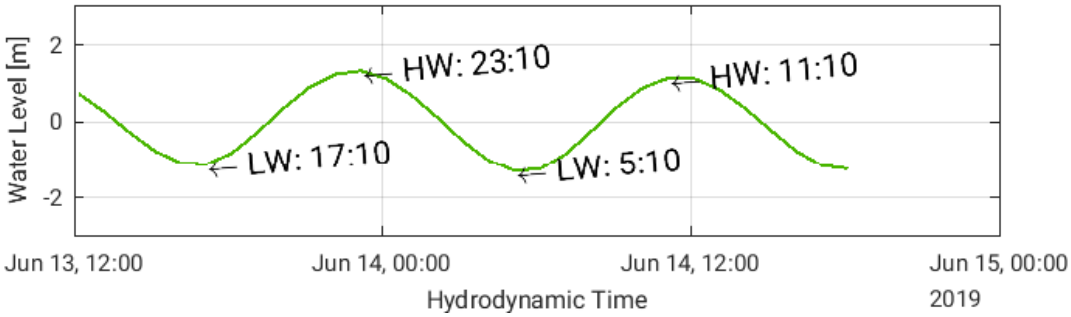

(a) Base case: Tidal wave during neap tide in the Outer Weser

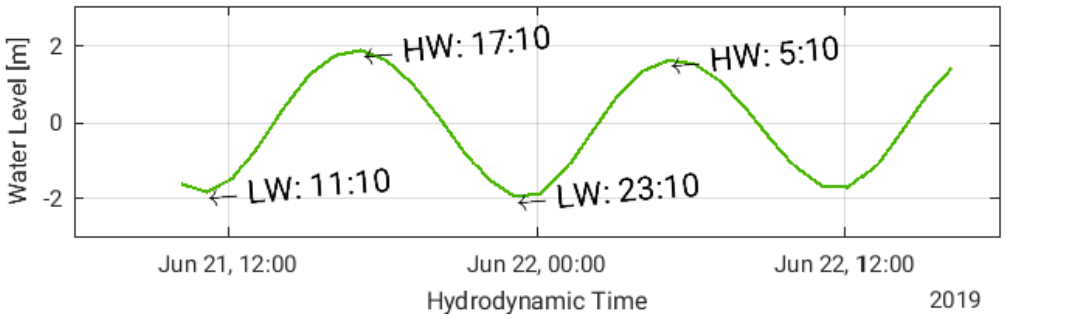

(b) Base case: Tidal wave during spring tide in the Outer Weser

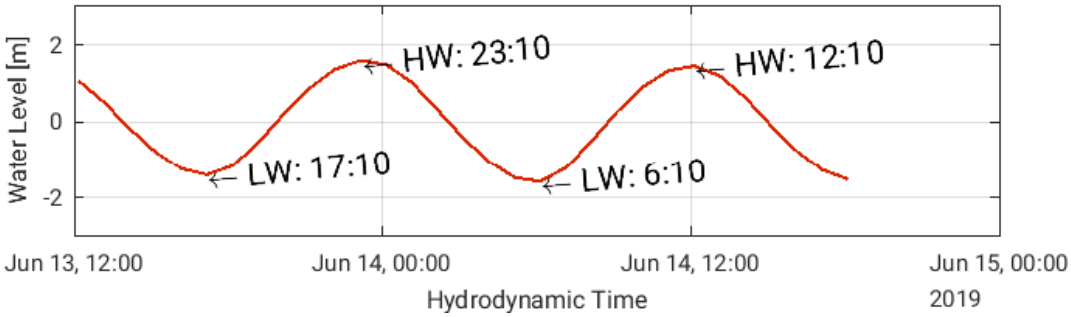

(c) Base case: Tidal wave during neap tide in the Lower Weser

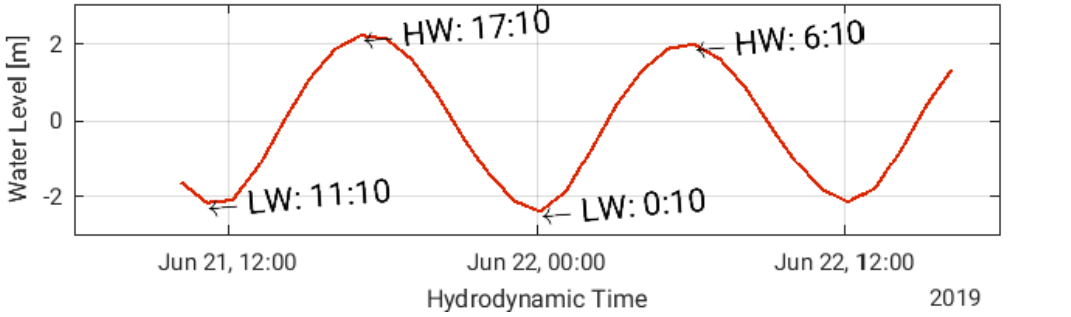

(d) Base case: Tidal wave during spring tide in the Lower Weser

Figure 6.3: Base case: Comparison of the tidal wave during spring and neap tide in the Outer and Lower Weser

6.1.2. Morphodynamics

For the base case simulation, the same questions that were defined in section 3.2 in chapter 3 arise. The first one questiones if the simulation reaches a kind of equilibrium stage.

Morpholocial Equilibrium Figure 6.5a shows the cumulative bed load transport over a cross-section in time. It shows that the system is generally importing sediment since the grid is defined positive from the Lower Weser onward. After a positive start which only lasts for the first two hundred MY, the next few hundred MY reveal a significant increase in the bed load transport that is directed southwards, indicated by the overall negative values. Around the morphological year 650, the general behavior of the cumulative bed load transport averaged over the cross-section changes: Instead of continuing the negative trend that can be observed in the years before, it changes to an almost constant line in time. This shows that the system south of the cross-section where the bed load transport is averaged imports sediment in the same order of magnitude as it exports.

Looking at a section of the cumulative bed load transport averaged over the cross-section 75 (figure 6.5b), it gets visible that every spring-neap-tidal-cycle and even each individual tide can be detected. The plot should be read having in mind that every year of hydrodynamics is amplified with a MORFAC of 400. Thus, the period where the morphological time scale indicates 400 years is equivalent to one year of hydrodynamics hence ~ 25 spring-neap-tides can be expected. Combining the transport at each temporal point, after the morphological year 650, they roughly average out.

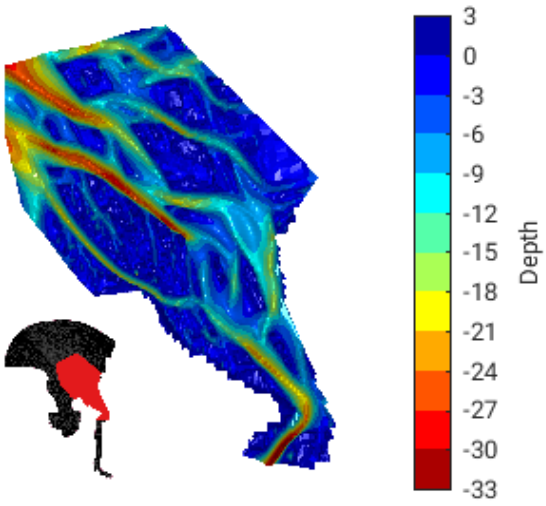

Figure 6.4: Bathymetry at t = 650

Another idea is to look at the development of depth contours over time: Theoretically, if any kind of equilibrium is reached after some time, the hypsometry should remain roughly the same and, thus, could be included as a kind of measurement that indicates equilibrium. Figure 6.5c reveals the hypsometry for the AOI over time. As indicated by the plots in figure 6.5, a kind of equilibrium can be indicated after 650 MY. Figure 6.4 shows the depth distribution in the AOI at t = 650. A clear single channel has developed coming from the Lower Weser part of the model with a fairly large depth. According to figure 6.5a, the bed load transport reaches a generally constant value in time in cross-section 75. Since that cross-section is located roughly around the end of the deep channel coming from the south, it reveals that this channel has built up to its equilibrium state. However, the more northern two thirds of the AOI show more small channels and multiple side channels. Due to the number of small channels, it is not possible to clearly distinguish two main channels out of the seen channels. Figure 6.4 can be seen as the starting point of the development of channels and shoals northwards from cross-section 75.

The hypsometry over time for the AOI supports this observation: A lot of changes in the hypsometrical composition can be found in the first 650 years of development. The build-up phase continues less significantly, roughly until 1100 years of morphodynamic evolution. From that year onwards the changes in the hypsometry are less continuous and show just small variations compared to the spin-up part at the beginning. Consequently, the detailed visual analysis of the shoal and channel development starts at a later point of morphodynamic evolution.

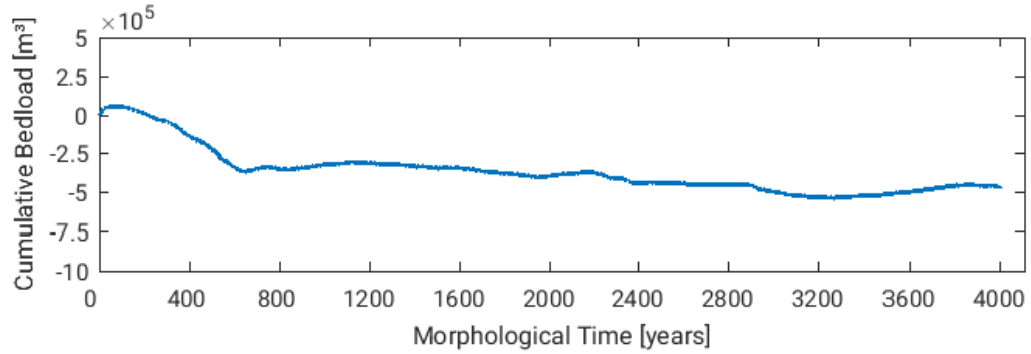

(a) Base case: Cumulative bed load transport

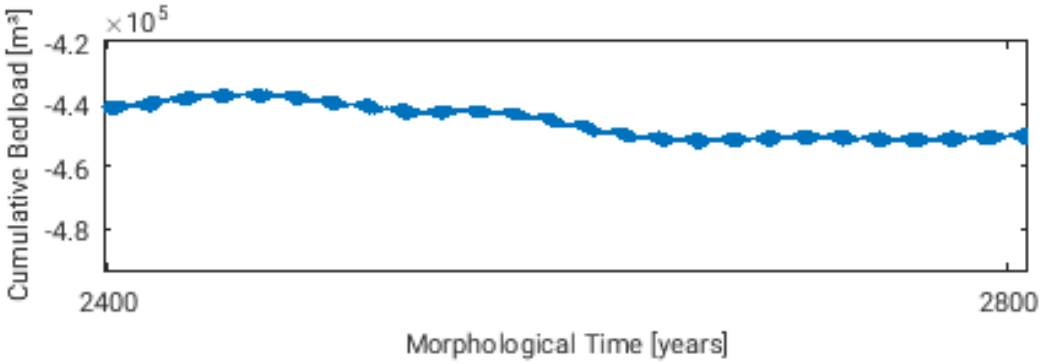

(b) Base case: Zoom into the cumulative bed load transport

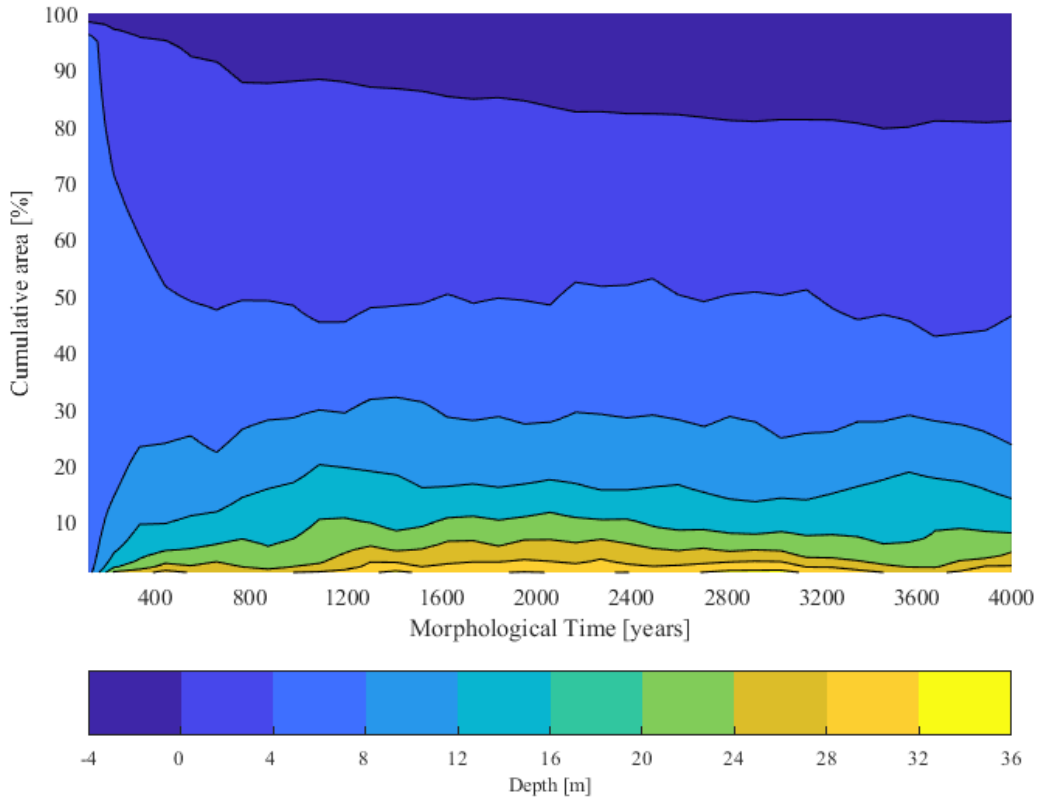

(c) Base case: Hypsometry over time inside the AOI

Figure 6.5: Base case: Equilibrium state for the morphodynamics in the AOI

Alternation Pattern After 1100 years of morphodynamic evolution (picture (a) of figure 6.6), one main channel can clearly be observed. It evolves from the small (~ 1 km) and deep (~ 33 m) channel that comes from the Lower Weser and widens around the bend where the city of Bremerhaven is located. The wide part has an extend of around 7 km length in direction of the channels axis, a width of around 3-4 km and is relatively shallow (~ 12 m). When carefully looking at the wide part, the tendency can be noticed, that a second channel develops on the eastern end of the wide channel. There is just the starting of a division visible located roughly in the middle of the funnel shaped Outer Weser part. The main channel itself gains depth from the middle until the end of the funnel shaped part increasing the depth from ~ 12 m to around 32 m. The width of that channel remains the same until the other tidal channels reach down from the North Sea.

Picture (b) of figure 6.6 shows the AOI after 1800 years of evolution. Here, the one main channel that was present in (a) has changed in the funnel shaped part: After the channel approaches the AOI from the Lower Weser identically as in (a), a different channel pattern is visible. In the southern bend, the channel has the tendency to propagate into the northwestern direction. Eastern of this tendentious western channel development,there is a rather shallow channel part that spreads widely up to the eastern domain end of that part and introduces the start of a channel in the east. The eastern channel starts more or less at the same latitude as the western channel ends. From there on, on the western side, a shallow tidal shoal reaches into the middle of the funnel shaped AOI where there is a tidal channel with a depth of around 20 m on the eastern side. This eastern channel splits into a short part directed northwards and a wide part directed northwestwards that links to the deep channel that is (the same as in (a)) coming from the North Sea.

A bit less than 400 years later, after 2150 years of morphodynamic development, the channel shoal development shows a different structure than in (a) and (b). Again, the channel coming from the Lower Weser has the same size and structure as in (a) and (b), but the channel evolution after the bend is different. In (c) the channel splits right at the southern end of the funnel shaped part of the AOI into two channels: A straight, relatively wide western channel that has a length of around 15 km and an eastern channel that is rather bowed and narrow. At the latitude where the channel divides into two, the western channel is much wider (~ $2-3$ km) and deeper (~ $20-24$ m) compared to the eastern channel (~ $0.2-0.3$ km width and ~ $10-15$ m depth). In the middle of the AOI, the eastern and western channel are progressing parallel towards northwest with similar depths (~ 15 m) and a long (~ 10 km), narrow (~ 1 km) tidal shoal in between them. At the northern third of the AOI where the western channel has its shallowest part (~ 10 m) the eastern channel spreads into a very short and shallow branch that tends to connect to the western channel directed northwestwards. The other branch is deeper (up to ~ 20 m) and continues northwards for 4 to 5 km until it connects with the western channel through a convex bow that closes off flowing almost westwards. The bow circles an egg-shaped tidal shoal that has evolved at the northern end of the long narrow shoal that has been described before. There are some side channels that flow from the bow towards north and northwest, but the significant part connects to the deep and long channel that has been indicated in (a) and (b) as well.

After 2880 years of morphodynamic evolution, the channel and shoal situation is a different one (picture (d) in figure 6.6). From the eastern channel that has been described in the latter passage just a fragments are left. Instead, the channel coming from the south spreads after the bend into two channels that reunite around 4 to 5 km later along the channel axis. The channels on both sides are equally deep (~ 18 m) and have the same narrow extend. They are divided by a low-lying area of roughly 10 m depth, a width of around 2 km and a length of approximately 3 km. After the two channels have joined around the mid latitude of the funnel shaped area in the AOI, they continue as one narrow channel following the direction of the western channel straight until the end of the funnel shaped part. Here, the channel has a depth of around 20 m. Before the channel connects to the deep channel coming from the North Sea, a shallower part interrupts the continuously deep channel structure: The 10 m deep shallow feature crosses the channel one diagonally, coming from the northwest and progressing towards the southeast.

Only a comparatively short time later, after 3010 MY, the channel pattern has rearranged in a different pattern. Here, two channels can be recognized, whereby the eastern channel is almost interrupted by the presence of a tidal shoal. The starting point, as in all other pictures, is the channel coming from the Lower Weser. In comparison to the pictures (a) to (d), the division of the channel occurs a few kilometers further north. Before the channel splits up, it widens and loses depth (from ~ 33 m depth towards $12-14$ m depth) at the same time. Around 4 kilometers north of Bremerhaven, a tidal shoal (~ 2 km width and ~ 3 km length) can be

observed which divides the channel into a very narrow (< 1 km) and shallow (< 8 m) eastern channel and a wider (~ 2 km) and deeper (~ 22 m) channel that flows relatively straight towards northwest. The second tidal shoal (~ 1.5 km width and ~ 3 km length) is located at the northern end of the funnel shaped part of the AOI. The two tidal shoals are divided by a wide and shallow junction between the eastern and western channel. In the northern third of the funnel shaped AOI, the eastern channel is more clearly visible. It has the same width as the western channel at this latitude (~ $1-2$ km), but with a depth around 20 m, it is almost twice as deep as the western channel (~ 11 m).

Close to the end of the simulation, after 3950 years of morphodynamics, the channel pattern has changed again. On a large scale, two channels can be detected again, but they differ in size and extend from the channel pattern that has been observed after 3010 MY. Instead, they reveal some similarities with the channel pattern after 1800 MY: Coming from the Lower Weser, the one channel that does not change throughout the simulation period after the morphodynamic equilibrium is reached tends to continue flowing towards northwest. After only a few kilometers the channel significantly loses depth until it reaches a depth of around 10 m. Parallel, on the eastern boundary of the funnel shaped area, a channel develops that gains depth where the former channel had lost depth. The channel coming from the south and the channel on the eastern border are connected by a mid-deep part that has a depth of around 10 m and can clearly be distinguished from the tidal flats. The eastern channel continues northwards until the end of the funnel shaped part of the AOI where it turns into a shallower and very narrow channel that splits up into a north flowing part and a northwest flowing part. At the latitude in the middle of the eastern channel where it is developed most, a western channel starts to evolve starting with a depth of 11 m. At the end of the funnel shaped area, it connects with the main tidal channel coming from the North Sea. Summarizing the spatial pattern of picture (f) of figure 6.6, there is a western channel that is interrupted in the middle of the funnel shaped part and there is a western channel that is exclusively located in the middle part of the funnel shaped area, disregarding the mid-deep parts that are connecting both channels.

In a nutshell, the spatial channel and shoal patterns were described for six different temporal points of the base case simulation. It has shown that even after some kind of equilibrium has been developed, the AOI is mophodynamically still very active. During the description and analysis in the AOI, the focus has been placed on the funnel shaped part and its northern extend within the AOI since the two relevant channels that are the reason for this investigation are located there. Comparing the observations made, it reveals that there are channel patterns that can be found in relatively similar to each other at different moments in time. For the base case, this can be found for the plots of (b) and (f) where the western channel is interrupted and the eastern channel is mostly present in the middle part. Furthermore, (c) and (e) have some similarities where there are two channels that are divided by tidal shoals and where the western channel is stronger in the southern part and the eastern channel is relatively strong in the northern part just before the junction. Broadly spoken, there can also be found some comparable patterns between (a) and (d) where no clear two channel system is present, but instead, a relatively wide single channel crosses the area of interest from south to northwest. These similarities between the bathymetries at different points in time can be an indication for a periodic behavior that might favor the alternation of channel dominance. Looking at the individual plots of figure 6.6, there is something that could be seen as an alternation: In plot (b), the deeper channel is located at the eastern side, in figure (c), it is clearly located on the western side. While there is no dominant channel observed in picture (c), there is a dominance of the western channel in (e) and a dominance of the eastern channel in (f). Consequently, the dominant channel alternates.

The question that needs to be answered now, according to the investigation concept in chapter 3, is whether a period can be assigned to the alternation pattern observed.

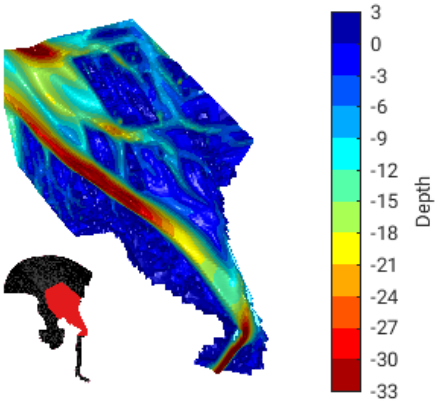

(a) Bathymetry at t = 1100

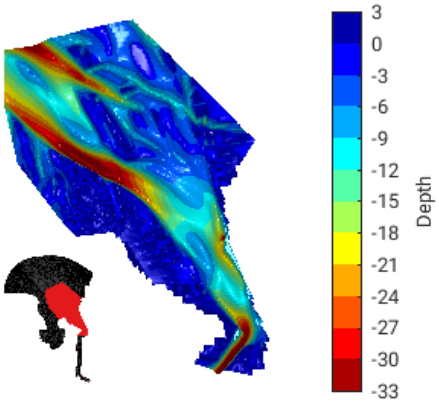

(b) Bathymetry at t = 1800

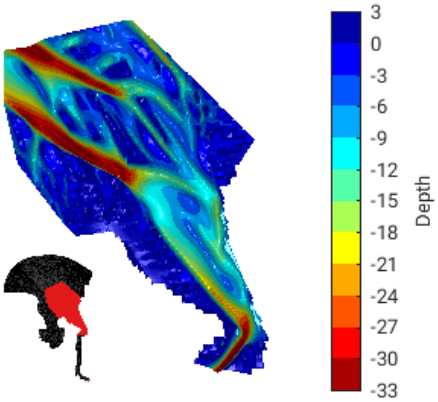

(c) Bathymetry at t = 2150

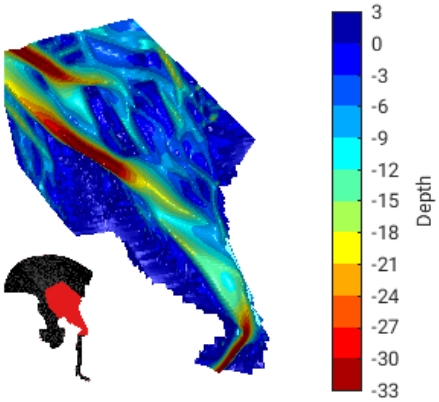

(d) Bathymetry at t = 2880

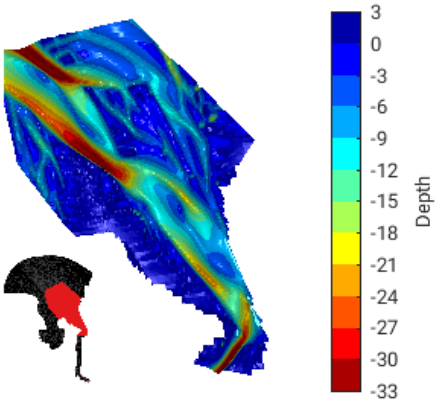

(e) Bathymetry at t = 3010

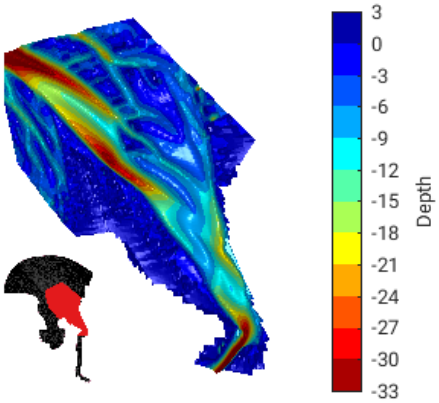

(f) Bathymetry at t = 3950

Figure 6.6: Base case - bathymetry at different points in time

Alternation Period In order to assign a period to the presumably recurrent alternation pattern of the two channels found in the plots of figure 6.6, the scenario EM2 (see 4.3.2 in chapter 4) is applied. For a better visualization, the cross-section chosen in chapter 4 is plotted over time for the base case simulation (figure 6.7a). The y-axis shows the relevant part of the cross-section 75 where morphodynamic activities are taking place. According to figure 6.5a and the analysis of the equilibrium state for the AOI, the plot should theoretically be analyzed after 2.5 years of hydrodynamics or after 1100 years of morphodynamics. However, when searching for periodic patterns in figure 6.7a, a remarkable scheme can be found twice over the simulated time: Starting with a very deep channel on the western side (the southern one in figure 6.7a) that then widens until it covers almost the whole channel area. While widening, the channel depth gets less deep, and at a depth of a bit more than 10 meters, the eastern channel starts to deepen resulting in a cross-section where the eastern (northern in figure 6.7a) channel is deeper than the western channel which is not even clearly visible anymore.
This development can be observed twice:

Starting after 600 MY until 1400

Starting after 2000 MY until 3000

Additionally, after the second occurrence of the described pattern, another alternation pattern appears which differs from the latter one. From 3000 to 3800 morhoplogical years another shift in the deepest channel can be found, even though it is less clearly visible. And before the simulated time is over, the dominant channel shifts again from the eastern to the western channel.

Since it seems difficult to address a period to the patterns that can be identified in figure 6.7a, the scenario EM2 provides a more simplified plot which might indicate a period more clearly. As presented in chapter 4, the idea is to categorize the cross-sectional state by correlating it with predefined cases. The cases are grouped according to the dominance of a channel and, thus, can indicate when the dominance within the two channel system is changed.

The tendencies that have been observed in figure 6.7a are now worked out more clearly in figure 6.7b: Looking for a confirmation of the findings so far and, thus, starting to look at the plot at 600 MY, the system is clearly dominated by the western channel. The correlation coefficient that is always above 0.8 in the temporal range of 600 - 1000 indicates that the cases that reveal a western dominance are well represented in this part. A short phase (around the point of 1100 MY) follows where both channels are equally dominant or where there simply is only one wide channel. Afterwards, an eastern dominated period is present for around 300 years, followed by a phase (1400 MY - 1800 MY) of no dominance. Next, the western channel is dominant again for a relatively long period (1800 MY to 2600 MY), followed by a short phase of equal dominance and a short phase where the eastern channel is dominant again (2850 MY - ~ 3000 MY). The last three periods have previously been described as the second section with a remarkable pattern. The analysis through method 2 does confirm the observations: There is indeed a pattern of channel alternation that repeats itself. With the plot 6.7b, these similar periods can also be compared quantitatively revealing that they show the same pattern, however with different dimensions of the individual parts within the alternation pattern. Lastly, the mentioned alternation pattern that differs from the two ones previously described is clearly indicated by the correlation analysis as well. After a very short phase of the western channel being dominant, a short period of equally dominant channels follows. Subsequently, a long phase of eastern dominance with a very high correlation coefficient ensues. The high correlation coefficient indicates that over the whole period, the time variable cross-section and a predefined case with an eastern dominance are almost identical.

Overall, the high values for the correlation coefficient are remarkable. One reason is that a number of cases that are included in the analysis are defined by the base case simulation and, thus, are matching at one point in time. But it also shows that there are morphological states that are appearing multiple times throughout the simulation period.

Based on the analysis of figure 6.7b, it is difficult to define a definite alternation period. One reason is that the three alternation patterns observed are not a large number of samples in order to indicate a verified trend. Secondly, two patterns that are similar with a period of around 1400 MY to 1600 MY can be defined, but the third observed alternation pattern does not fit to that period. If a period needed to be assigned for the overall alternation, a linear regression could indicate a period at which the change from western to eastern dominance occurs. Taking the temporal middle of the eastern dominant periods (1200, 2900, 3500) and using them

in a linear regression results in the following formulation:

$$Y = 230 + 1150 * X \tag{6.1}$$

This means a return period of 1150 MY can be assigned to the overall alternation. When looking at only the two first very similar alternation patterns, a return period of 1700 is calculated. It needs to be stated that no distinctive return period can be assigned.

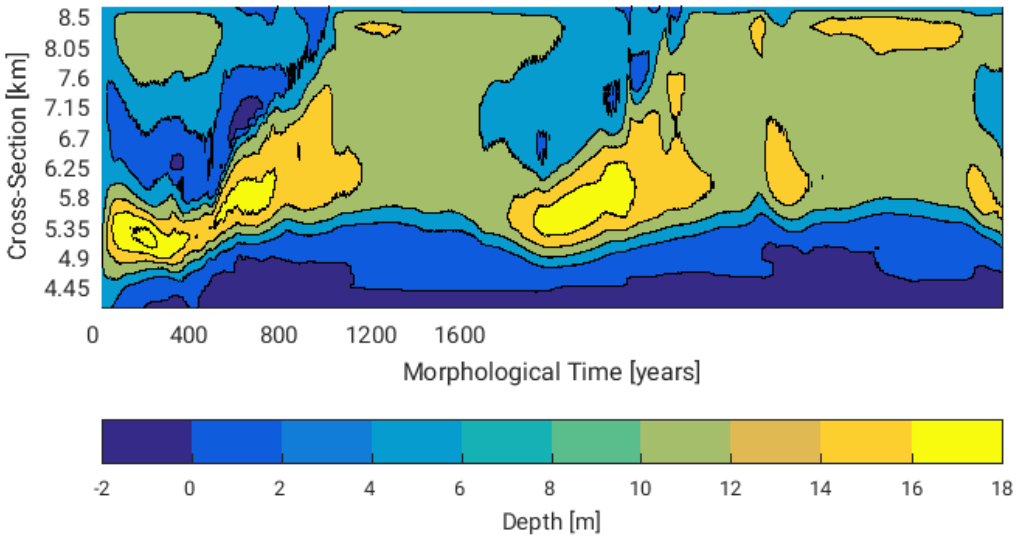

(a) Base case: Cross-section 75 over time

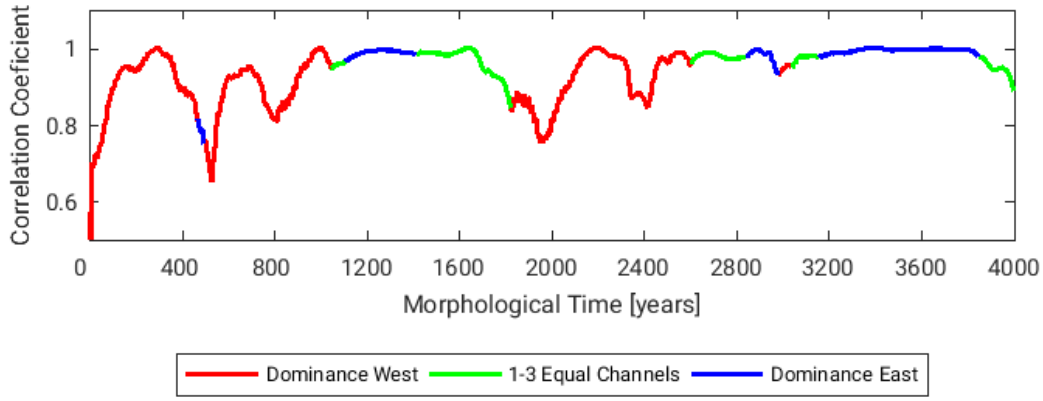

(b) Base case: Cross-section 75 cases analysis

Figure 6.7: Base case: Alternation analysis

Overall Representation Analysis In order to get an indication how representative the predefined cases are for this base case simulation, the determination coefficient is presented in table 6.1. The determination coefficient shows how representative a case is for the whole time series of cross-sections that have been extracted from the base case simulation. The idea is to indicate which cases are most suitable for the overall representation of the base case (with the help of the determination coefficient). By looking at the distribution of the best fitting cases between the three categories of the cases, insight can be gained about which dominance is overall favored.

Table 6.1 reveals that the highest representation is attained by an equal dominance case with over 50 % representation. Additionally, there are two cases around 40 % of representation, one with a higher representation for an eastern dominance and one with a lower representation for a western dominance. Lastly, three cases with a bit more than 30 % can be found where each of the three categories are represented once. Based on these representations, the base case can be seen as a simulation where both a west-dominant channel and an east-dominant channel are equally present. Since it is known from the former analysis that the dominance of one side is not continuous but changes over time, it can be concluded that the alternation pattern is also balanced over time.

Case	Description			r^2 [%]
	No of Channels	Dominance	Extend	
1	2	West	Narrow	1.2
2	1	West	Narrow	32.7
3	1	West	Wide	38.9
4	2	Equal	Wide	8.7
5	2	Equal	Small Hump	53.3
6	3	Equal	Wide	30.3
7	2	East	Narrow	6.4
8	1	East	Narrow	31.3
9	1	East	Wide	40.5

Table 6.1: Determination coefficient (r^2): Cases vs base case simulation

6.2. Scenario: Kelvin Wave

Morphological Equilibrium As for the base case, it needs to be determined if and after which time period the model of the Weser estuary will reach a kind of equilibrium, if there is no Kelvin wave included in the boundary condition. The first indicator is the cumulative sediment transport averaged over a chosen cross-section. The cross-section is the same as for the base case and the result is shown in figure 6.8a. The plot indicates that around the point of 800 MY the cumulative transports starts to converge to a more constant value. From the start until 800 MY a cumulative transport of around -300 000 m³ has developed, whereas from 800 MY until the end the cumulative transport negatively increases with -180 000 m³ over 3200 MY to a value of roughly -480 000 m³.

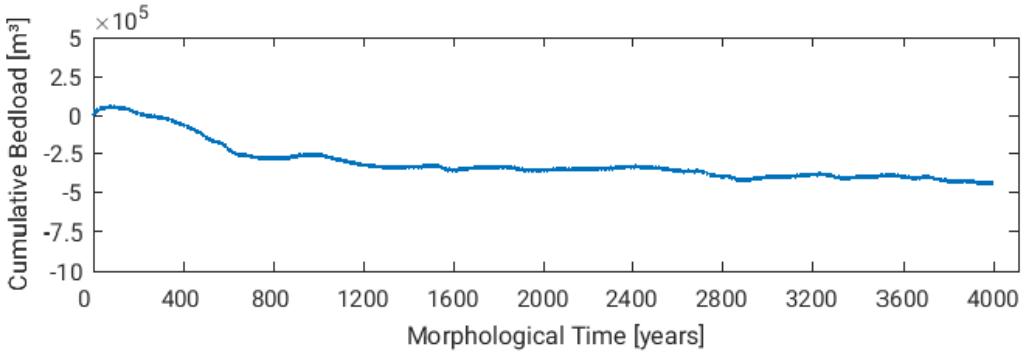

(a) Kelvin wave: Cumulative bed load transport

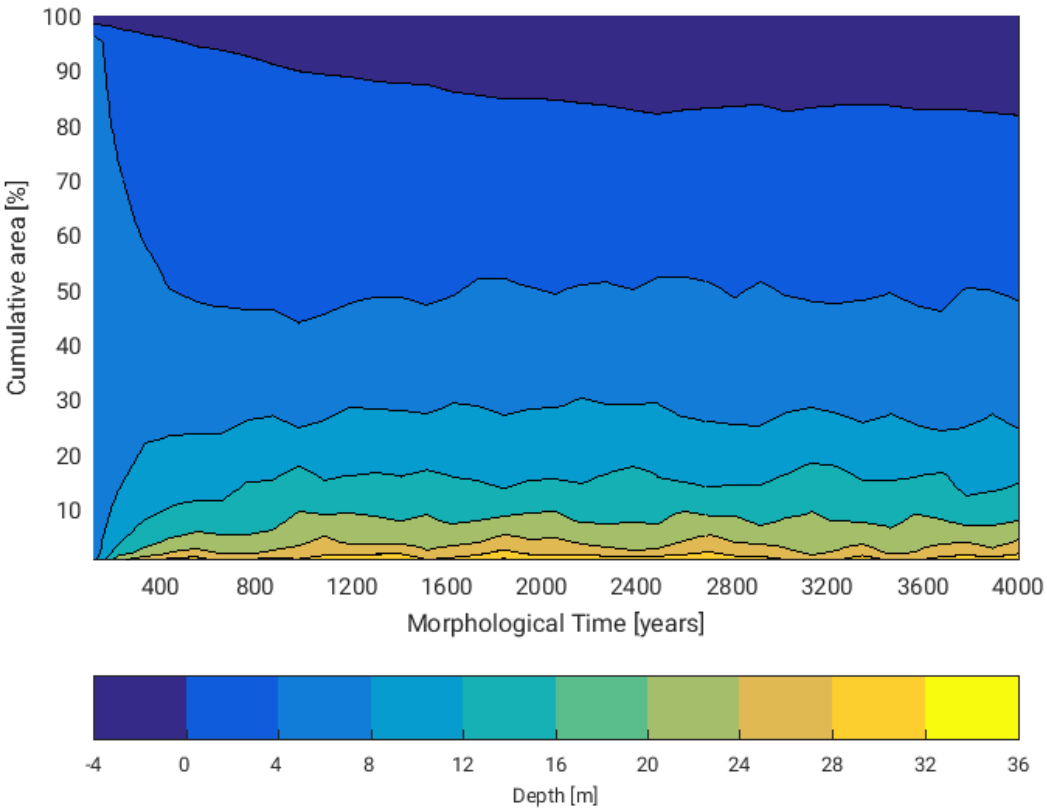

(b) Kelvin wave: Hypsometry over time inside the AOI

Figure 6.8: Kelvin wave: Equilibrium state in the AOI

There are still small variations but in comparison to the constant negative growth of the cross-sectional cumulative sediment transport it can be considered as a relative constant value. As in the base case just looking at the cumulative sediment transport can be tricky and therefore the hypsometry of the AOI over time is used as a second indicator for morphological equilibrium. Following the hypsometric plot that is shown in figure 6.8b the point of 800 MY seems to be reasonable, since almost all depth ranges have reached the extend that they keep for the rest of the simulation time. The only exceptions are the deep parts (below 16 m) and the area above zero, the tidal flats. The supra-tidal zone requires a longer time to build up since an equilibrium extend is reached after around 2400 years of morphodynamic development. For the deep parts the morphodynamic equilibrium development is reached after around 1100 MY which is close to what has been observed in the base case. The same conclusion can be drawn when looking at the hypsometry for the full model domain over time (see appedix E), where the long spin-up phase for the tidal flats is less clear due to the extensive land masses that are included in the model domain, but still can be found. Since the main goal is to look at the channel pattern, it is assumed that the initial adaption phase where sediment is imported to the Lower Weser part ends after 800 MY. Now, that the spin-up time for the morphodynamics is known the simulation results can be described and analyzed regarding alternating channels and a alternation period.

Channel / Shoal Pattern The bathymetries of figure 6.9 show the development of channels and in the AOI for selected points in time. The simulation results of the full model domain can be found in figure D.2 in appendix D. When comparing the bathymetries of figure 6.9 with the bathymetries of the base case a few aspect can be found that are different for the scenario Kelvin wave: First of all, the deep channel that comes from the North Sea and approaches the AOI is located a bit more south which is especially clear in the first two plots of figure 6.9. The one channel coming from the Lower Weser however is the same and appears at the same location as for the base case. Other than that, the channel pattern is generally not strikingly different, although it does not show a periodic behaviour as it does in the base case simulation. Furthermore, an alternation is less clearly visible from the bathymetries, compared to the base case simulation. But still an alternation can be found on small scale when looking at the deepest channel inside the funnel shaped part of the AOI, where it varies as following:

- (a) western channel
- (b) eastern channel
- (c) western channel
- (d) equally / eastern channel
- (e) western channel
- (f) equal / lat. dependent

According to the bathymetries of figure 6.9 there is an alternation, but it is less clear than in the base case simulation. Assigning a period to these patterns is not possible from just looking at the bathymetries, which is why the EM2 gets applied. A more tangible analysis is given by looking at cross-sections and their evolution in time where quantitative information about the dominance of a channel and its location are provided. As for the base case, cross-section 75 is selected representative for the AOI. Figure 6.10 shows the development of the cross-section over time for the Kelvin wave scenario. By looking at the development of the deepest points (indicated by the yellow/orange contour fields) along the cross-section axis in km, it gets visible that after the spin up time there are two channels. Although, for most of the time the western channel (the southern one in figure 6.10) is deeper than the eastern one, but still some periods can be found where the eastern channel has a higher depth than the western channel and can thus be considered as more dominant in these periods.

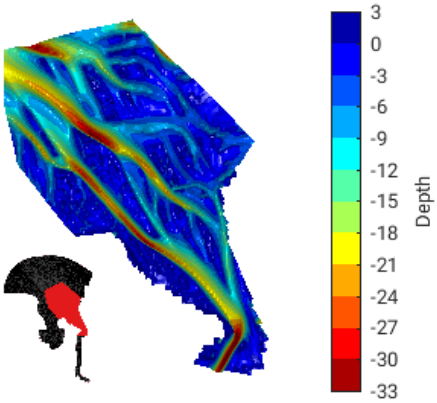

(a) Bathymetry at t = 800

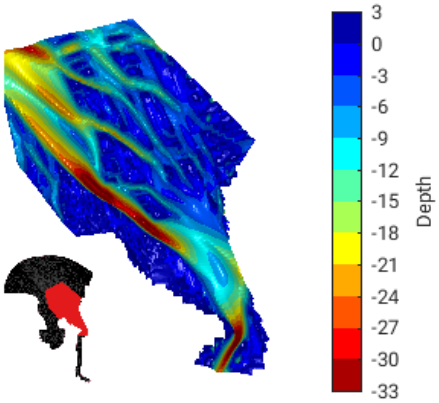

(b) Bathymetry at t = 1200

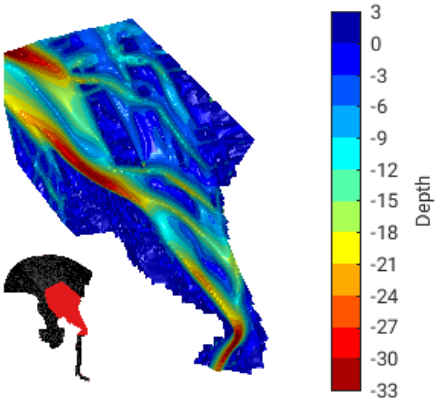

(c) Bathymetry at t = 1600

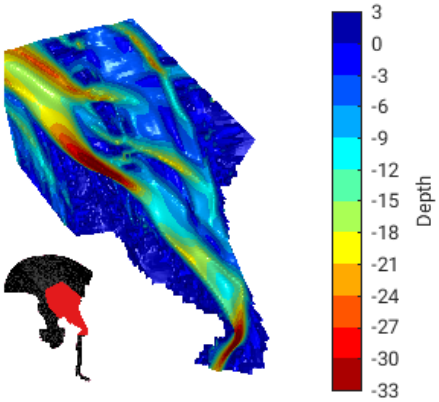

(d) Bathymetry at t = 2200

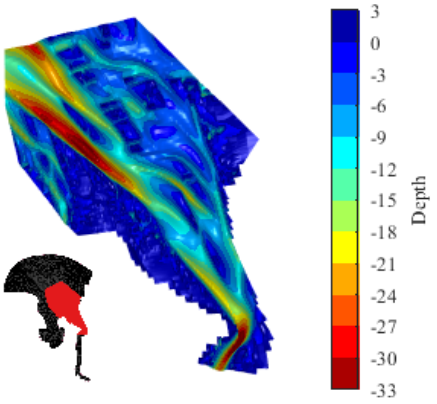

(e) Bathymetry at t = 2800

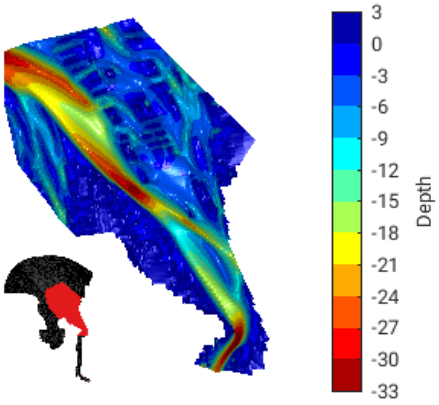

(f) Bathymetry at t = 3600

Figure 6.9: Scenario: Kelvin wave - bathymetry at different points in time

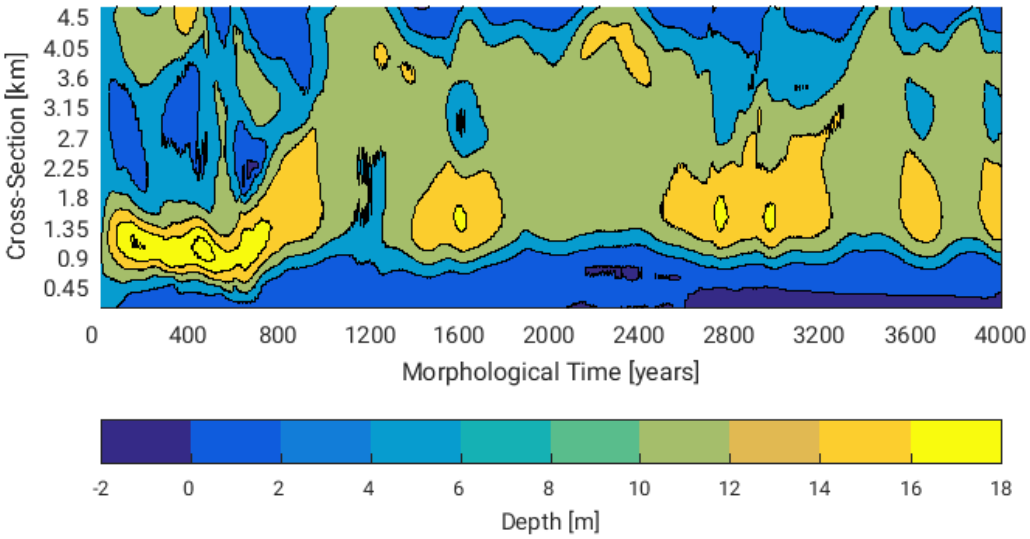

Figure 6.10: Cross-section 75 plotted over time for scenario Kelvin wave

Alternation Period In order to specify a possible period of the alternation, the EM2 yields a plot where the dominance is determined and clearly distinguishable. Figure 6.11 indicates the location of different dominance situations by color. Since for the Kelvin wave scenario red is the dominating color of the plot, it indicates that over the whole simulation period the western channel is mainly the dominant one. There is a short period ($\sim 1120 - 1300$ MY) where the eastern channel is dominant. Apart from that, there are several phases where there are two channels which are equally deep and wide (around the MY 1090, 1400, 2300, 3450, 3850) as indicated by the green color. this means that the cross-sections at these points in time do have a higher correlation with the equal dominance cases than with the eastern dominance cases. In figure 6.10 in the period of 2200 MY to 2500 MY it looks as if the depth is higher at the eastern channel than it is at the western channel or in the area in between. Due to the representation as a filled contour plot this might be misleading, since figure 6.11 indicates a higher similarity with the equal cases. Additionally, when looking to the bathymetry of picture (d) of figure 6.9 it gets clear that at his point in time there is no dominance by the eastern channel, even though it might be a bit deeper. But the depth difference between the two channels is small in comparison to the depth itself and thus it is classified as an equal dominant system. Summarizing, no period can be assigned to the alternation of the dominance between the western and the eastern channel. Instead, it seems as if there is an alternation between western dominance and equal dominance. Applying a linear regression, an estimation of a temporal period can be gained which fits best to the observation made. Using the temporal middle of the periods where there is an equal dominance between the channels (as stated above) a time series can be generated as input for the regression. Starting from 800 MY the linear regression results in:

$$Y = 147 + 757 * X \tag{6.2}$$

This indicates that there is an alternation period between western dominance and an equal dominance of around 757 MY.

Overall Representation Analysis This perception is supported by the determination coefficients of table 6.2. They reveal that all cases which represent an eastern dominant channel are less than 10 % representative for the whole time series. In contrast to the eastern dominance the western dominant cases are best represented: Case 2 and 3 show the highest and the third highest representation in this time series with more than 35 % and 25 %. The cases representing an equal depth have the second and fourth highest determination coefficient and thus can be considered as second relevant classification with a representation of once more than 25 % and once more than 20 % for this scenario.

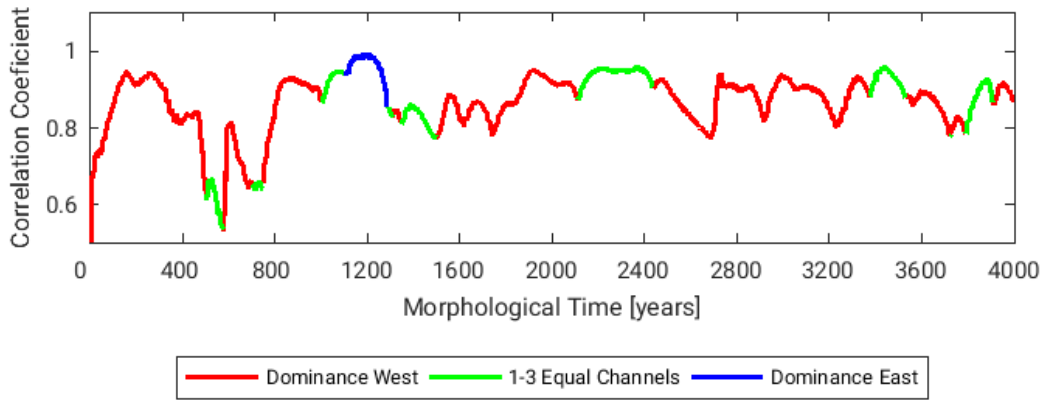

Figure 6.11: Cross-section 75 analyzed for channel dominance by comparing cases to the cross-section in time for scenario Kelvin wave

Case	Description			r^2 [%]
	No. of Channels	Dominance	Extend	
1	2	West	Narrow	10.5
2	1	West	Narrow	37.6
3	1	West	Wide	26.2
4	2	Equal	Wide	27.4
5	2	Equal	Small Hump	23.8
6	3	Equal	Wide	11.7
7	2	East	Narrow	4.9
8	1	East	Narrow	9.5
9	1	East	Wide	9.4

Table 6.2: Determination coefficient (r^2): Cases vs scenario Kelvin wave

6.3. Scenario: Coriolis

Morphological Equilibrium For the Coriolis scenario a morphological equilibrium cannot be indicated as clearly as in the simulations presented before. Looking at the cumulative bed load transport, according to figure 6.12a, there are three trends that can be observed throughout the whole simulation time:

The first spin-up phase with a significant negative growth of the cumulative transport can be determined until 500 MY.

The second phase with a less drastic negative growth goes from 500 MY until 3600 MY.

The third phase is the almost constant phase at the end of the plot from 3600 MY till 4000 MY.

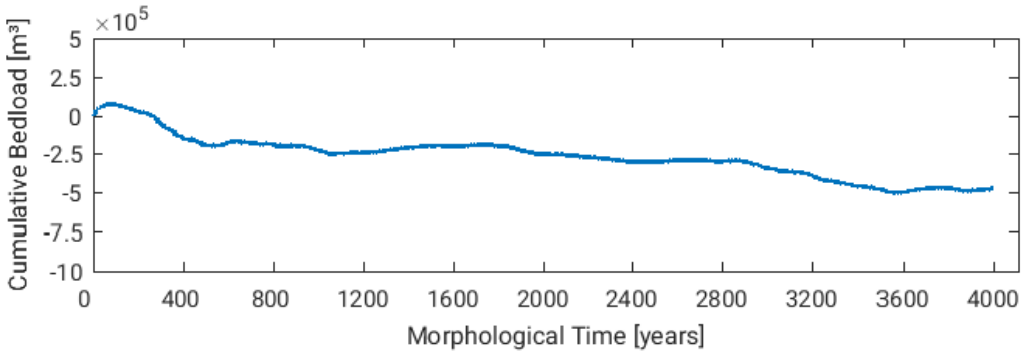

(a) Coriolis: Cumulative bed load transport

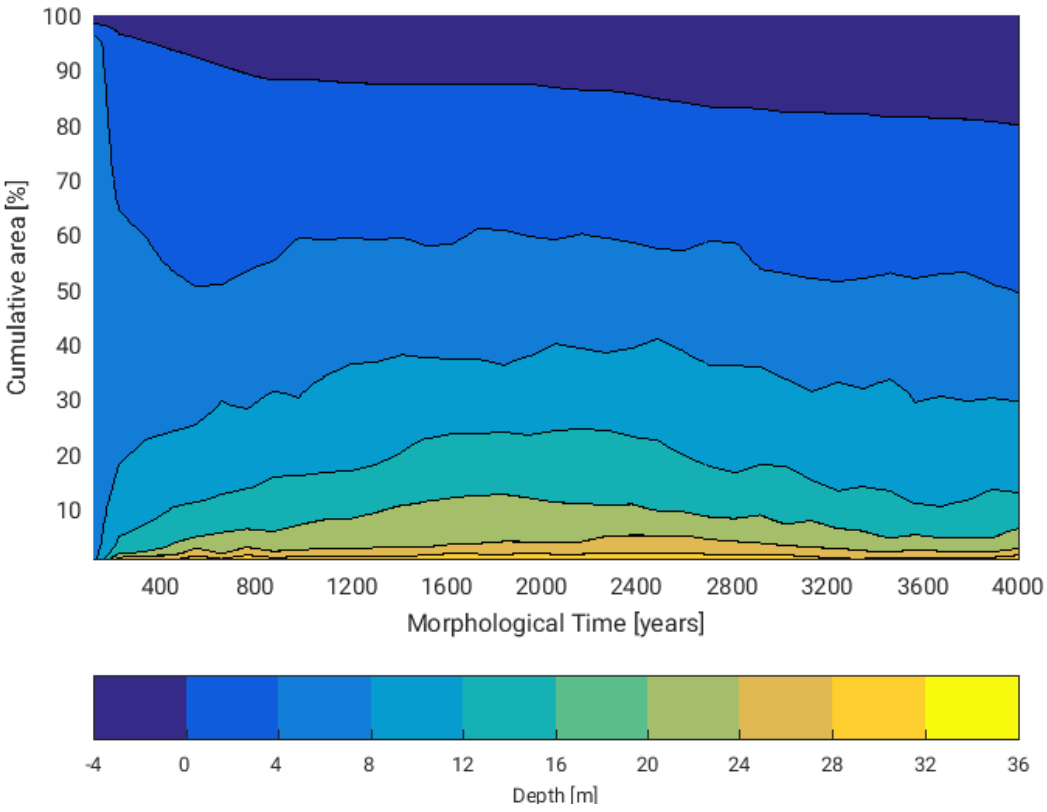

(b) Coriolis: Hypsometry over time inside the AOI

Figure 6.12: Coriolis: Equilibrium state in the AOI

The graphical trends are also indicated by the cumulative transport values at the beginning and end of each phase:

Within the first phase, around -200 000 m³ are imported within 500 MY.

In the second phase, the cumulative transport increases from -200 000 m³ till -450 000 m³ within 3100 MY.

In the last phase the cumulative transport remains roughly the same.

In order to determine if the morphology is getting to an equilibrium after the first phase or if it does get to an equilibrium at the end of the second phase close to the end of the simulation time, the development of the hypsometry over time is plotted. Generally, the hypsometry over time (figure 6.12b) does support the observation of a spin-up phase up until the MY 500. At that point in time all depth layers have developed to their full extend except the layer representative for the tidal flats which corresponds more with the second phase and has build up after more than 3000 years of morphodynamics. A clear indication for the striking change in the cumulative bed load transport at 3600 MY cannot be found in figure 6.12a. Based on the plots of figure 6.12 the spin-up phase is concluded to be 500 MY.

Channel / Shoal Patterns The simulation results of the Coriolis scenario are shown in figure 6.13 and can be compared to the base case scenario in order to investigate the influence of Coriolis on the development of channel and shoals. When comparing the depth contours of figure 6.13 with the results from the base case, a few differences are striking:

There are multiple channels that are approaching the AOI from the north.

The multiple channels from the north continuously unify with proceeding simulation time.

The unified channel from the north is not as deep as the channel from northwest but significantly wider.

The channel which flows from the northwest in the AOI is narrower in the Coriolis scenario compared to the base case.

The eastern channel seems to be deeper in the funnel shaped part most of the time.

Apart from the differences with the base case there are also some patterns that are mentionable. For most of the simulation time there are two channels that are relatively easy to distinguish, whereby the split into the two channels often happens in the middle of the funnel shaped part of the AOI. As the simulation time passes, the influence of the wide channel coming from the north side of the model domain increases and also influences the dominance of the eastern channel. However, as indicated by picture (e) of figure 6.13 there are also periods, where there is no clear dominance of the eastern channel in the whole AOI, although the overall eastern channel dominance is striking.

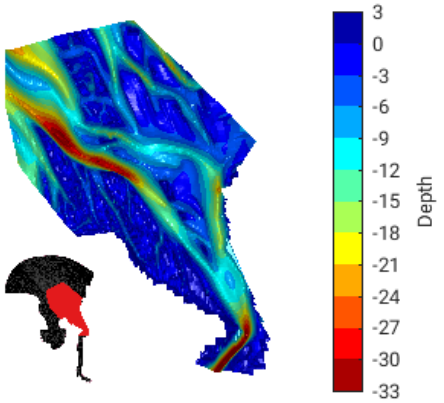

(a) Bathymetry at t = 500

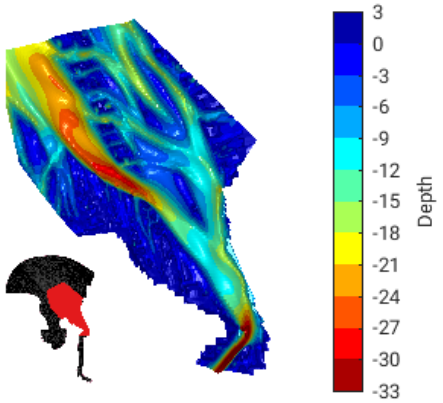

(b) Bathymetry at t = 1300

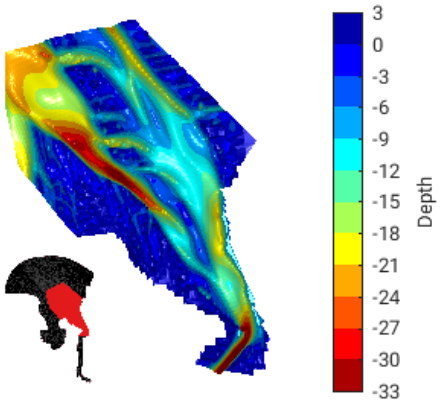

(c) Bathymetry at t = 2000

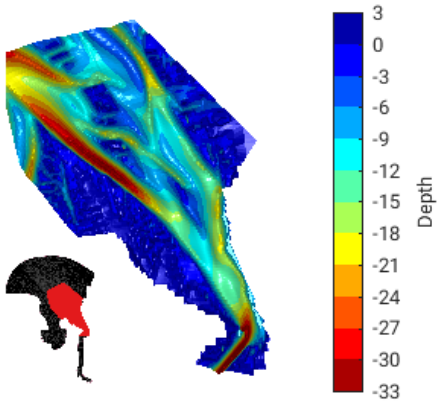

(d) Bathymetry at t = 2600

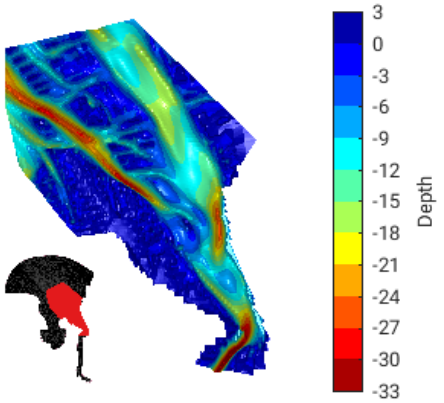

(e) Bathymetry at t = 3200

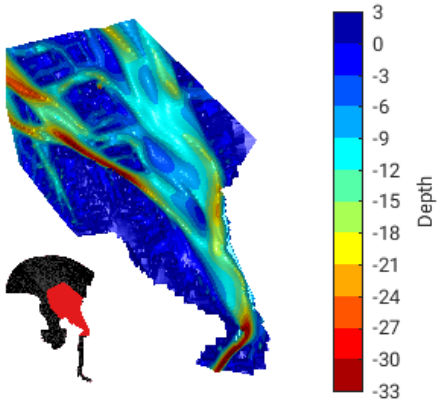

(f) Bathymetry at t = 3600

Figure 6.13: Scenario: Coriolis - bathymetry at different points in time

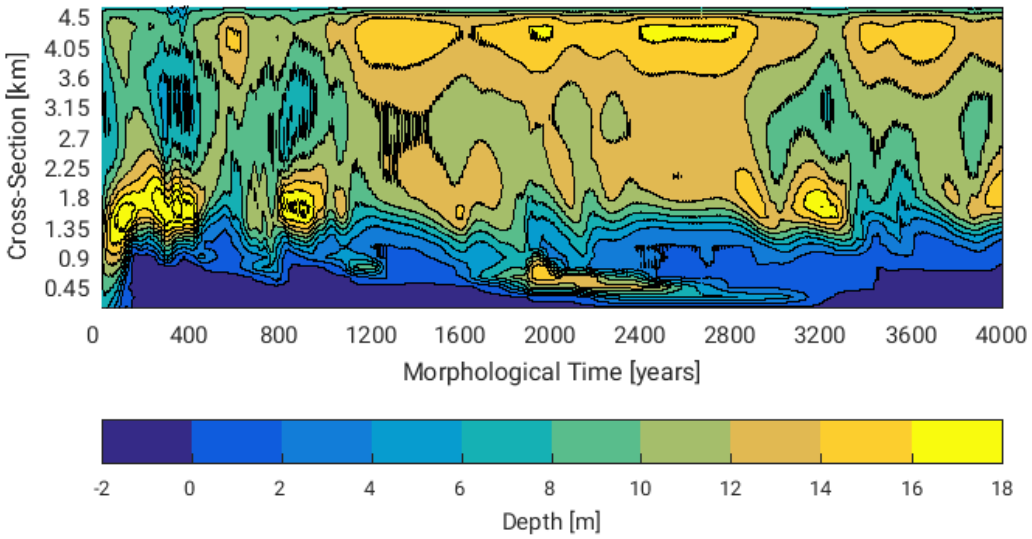

Figure 6.14: Cross-section 75 plotted over time for scenario Coriolis

Alternation Period For the assignment of a period to possible alternation pattern the cross-sectional development in time is examined. The first thing conspicuous in figure 6.14 is the presence of many wriggles along the individual contour lines. It could be reasoned that a high density of wriggles indicates morphodynamic activities in between two contour depth categories, since these are defined discrete. Furthermore, it is remarkable that the contour lines of several contour categories are aligned close to each other, especially in the parts between the tidal flats at the bottom of figure 6.14 and the channel pattern more centered. These closely aligned contour lines indicate high gradients from the tidal flats to the channels. Despite the striking arrangement of contour lines figure 6.14 supports the observations from the bathymetric plots: The eastern channel (at the top of figure 6.14) is the most dominant channel for most of the simulated time. Additionally, it reveals that starting from 500 MY there are periods where the western channel is more dominant than the eastern channel, at least in the cross-section 75. The western dominance can be found after 900, 1600, 3200 and 4000 MY. When looking at the second plot of EM2, figure 6.15, the mentioned western dominance cannot be found. Instead, the method reveals equal dominance for the points after 1600 and 4000 MY. Furthermore, the western dominance at 3200 MY is indicated for such a short period that it is hardly recognizable. The only clear indication of western dominance is during the spin-up time and after 900 MY. For the rest of the plot, an alternation between equal dominance and dominance of the eastern channel is found. It could rise doubts about the definition of the cases if the observations from figure 6.14 cannot be found in figure 6.15. Since the correlation coefficient itself is remarkably high and close to one, it can be assumed that the analysis is (according to the predefined cases) accurate. In order to determine a period, the same procedure as before is applied: Generation of a linear regression. Using the temporal center of the eastern dominance periods as input for the regression analysis results in an input array of [600, 1250, 2700, 3500] and a regression formulation of:

$$Y = 1015 * X - 525 \tag{6.3}$$

This would assign an alternation period of 1015 MY which is a bit more than an intuitive estimation according to figure 6.14 would indicate.

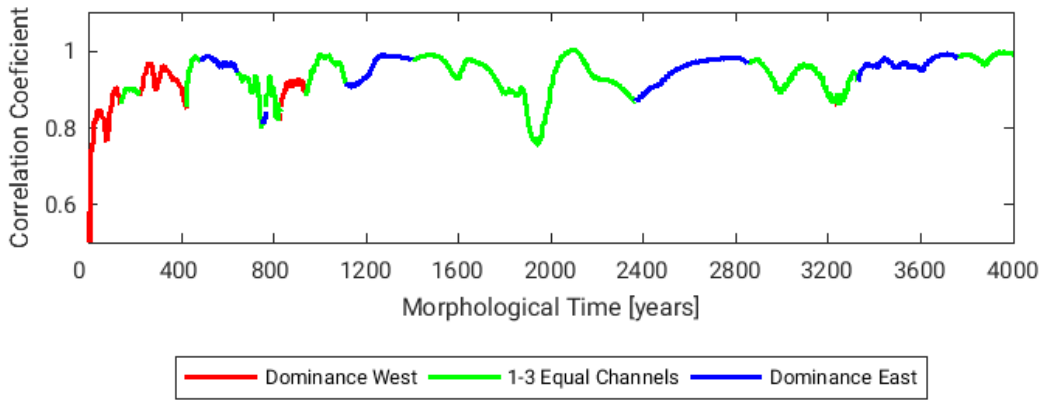

Figure 6.15: Cross-section 75 analyzed for channel dominance by comparing cases to the cross-section in time for scenario Coriolis

Overall Representation Analysis When looking at the representation of the individual cases, the speculation that has been made in the latter paragraph gets confirmed. It was stated that the second best correlation coefficient case at one point in time will not be indicated, even though the correlation coefficient might be high. Two cases that are representing a western dominant channel have representation of almost 45 % and over 20 % for the whole time series. But apart from the beginning, one short (around 900 MY) and one very short period (around 3200 MY) western dominance does not appear much in figure 6.15. The reason is that four other case have a representation value of more than 50 %. The case with the highest representation is case 5 which indicates an equal dominance or almost one unified wide channel with a representation of almost 75 %. Furthermore, with over 65 % case 9 (indicating eastern dominance) has a very high (second largest) representation for the whole time series as well. Together, with case 6 and 8 which are indicating equal dominance and eastern dominance, both with over 50 % of representation, theses cases characterize the overall behavior of the scenario Coriolis.

Case	Description			r^2 [%]
	No. of Channels	Dominance	Extend	
1	2	West	Narrow	0.7
2	1	West	Narrow	22.0
3	1	West	Wide	44.2
4	2	Equal	Wide	8.8
5	2	Equal	Small Hump	73.2
6	3	Equal	Wide	52.6
7	2	East	Narrow	15.9
8	1	East	Narrow	57.6
9	1	East	Wide	65.5

Table 6.3: Determination coefficient (r^2): Cases vs scenario Coriolis

6.4. Scenario: Waves

Morphological Equilibrium In order to find the morphological spin-up time for the wave scenario, the cumulative cross-sectional transport and the hypsometry over time are plotted and analyzed. The cumulative bed load transport can be divided into two phases: In the first phase (from 100 MY to 650 MY) the cumulative bed load shows a negative linear growth where sediment is imported (up to -300 000 m³) in the system south from the cross-section. The second phase starts from the morphological year 650 and goes until the end of the time series. It reveals an almost constant rate of sediment leaving and entering the system so that within around 1000 MY the cumulative transport increases from 300 000 m³ to 380 000 m³. This linear part can be considered the morphological equilibrium state. In order to confirm this estimation the hypsometry

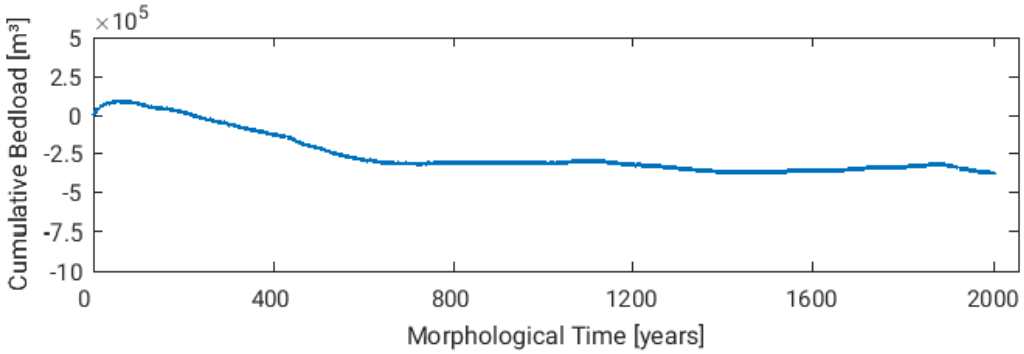

(a) Wave: Cumulative bed load transport

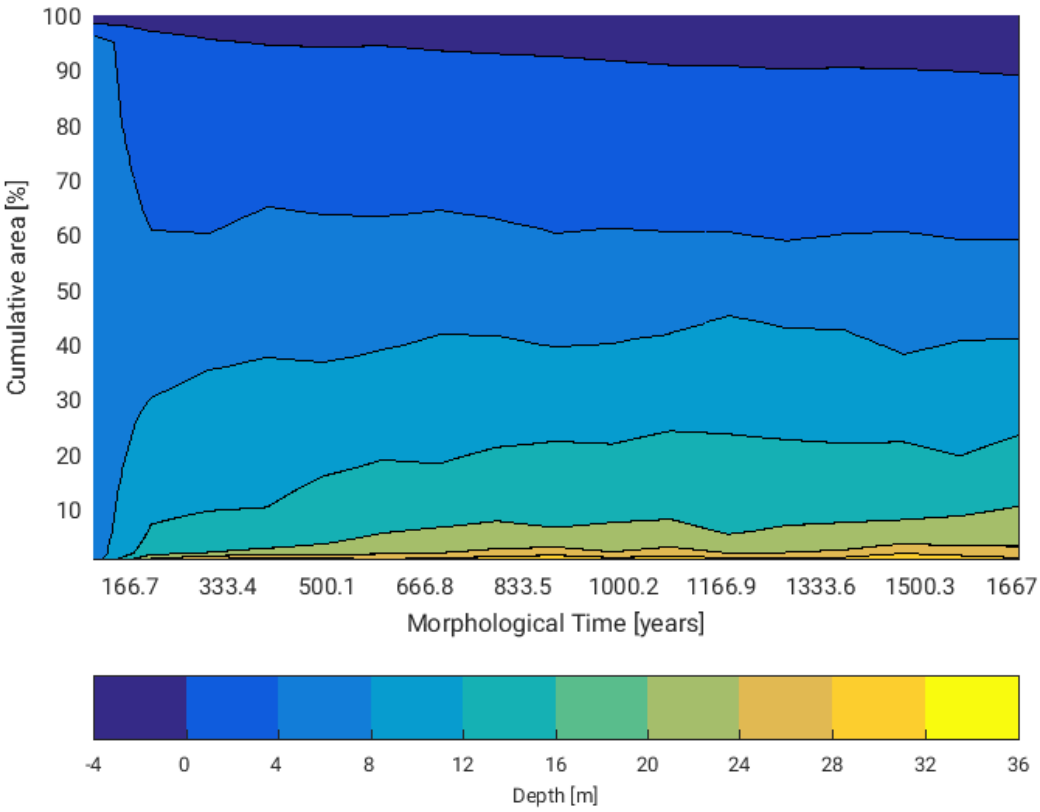

(b) Wave: Hypsometry over time inside the AOI

Figure 6.16: Wave: Equilibrium state in the AOI

of the AOI is plotted over time ((b) in figure 6.16) and can be investigated regarding an equilibrium as well. According to the hypsometry, a morphological equilibrium could be reached after 650 MY but it is not as clearly indicated as in part (a) of figure 6.16. The tidal flats (in dark blue) do not reach a clear equilibrium state

within this scenario simulation period, and the initial depth contours show that the tidal flats are reaching their equilibrium extend relatively fast. However, taking the contour section of 12-16 m depth into account and considering the observations described, it can be confirmed that the assumption of an equilibrium state after 650 MY is justified.

Channel / Shoal Pattern The bathymetries presented in figure 6.17 show the morphodynamic development of the AOI under the influence of waves. The depth contours generally differ from the bathymetries of the base case and of the first two scenarios. A general eastern tendency is clearly visible: The channel which comes from the north and flows out of the AOI in the western end of the Hohe Weg tidal flat area is much stronger (in terms of depth and extend) in this scenario than it is for the previously presented simulations. Consequently, the wadden area of the Hohe Weg has shifted towards the east as well (e.g. compared to the base case).

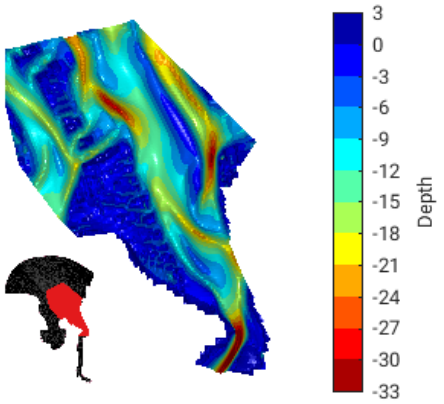

(a) Bathymetry at t = 650

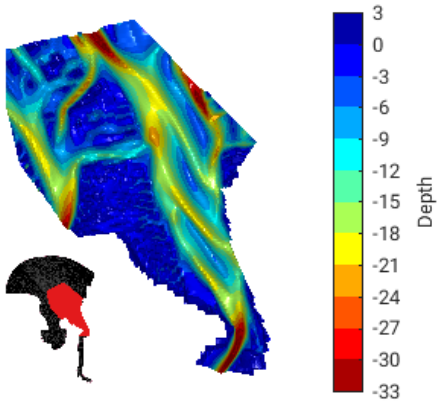

(b) Bathymetry at t = 900

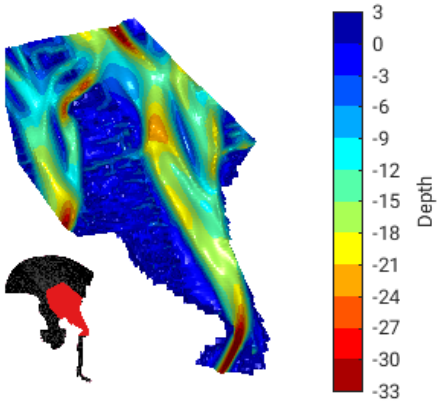

(c) Bathymetry at t = 1200

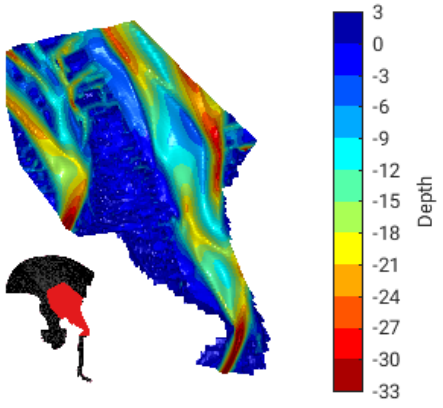

(d) Bathymetry at t = 1750

Figure 6.17: Scenario: Wave - bathymetry at different points in time

Furthermore, the tidal channel coming from the Lower Weser (having the same dimensions as in all previous

simulations) continues almost straight towards the northern end of the AOI and does not tend to flow towards the northwest part of the AOI as it appeared for the base case and the Kelvin wave scenario. Looking at the channel pattern in the AOI, a channel system develops where multiple channels can be seen at different location. A remarkable difference to the base case and previously described scenarios is the presence of extensive mid-deep/mid-shallow areas along the channel system. At some points in time there are two channels ((a), (d) and partly (b) of figure 6.17) as indicated in the base case. In picture (b) of figure 6.17 there are three channels arranged parallel to each other, staggered above each other coming from southeast and flowing towards northwest. At (c) there is mainly one channel in the funnel shaped area of the AOI, and for the other pictures there seems to be a small variation in the location of the deepest channel with a small tendency towards the east.

Alternation Period Next, it should be checked if through EM2 an alternation pattern can be identified and a period assigned. Figure 6.18 can give an overview about the channel development in the predefined cross-section that has been chosen to be representative. Starting with the investigation from the previously defined point of morphological equilibrium after 650 MY, some striking patterns are identified:

There are two channels clearly present at some point and evolved into one channel at other points.

The whole channel area is relatively deep.

The channel/channels itself are in quantity deeper as in the previous simulations.

The gradients between the tidal flats and the deep channels are relatively high.

A channel that is first present on the western side develops to a channel only present on the eastern side .

Taking the correlation analysis into account as well (figure 6.19) it reveals a clear pattern. After the spin-up time, there is an eastern dominance that changes into an equal dominance situation when the eastern channel looses depth while the western channel develops. As the western channel gains depth intensively, it becomes the dominant channel as indicated in figure 6.19 from 800 MY to 1200 MY. This changes when the western channel migrates towards the east and becomes the eastern channel with an increased depth, while there is no channel developing again on the western side. Consequently, figure 6.19 indicates eastern dominance from 1200 MY onward. After a certain time, a channel starts to develop on the western side again so that there are two channels again. But as the western channel does not reach the same depth as the eastern channel, it does not introduce an equal dominance situation until the end of the simulation period. Thus, during the simulation period one alternation is observed (dominance east - dominance west - dominance east). This one pattern is not enough to assign a period since it would introduce considerable uncertainties.

Overall Representation Analysis The figure 6.19 shows a correlation coefficient that is relatively low at the beginning but increases in time. After 1200 MY it has an average value of about 0.9. In order to quantify the observed pattern in the previous analysis, the determination coefficient is applied. The highest representation for the wave scenario can be found in combination with case 8 which has a representation of over 35 %. It represents eastern dominance which is in alignment with the visual observations made in figure 6.17. Surprisingly, case 5 which represents an equal dominance has the second largest representation for the time series although it does not appear much in figure 6.19. Also the third and fourth highest representation values belong to the eastern dominance category with a representation of about 23 %. Apart from that the western dominance category is hardly representative for this scenario. Two out of three cases are representative for less than 10 % of the time series and the highest case has a representation of 11.4 % which is significantly lower than the other cases. Comparing the numbers of the western dominance category with the plot of figure 6.19 it seems surprisingly that the plot indicates a western dominance phase for a considerable period. Nevertheless, the overall result clearly indicates the domination of the eastern channel that has been observed and described in the paragraphs above.

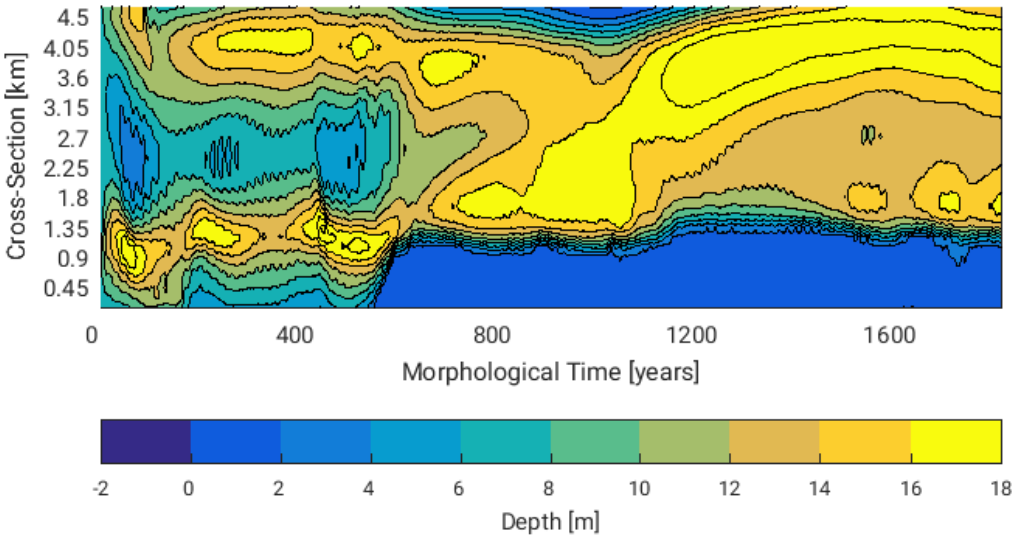

Figure 6.18: Cross-section 75 plotted over time for scenario Wave

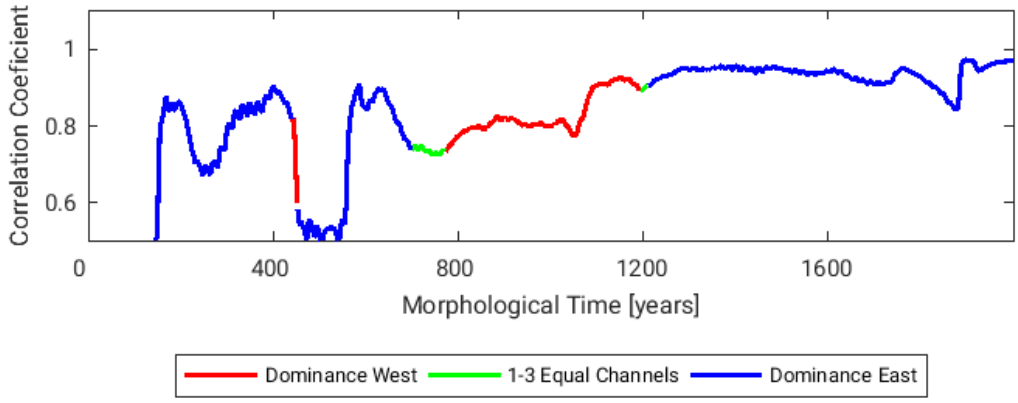

Figure 6.19: Cross-section 75 analyzed for channel dominance by comparing cases to the cross-section in time for scenario Wave

Case	Description			r^2 [%]
	No. of Channels	Dominance	Extend	
1	2	West	Narrow	5.8
2	1	West	Narrow	3.9
3	1	West	Wide	11.4
4	2	Equal	Wide	6.9
5	2	Equal	Small Hump	25.8
6	3	Equal	Wide	19.2
7	2	East	Narrow	23.1
8	1	East	Narrow	35.7
9	1	East	Wide	23.2

Table 6.4: Determination coefficient (r^2): Cases vs scenario Wave

6.5. Scenario: Extreme River Discharge

Morphological Equilibrium As for the other scenarios the analysis of this scenario starts with the investigation of a morphological equilibrium. Beginning with the cumulative bed load transport plot, the first striking detail is that the extreme river discharge scenario is the first scenario where the cumulative bed load transport is positive over time. It means that sediment is exported from the model domain south from the predefined cross-section due to the high discharge. Nevertheless, a point can be found where the initial growth of transport (from 0 m³ to around 400 000 m³ within 800 MY) is changing into a more constant progress (from 400 000 m³ till 420 000 m² within 3200 MY). Consequently, according to plot (a) of figure 6.20, this change can be localized after around 800 MY.

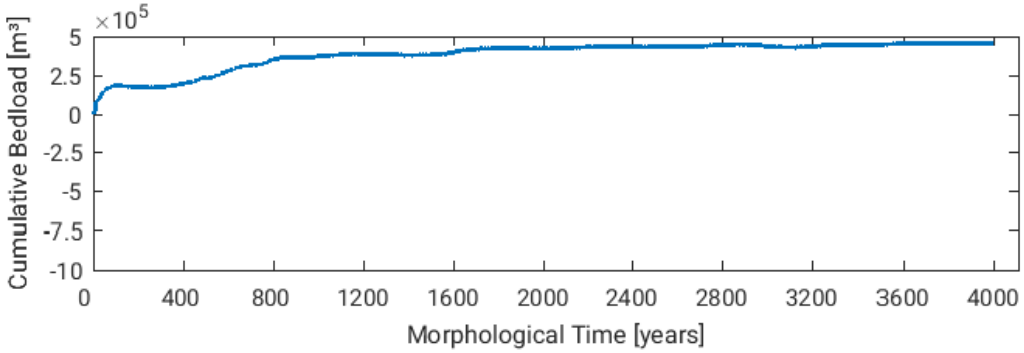

(a) Extreme river discharge: Cumulative bed load transport

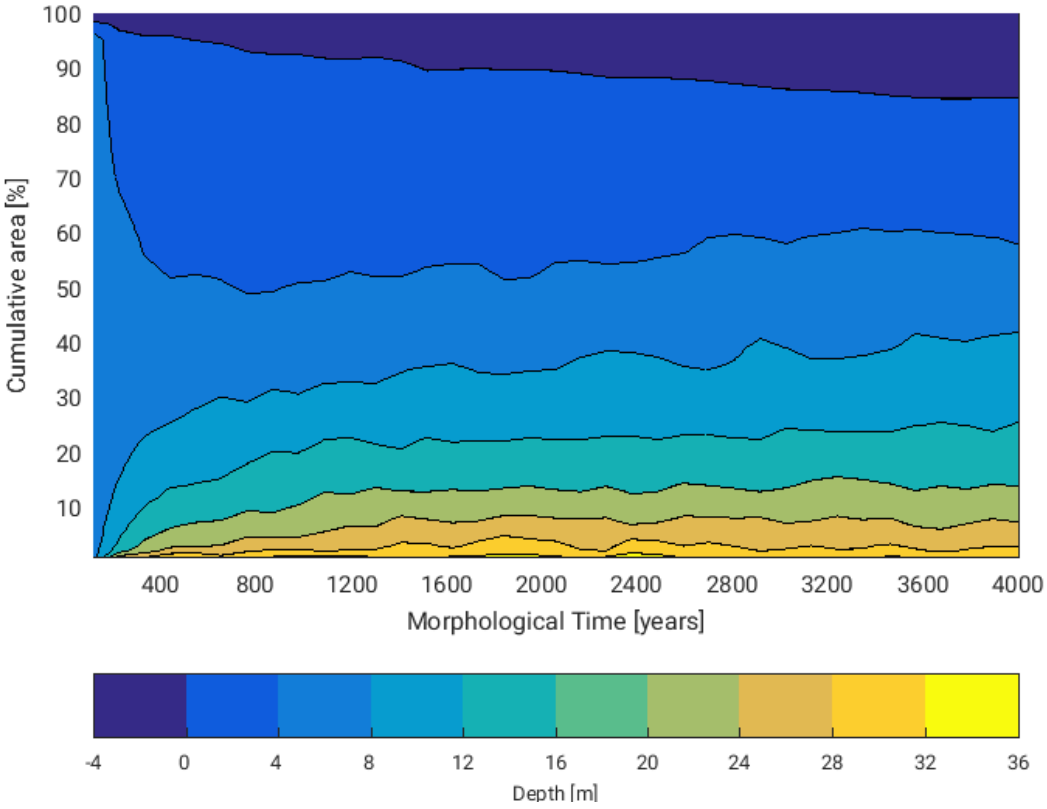

(b) Extreme river discharge: Hypsometry over time inside the AOI

Figure 6.20: Extreme river discharge: Equilibrium state in the AOI

To ensure that this observation is not misleading for further investigations, the hypsometry over time is plotted and analyzed. Similar as for the other scenarios, the hypsometry develops relatively fast and remains the same after a short spin-up phase. The spin-up time could indeed be estimated as 800 MY since from that mo-

ment onward there are just slight changes in the hypsometry, except for the contour category that represents the tidal flats. There, an equilibrium could be found after around 3600 MY but since the focus is put to the channels which develop relatively fast, this can be neglected in this analysis.

Channel / Shoal Pattern The bathymetric results of the extreme discharge scenario are shown in figure 6.22 and reveal some remarkable channel and shoal pattern: In the first two plots, after 800 MY and after 1200 MY there is a deep channel that originates in the center of the funnel shaped part of the AOI and then progresses strongly to the northwest, passing the northwestern corner of the funnel shaped part. In all previous simulations there has not been a channel drifting that far towards the west on that latitude. Later, the channel develops further east which can be observed in plot (c), (d) and (e) of figure 6.22. Additionally, except for (a) there are always two channel present in the funnel shaped part of the AOI. Over the whole time the eastern channel is deeper in the middle and northern section of the funnel shaped part of the AOI whereas the western channel is deeper on the southern part of the AOI when the two channels are splitting at the end of the Lower Weser. After 1200 MY on a small scale but increasing along the channel axis from (b) to (d). In (c), (d) and (e) the two channel are divided by a long and very narrow tidal shoal that can mainly be seen as a subtidal shoal. Furthermore, it is striking that the plots after 2000, 2700 and 3600 MY look fairly similar regarding the two channel arrangement. It seems as if the eastern channel is a bit deeper in the funnel shaped area.

Looking at figure 6.21, it can be controlled if the observation from the bathymetric plots can be confirmed by plotting the cross-section over time. This plot is used here to describe the morphological pattern that at first do not fit to the overall behavior of the previously described channel pattern. First of all, after 800 MY there are two channels present in the cross-section for most of the remaining simulation time. The two channels are clearly visible and generally have a relatively wide extend. Furthermore, from 800 MY until 1600 MY the eastern channel seems to be the dominant one, followed by a period where both channels are present with roughly the same depth until the morphological year 2500. From there on it looks like the western channel is more dominant, although from the morphological year 3000 onward a deep channel develops in the eastern area again. This description matches with the observations that have been made for the southern part of the AOI and will be set into context in the next chapter.

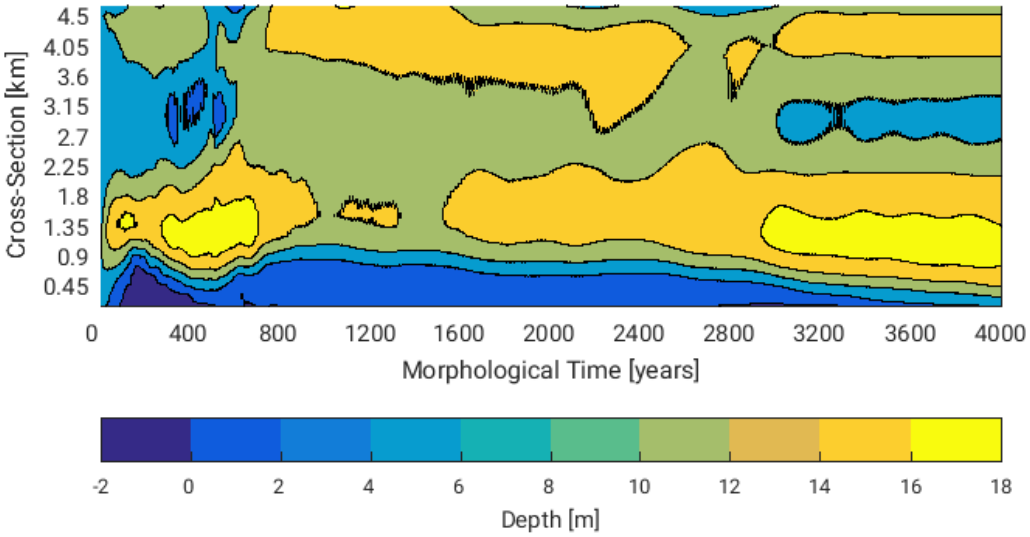

Figure 6.21: Cross-section 75 plotted over time for scenario extreme river discharge

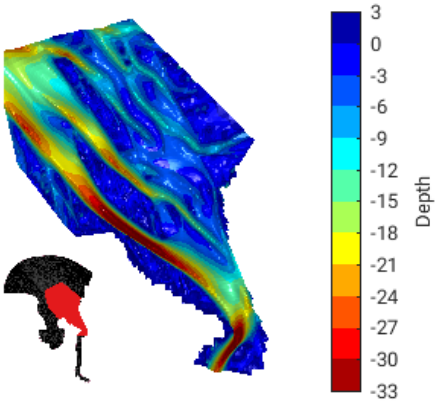

(a) Bathymetry at t = 800

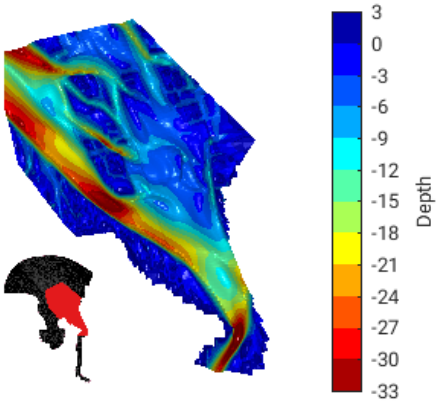

(b) Bathymetry at t = 1200

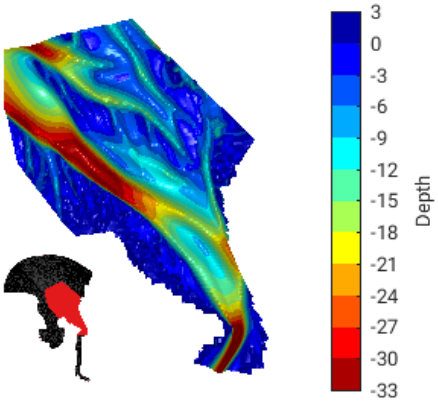

(c) Bathymetry at t = 2000

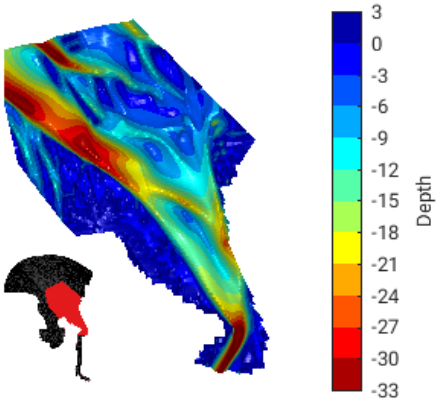

(d) Bathymetry at t = 2700

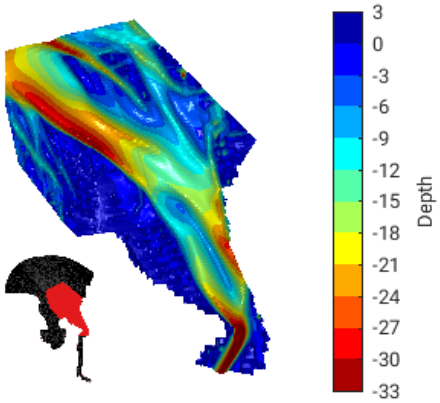

(e) Bathymetry at t = 3600

Figure 6.22: Extreme river discharge: Bathymetry at different points in time

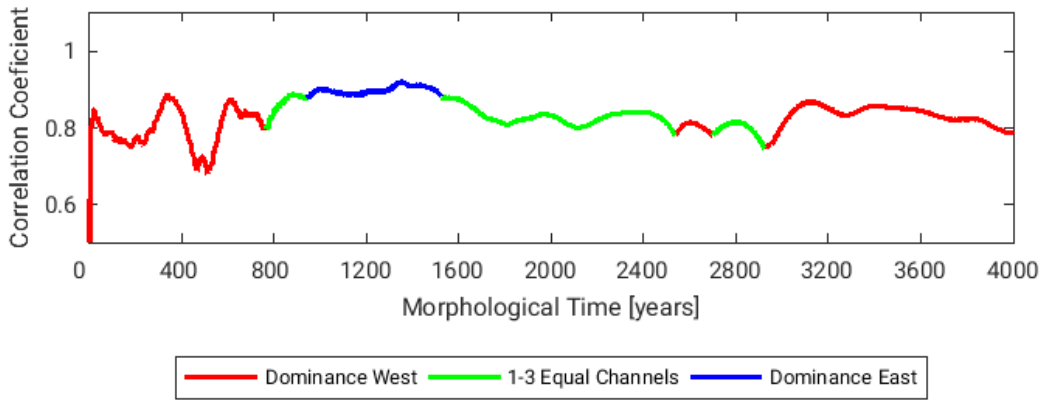

Figure 6.23: Extreme river discharge: Cross-section 75 cases analysis

Alternation Period In relation to the description given in the latter paragraph, it is checked if there is a period that can be assigned to some kind of alternation pattern. As described before, there has been a change in the location of the dominant channel, but in order to investigate if a periodic alternation can be observed the second plot from EM2 is analyzed: Starting with the morphological equilibrium state (defined at the beginning of this section) there is first a short period of equal dominance, followed by a phase of eastern dominance as described for the bathymetric plots. From 1500 MY a long period of equal dominance follows. Next, something that could be described as alternation pattern can be observed. At first, there is a very short phase of western dominance, secondly, a short period of equal dominance and at the end, a quite long section where the western channel is deeper and thus dominant. These indications from figure 6.23 match with the observations done in the latter paragraph. However, according to the descriptions it seems as if there is no clear alternation pattern visible that would follow a specific scheme. Instead, it reveals the general tendency towards western dominance in the southern part of the AOI but does not represent the development in the middle and northern part of the AOI.

Overall Representation Analysis Including the determination coefficient in the scenario investigation the analysis that have been made so far can be confirmed: The two best representations for the whole time series are given by cases of the category western dominance with over 40 and 36 % of representation. This supports the observations that the western channel seems to be more dominant in the southern part of the AOI of this scenario. Furthermore, the ambiguous observations about the alternative domination situations can be found in the overall representation. Both categories of equal and eastern dominance have two cases that are between 20 % and 30 % of representation and one case between 10 % and 20 %. Consequently, they can be considered as equally important as a secondary state in the southern part.

Case	Description			r^2 [%]
	No. of Channels	Dominance	Extend	
1	2	West	Narrow	36.0
2	1	West	Narrow	41.2
3	1	West	Wide	12.2
4	2	Equal	Wide	22.8
5	2	Equal	Small Hump	27.5
6	3	Equal	Wide	18.0
7	2	East	Narrow	26.4
8	1	East	Narrow	22.1
9	1	East	Wide	11.2

Table 6.5: Determination coefficient (r^2): Cases vs scenario extreme river discharge

6.6. Scenario: No River Discharge

Morphological Equilibrium The morphological equilibrium is, as done already for the other scenarios, determined by the cumulative bed load transport and the hypsometry of the AOI over time. The overall cumulative bed load transport has a negative value that is raising negatively within two phases: The first phase goes from 0 MY until 800 MY and can be characterized by a linear negative growth that reaches a value of -500000 m³ of bed load that are imported to the Weser estuary south from the current cross-section. From 800 MY until the end of the simulation there is an almost constant, slightly linear negative growth which increases the imported amount of bed load up to a value of - 1000000 m³. The cumulative transport is not constant in time so that it seems as if there is no real equilibrium. However, the almost constant and slightly inclined linear trend of the cumulative transport indicates that a state has developed which could be seen as a equilibrium state for this scenario. Consequently, part (a) of figure 6.24 indicates an equilibrium after 800 MY.

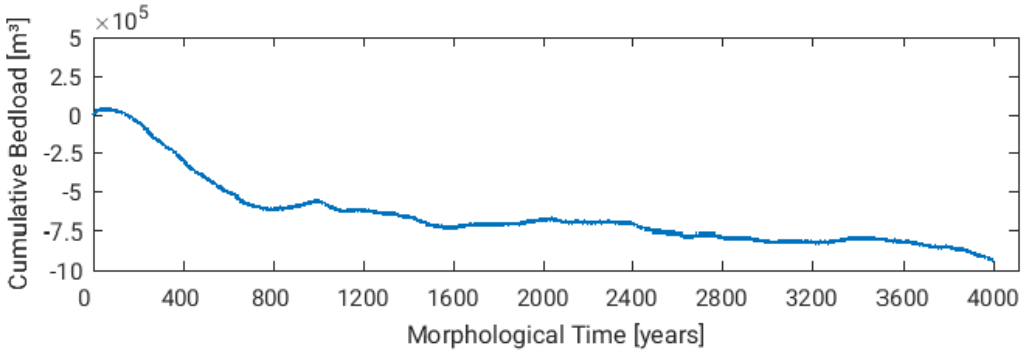

(a) No river discharge: Cumulative bed load transport

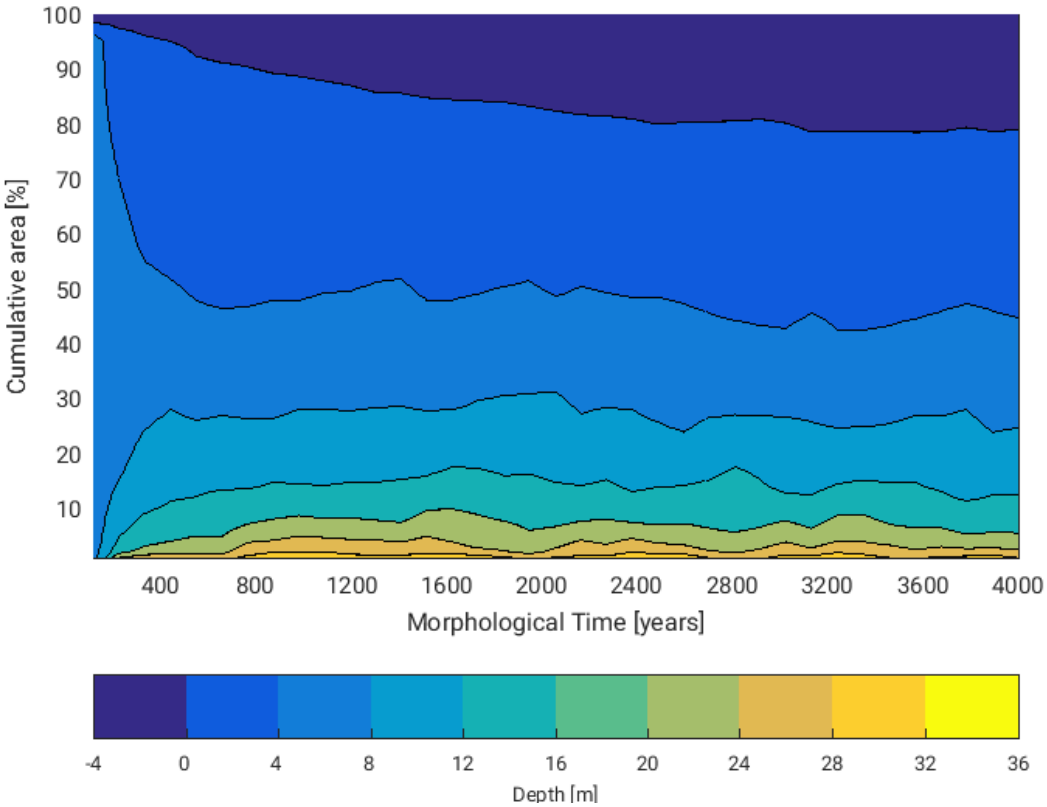

(b) No river discharge: Hypsometry over time inside the AOI

Figure 6.24: No river discharge: Equilibrium state in the AOI

Plot (b) of figure 6.24 indicates a relatively fast arrangement of the different depth contours in the AOI. Apart

from the depth contour range that represents the tidal flats (similar as in the other scenarios), all depth ranges are build up to an extend that they roughly keep until the end of the simulation period. It is challenging to specify one point from where on the depth ranges remain the same. Nevertheless, it seems reasonable that the point at 800 MY can be seen as the point where morphological-wise an equilibrium is reached.

Channel / Shoal Pattern The morphodynamic pattern that develop over time are described as follows: Even though there is no discharge from the river, the channel coming from the Lower Weser is at the same location and has the same dimensions as in the previously investigated scenarios. The same accounts for the one or two channels that are approaching the AOI from northwest coming from the North Sea. In between the channel coming from the Lower Weser and the channel coming from the North Sea there are two channels present most of the time ((a), (b), (e) and (f) in figure 6.26). Here, in the funnel shaped part of the AOI the western channel is present more often and more clearly, being wider and deeper than the eastern channel as in plot (c). At some points the eastern channel has the tendency to get very narrow ((b) and (c) of figure 6.26) and even detached from the western channel in the southern part of the funnel shaped area ((c) and (d) of figure 6.26). The western channel connects the channel from the Lower Weser with the channel from the North Sea relatively straight from southeast to northwest, whereas the eastern channel tendentiously first flows more northwards before it takes a path parallel to the western channel until the joint. Compared to the base case and other scenarios, at some points in time quite extensive tidal flats develop in between the two channels.

For an additional and more schematic analysis of the channel and shoal structure over time figure 6.25 is investigated as well. It reveals that the western channel (the yellow and orange area at the mid-bottom of the plot) can be indicated very clearly, whereas the eastern channel exists just temporary or as one wide channel where both the western and the eastern channel are connected with each other. Furthermore, it is remarkable that except for a very short time around 3600 MY the eastern channel in cross-section 75 is not deeper than 14 m. Together with the fact that the western channel is generally deeper or equally deep as the eastern channel it can be concluded that there is no alternation between western dominance and eastern dominance.

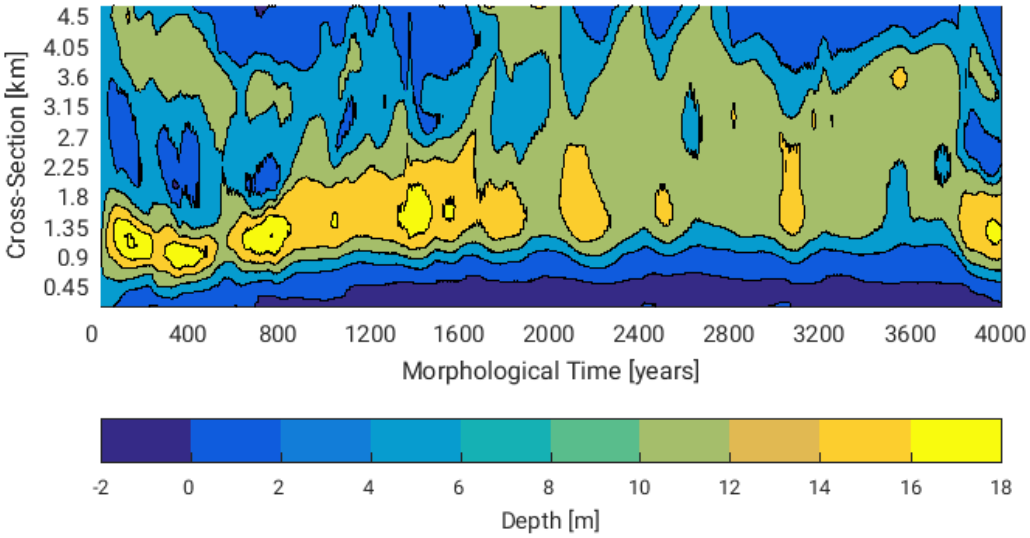

Figure 6.25: Cross-section 75 plotted over time for scenario no river discharge

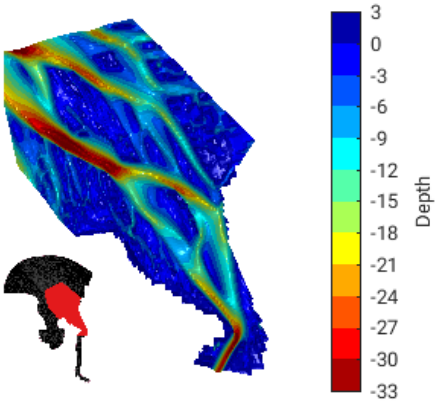

(a) Bathymetry at t = 800

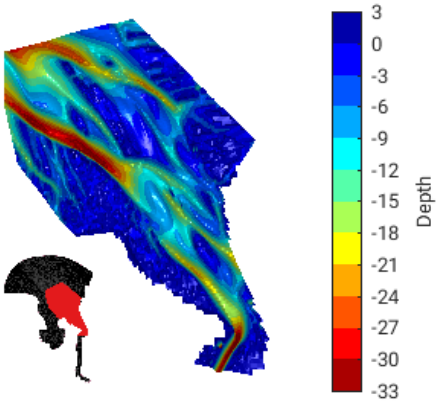

(b) Bathymetry at t = 1200

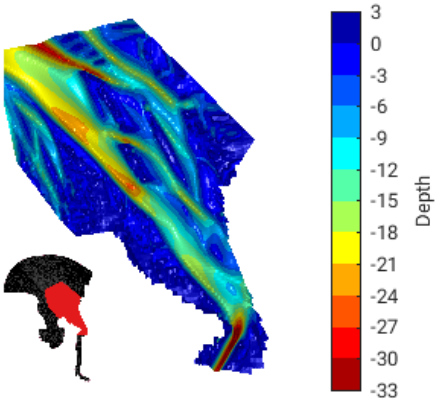

(c) Bathymetry at t = 1900

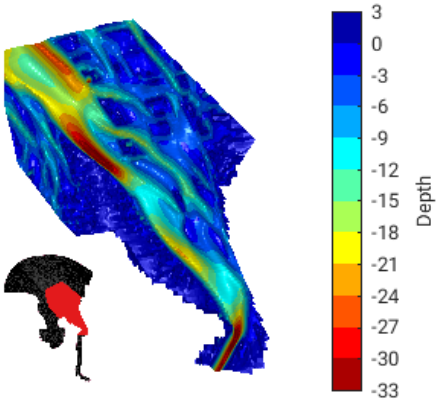

(d) Bathymetry at t = 2600

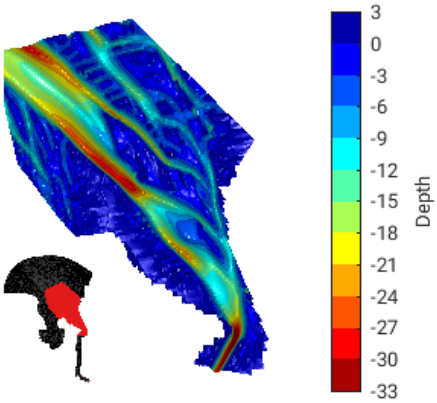

(e) Bathymetry at t = 3500

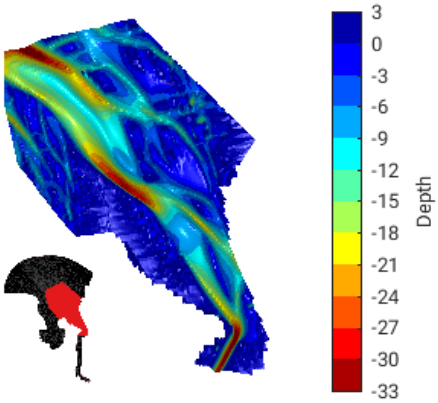

(f) Bathymetry at t = 3900

Figure 6.26: No river discharge: Bathymetry at different points in time

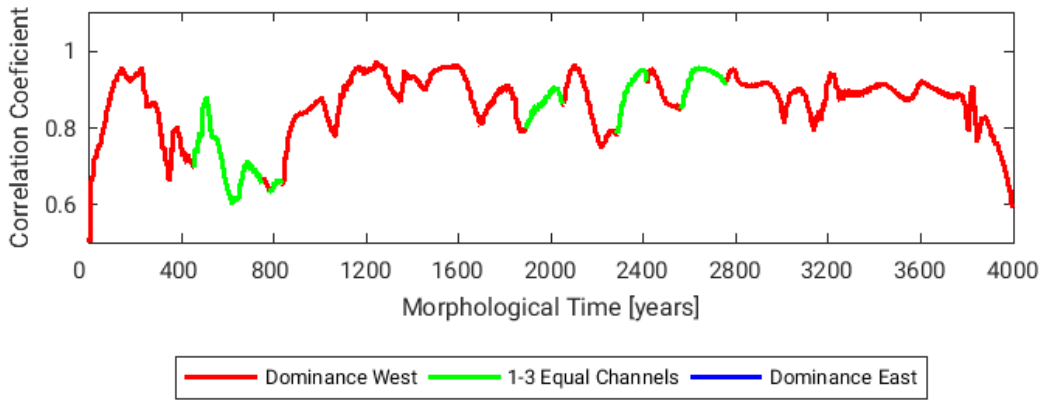

Figure 6.27: No river discharge: Cross-section 75 cases analysis

Alternation Period As stated in the previous paragraph, no alternation between eastern channel dominance and western dominance can be observed in figure 6.26 and 6.25. Nevertheless, since an alternation between the western channel dominance and equal dominance is observed, a period could be assigned to this pattern. This would also include the case where just one wide channel covers the center of the AOI as it has been described in figure 6.26 for some points in time. The second figure of EM2 (figure 6.27) should give an indication if there is an alternation period. The correlation case analysis shows the expected dominance of the western channel over time. Furthermore, the temporal equal dominance is confirmed by the correlation analysis as well and indicated by the plot. An exception that indicates a need of improvement for the EM2 can be found around the point 3500 where the depth contours clearly indicate the presence of an eastern channel, but the cases defined for the correlation analysis gives a better fit for the western than for the eastern dominance in this specific case. As a manual correction this point is taken into account in the linear regression in search for a period between the western dominance and the equal dominance. Thus, the input for the linear regression is 1950 MY, 2350 MY, 2700 MY and 3500 MY.

$$Y = 1375 + 500 * X \tag{6.4}$$

Consequently, a related period would be 500 MY.

Overall Representation Analysis The determination coefficient gives distinct results: The category that indicates dominance of the western channel has the highest representation with almost 40 %, 25 % and 10 %. In contrast, the eastern dominance category twice has a representation just above 5 % and once less than 3 %. The equal dominance category confirms the findings of the previous passages as well, since it has the second highest representation with 28 %, 18 % and 7 %. Consequently, the western dominance is much stronger than the equal dominance.

Case	Description			r^2 [%]
	No. of Channels	Dominance	Extend	
1	2	West	Narrow	10.6
2	1	West	Narrow	38.3
3	1	West	Wide	25.2
4	2	Equal	Wide	28.4
5	2	Equal	Small Hump	18.7
6	3	Equal	Wide	7.6
7	2	East	Narrow	2.6
8	1	East	Narrow	5.6
9	1	East	Wide	5.6

Table 6.6: Determination coefficient (r^2): Cases vs scenario no river discharge

6.7. Scenario: Increased Tidal Range

Morphological Equilibrium As for the previous scenarios, as a first step in analyzing the simulation results it is checked if a morphological equilibrium is reached at some point. Plot (a) of figure 6.28 gives an overview about the bed load transport development in time, where the cumulative transport can be divided into two phases, similar as for most of the other scenarios:

The first phase starts with the beginning of the scenario simulation and goes until 1100.

The second phase begins with the end of the first phase and continues until the end of the simulation.

During the first phase a steep linear negative growth characterizes the cumulative transport. Within the 1100 MY it reaches a value of around 480 000 m³. In the second phase the cumulative transport varies around a constant value of 480 000 m³ so that at the end there is no growth or loss in the cumulative bed load transport. The second option to investigate the existence of an equilibrium state for the scenario is an analysis of the

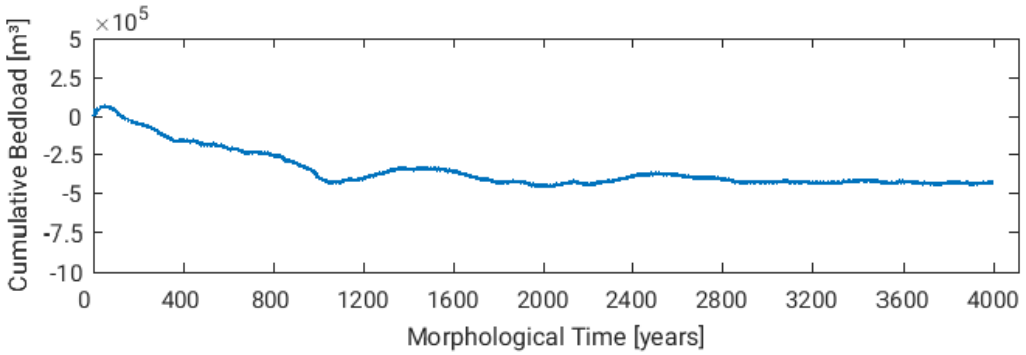

(a) Increased tidal range: Cumulative bed load transport

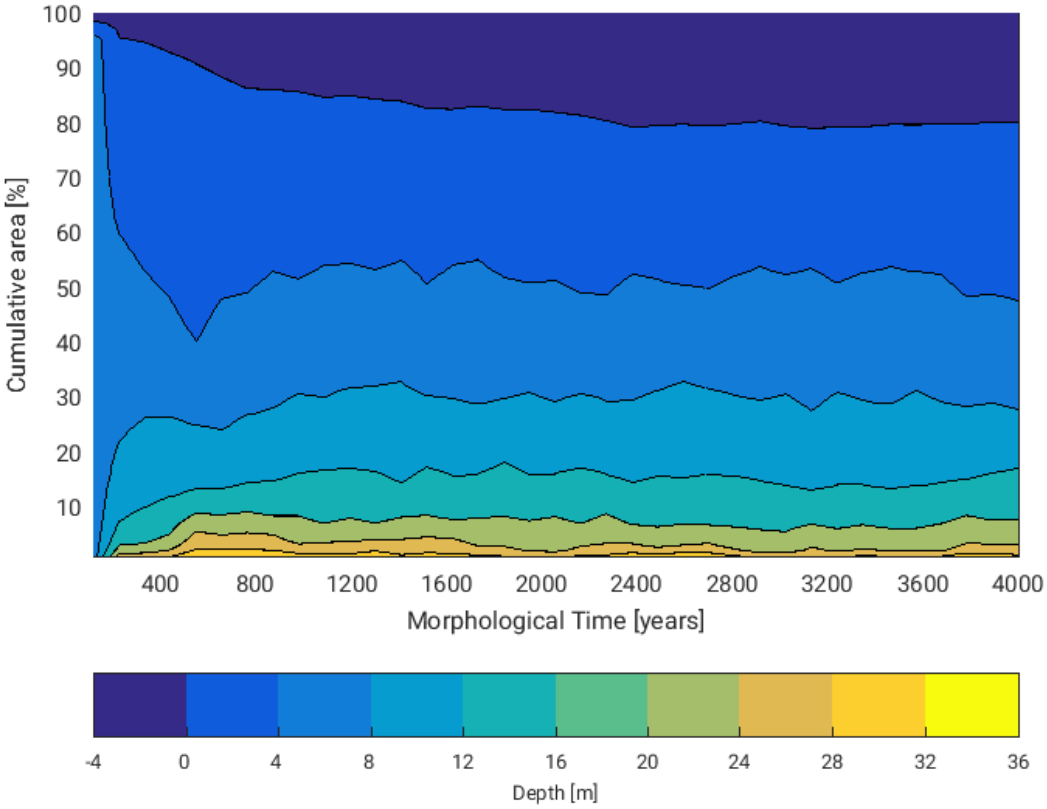

(b) No river discharge: Hypsometry over time inside the AOI

Figure 6.28: Increased tidal range: Equilibrium state in the AOI

hypsometry over time. Part (b) of Figure 6.28 shows the development of the different depth contour sections for the AOI of the model domain over time. After the initial state and a short dominance of the depth section 0-4 m around point 550 MY all sections are getting to an extend that remains roughly until the end. The only exception is the development of the tidal flats which takes a spin-up time much larger than the spin-up time for the development of channels. The tidal flats reach an equilibrium after around 2400 MY. The remaining depth sections are in an equilibrium state earlier. Since it is not easy to determine the spin-up time from the hypsometry alone, it is used as a confirmation analysis for the previously made observation where an equilibrium is reached after 1100 MY.

Channel / Shoal Pattern Analyzing the bathymetric results gives some inside on the effect that an increased tidal range has on the development of tidal flats and tidal channels. A striking pattern which can be observed is that there are two channels present in most of the plots inside the center of the AOI ((a), (d), (e) and (f) in figure 6.29). More specifically, the channels show different depth patterns over time:

There are phases where the western channel is deeper (picture (b)) .

In other phases the eastern channel has a higher depth (picture (f)).

As in the other scenarios, the channel coming from the Lower Weser is at the exact same location as for the base case. Furthermore, the main channel that comes from the North Sea and enters the AOI from the northwest corner, is at the same location as in the base case. There are also small side channels that approach the AOI from the north. Side channels from the north could have been observed in other scenarios as well, but here, in this scenario there is a side channel visible in (b) to (f) of figure 6.29 that seems to connect to the eastern channel in the funnel shaped part of the AOI. It is relatively deep, narrow and does not vary much in shape and extend, in contrast to the two channels connecting the channel from the south with the channels from the north. As already introduced in the beginning of this paragraph, different situations are found where the depth contours differ between the two channels and are almost reversed. Where (d) and (e) show a similar depth pattern of two channels that are almost equally deep, there is a three phase turn of the deepest channel in plot (c) for example. At the southern part of the funnel shaped part, the eastern channel is the deeper one. In the middle the eastern channel does hardly exist as a very narrow and shallow side channel, whereas the western channel is clearly deeper and wider with a depth of around 30 m. In the most northern part, the western channel is still present and also keeps its width, but the eastern channel that comes from the north has a higher depth while it has more or less the same width. Another example is plot (f) where the eastern channel is dominant in the south and intertwines with the western channel which is more dominant in the north. Summarizing, figure 6.29 reveals a variety of different channel and shoal patterns over time that can easily be categorized but not easily be converted into a scheme of recurring patterns.

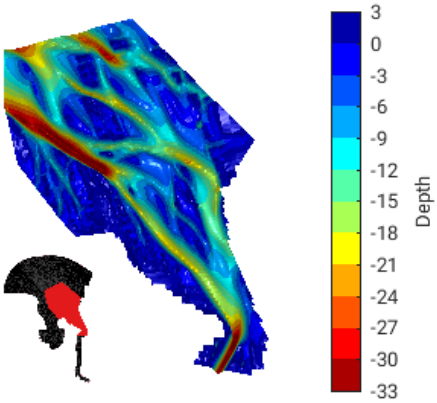

(a) Bathymetry at t = 1200

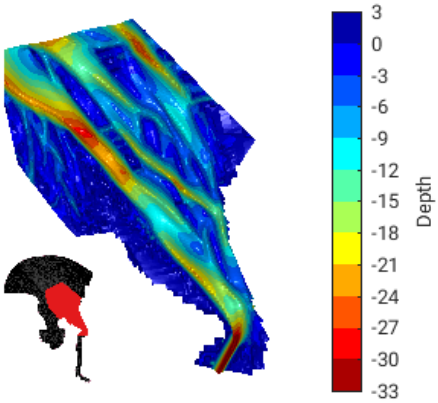

(b) Bathymetry at t = 1900

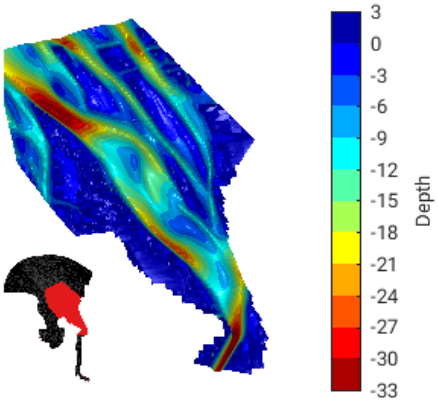

(c) Bathymetry at t = 2300

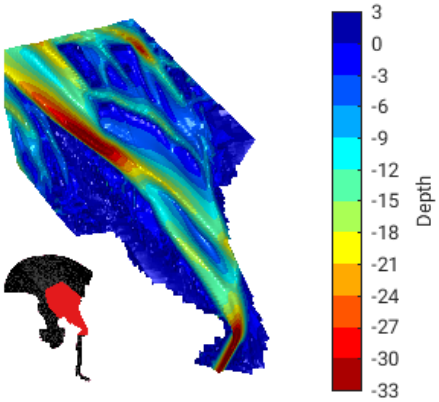

(d) Bathymetry at t = 2600

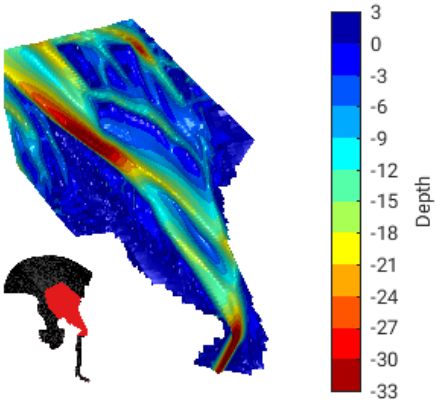

(e) Bathymetry at t = 3500

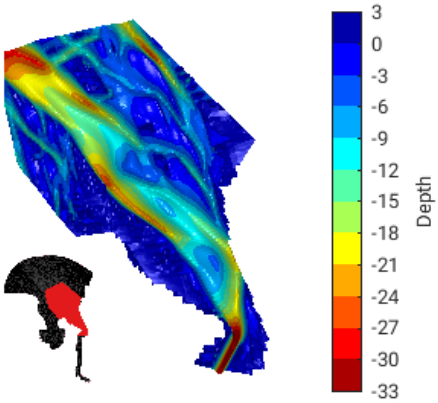

(f) Bathymetry at t = 3900

Figure 6.29: Increased tidal range: Bathymetry at different points in time

Alternation Period What has been difficult in the latter paragraph will be done in this paragraph: Searching for recurring patterns and assign a period to it, if possible. By means of EM2 the channel pattern is schematized so that figure 6.30 gives the location of the tidal channels over time along the cross-section 75. Starting at 1100 MY (the equilibrium state) three schematically recurrent pattern can be found: First, a quite deep channel develops on the western side (bottom of the plot) which after a period of 200-400 MY decreases in depth until there is an equal depth along the inner part of the cross-section, followed by a channel that develops on the eastern side (top of the plot) whereas the western channel has disappeared. This pattern can be found three times although the dimensions do not always match with the previously described ones.

A squeezed version of that pattern is found from 1100 MY to 1400 MY.

It is also found with an extensive western channel (lasting for 600 MY) from 1400 MY until 2600 MY.

Lastly, it is found with a comparatively small western channel from 3000 MY until 3800 MY.

In order to assign a period to this behavior the second plot from EM2 is analyzed (figure 6.31). Since in the first phase where the recurrent pattern has been indicated the eastern channel at the end of the schematic pattern is very small and the depth at the location of the western channel is relatively deep, it is not recognized as easterly dominated. Thus, this first period needs to be taken into consideration carefully when looking for alternation patterns. The second detection is clearly indicated in figure 6.31, where a first intensive period of western dominance is followed by a short period of equal dominance and completed by a clearly indicated period of eastern dominance. The same accounts for the third appearance of the described pattern, although the period of western dominance is shorter and the period of equal dominance is longer compared to the second time. If the first indicated pattern is taken into account (even though it does not meet the full described pattern in figure 6.31) and the temporal center of the recurrent pattern would be considered as well, the resulting linear regression would be:

$$Y = \frac{200}{3} + 1075 * X \tag{6.5}$$

Whereas, if only the recurrent pattern indicated by figure 6.31 is taken into account, the resulting equation would be:

$$Y = 600 + 1400 * X \tag{6.6}$$

Summarizing, the period of the alternation pattern for the scenario increased tidal range would be 1075 MY when taking the all three patterns into account and 1400 MY when only considering the overall fully matching alternation patterns.

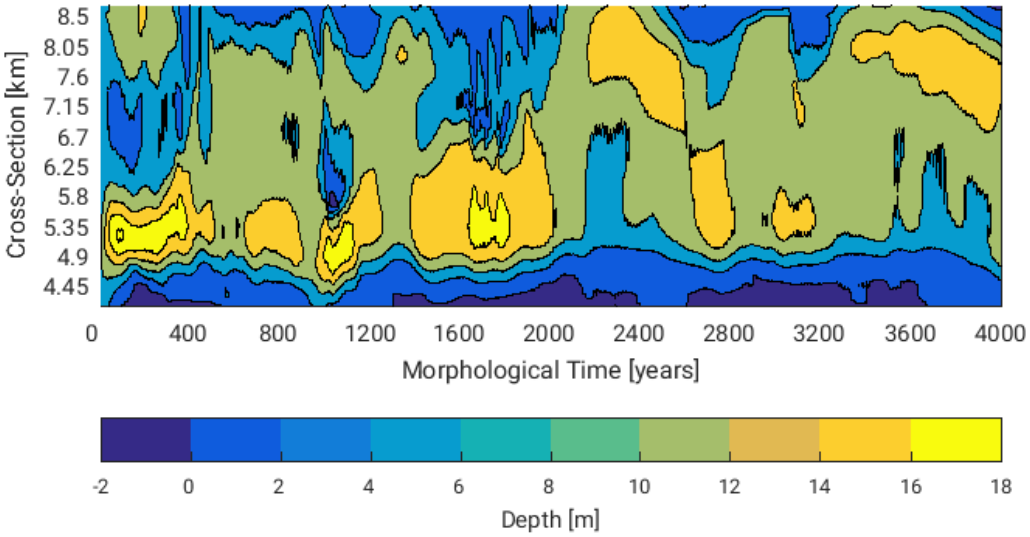

Figure 6.30: Increased tidal range: Cross-section 75 over time

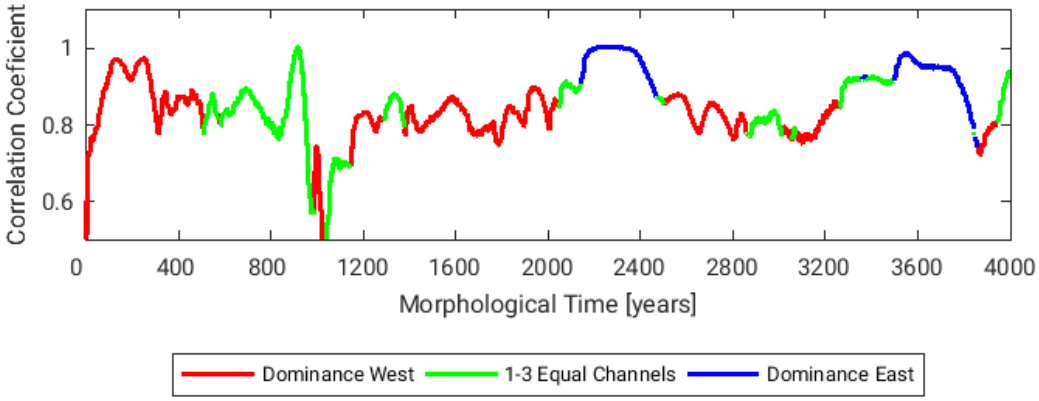

Figure 6.31: Increased tidal range: Cross-section 75 cases analysis

Overall Representation Analysis In order to quantify the observations made in figure 6.30 and 6.31, the determination coefficient is applied to indicate the representation of the individual cases for the scenario cross-section. In figure 6.31 the colors that have the highest appearance are red and green, thus it would be expected that the categories western dominance and equal dominance have the highest representation rates. Indeed, both categories have one case with over 30 % of representation, one case with around 25 % representation and one case with over 10 % of representation for the whole time series. The third category of eastern dominance, colored blue, is only indicated twice for a relatively short period in the correlation coefficient plot. With twice slightly more than 10 % and once below 10 % the eastern dominance cases are poorly representative for this scenario, even less than what would have been expected from the two peaks in figure 6.31. The reason is that for some periods in this scenario the correlation coefficient for the eastern dominance cases is getting negative, which decreases the mean correlation coefficient that is the square-root of the determination coefficient indicated in table 6.7.

Case	Description			r^2 [%]
	No. of Channels	Dominance	Extend	
1	2	West	Narrow	14.0
2	1	West	Narrow	31.3
3	1	West	Wide	25.3
4	2	Equal	Wide	32.6
5	2	Equal	Small Hump	24.5
6	3	Equal	Wide	12.9
7	2	East	Narrow	8.3
8	1	East	Narrow	13.1
9	1	East	Wide	10.9

Table 6.7: Determination coefficient (r^2): Cases vs scenario increased tidal range

7 Discussions

The discussion for this project is split into three parts in order to give account to the different questions that are aimed to be answered within this project. Therefore, firstly, the analysis of the results (chapter 6) is elaborated, secondly, the general investigation approach (chapter 4) will be reflected and thirdly, an outlook about potential investigations that could be built up on this project is given.

7.1. Discussion of the Results

7.1.1. Reflection on of the Base Case

Hydrodynamics In the subsection 6.1.1 the base case hydrodynamics are presented in three categories:
The equilibrium tide is a result of the combined effects of the flat bed as an initial bathymetry and the initial conditions for the water level. Since it is model related it can neither be compared to measurements from reality nor to the hydrodynamic spin-up time of other models applied at BAW due to the absence of the flat bed topography in these. However, it is seen as a positive sign for the model that an equilibrium is reached at some point and additionally, it is seen as a confirmation for the long simulation period.
As a second aspect the development of the tidal range in the Weser estuary is plotted and explained. It reveals an increase of the tidal range from the Outer Weser estuary to the Lower Weser estuary. This development is matching with the present day tidal range characteristics in the Weser estuary. However, as indicated in figure B.1 the historical tidal range that is aimed to be reproduced shows a decrease of the tidal range towards the Lower Weser estuary. It decreases until the tidal range is small enough to be assumed negligible and let to the definition of the model extend (section 4.1). On the one hand, the considerable tidal range that can be found in the model at the southern open bounday while there has been assumed to be a negliglible tidal range is questioning the applicability of the model. On the other hand, the tidal range at Bremerhaven (and consequently the AOI) in the model is around 4 m and 3.8 m in reality [22] which is a quite good match. Furthermore, the southern open boundary is relatively far away from the AOI and thus does presumably not have a very strong influence on the generation of the morphodynamics in the Outer Weser esturay. Nevertheless, the contradiction between the tidal range of the model and of the historical measurements is an important factor that should be considered and improved when continuing working with this model. A simple explanation is found in the roughness height predictor that has been taken from the Weser model by Herrling [13] without further adjusting. Herrling calibrated the model such that it represents the present hydrodynamics whereas the model in this project simulates the past. Consequently, the assumption that the roughness height predictor will be representative for the historical situation as well was conditionally not correct. It is not sure that the roughness height predictor is the only cause of the increasing development of the tidal range and optional future simulations will need to prove this hypothesis.
As the third aspect the tidal dominance is schematically indicated. The base case simulation reveals a symmetric tidal flow in the Outer Weser and a flood dominant tidal flow in the Lower Weser estuary, both during spring and during neap tide.
As introduced in chapter 2 the nowadays tidal-flow-dominance of the Weser estuary is a bit more complicated. However, in a broad sense the simulated tidal-flow-domination does match to the observations described by Zorndt [48]. A comparison with the historical situation is more difficult, due to the lack of documentation from the historical tidal dominance. Still, for the Lower Weser that has been modeled at its his-

torical state by Herrling [14], the flood-dominant behavior found in the simulations can be validated. For the Outer Weser it is not possible to give a valid assessment with the current information acquired.

Morphodynamics The principle morphodynamics of the base case simulation show a relatively good fit to the historical shoal and channel system. Since the Outer Weser morphodynamics have been applied as the calibration criteria and been described in chapter 5, the review of the overall morphodynamics is kept short: The large scale morphodynamics, by means of the number of channels, their locations and the overall alternating pattern, are represented well by the base case model. More specifically, the two main channels that are characteristic for the Outer Weser estuary, the Jade channel and the channel that develops in the north west of the model domain can be found in the historical charts and party can be recognized in nowadays bathymetries. Furthermore, the extend and height of tidal shoals in the whole model domain generally matches the historical and present observations. Together with the fact that the morphydynamics show a clear alternation pattern, all aspects together form the well representative features of the morphodynamics.
Less good represented aspects can be found in the channel depths. Generally, the model is overestimating the depth of the channels by an order of magnitude, which might be linked to the roughness height predictor, that has not been calibrated in this project. Additionally, small scale features, such as side channels and the migration of dunes and ripples (described in chapter 2) have been determined as less important for the purposes of this model and thus are not well represented as well. Furthermore, the timescale of the alternation pattern differs drastically from the historically observed and described one. Instead of 60-70 years or 110-120 years the base case simulation reveals an alternation period of 1150 MY. The reason for this discrepancy might be found in the intentionally introduced denotation "MY (morphological years)". The hydrodynamic results are multiplied with a constant factor that represents the number of morphodynamic developments equal to the given factor with the same hydrodynamic conditions. Since this MORFAC has been chosen to be large it tends to distort the results gained. It is a clear disadvantage and results in qualitative results rather than quantitative.
Due to the simplification made within this project, the model generated represents very specific features of the Weser estuary only. Its morphodynamic representation is restricted to the Outer Weser part, since this has been the calibration focus. The model has been build-up in order to investigate macro-scale features, consequently, it is not suitable for micro-scale investigations. Additionally, results should be seen on a qualitatively level rather than on a quantitative one. Generally, looking at the morphodynamics, the model most likely has the ability to serve more and other duties than the once defined within this project, but that would necessarily require model improvements. At the current state, the model is suitable to look at the large scale development of the morphodynamics and the qualitative results of alternating patterns.

7.1.2. Reflection of the Scenario Results

In the latter chapter the simulation results have been presented and described. Chapter 3 presents the derivation of the scenario composition and introduces the reasoning for the selection of each individual scenario. Following this argumentation, the scenario simulations are now being analyzed regarding two categorizations:

1. Do the scenario simulations reveal changes within a system or do they indicate the development of a new system?

2. What scenario induced variations in the alternation of the two channel system can be found?

By categorizing the scenarios a structured analysis is enabled that can sort the scenarios according to their effect. The first question examines the effect of the different model set-ups and consequently different influences on the generation of tidal flats and tidal channels. This investigation is done by looking at the characteristics of the estuarine system. Insight can be gained by analyzing the characteristics; whether the external force introduced in the individual scenario is changing the arrangement of tidal channels and shoals within a system or if the scenario simulation changes the estuarine system itself.
The second question is used for identifying the interpretation of alternation patterns in case they are existing in the scenario. If that is the case and a period has been assigned to an alternation pattern, relations can be built-up between the external forces and the alternation period.

Kelvin Wave

1. Comparing the hypsometries over time generated for the whole area (appendix E) reveals no significant differences. The Kelvin wave scenario shows less channel areas that are between 20 and 24 m of depth but include deeper channel areas (>24 m depth). Since the percentage of supra-tidal, inter-tidal, sub-tidal and channel zones is roughly the same, it is taken as an indication that the Kelvin wave scenario simulation is reproducing the same tidal system as the base case. Looking at the bathymetry plots of the Kelvin wave scenario and the base case supports this conclusion, since the tidal channels shown in the bathymetries are similar in location and dimension compared to the base case. Another indication is the spin-up time for a morphological equilibrium state. For both the Kelvin wave scenario and the base case the deep areas are in equilibrium after around 1100 MY whereas the supra-tidal areas need a higher spin-up time. This could be an indication for the same tidal prism to develop, but the evidence cannot be given, since an analysis of the hydrodynamics is not yet included in this project.

2. When comparing the results of EM2 the Kelvin wave scenario has a comparable alternation pattern to the base case, but with a significant difference: Instead of an alternation of the eastern and western channel, there is an alternation of the western channel with an equal dominance situation. Figure 6.11 indicates the missing of an eastern dominance periods except for one happening. Additionally, the period of the alternation between the western dominance and equal dominance has been analyzed to have a period of 757 MY which indicates a shorter alternation interval compared to the base case. Furthermore, the simulation, excluding the Kelvin wave, results in strong dominance of the western channel. The determination coefficient in the Kelvin wave scenario shows the same percentage as the most representative western dominance case in the base case simulation (37.6 vs 38.9). The highest percentage that is representing the equal dominance and the eastern dominance categories in this simulation, are factor 2-4 smaller compared to the base case simulation, which is including the Kelvin wave.

Summarizing, the research question asking for the influence of the Kelvin wave can be answered at least schematically: The Kelvin wave introduces a stronger eastern channel. This reasoning is possible, as the simulation disregarding the Kelvin wave shows almost the same western channel, but a less dominant eastern channel. Consequently, by increasing the overall dominance of the eastern channel due to the Kelvin wave, the morphological time that is needed to change the bathymetry temporarily back to a western dominance increases. This explains the shortening alternation period that has been determined in the result description of the Kelvin wave scenario.

Coriolis

1. Disregarding Coriolis inside the model domain causes some distinct changes and at the same time similarities in the estuarine system: Looking at the hypsometry of the full model domain over time (see appendix E) reveals a virtually identical development of the supra-, inter- and sub-tidal zones. Furthermore, the percentage of areas that are deeper than 20 m is with 10 % the same for the simulation with and without Coriolis. But the composition of these 10 % over time differs significantly: In the simulation without Coriolis, areas with a depth between 20 m and 30 m are strongly present whereas areas deeper than 32 m are hardly found. In contrast, the simulation including Coriolis reveals areas with more than 32 m for 2/3 of the simulation time covering half of the previously mentioned 10 %. Including the description of the bathymetrical differences (see chapter 6) a different arrangement of the channels is indicated. The changes that are caused by excluding Coriolis are clearly visible. Even though there are still two channels visible in the AOI they indicate a different development. In contrast to the base case simulation the Coriolis scenario reveals a channel division at a higher latitude. Furthermore, the two channels remain as individual channels (one flowing towards northwest and one flowing towards north) rather than joining after a distance of 10 km as in the other simulations. Over time the channel that approaches the AOI from the north grows in width, gets slightly deeper and becomes the eastern channel. The channel that comes from the northwest gets narrower while keeping its depth. Even though the system has changed the spin-up time is in the same order of magnitude (650 MY including Coriolis and 500 MY excluding Coriolis).

2. The simulation excluding Coriolis introduces a new estuarine system. Nevertheless, a cyclic behavior can be observed and is described in chapter 6. There, a recurrent pattern of eastern dominance

and equal dominance has been indicated, which is consistent with the previous descriptions. However, it needs to be kept in mind, that the period analysis in chapter 6 is based on the analysis of one cross-section which is geographically located at a latitude where the channel in this specific scenario is mostly not divided yet. The period that is indicated is 1015 MY and is in the order of magnitude of the alternation period that has been assigned to the base case simulation.

Summarizing, the influence of Coriolis in the system is significant. Not considering the effect of Coriolis is introducing the development of an estuarine system that cannot be considered to be the same as in a comparable case in which Coriolis is included. Nevertheless, a cyclic behavior has been found that has a period in the same order of magnitude, regardless of considering Coriolis or not. Consequently, in accordance to the hypothesis that has been stated in conceptual investigation description (chapter 3), Coriolis does not have an influence on the cyclic (alternation) pattern, but is possibly one component that influences the concentration of the water masses approaching the AOI from northwest. Furthermore, in this model, Coriolis is enhancing the development of the western channel in the lower latitudes of the AOI.

Wave

1. The constant consideration of waves with slightly exaggerated wave conditions is leading to the development of a new estuarine system. A first indication for the formation of a different system is found in the hypsometry of the full model domain over time (see appendix E): The supra- and inter-tidal zones compose a percentage of 60 % in the base case whereas the two depth zones amount to a percentage of 50 % in the scenario simulation including waves. Furthermore, deeper lying areas are more present in the wave scenario than in the base case, as the areas having a depth between 8 m and 16 m are covering twice as much space when waves are taken into consideration. The very deep areas however are more present in the base case, since the hypsometry of the wave scenario hardly indicates a depth of over 24 m. Consequently, the influence of waves is reshaping the bathymetry in such a way that the very deep area disappears and the percentage of mid-deep areas increases. This can clearly be observed in figure 6.17 where the mid-deep parts are visible as wide and relatively shallow channels. Additionally, figure 6.17 reveals a drastic shift of the full channel pattern towards the east, resulting in the most dominant channel being converged close to the eastern land boundary. Even though a different system develops, the cumulative bed load transport over the cross-section 75 remains the same, with or without waves included. Together with the identical spin-up phase this indicates that waves are not influencing the tidal prism that builds up in the Lower Weser, but does reshape the bathymetry in its cross-sectional arrangement.

2. As stated in the results chapter (6), there is neither the visibility of an alternation of the channel dominance nor an indication of the cyclic behavior by EM2. This could also be caused by the short simulation period, which only allows a qualitative analysis of the influence of waves.

The influence of waves on the morphodynamics is significant and should not be underestimated. The results of the wave scenario show the development of a different estuarine system which is in accordance to the theoretical categorization of estuaries stated in chapter 2. Since the simulation is limited to around 2000 years of morphodynamic development, it can only be considered qualitatively, due to the long computational time. The conclusion of the wave scenario implies that waves do have a strong influence on the generation of shoals and channels in the Outer Weser and consequently should be taken into account when modeling the morphodynamics. Moreover, no sign of wave influence on the development of a two channel system can be detected. Since most severe storm events come from northwest (as simulated in the model) the influence of waves should support the eastern channel more than the western channel and generally flatten the bathymetry. However, due to the presence of a two channel system in all other simulations (without waves) it can be reasoned that waves are not the predominant force responsible for the development of the two channel system.

Extreme River Discharge

1. The extreme discharge scenario reveals several significant differences when looking at the hypsometry and the cumulative bed load transport over time. The first and most striking difference between the base case simulation and the extreme river discharge simulation is that the latter does export sediment from the Lower Weser towards the Outer Weser and further offshore, as seen in the cumulative sediment transport of figure 6.20a. This indicates that the net currents are directed offshore which is caused by an overruling of the tidal currents by the high river discharge. The second difference is found in the hypsometry of the full model domain over time. An equilibrium state of the supra-tidal zone is reached much faster in the extreme discharge scenario (after 2000 MY instead of 3600 MY). Additionally, the channels that develop in the extreme discharge scenario are generally deeper, which is indicated by the amount of areas below 32 m (yellow color in figure E.5). Moreover, in this scenario simulation the subtidal zone is more extensively present in contrast to the base case simulation. The bathymetries show the development of two steady channels with larger depths in the funnel shaped part of the AOI, where the western channel is generally deeper in the southern part and the eastern channel in the middle and northern part.
   The number of channels and their general arrangement in the AOI are indicating that the estuarine system is still the same, whereas other facts indicate that this hypothesis is misleading. Since the channels are pretty stable in depth and location (other than the base case) and since no cyclic behavior has been indicated, this scenario could also be considered as being a new system. The positive cumulative sediment transport is an indication for that as well.

2. As described in chapter 6 there is no alternation period that can be observed. A reason might be that for the whole model domain the characteristics have changed, although two channels clearly have developed in the AOI. Even a general cyclic pattern cannot be distinguished from the general long term morphodynamic activities.

Recapitulating, the extreme discharge seems to change the character of the estuarine system, but still there are two channels in the funnel shaped part of the AOI. This scenario does not prevent the development of the two channels, since both channels are clearly distinguishable. Due to the fact that both channels neither disappear over time nor vary much, as seen in other simulations, a cyclic behavior is absent. Consequently, when river discharge is overruling the tides, the alternation of the channels that has been found in other cases is overruled as well. Lastly, according to the bathymetrical plots, the river discharge seems to support the eastern channel, especially in the mid-north of the funnel shaped area.

No River Discharge

1. In contrast to the extreme river discharge scenario this scenario with no river discharge, does not result in a new estuarine system. Instead, no discharge introduces a fairly similar channel and shoal pattern in the AOI. One conspicuity is that over time the no discharge scenario reveals slightly less deeper channels that are approaching the AOI from the North Sea. It can be seen in the bathymetries and additionally in the hypsometry of the AOI over time, where the areas below 24 m are less strong appearing compared to the base case. The western channel is deeper (most of the time and for most of the funnel shaped area of the AOI), although there can be found variations. At those times, with two channels present, the tidal shoals in between them are clearly visible and have a comparatively high elevation. Another observation is the high import of sediment into the Lower Weser due to the absent river discharge. The cumulative bed load transport is almost doubled and upstream directed. Nevertheless, even though the river discharge is neglected in this scenario, there is not an observation that would clearly indicate a change of the system. Instead, there are some small changes in the arrangement of the channels and in the governed dominance.

2. Since the system does not change as the river discharge is set to zero, a cyclic pattern is expected. Indeed the analysis of the alternation period in chapter 6 reveals a return period of 500 MY which is half of the alternation period found for most of the other simulations. However, it should be kept in mind that some assumptions and uncertainties are included in this period. Nevertheless, as a qualitative result it is remarkable that the absence of the river discharge has such a huge influence on the cyclic period.

Summarizing, the absence of river discharge does not introduce a new estuarine system. Consequently, the river discharge that is present in the base case does not represent the most dominant force. Since river discharge is absent and tidal channels divided by a considerable tidal shoal are found in the funnel shaped part of the AOI, it can be concluded that the development of two tidal channels is not primarily caused by the river discharge. Additionally, it can be concluded that the river discharge is favoring the eastern channel, since the western channel is more dominant in this scenario than in the base case. This observation is also in alignment with the conclusions made for the extreme river discharge scenario. Furthermore, this scenario reveals the alternation period that is exclusively introduced by the tides with a value of 500 MY, although this value needs to be treated carefully.

Increased Tidal Range

1. From all scenarios the increased tidal range scenario is the most similar one to the base case. Except a slightly increased percentage of the sub-tidal zone and the deep channel areas (>32 m depth) in the hypsometry of the model domain over time, there is no significant difference in the overall depth distribution. When looking at the development of the shoals and channels over time, both this scenario and the base case simulation reveal a relatively similar pattern, although there are more side channels approaching the AOI in this scenario. The most recognizable difference between the base case and the increased tidal range simulation is the spin-up time. Compared to the base case, it takes almost double of the time for the increased tidal range to reach a morphological equilibrium, although both system are importing the same amount of sediment. Nevertheless, the increased tidal range scenario results in the same estuarine system as the base case.

2. The alternation period that has been found for the increased tidal range scenario depends on the interpretation of the results. If the first visible eastern dominance pattern is considered, the alternation period would be estimated to be 1075 MY, which is basically the same alternation period as the one described for the base case simulation. If only clearly indicated alternation signals are taken into account, as done for the base case, the period would be determined to be 1400 MY, which is an increase of the return period of around 25 %.

Summarizing, an increase of the tidal range does not change the estuarine system, which is in accordance with the reasoning that has been presented in the investigation concept of chapter 3. However, the increased tidal range does lead to a different alternation period, which is an increase of 25 % equivalent to an alternation period of 1400 MY. Hereby, it needs to be considered, that this result is not unambiguous, but reasonable.

7.2. Conclusion

With the development of the investigation concept and the resulting scenario composition, two research questions have been defined: The first research question looks into the causing force that is creating two channels in the funnel shaped part of the Outer Weser, whereas the second aims to indicate the reason for the presence of a recurrent alternation pattern.

For the development of a two channel system, the Kelvin wave / Coriolis, wind waves and river discharge have been selected to be the potential source generating two channels. After simulating, describing and analyzing the results, it can be stated that the generation of two channels is mainly caused by the tides. The presence of two channels, when no river discharge is applied, leads to the conclusion that the river discharge cannot be the main driving mechanism. Additionally, the extreme river discharge scenario reveals that it does not enhance the generation of two channels. Instead, it results in a constrained tidal shoal dividing the two channels which tendentiously could lead to the formation of only one channel if the river discharge overruled the tidal wave even more. The hypothesis is that the high discharge is forming a new estuarine system, where baroclinic tidal processes are stronger present than batotropic ones. Furthermore, the Kelvin wave and Coriolis were not detected as the cause for the creation of two channels. However, both (seem to) have an influence on enhancing one of the channels: The Kelvin wave favors the creation of an eastern channel, whereas Coriolis raises the depth of the western channel inside the model domain. Lastly, wind waves have been considered as strongly influencing but not as the main factor that is causing the generation of two channels. Since none of the chosen scenarios can indicate another driving mechanism than the tides, it is concluded that the combination of the tides and the geometry of the estuarine basin are causing the development of two main channels. Thus, the geometry might be the most important influence for the number of channels generated in the Outer Weser estuary. The same conclusion has been drawn by Dam et. al. [6] when they performed a hindcast of the morphological changes over 110 years in the Western Scheldt. In their research they stated that the combination of tides and estuarine geometry determines the allocation of the channel and shoal patterns. Furthermore, the scenario simulations have partly revealed that the different forces are enhancing one of the two channels of the Outer Weser:

* Kelvin Wave → Eastern Channel
* Coriolis → Western Channel
* Wave → Eastern Channel
* River Discharge → Eastern Channel

Variation in the river discharge, wind waves and variations in the tidal range have been selected as a possible source for the occurrence of the alternation. After the investigations of the previous chapters, it can be concluded that the alternation period is dependent on the tidal domination in the Weser estuary and the depth of the channels. This includes a combination of tidal range, river discharge and waves. The conclusions are based on the results of the increased tidal range, where a larger alternation period could be indicated due to larger channel depths. In the simulation of no river discharge the alternation phase is decreased significantly. Moreover, during extreme river discharge, with the river flow being assumed to overrule the tidal currents, no alternation could be determined. Wind waves cannot be analyzed comprehensively, but their influence is considerable. Additionally, a tide without a phase difference along the open boundary results in a shorter alternation period. Neglecting the Kelvin wave introduces a weaker presence of the eastern channel resulting in a lower alternation period since less depth needs to be changed in order to complete an alternation cycle. This effect is artificially generated and should not be considered when investigating the causing forces of the alternation period.
Generally, it is difficult to assign a discrete alternation period that would match the historically observed one for two reasons: One reason can be found in the rare information that exists from the natural alternation observation since a somehow natural state has only been present until the end of the 19th century. Furthermore, the scientists presented in chapter 2 who dealt with the alternation of the two channel system indicate an alternation period that varies between 60-70 years and 110-120 years. Göhren [11] even questions whether it is possible to assign an alternation period from a perspective nowadays. Another reason might be that applying a MORFAC (especially such a high one) does strongly influence the simulation results. Thus, it has a considerable impact on the number of years that have been indicated as the alternation period linked to the

scenarios. As a result, the indicated recurrent periods are distorted and do not match any historically indicated values anymore.
On the one hand, the simulations done indicate that the alternation period is not linked to any time scale that has been introduced to the model. Furthermore, based on the simulation results, it is reasoned that the alternation period is influenced by tidal dominance. Consequently, it could be concluded that the alternation period found in the simulations is a result of the interaction between the tidal wave and the basin geometry since the latter would be the possible source left. On the other hand, since the insights gained by the scenario simulations can only be considered qualitatively rather than quantitatively, such conclusions based on the distorted alternation period would be questionable. In a nutshell, this project is stuck when it comes to finding a defined answer to the reasons for the alternation and the according period. But some more insight has been gained on which aspects have an influence and what theoretically could be the cause.

The overall findings of the scenario simulations are summed up in figure 7.1. Here, the scenario and the reference simulation are plotted according to their characteristics regarding channel dominance and morphodynamic activity. The method behind this plot can be found at the end of subsection 4.3.2.

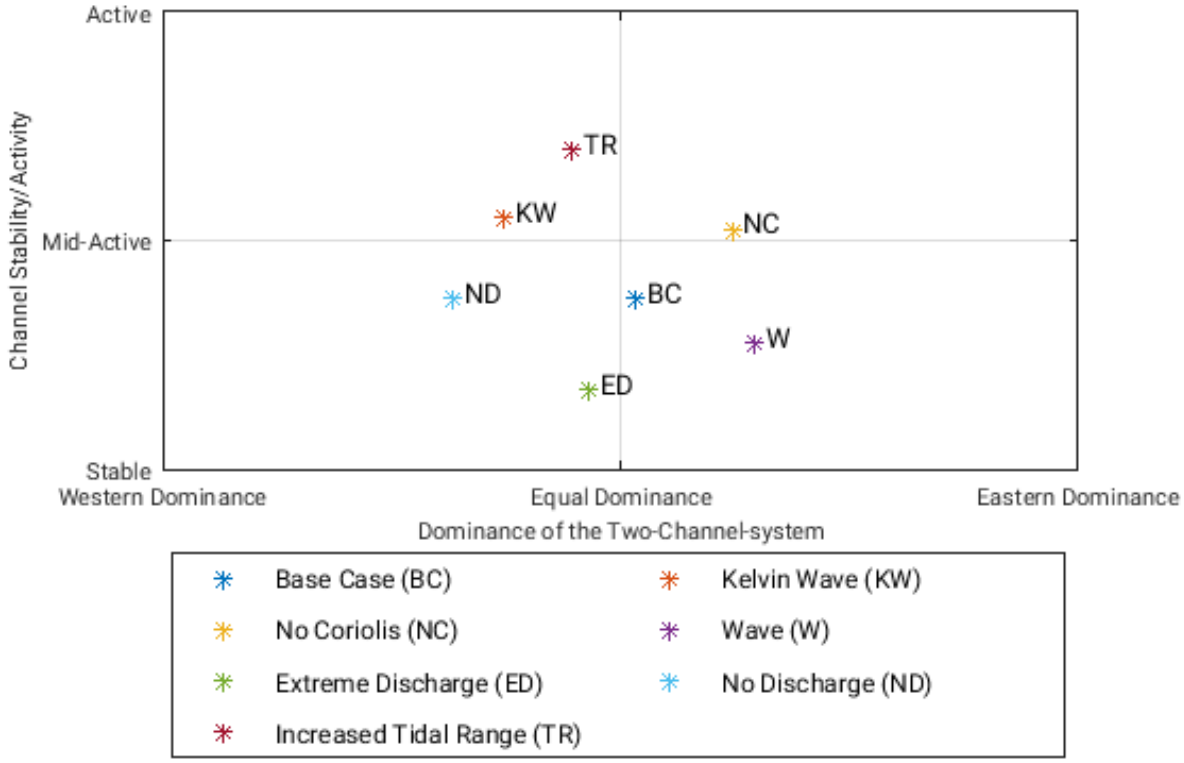

Figure 7.1: Comparison of the simulations in a conceptual way - including the channel dominance on the x-axis and the channel activity on the y-axis

The figure reveals a number of interesting aspects, starting with the arrangement of the scenarios around the base case simulation. In a broad sense, the scenario simulations are arranged circular around the base case simulation, indicating that the selected model configurations cover the various aspects of the two investigated morphodynamic features.
Considering the y-axis of figure 7.1, the simulations of the base case and of no river discharge show the same value of morphodynamic activity. In both cases, the same tidal range is applied on the northern open boundary, but with a discharge difference of 325 m^3/s at the southern boundary. Since the indicated activity is the same, it could be concluded that a river discharge of 325 m^3/s has no effect on the morphological activities. But this conclusion should not be made without further investigations. At the simulations with no Coriolis and no Kelvin wave, again the same tidal range is present at the open boundary and the same river discharge is introduced at the southern open boundary. Still, the latter two scenarios show significantly more morphological activity than the base case and the no river discharge scenario and almost the same activity when compared to each other. Since the only difference is found in the way the tidal wave propagates in and

through the Weser estuary, a possible reasoning could be that variations in the tidal wave propagation in the estuary have a significant influence on the morphological activity of the estuary itself. Additionally, when taking the wave and extreme river discharge simulation into account where the tidal wave is overruled by the waves/discharge, less morphodynamic activity is observed which is in alignment with the previously stated hypothesis. Moreover, the increased tidal range shows the highest activity which is probably a result of the stronger forcing of the tides inside the estuary. Summing up the findings from the y-axis, a dependency of the morphological activity on two factors can be indicated: First, the way the tidal wave propagates through the estuary and second, the relative domination of the tidal range.
Looking at the x-axis the general finding is that all scenarios are closer to the equal dominance state than to a western or eastern dominance state. Additionally, it is convenient and interesting that the base case simulation is close to the ideal equal dominance state according to the method applied for determining the channel dominance (see end of section 4.3.2). Within a small tolerance margin the extreme river discharge simulation is also close to the ideal equal dominance state. From the simulations left, three scenarios can be found on the western dominance side of figure 7.1. Ascending in western dominance tendency, these scenarios are: Increased tidal range, no Kelvin wave and no river discharge. The conclusion drawn from this arrangement is the dependency of western domination on the relative dominance of the tidal wave. In the no river discharge scenario, where the highest western dominance is indicated by figure 7.1, this theory is supported since here, the development of the channels is 100 % tidally driven. Furthermore, it can be assumed that an increased tidal range is leading to a higher relative influence of the tides on the morphology. Since the tidal range is only increased by 10 %, the resulting effect is less strongly visible as it is for the scenario with no river discharge, where the relative influence of the tides is 100 %. However, a reasoning for the slight western dominance for the extreme river discharge is missing, yet. An explanation could be that the method applied in order to determine the dominance state has a certain error margin which covers the difference between the base case and the extreme river discharge scenario. Following this theory, the reasoning would be that the river discharge itself does not introduce eastern dominance, it only can balance out the tendentious western dominance introduced by the tides into an equal dominance state as found for the base case and the extreme river discharge simulation. Nevertheless, this reasoning is questionable and further studies are recommended including simulations with a step-wise increased discharge starting from zero. Apart from that, the simulation with no Kelvin wave also shows a tendency towards western dominance. Contrary, the scenario with no Coriolis shows a stronger eastern domination. Both scenarios are revealing the same *dominance-difference* to the base case simulation which implies that both effects are balancing each other out when included. The Kelvin wave is approaching the model domain from the north west. Thus, the eastern land boundary of the funnel shaped part of the Weser estuary functions as the cut bank which forces a propagation of the wave towards the south. Consequently, the eastern channel gets enhanced when the Kelvin wave is included. The opposite applies for the effect of Coriolis. Here, as described earlier, the tidal wave propagating through the Weser estuary gets deflected to the right. In this case, during flood-flow, this would give a preference to the western channel. Since both the scenarios disregard the Kelvin wave/Coriolis, the simulation results show the reversed channel enhancement. The last simulation that shows the same order of eastern dominance tendency as the no Coriolis scenario is the wave scenario, where wind waves are added. Since only one wave direction is introduced constantly over time from north west, a general shift towards south east can be expected and is revealed by the simulation analysis as well. Here, the assumption is that the significant wave height applied determines the amount of eastern dominance.
Summarizing, the following table represents the results of this project in comparison to the base case:

Force	Enhanced Channel (v)	Δv_{rel}	Channel Activity (θ)	$\Delta\theta_{rel}$
Kelvin wave	Eastern Channel	25.5 %	Increased	46,6 %
Coriolis	Western Channel	24.4 %	Increased	40.0 %
Wave	Eastern Channel	29.2 %	Decreased	26.6 %
Extreme River Discharge	Western Channel	06.8 %	Decreased	53.3 %
No River Discharge	Western Channel	36.7 %	No tendency	00.0 %
Increased Tidal Range	Western Channel	10.7 %	Increased	86.6 %

Table 7.1: Channel Enhancement in the Different Scenarios

7.3. Concept Reflection

In chapter 3 the modeling concept applied in this project has been reasoned and described. Reflecting the investigation concept is split into two parts: The first part is aligned to the modeling approach of applying a flat bed as an initial bathymetry. The second part is reviewing if the investigation concept is suitable for answering the research questions that have been defined in the project proposal.

The first question is whether reasonable results can be achieved when applying a flat bed to the Outer Weser estuary and let morphology develop freely - in other words: Does the flat bed modeling approach work for the Outer Weser estuary? Multiple aspects reason that the application of a flat bed modeling concept to the Outer Weser can be seen as successful:

- All simulations have reached a morphological equilibrium state
- A reasonable channel and shoal pattern develops in the standard simulations
- The remarkable two channel system is developing
- The characteristic recurrent alternation of the two channels can be modeled with this approach
- The Jade has been reproduced well regarding location and dimension

Considering the five statements above, the flat bed modeling approach can be seen as an appropriate method in order to investigate the influences of different forcings on the Weser estuary. However, when looking at the simulation results and the remarkable reproductions of the Western Scheldt estuary that are achieved by Van der Wegen and Roelvink (2012) [39] the simulation results gained in this project do not seem to have the same level of reproduction. Disregarding the expertise of Van der Wegen and Roelvink for the Western Scheldt estuary and long term morphodynamic modeling, a reason for the less detailed representation of the simulations in this project could be the incomplete calibration, where the roughness height predictor and the channel depth calibration have been excluded from the calibration due to a shortening of the available calibration time (see section 5.6). A consequence of this compromise is that the tidal range is increasing throughout the Lower Weser instead of decreasing, so that the assumptions underlying the chosen end of the model domain are not valid anymore (see section 4.1).
Additionally, the Outer Weser estuary is lesser geometrically influenced, in comparison to the Western Scheldt. The wide area of the model domain raises more options for a possible development of channels and shoals. As concluded in section 7.2, the geometry is probably the condition that together with the tidal wave will define, how many channels will be generated and where. Consequently, hypothetically spoken, the more restrictions the geometrical shape of an estuary would introduce, the better results can be expected by a flat bed model. Incorporating this reasoning, other estuaries that are less wide and more influenced by a distinct geometry would probably give a close representation of the natural shoal and channel pattern. In the German Bight, the Weser estuary is the widest and maybe also the geometrically most unrestricted estuary. Applying the flat bed modeling approach in the other estuaries might thus not only be interesting, but also promising. Considering, that the less constrained Weser estuary gives a fairly similar shoal and channel pattern and additionally includes characteristics that have been defined as the most important ones, supports the conclusion of applicability of the flat bed modeling concept for the Outer Weser estuary.
Nevertheless, for the morphodynamic representation there is potential for model improvements. As stated in chapter 5 the model itself has not yet reached its maximum representation for the historical natural state of the Weser estuary (see section 5.5 for improvement suggestions).

The second reflection is whether the investigation concept is appropriate to provide an answer for the two research questions. Recapitulating the results and analysis from all simulations, the conclusion drawn is that the investigation concept is generally suitable for answering the first research question, but it is not adequate for investigations on the second research question.
The problem lies in the application of the MORFAC as mentioned earlier. With the MORFAC the morphodynamic response to the hydrodynamics is accelerated which theoretically allows simulations that are representative for the morphological development of centuries to millennia. Simulating the morphological development from a flat bed until a morphodynamic equilibrium is reached is only feasible when applying simplification and accelerating methods like the MORFAC. The drawback of the (high) MORFAC in this case is the distortion of the time scale. Since the time scale is the most important parameter in order to compare

and differentiate the alternation pattern of the scenario simulations, a method that is manipulating the results considerably cannot lead to results that are matching to historically documented alternation periods. Consequently, it is questionable, if the MORFAC approach can be used validly and thus, if the flat bed modeling is the right method to investigate the influences of different forces on the alternation phenomenon. The results of this project and the considerable differences between the alternation periods simulated and historically observed, indicate that a flat bed model (including the MORFAC) is not suitable for this kind of investigation. However, as also shown in this project, the flat bed modeling approach can give qualitative results for variations in the alternation period, which can be applied in order to categorize the various effects of different influences on the alternation pattern. Still, a comprehensive investigation for this specific question is not possible.

7.4. Outlook

During this project a lot of new investigation idea raised that could not be realized, due to the time limitation of this project. Consequently, there are some ideas that could be considered by other contributors and following projects. Apart from the modeling recommendations of chapter 5 it would be conductive to enlarge the simulation period such that at least 20 years of hydrodynamics are computed. The increased simulation period could give more comprehensive results regarding the alternation period and overall equilibrium development. Additionally, a few more ideas could not be included in this project yet, but would give further insight. The prioritized suggestions are:

1. Finding of theoretical solutions: A schematized initiation analysis where the estuary is idealized as a funnel shaped estuary with straight lines according to the principle of Van Veen [44]

   The first point of the unrealized ideas is about a study that could indicate how the geometrical shape of the estuary is influencing the development of multiple channels. By starting with a straight funnel shaped estuary that is in length and width schematically equal to the Outer Weser estuary and adding the Lower Weser as a straight long and narrow channel the most simplified version of the Weser estuary could be tested. In a next step, the Lower Weser channel could be attached to the funnel shaped part in a more realistic way, by inclining it as much as it is inclined nowadays. Inspired by the studies made by Van Veen [44] the results could give an idea of the channels development most simplified. This study would be a preliminary study, whereupon the scenarios simulated in this project could be put into context. Especially, by increasing the precision of the representative estuarine geometry (from very schematic to 100 % realistic) could clarify, if the hypothesis about the estuarine geometry being the factor that determines the the number of channels and their locations the most is valid.

2. Indication and investigation of the ebb- or flood-dominance of two channel system itself and the two channels individually

   The second idea that has not been included yet, is if the scenarios are flood- or ebb-dominant. Ebb- and flood-dominance is determined by the tidal asymmetry and can thus be analyzed by looking at the tidal components or the plotted tidal wave. The reason why it would be interesting to look at the dominance of the tidal system is that the Weser estuary in reality is quite complex as described in chapter 2. It would be interesting to see, if this complex tidal flow domination differs between the selected scenarios. Additionally, a distinction can be made whether the different scenarios are enhancing a flood- or ebb-channel and if a schematizations can be found within these pattern. Especially, when the river discharge is exaggerated or neglected more insight could be gained by analyzing whether the western channel or the eastern channel can be indicated as a flood- or ebb-channel. Furthermore, the Kelvin wave and Coriolis might have an influence on the ebb- and flood-channel development and taking that into account would add value to the current investigations.

3. Analyze the length scale of the two channel system and check if that can be linked to a time scale

   The third idea that has not been included is the analysis of the length scale of the two channel system. Within and between each scenario the length scale of the two channel system from the division to the junction varies. The question is, if this variable length can be linked to any time scale that thus could be determined to be responsible for this development.

4. The Analysis of the hydrodynamics in order to see dominant regime (wave/river flow/ tides) varies between the scenarios, through investigations of the tidal wave inside the model domain

   The fourth that could not be realized is the analysis of the velocities during flood- and ebb-flow. Especially, when waves, extreme discharge and no discharge are simulated it is assumed that these forces can influence the tidal flow. By analyzing the velocities along a cross-section it could be provide the necessary information needed in order to prove the assumptions.

5. Salinity concentration and the estuarine turbidity maximum could be considered as a process/phenomenon and its effect examined

With the fifth idea of further investigations deals with the question if salinity gradients along the estuary and the estuarine turbidity maximum have an influence on the development of the channel and shoals. In the Weser estuary the estuarine turbidity maximum is influencing the flocculation of fine sediments and is responsible for todays dredging activities in that area [22]. Considering this aspect might have an effect on the bathymetry evolving.

6. An Analysis of the tidal system that develops by means of the width average depths calculation along the Weser channel axis

   The sixth point aims for an investigation of the estuarine regime that is developing in each scenario. In order to differentiate the systems that are present when the morphological equilibrium is reached it can be beneficial to look at the sediment distribution throughout the estuary. The idea is to get an intuitive comparisons by looking at the width averaged depth along the channel axis and by plotting all depths one figure. As an additional investigation method it can link the development of estuarine system with the amount of cumulative bed load that has been in- or exported as indicated by the equilibrium analysis.

7. Additional cross-sections for the evaluation method 2

   The seventh idea is taking additional cross-sections and applying EM2 to them. By considering more cross-sections at different latitudes it can be contributed to a more comprehensive investigation of the two channel development in the Outer Weser.

8. Influence of the Holocene sediment distribution and bed composition on the development of channels in the Outer Weser estuary

   The eighth research suggestion is to look at the effect that a discharge has that varies in time. So far, in the scenarios there just has been applied a constant river discharge over time, whereas in reality, especially before the Weser has been restricted in its discharge by wires and dams, the Weser discharge differs during the seasons. It would be interesting to get an indication of the mixed effect of tides and different discharge ratios, even though the analysis and distinction of river and tidal influence might be challenging for this scenario.

9. Influence of SLR on the natural development of tidal channel and shoals

   The ninth idea came up, when looking at the flat bed modeling by Van der Wegen (2012) where he applied non erodible areas by investigating the sediment composition of the investigated estuary. By applying non erodible area or different sediment fractions as a bed layer composition, different simulation results could be expected.
   The ninth and last idea that is presented here, is that SLR could also influence the long term development of an estuary and could possibly reason historical behavior that has been observed as described in section 2.2. Sea level rise could have an influence on the tidal volume and thus on the dimensions of the tidal channels. On the long term tidal shoals are theoretically growing with SLR but does that also change the arrangement of channel and shoals is an interesting question, that would probably not add value to the current study, but could satisfy once curiosity and expectations.

8

Recapitulation

In this graduation project the morphological development of the Outer Weser estuary under the influence of different forcing has been investigated. The Outer Weser together with the Lower Weser forms the estuarine part of the Weser. The scope of the project lies on the two channel system, a conspicuous pattern of two tidal channels that are traversing the extensive tidal flats of the Weser estuary from south to northwest and vice versa. Until the constructions of training walls and gronyes at the end of the 19th century. The two channels have been characterized by an alternation pattern, where the western and the eastern channel dominate each other recurrently. Yet today neither the reason for the development of the two channels nor the origin of the alternation pattern is fully understood. In order to gain some insight in these open research question, a mophodynamic model of the Outer Weser has been generated by applying the process-based modeling toolbox Delft 3D. As an investigation approach it has been decided to run long-term morphodynamic simulations with different model set-ups so called scenarios. In the various scenarios the different forces which could be responsible for the development of two channels and/or the alternative behavior are added or excluded from a base case simulation in order to investigate the individual influence of each force. Since the goal is to get a clear distinction of the different influences the model is simplified and as many processes as possible have been excluded. Based on the need of a simulation that is as little influenced by initial conditions as possible it has been decided to apply a flat bed bathymetry in order to let the tidal channel and shoals develop freely. In combination this set-up is leading to a schematized model that is able to predict the long-term development of macro scale morphology by including a high MORFAC (a factor that is multiplying the sediment transport resulting from the hydrodynamics) .
The simulated scenario composition has been chosen by looking at constantly present forces for the first research question and periodically varying forces in search of an explanation for the alternation. By reasoning the main influences on the estuary being the tidal movements, wind waves and river discharge the scenario composition has been generated. The scenarios for the first research question are the effect of the Kelvin wave, Coriolis, wind waves and river discharge. The second research question is aimed to be investigated by the scenarios wind waves, extreme river discharge, no river discharge and an increased tidal range which takes account for seasonal effects, SLR and the nodal tide.

The analysis of the results has been done by examine several points. Firstly, it has been estimated if and when the scenario simulation reaches a morphologic equilibrium. Secondly, it has been checked if the simulations are showing an alternation pattern of a two channel system. And thirdly, it has been investigated if a return period can be assigned to an alternation pattern, if present. The first aspect has been carried out by an analysis of the cumulative bed load transport averaged over a cross-section and by looking at the hypsometry over time. The second aspect has been investigated by plotting the bathymetry of the AOI at several points in time and applying EM2. The last aspect has been analyzed by detecting the dominant channel over time (EM2), by determine recurrent patterns and by applying these results in a linear regression. The evaluation method 2 has been developed in order to have a tool that can indicate the location and depth of the tidal channels in the AOI and investigate the related alternation period if existing. As a first step in EM2, a predefined cross-section (which is located in the funnel shaped part of the AOI) has been plotted over time. The resulting contour plot gives an overview of the development of the two channels in time at the specific location. Furthermore, EM2 analyzes the alternation period, by correlating the cross-section over time with nine

pre-defined cases. Each case is representing a morphological state of the cross-section that indicates western dominance, equal dominance or eastern dominance. Afterwards the highest correlation coefficient is plotted and colored with respect to the dominance situation indicated by the according case. By analyzing the sequence of the colors, alternation pattern can be spotted and in case they occur recurrently, being assigned to a return period by means of a linear regression calculation. Combining these methods, the influence of each factor on the research question can be investigated.
The model domain is chosen to include the Lower Weser and the Jade Bay next to the Outer Weser which is the area of interest in this project. The model grid is generated such that it has a higher resolution in the Outer Weser part, whereas the Lower Weser and the Jade bay are less detailed represented. The initial depth that is assigned to the flat bed has been estimated by averaging the todays bathymetry. One sediment fraction is defined with a grain size of 200 μm in the whole area and Engelund Hansen is applied as the sediment transport formula with an α_{Bn} of 7.5 and a MORFAC of 400. At the open boundary on the North Sea side the tidal components O1, K1, M2, S2, M4, MS4 and M6 are used with a reflection coefficient of 10 000 and at the open boundary on the river side a constant discharge of 325 m^3/s is applied, with a reflection coefficient of zero.

The results of the base case simulation generally show a good representation in the Outer Weser estuary. A two channel system clearly develops and also the alternation pattern can be detected. Regarding the historic locations and depths of the two channels the base case has some potential for improvements, but qualitatively the results are reasonable. In the base case simulation the morphological equilibrium is reached after 650 MY. Furthermore, a two channel system develops at several periods in time, and according to EM2 an alternation cycle can be observed three times, starting with western dominance and continuing with a period of equal dominance, followed by a period of eastern dominance. The alternation period assigned to these pattern is 1150 MY according to the linear regression.
In the first scenario where the Kelvin wave has been excluded, an equilibrium is reached after 800 MY. The scenario shows a development of a two channel system including an alternation. In contrast to the base case simulation, a stronger development of the western channel can be observed when the Kelvin wave is not considered. An alternation between western dominance and equal dominance is evaluated by EM2, and a return period of 757 MY has been assigned. Consequently, the Kelvin wave supports the development of the eastern channel within the two channel system.
In the Coriolis scenario, where the Coriolis effect has not been considered in the simulations, a morphological equilibrium is reached after 500 MY. Again, a two channel system is clearly visible, even though the deviation into two channels appears at a slightly higher latitude as in the base case. Additionally, a general shift towards the east is observed in the bathymetries. In the Coriolis scenario an alternation between the eastern dominance and equal dominance has been indicated with a period of 1015 MY. From the scenario simulation it can be reasoned that the Coriolis effect has a significant influence and is enhancing the development of the western channel.
In the wave scenario the equilibrium state has been indicated after 650 MY. Partly, a two channel system develops but within a different estuarine system where a general shift of channels towards the east is observed. The influence of waves introduces more shallow and wide channels that do not have the same characteristics. An alternation pattern has not been detected due to the comparable short simulation period and the different estuarine system. It is concluded that the influence of waves is significant and should not be neglected.
When extreme river discharge is applied to the model some kind of equilibrium is reached after 800 MY. A two channel system is clearly seen, divided by a narrow and long tidal shoal. This channel arrangement seems to be stable over time as indicated by EM2 with a western dominance in the southern part and an eastern dominance in the middle and northern part. The conclusion of this scenario is that the extreme discharge leads to a disappearance of the alternation and no enhancement of one of the two channels.
In the scenario that excludes the river discharge an equilibrium state is reached after 800 MY. By the visual inspection and EM2 a two channel system is detected which also contains a cyclic pattern. The recurrent pattern changes between a western dominance and an equal dominance situation. The linear regression, determined from the results of EM2, gives a return period for the cyclic pattern of 500 MY. Generally, the scenario shows an enhancement of the western channel. Consequently, the tidal wave has been concluded to be the solitary force in the development of the two channels, which have an alternation period that is significantly smaller, when disregarding the river discharge.
When analyzing the increased tidal range scenario a morphological equilibrium state has been found after 1100 MY. Furthermore, a two channel system develops that has a remarkable resemblance with the base case scenario. The EM2 supports this observation when looking at the cross-section over time. As the scenario

is similar to the base case simulation an alternation pattern is also determined varying between eastern and western dominance with a period of 1400 MY. This period indicates an increase of 25 % of the alternation period, but is not unambiguous. The conclusions drawn from this scenario are that the increased tidal range also increases the alternation period and shows similarities to the base case which implies a direct dependency on the tidal forcing/domination.

Combining the results of all scenarios for the first research question it has been concluded that the development of the two channel system is mainly caused by the tides in combination with the basin geometry. It is reasoned based on the no river discharge scenario, where a two channel system is found without the influence of waves or river discharge. Additionally, it has been observed that in the scenarios where the kelvin wave and Coriolis are excluded there are still two channels present, which supports the conclusion drawn. Furthermore, no enhanced development of the two channels is found in the extreme discharge scenario which is also in alignment with the previous findings. In this study the influence of waves could not be answered comprehensively, but it is shown that the influence of waves is significant and should be considered when modeling the Outer Weser estuary.
For the second research question it is found out that the alternation period depends on the domination of the tides and the depth of the channels. In case where the tides are the only forcing the alternation period is determined to be shorter than for the simulations including river discharge, due to the strong domination of the tidal wave. Furthermore, if the tidal flow is overruled by wave actions or by extreme discharge from the river, no alternation pattern has been observed, at least not within the simulation period. Moreover, when increasing the tidal range, indications are found that the alternation period increases as well due to the large channel depths that needs to be adapted by the alternation. Additionally, since the alternation period is not linked to any period that is externally introduced, it could be reasoned that the alternation period is a geometrically initiated phenomenon. However, the simulation results are not sufficient to prove this hypothesis comprehensively.
However, a comprehensive analysis is not feasible within the project duration and thus further research is highly recommended. It has been indicated that it could improve the model results significantly by applying multi-fractional sediment in the model with a lower MORFAC, a detailed calibrated roughness height predictor and under the consideration of further processes (for example waves). Additionally, the evaluation method could be improved by more analysis for a longer time span in order to gain more alternation cycles that can be examined.

A

Historical Maps

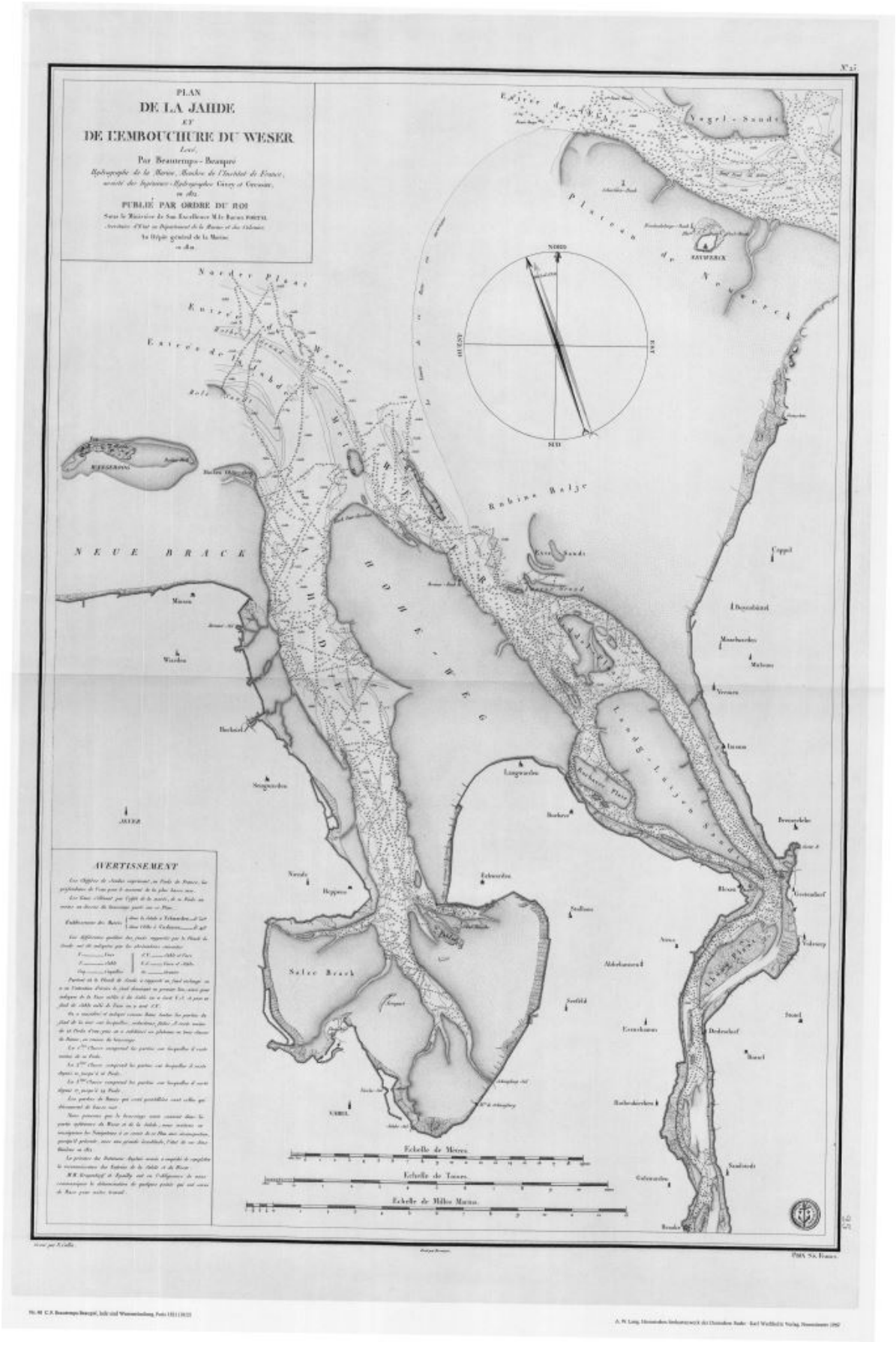

Figure A.1: Historical Map of 1812

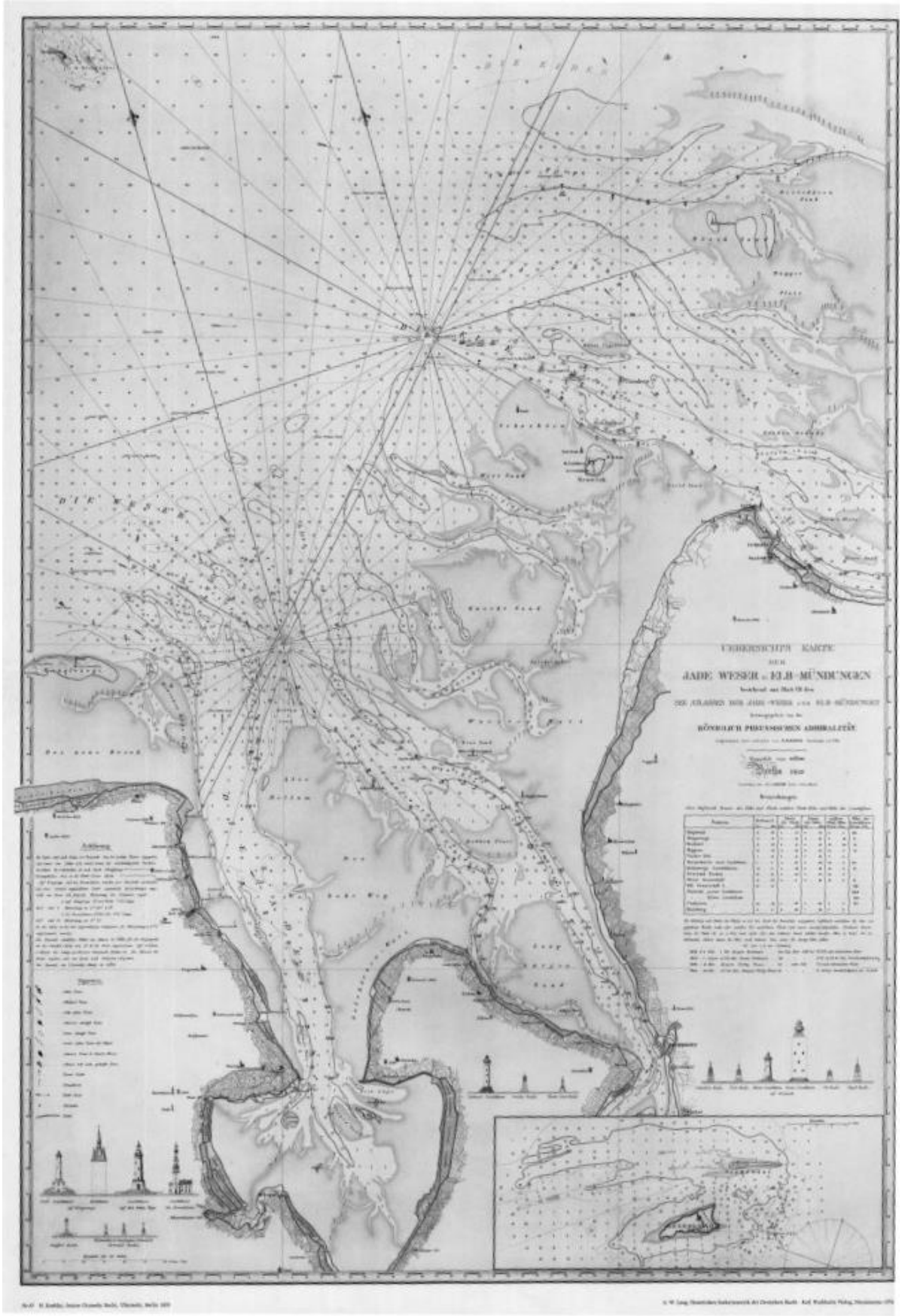

Figure A.2: Historical Map of 1859

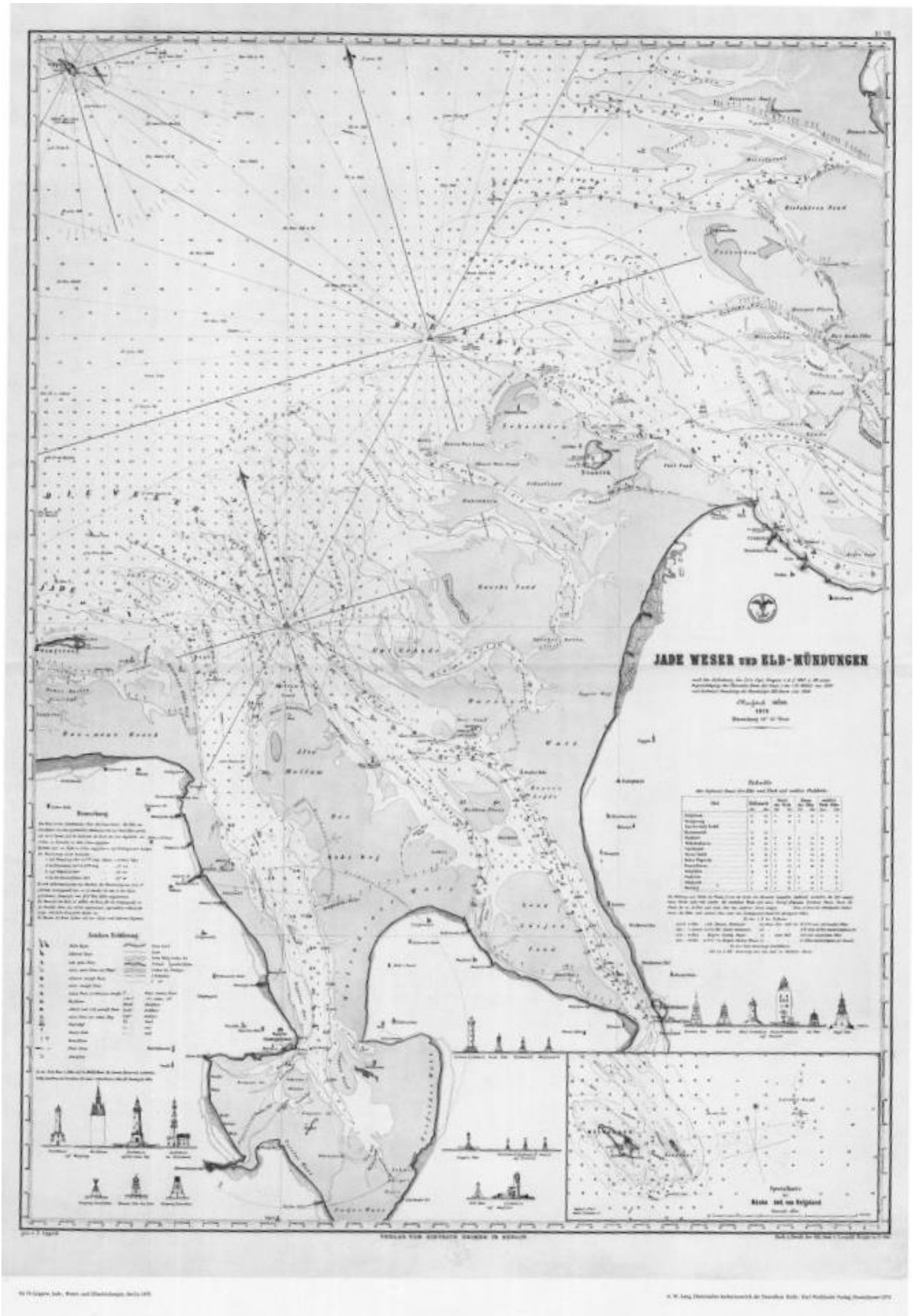

Figure A.3: Historical Map of 1870

B

Method

B.1. Model Set-Up

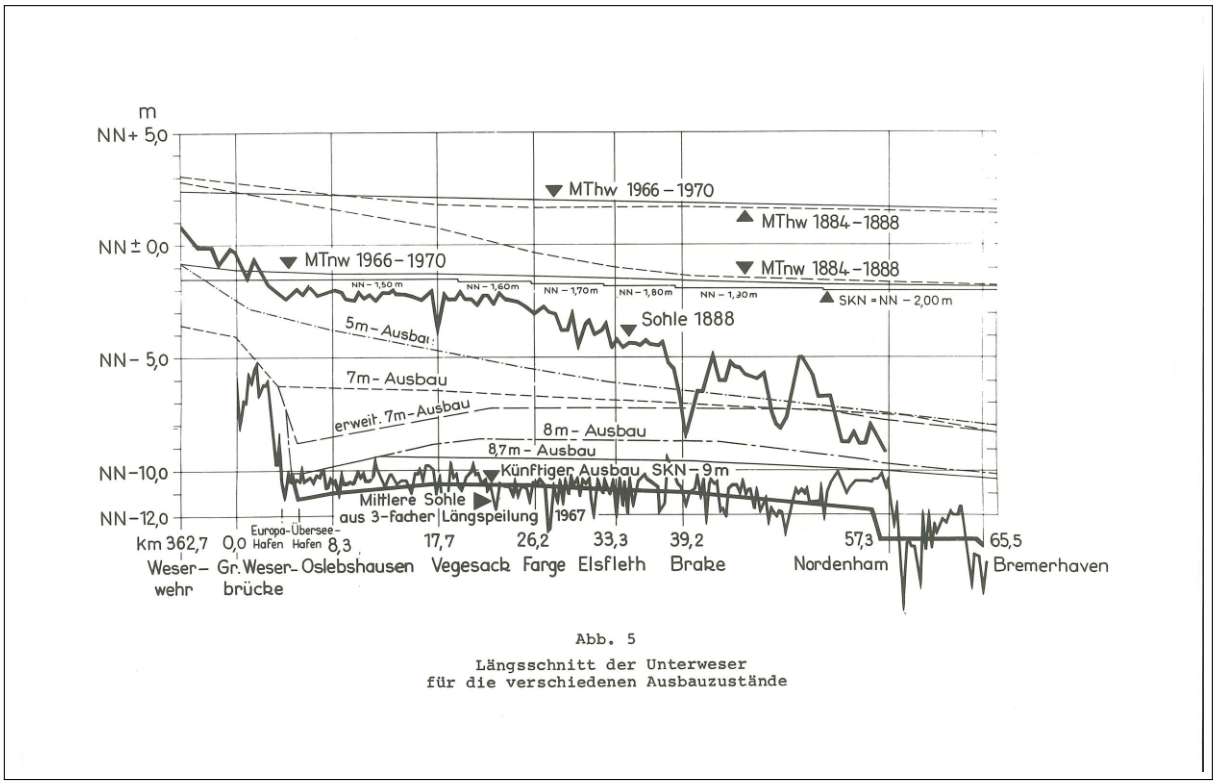

Abb. 5

Längsschnitt der Unterweser
für die verschiedenen Ausbauzustände

Figure B.1: Width Averaged Depth and Tidal Range in the Lower Weser 1884 - 1888

B.2. Scenario Set-Up

B.2.1. Kelvin Wave

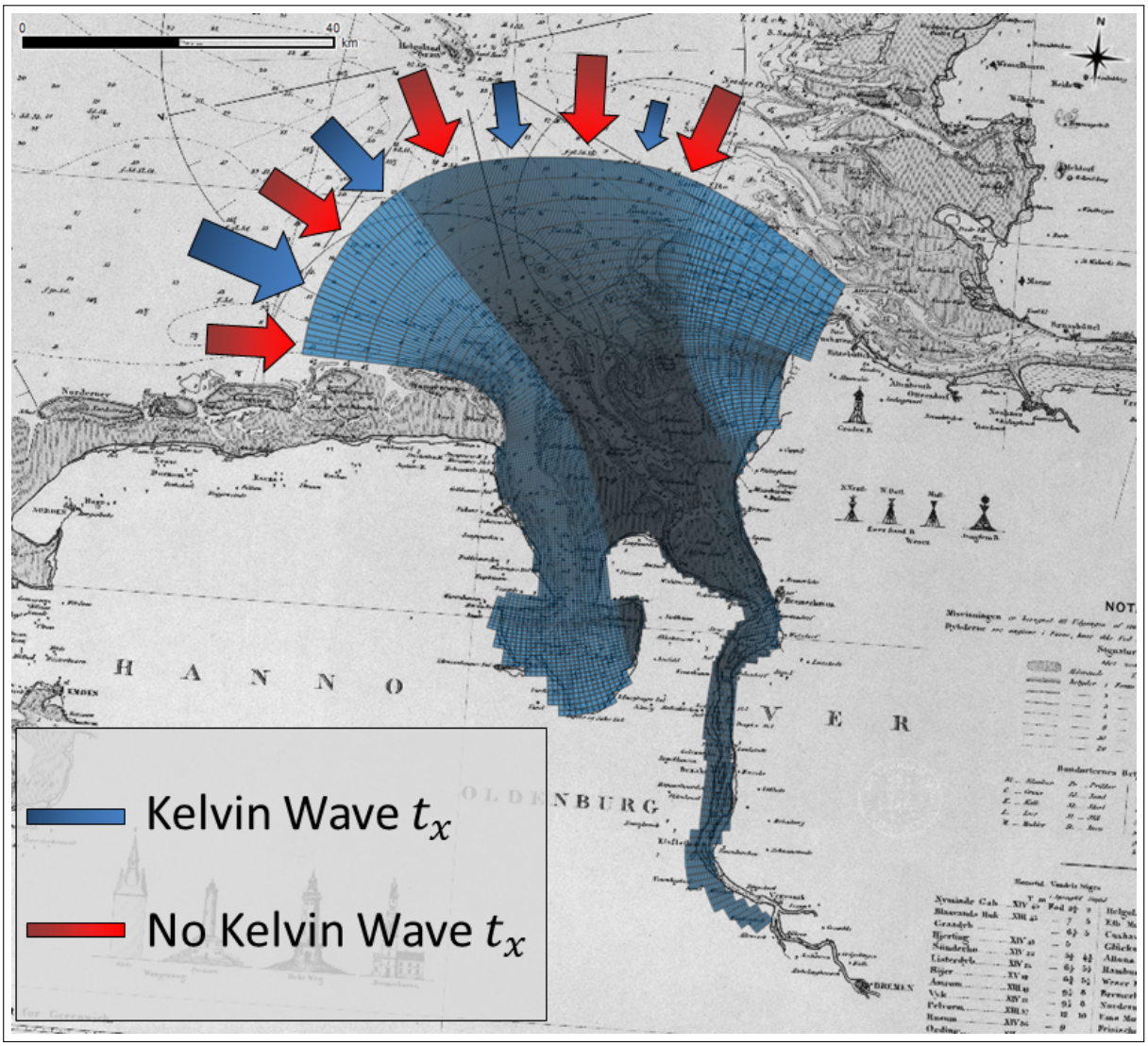

Figure B.2: Influence of the Kelvin Wave on the Open Boundary

B.2.2. Wind and Waves

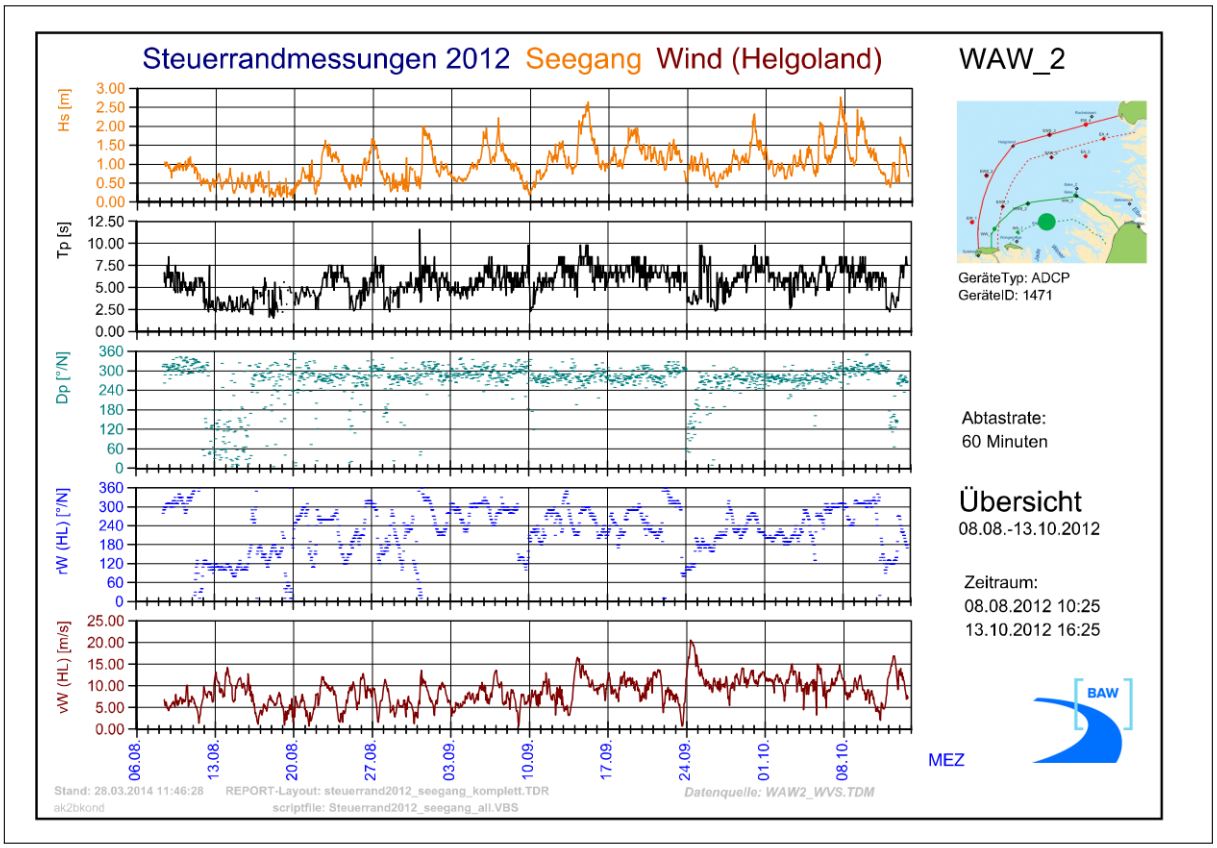

Figure B.3: Wind and Wave Measurements Taken Outside the Outer Weser Estuary in 2012

B.3. Evaluation Method 2

Figure B.4: Cross-Section 75 - Location for the Application of Evaluation Method 2

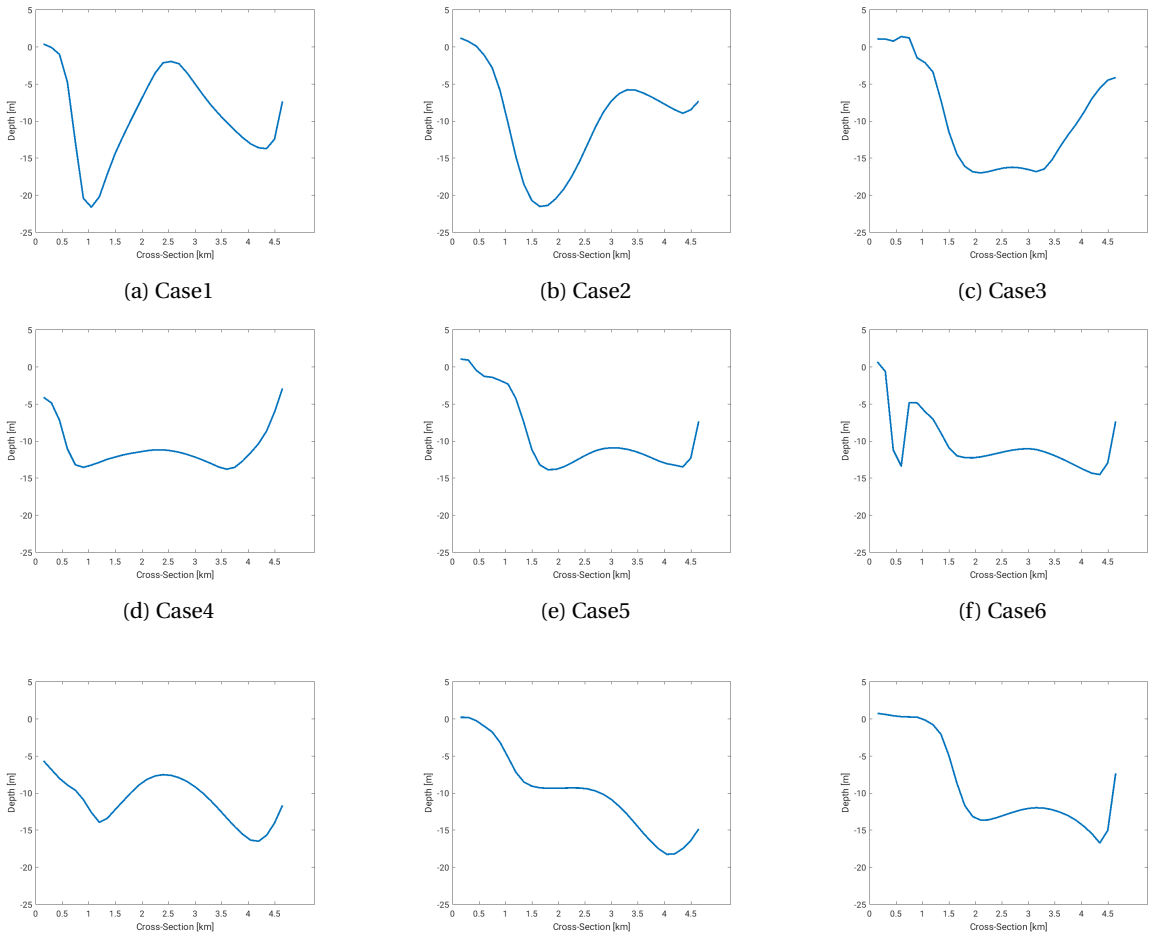

(a) Case1 (b) Case2 (c) Case3

(d) Case4 (e) Case5 (f) Case6

(g) Case7 (h) Case8 (i) Case9

Figure B.5: All Cases That Are Used for the Correlation Analysis

C

Calibration

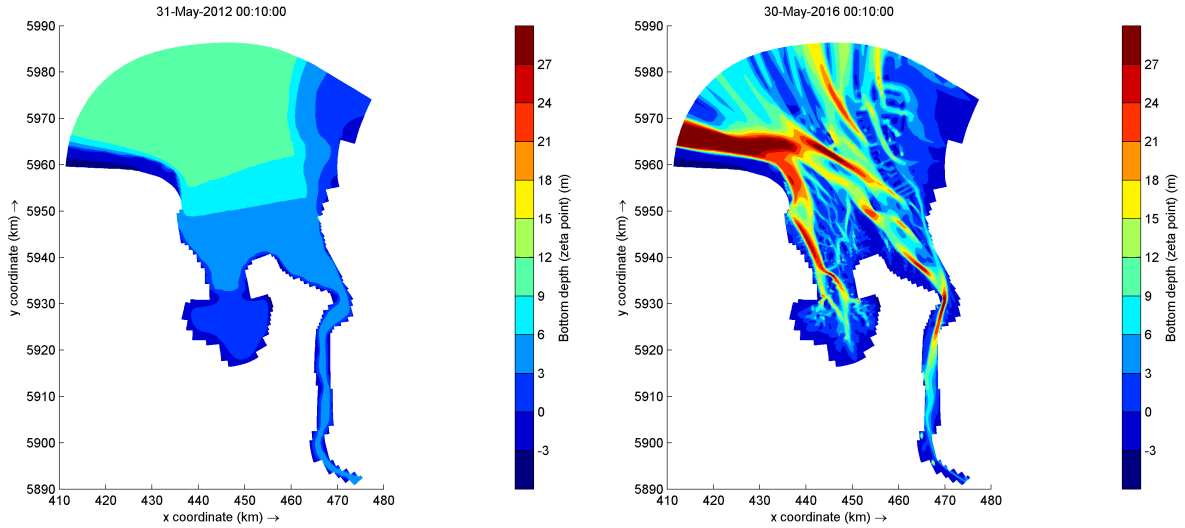

(a) Initial Bathymetry 1

(b) Bathymetry after 4 MY

Figure C.1: Examples 1 for the Bathymetrical Results

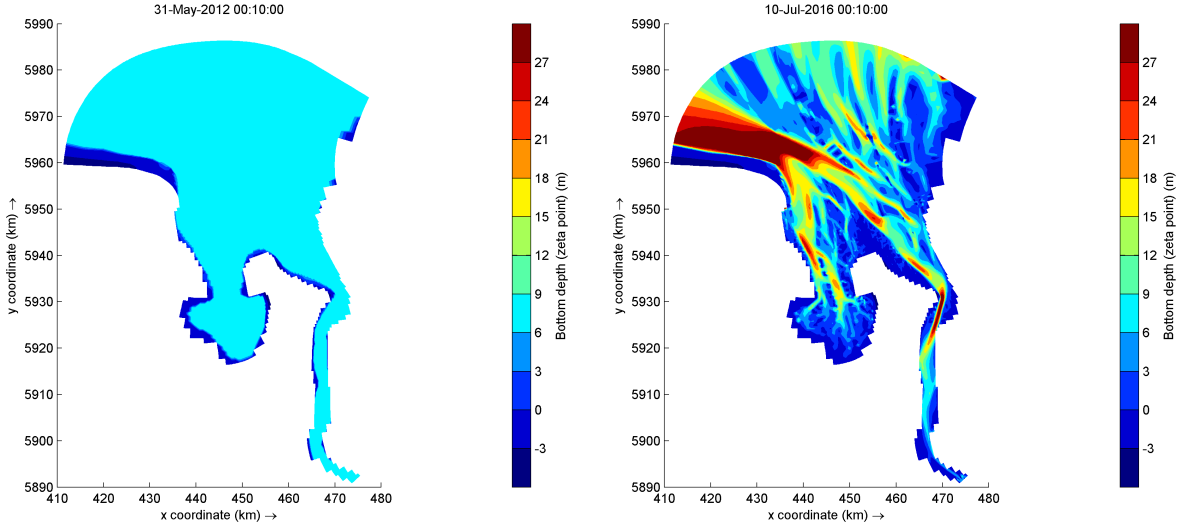

(a) Initial Bathymetry 2

(b) Bathymetry after 4 MY

Figure C.2: Examples 2 for the Bathymetrical Results

D

Results

D.1. Base Case

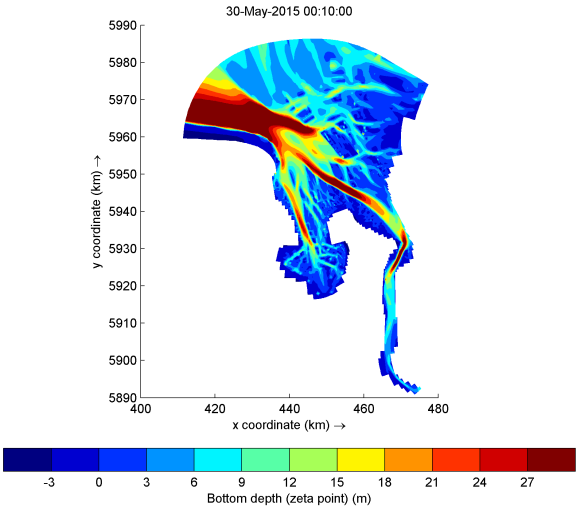

(a) Bathymetry at t = 1100

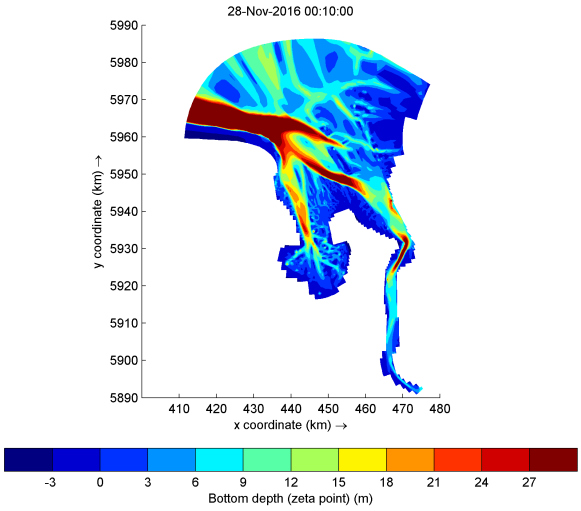

(b) Bathymetry at t = 1800

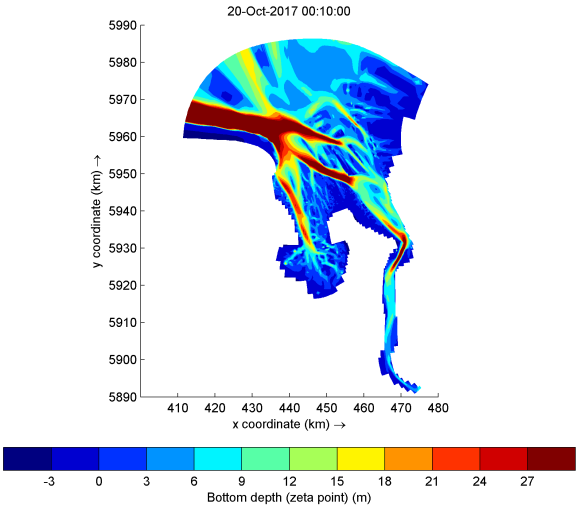

(c) Bathymetry at t = 2150

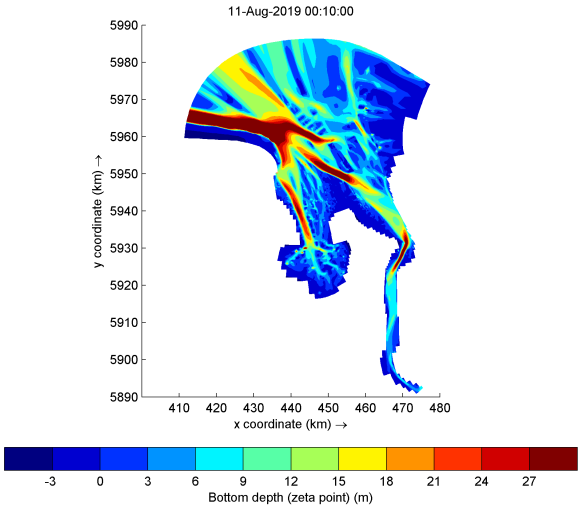

(d) Bathymetry at t = 2880

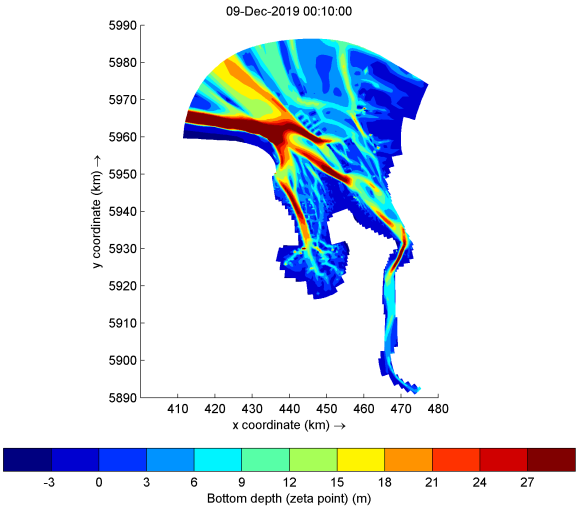

(e) Bathymetry at t = 3010

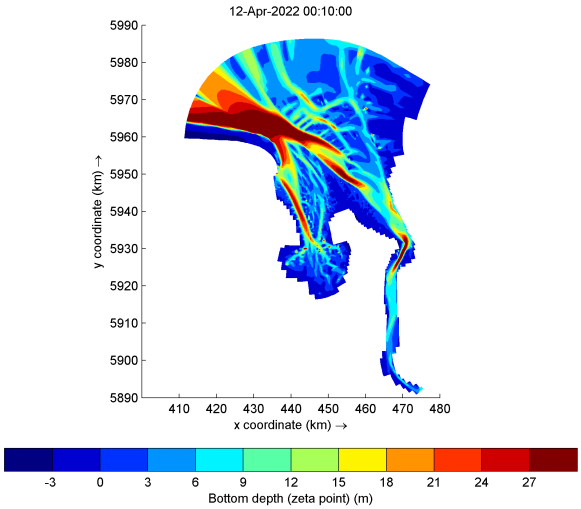

(f) Bathymetry at t = 3950

Figure D.1: Base Case - Bathymetry at Different Points in Time

D.2. Kelvin Wave

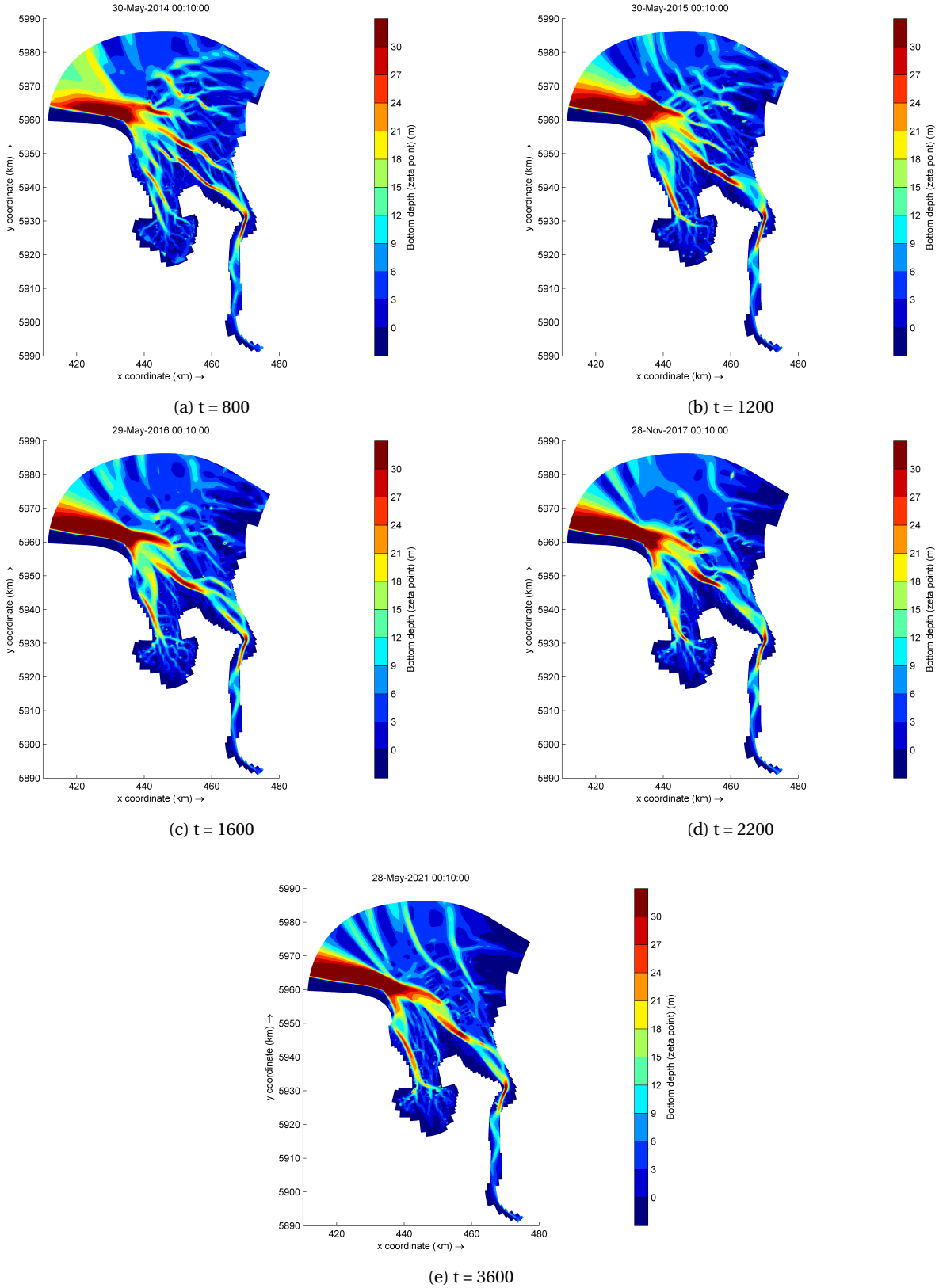

(a) t = 800

(b) t = 1200

(c) t = 1600

(d) t = 2200

(e) t = 3600

Figure D.2: Bathymetry of the Scenario Kelvin Wave at Different Points in Time

D.3. Coriolis

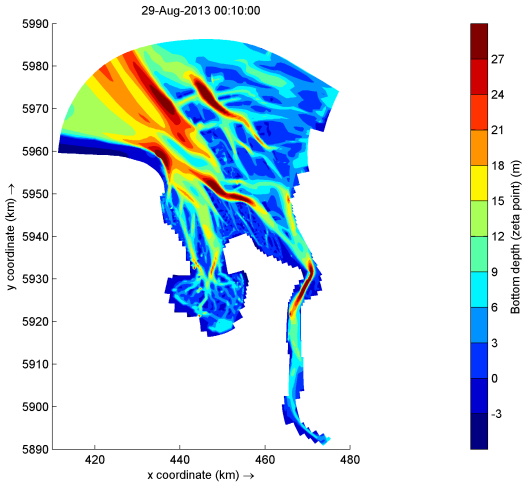

(a) Bathymetry at t = 500

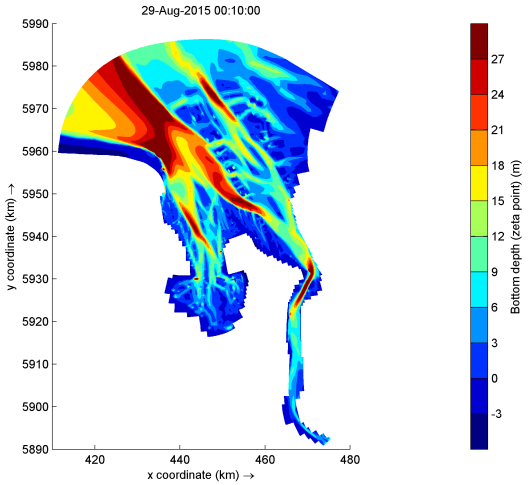

(b) Bathymetry at t = 1300

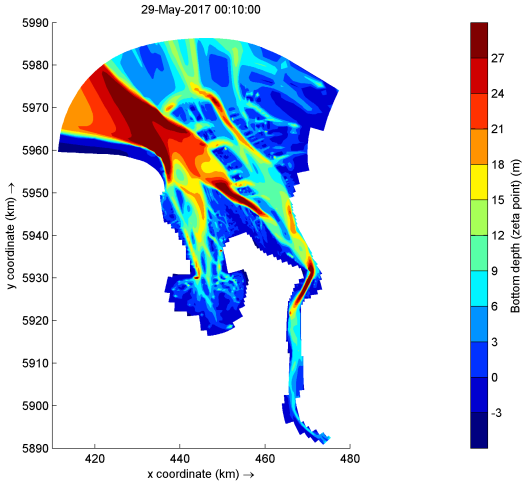

(c) Bathymetry at t = 2000

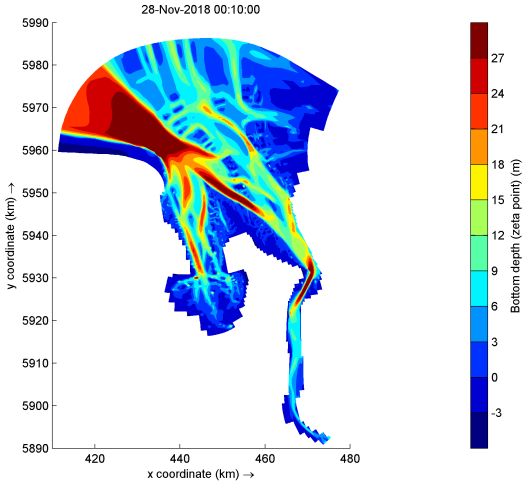

(d) Bathymetry at t = 2600

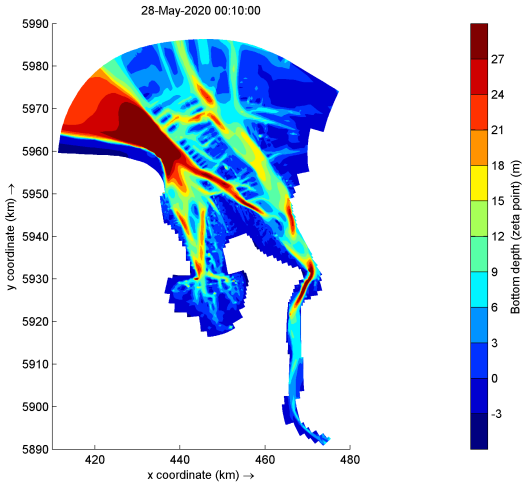

(e) Bathymetry at t = 3200

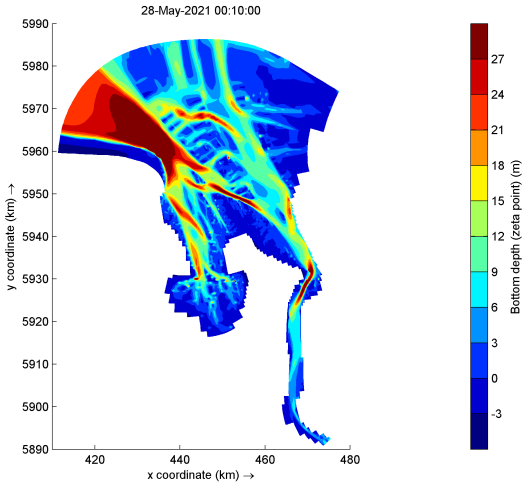

(f) Bathymetry at t = 3600

Figure D.3: Scenario: Coriolis - Bathymetry at Different Points in Time

D.4. Waves

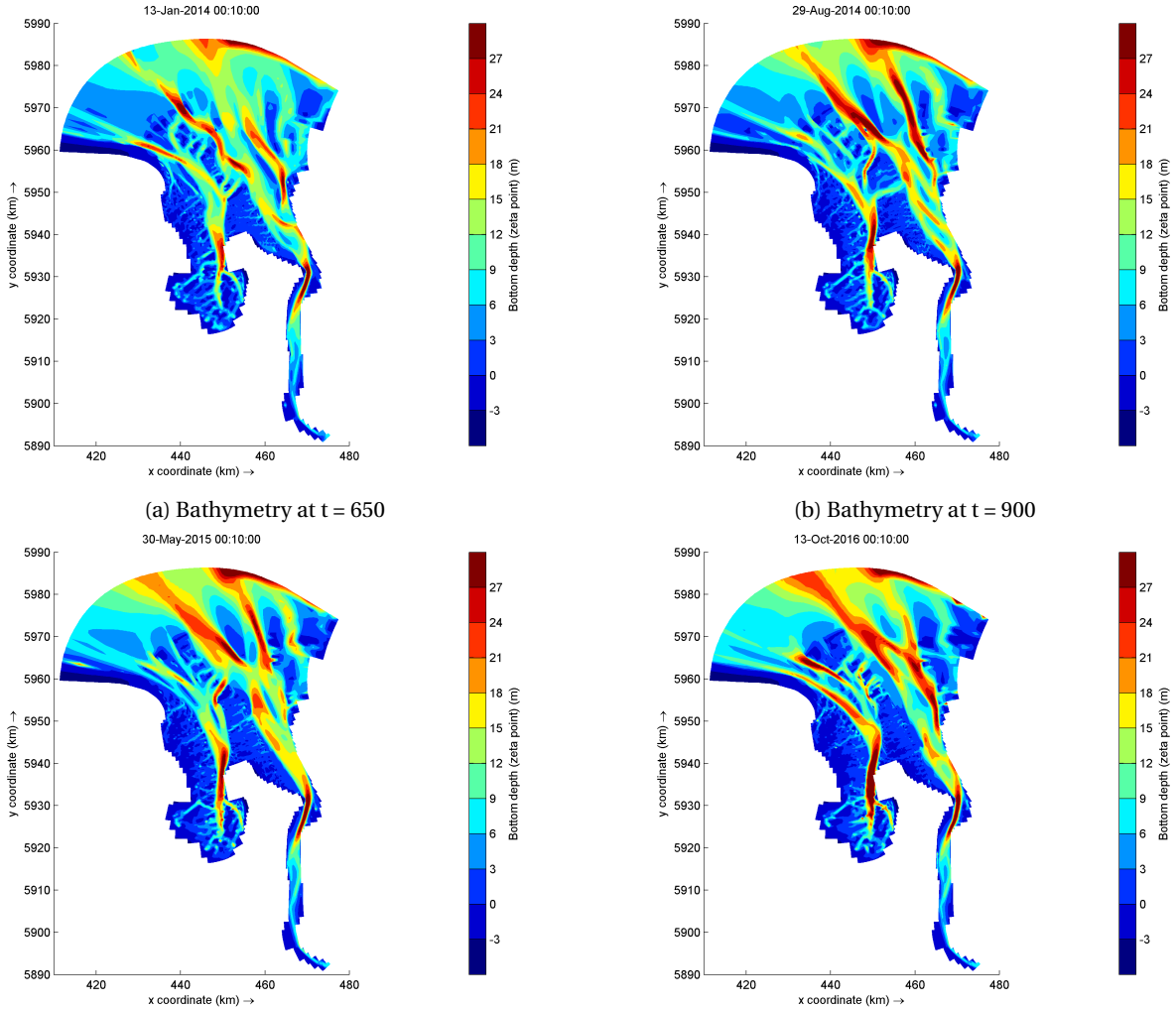

(a) Bathymetry at t = 650

(b) Bathymetry at t = 900

(c) Bathymetry at t = 1200

(d) Bathymetry at t = 1750

Figure D.4: Scenario: Wave - Bathymetry at Different Points in Time

D.5. Extreme River Discharge

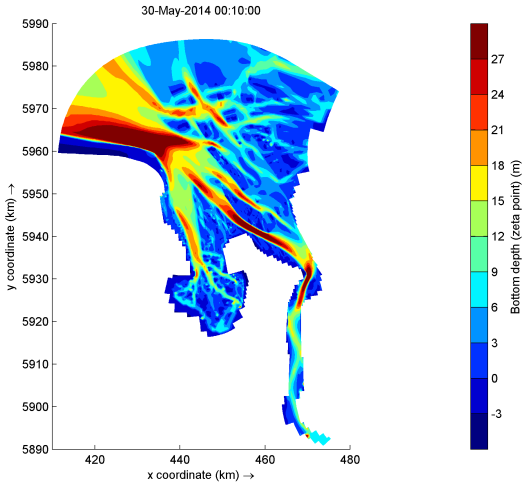

(a) Bathymetry at t = 800

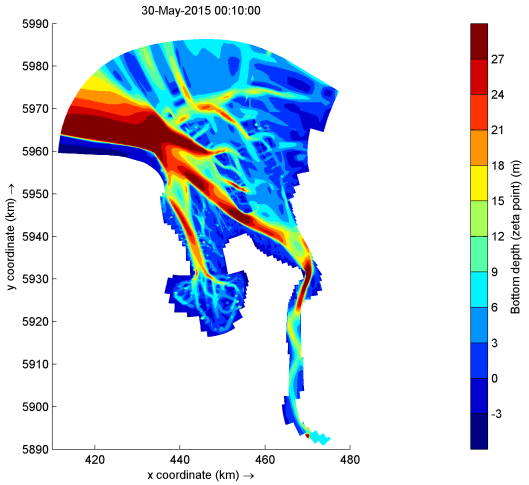

(b) Bathymetry at t = 1200

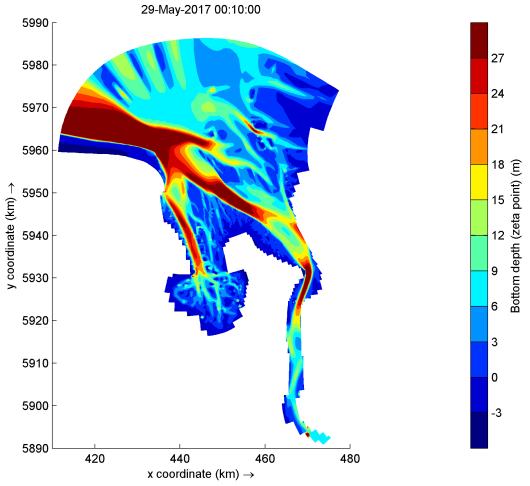

(c) Bathymetry at t = 2000

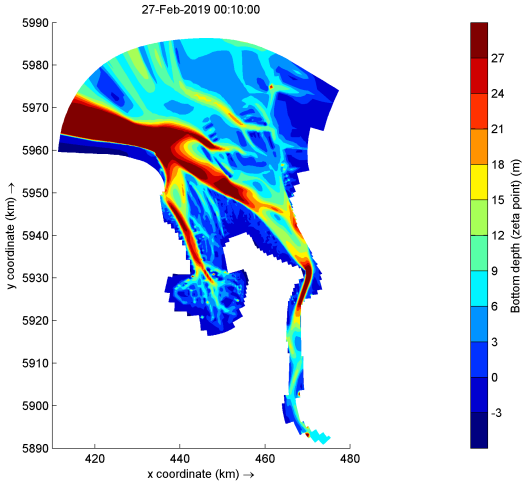

(d) Bathymetry at t = 2700

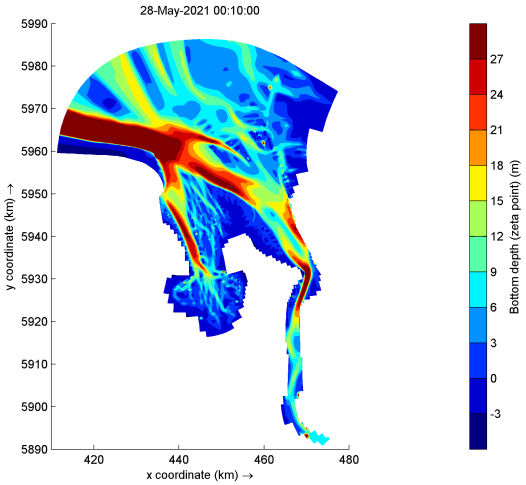

(e) Bathymetry at t = 3600

Figure D.5: Extreme River Discharge: Bathymetry at Different Points in Time

D.6. No River Discharge

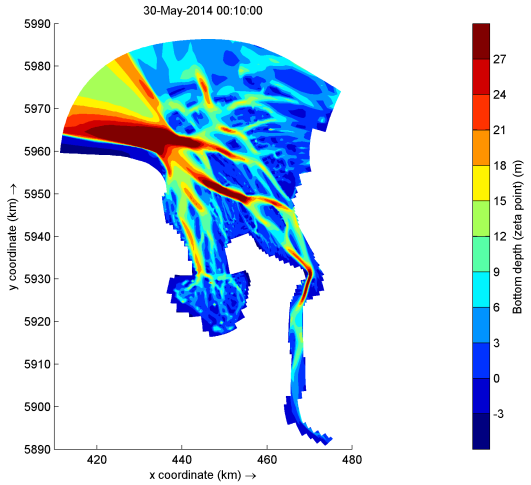

(a) Bathymetry at t = 800

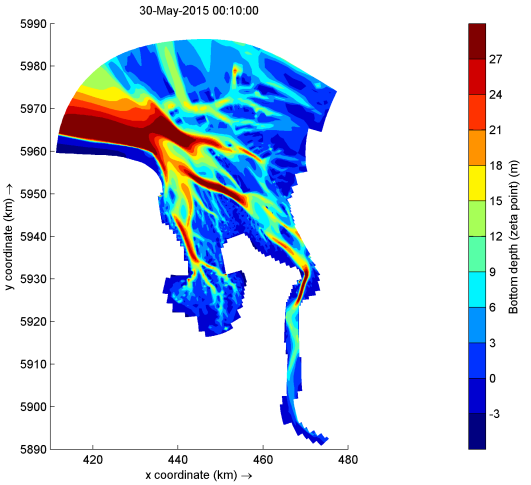

(b) Bathymetry at t = 1200

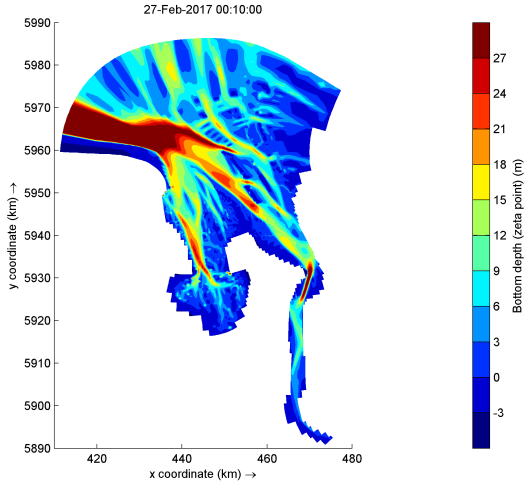

(c) Bathymetry at t = 1900

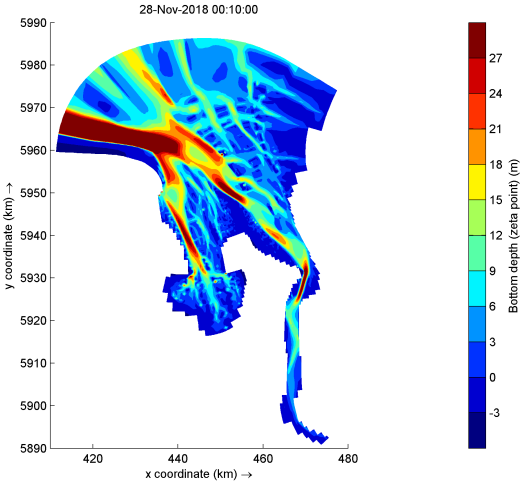

(d) Bathymetry at t = 2600

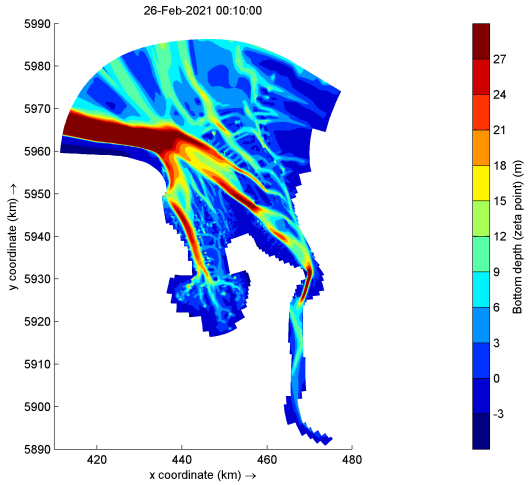

(e) Bathymetry at t = 3500

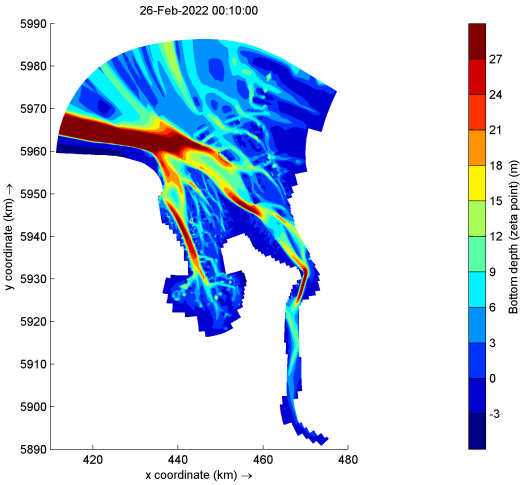

(f) Bathymetry at t = 3900

Figure D.6: No River Discharge: Bathymetry at Different Points in Time

D.7. Increased Tidal Range

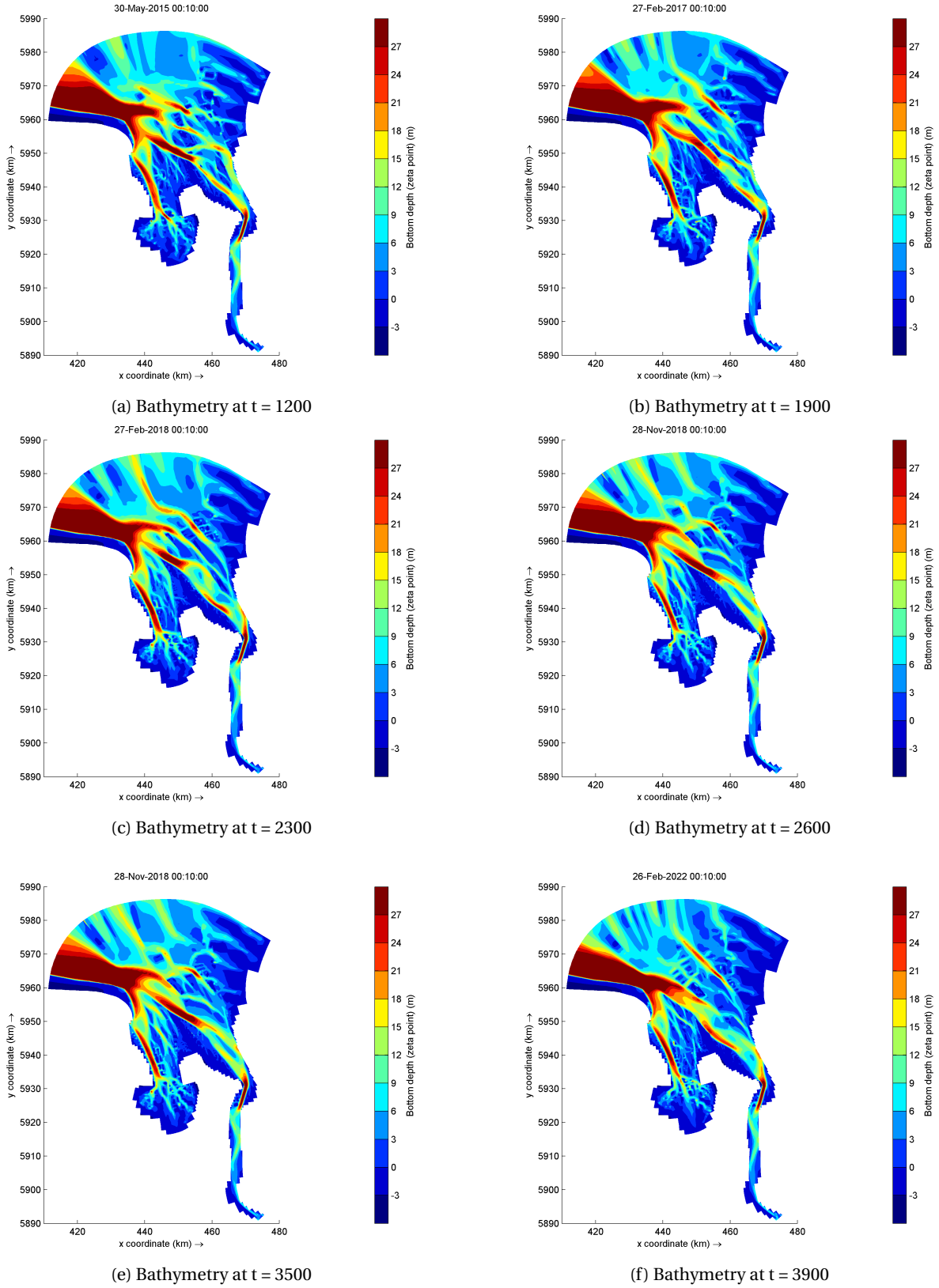

(a) Bathymetry at t = 1200

(b) Bathymetry at t = 1900

(c) Bathymetry at t = 2300

(d) Bathymetry at t = 2600

(e) Bathymetry at t = 3500

(f) Bathymetry at t = 3900

Figure D.7: Increased Tidal Range: Bathymetry at Different Points in Time

E

Hypsometrie of the Model Domain Over Time

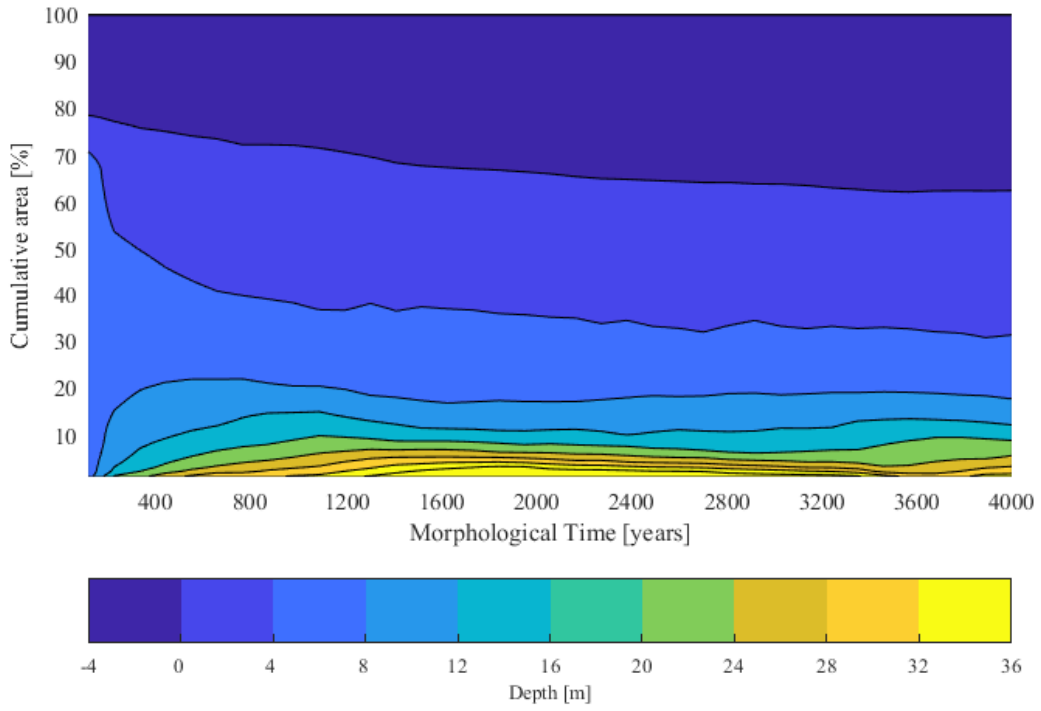

Figure E.1: Base Case: Hypsometry of the Full Model Domain Over Time

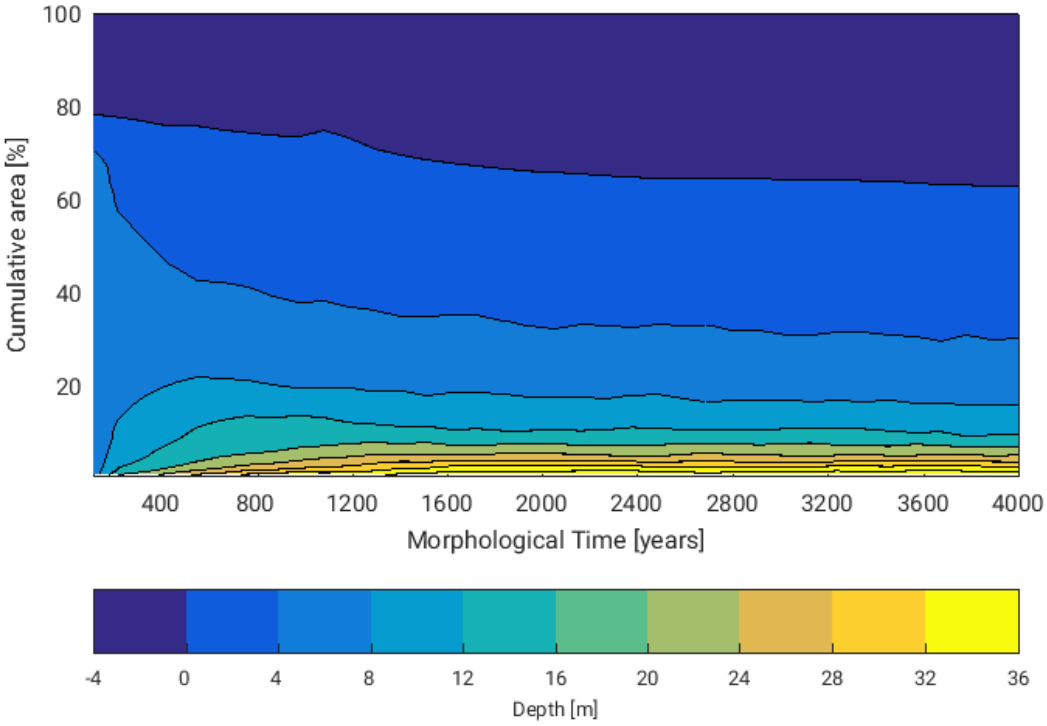

Figure E.2: Kelvin Wave: Hypsometry of the Full Model Domain Over Time

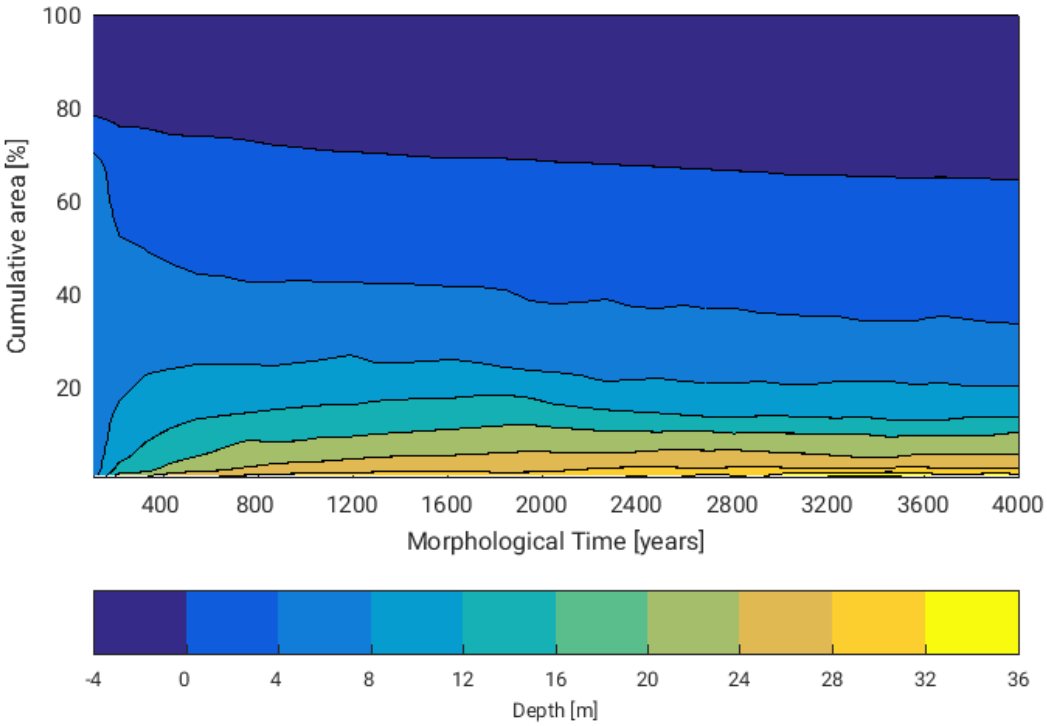

Figure E.3: Coriolis: Hypsometry of the Full Model Domain Over Time

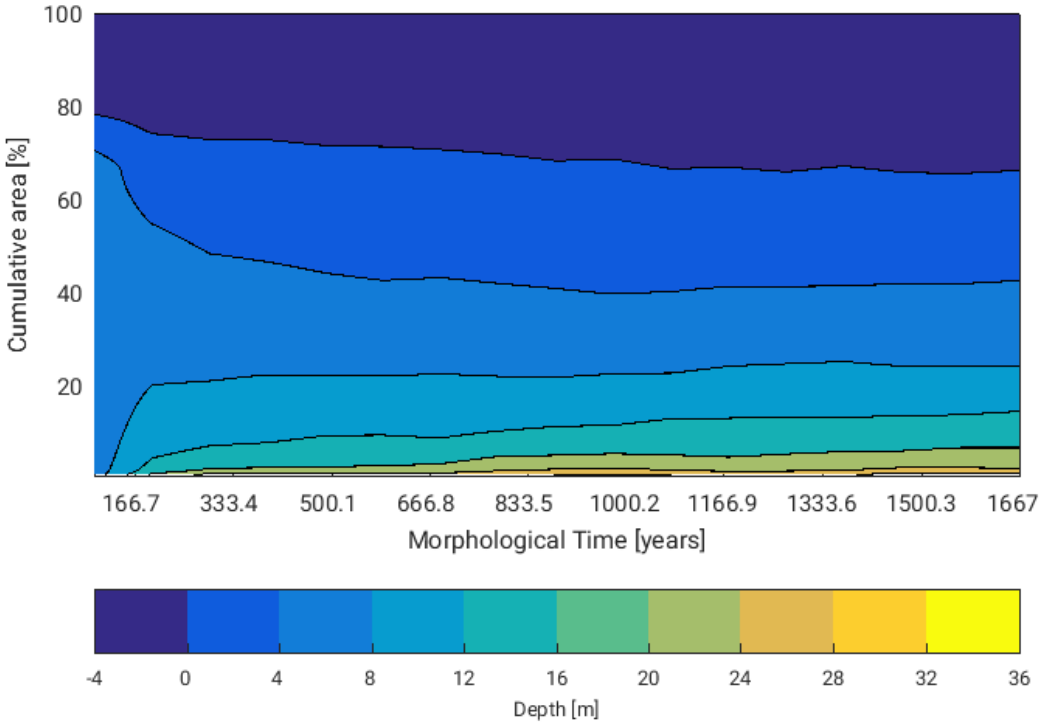

Figure E.4: Wave: Hypsometry of the Full Model Domain Over Time

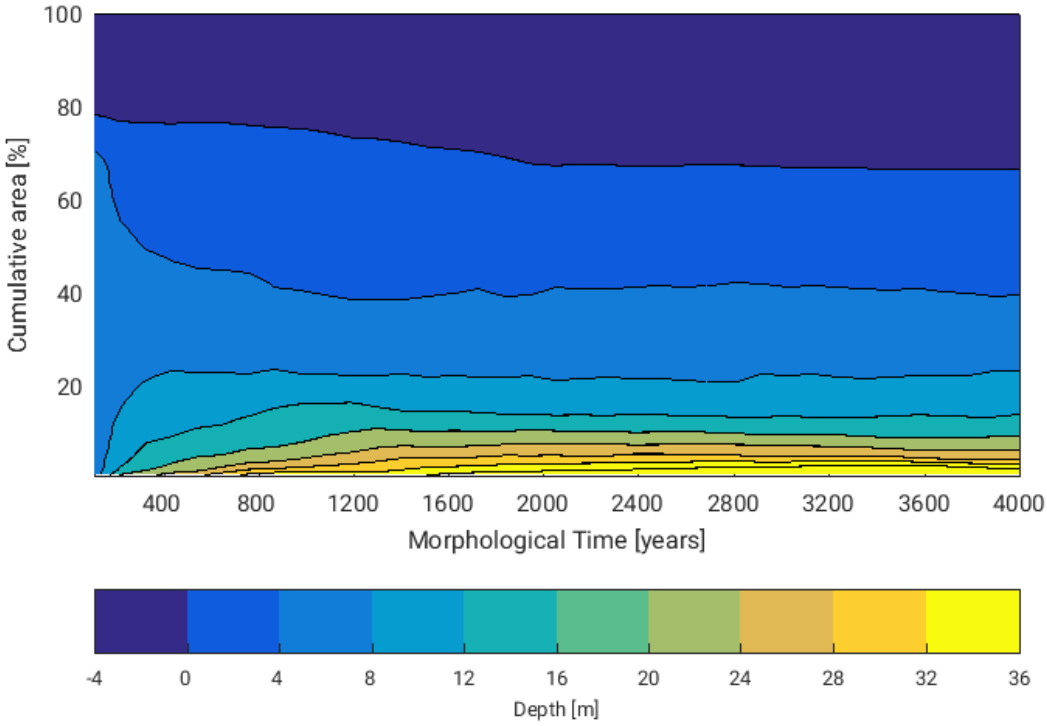

Figure E.5: Extreme River Discharge: Hypsometry of the Full Model Domain Over Time

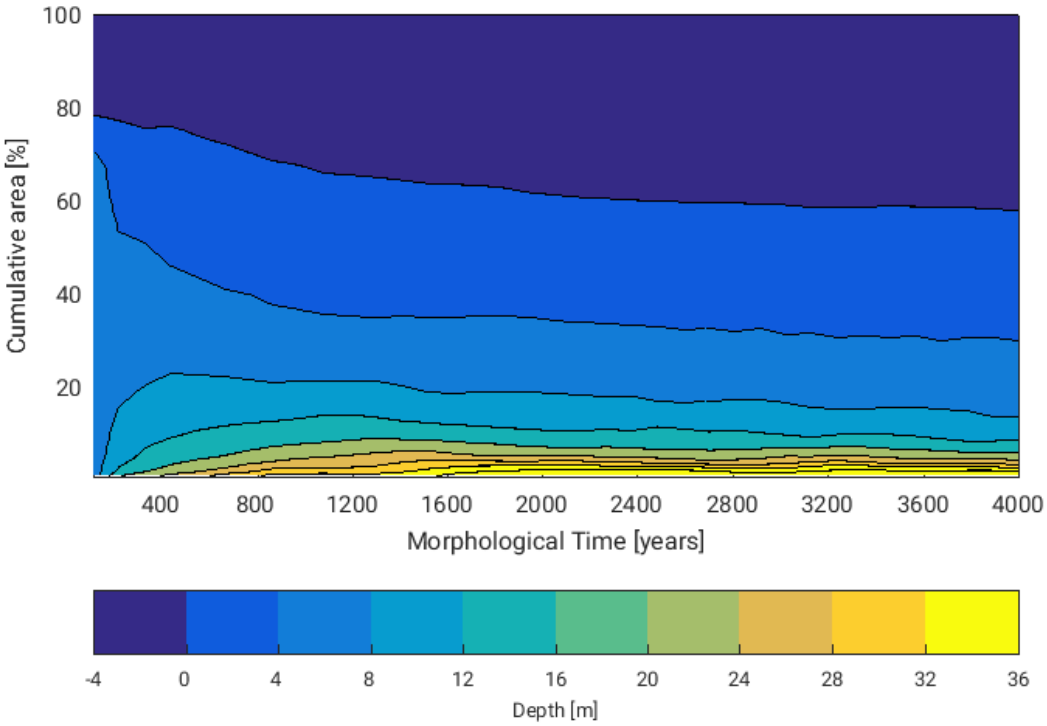

Figure E.6: No River Discharge: Hypsometry of the Full Model Domain Over Time

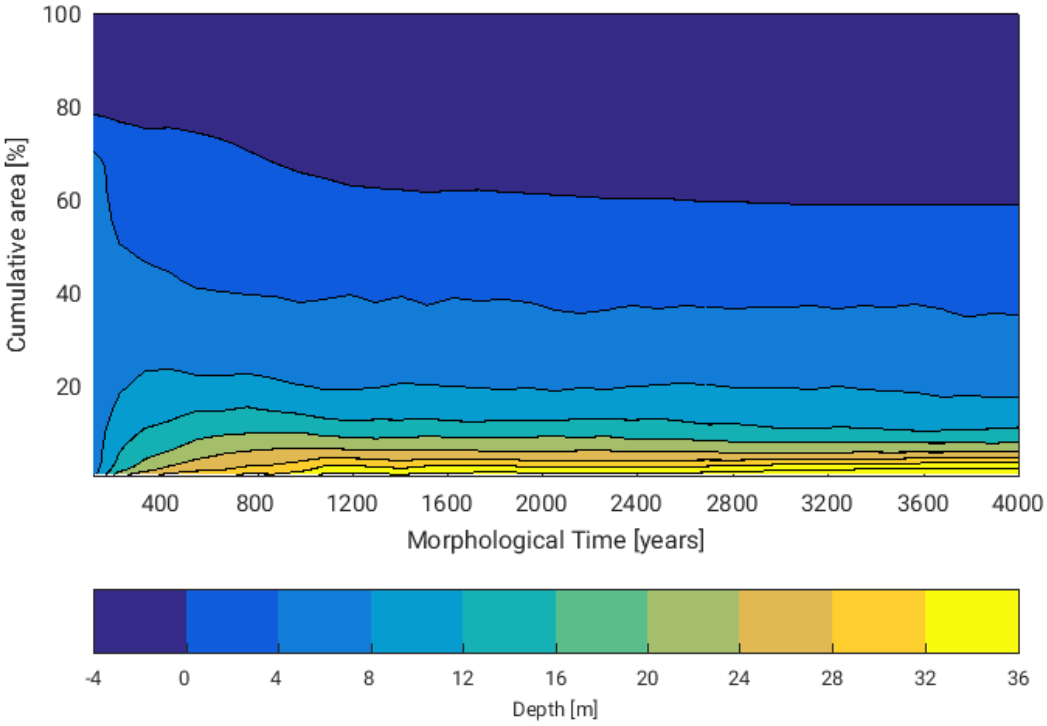

Figure E.7: Increased Tidal Range: Hypsometry of the Full Model Domain Over Time

Bibliography

[1] Deutsches Gewässerkundliches Jahrbuch: Weser- und Emsgebiet.

[2] Volker Barthel. Stability of tidal channels dependent on river improvement. In *Coastal Engineering 1976*, pages 1775–1789, New York, NY, 1977. American Society of Civil Engineers. ISBN 9780872620834. doi: 10.1061/9780872620834.103.

[3] J. Bosboom and A. J. H. M. Reniers. Scale-selective validation of morphodynamic models. *Coastal Engineering Proceedings*, 1(34):75, 2015. ISSN 2156-1028. doi: 10.9753/icce.v34.sediment.75.

[4] J. Bosboom and M.J.F. Stive. *Coastal dynamics I: Lecture notes CIE4305.* VSSD, Delft, version 0.3 edition, 2012. ISBN 9789065622860.

[5] R. Boyd, R. Dalrymple, and B. A. Zaitlin. Classification of clastic coastal depositional environments. *Sedimentary Geology*, 80(3-4):139–150, 1992. ISSN 00370738. doi: 10.1016/0037-0738(92)90037-R.

[6] G. Dam, M. van der Wegen, R. J. Labeur, and D. Roelvink. Modeling centuries of estuarine morphodynamics in the Western Scheldt estuary. *Geophysical Research Letters*, 43(8):3839–3847, 2016. ISSN 00948276. doi: 10.1002/2015GL066725.

[7] J. J. Dronkers. *Dynamics of coastal systems.* World Scientific Pub. Co, Singapore and Hackensack, N.J and Singapore and Hackensack, N.J, 2005. ISBN 978-981-256-207-4.

[8] F. Engelund and E. Hansen. A monograph on sediment transport in alluvial streams. *Technical University of Denmark 0stervoldgade 10, Copenhagen K*, 1967.

[9] C. T. Friedrichs and D. G. Aubrey. Non-linear tidal distortion in shallow well-mixed estuaries: A synthesis. *Estuarine, Coastal and Shelf Science*, 27(5):521–545, 1988. ISSN 02727714. doi: 10.1016/0272-7714(88)90082-0.

[10] W. E. Galloway. Process framework for describing the morphologic and stratigraphic evolution of deltaic depositional systems. 1975.

[11] H. Göhren. Beitrag zur Morphologie der Jade-und Wesermündung. *Die Küste, 13*, 13:140–146, 1965.

[12] A. Götschenberg and A. Kahlfeld. The jade. *Die Küste*, 74:263–274, 2008.

[13] G. Herrling, M. Benninghoff, and C. Winter. Morphodynamic model of the Outer Weser estuary: Model set-up and validation: MorphoWeser - Interim report 1.

[14] G. Herrling, J. Elsebach, and A. Ritzmann. Evaluation of changes in the tidal regime of the Ems-Dollard and Lower Weser estuaries by mathematical modelling. *Die Küste*, (81):353–368, 2014.

[15] D. Hydraulics. Delft3D-Wave user manual, .

[16] D. Hydraulics. Delft3D-FLOW user manual, .

[17] D. L. Inman and C. E. Nordstrom. On the tectonic and morphologic classification of coasts. *The Journal of Geology*, 79(1):1–21, 1971. ISSN 0022-1376. doi: 10.1086/627583.

[18] F. Kösters and C. Winter. Exploring German Bight coastal morphodynamics based on modelled bed shear stress. *Geo-Marine Letters*, 34(1):21–36, 2014. ISSN 0276-0460. doi: 10.1007/s00367-013-0346-y.

[19] F. Kösters, M. Karstens, and A. Plüß. Nordsee - Basismodell: Teil I: Allgemeine Übersicht.

[20] W. Krüger. *Meer und Küste bei Wangeroog und die Kräfte, die auf ihre Gestaltung einwirken.* 1911.

[21] G. Lang. Ein Beitrag zur Tidedynamik der Innenjade und des Jadebusens. *Mitteilungsblatt der Bundesanstalt für Wasserbau*, 86:33–42, 2003.

[22] D. Lange. The weser estuary: Heide, Holstein: Boyens. *Die Küste*, 74:275–287, 2008.

[23] G. R. Lesser, J. A. Roelvink, J.A.T.M. van Kester, and G. S. Stelling. Development and validation of a three-dimensional morphological model. *Coastal Engineering*, 51(8-9):883–915, 2004. ISSN 03783839. doi: 10.1016/j.coastaleng.2004.07.014.

[24] P. Milbradt, J. Valerius, and M. Zeiler. Das Funktionale Bodenmodell: Aufbereitung einer konsistenten Datenbasis für die Morphologie und Sedimentologie. *Die Küste*, (83):19–38, 2015.

[25] M. Müller, J. Y. Cherniawsky, M. G. G. Foreman, and J.-S. von Storch. Seasonal variation of the M 2 tide. *Ocean Dynamics*, 64(2):159–177, 2014. ISSN 1616-7341. doi: 10.1007/s10236-013-0679-0.

[26] A. H. Murphy and E. S. Epstein. Skill scores and correlation coefficients in model verification. *Monthly Weather Review*, 117(3):572–582, 1989. ISSN 0027-0644. doi: 10.1175/1520-0493.

[27] H. E. Pelling, M. J. A. Green, and S. L. Ward. Modelling tides and sea-level rise: To flood or not to flood. *Ocean Modelling*, 63:21–29, 2013. ISSN 14635003. doi: 10.1016/j.ocemod.2012.12.004.

[28] L. Plate. Die Weser als Seewasserstrasse: Bilanzbericht.

[29] L. Plate. Forschungen als Grundlage für den Ausbau der Aussenweser. *Deutsche Wasserwirtschaft*, (30): 66–74, 1935.

[30] H. Poppen. *Die Sandbänke an der Küste der Deutschen Bucht der Nordsee*. Mittler, 1912.

[31] H. Ramacher. *Der Ausbau von Unter-und Außenweser*. EV, 1974.

[32] R. Ranasinghe, C. Swinkels, A. Luijendijk, D. Roelvink, J. Bosboom, M. Stive, and D.J.R Walstra. Morphodynamic upscaling with the MORFAC approach: Dependencies and sensitivities. *Coastal Engineering*, 58(8):806–811, 2011. ISSN 03783839. doi: 10.1016/j.coastaleng.2011.03.010.

[33] J. A. Roelvink. Coastal morphodynamic evolution techniques. *Coastal Engineering*, 53(2-3):277–287, 2006. ISSN 03783839. doi: 10.1016/j.coastaleng.2005.10.015.

[34] J. A. Roelvink and A. J. H. M. Reniers. *A Guide to modeling coastal morphology*. World Scientific, Hackensack, NJ and London, op. 2012. ISBN 978-981-4304-25-2.

[35] G. Samu. Beitrag zur morphologischen Entwicklung der Außenjade. In *Mitteilungsblatt der Bundesanstalt für Wasserbau*, volume 38. URL `https://hdl.handle.net/20.500.11970/102999`.

[36] K. Schrottke, M. Becker, A. Bartholomä, B. W. Flemming, and D. Hebbeln. Fluid mud dynamics in the Weser estuary turbidity zone tracked by high-resolution side-scan sonar and parametric sub-bottom profiler. *Geo-Marine Letters*, 26(3):185–198, 2006. ISSN 0276-0460. doi: 10.1007/s00367-006-0027-1.

[37] Scientific American. Does water flowing down a drain spin in different directions depending on which hemisphere you're in? And if so, why? URL `https://www.scientificamerican.com/article/can-somebody-finally-sett/`.

[38] J. Sutherland, A. H. Peet, and R. L. Soulsby. Evaluating the performance of morphological models. *Coastal Engineering*, 51(8-9):917–939, 2004. ISSN 03783839. doi: 10.1016/j.coastaleng.2004.07.015.

[39] M. van der Wegen and J. A. Roelvink. Reproduction of estuarine bathymetry by means of a process-based model: Western Scheldt case study, the Netherlands. *Geomorphology*, 179:152–167, 2012. doi: 10.1016/j.geomorph.2012.08.007.

[40] S. M. van Leeuwen and H. E. de Swart. Intermediate modelling of tidal inlet systems: Spatial asymmetries in flow and mean sediment transport. *Continental Shelf Research*, 22(11-13):1795–1810, 2002. ISSN 02784343. doi: 10.1016/S0278-4343(02)00038-9.

[41] L. C. van Rijn. *Principles of sediment transport in rivers, estuaries and coastal seas*. Aqua Publications, Amsterdam, 1993. ISBN 90-800356-2-9.

[42] L. C. van Rijn. Unified View of Sediment Transport by Currents and Waves. I: Initiation of Motion, Bed Roughness, and Bed-Load Transport. *Journal of Hydraulic Engineering*, 133(6):649–667, 2007. ISSN 0733-9429. doi: 10.1061/(ASCE)0733-9429(2007)133:6(649).

[43] L.C van Rijn, D.J.R Walstra, B. Grasmeijer, J. Sutherland, S. Pan, and J.P Sierra. The predictability of cross-shore bed evolution of sandy beaches at the time scale of storms and seasons using process-based Profile models. *Coastal Engineering*, 47(3):295–327, 2003. ISSN 03783839. doi: 10.1016/S0378-3839(02)00120-5.

[44] J. van Veen, van der Spek, A. J. F., M. J. F. Stive, and T. Zitman. Ebb and flood channel systems in the netherlands tidal waters 1. *Journal of Coastal Research*, 216:1107–1120, 2005. ISSN 0749-0208. doi: 10.2112/04-0394.1.

[45] Volkhard Wetzel. Der Ausbau des Weserfahrwassers von 1921 bis heute. In *Jahrbuch der Hafenbautechnischen Gesellschaft*, volume 42, pages 83–105. doi: 10.1007/978-3-642-52298-7{\textunderscore}4.

[46] C. Wienberg. *The impact of dredge spoil dumping on coastal morphodynamics monitored by high-resolution acoustic measuring instruments (outer Weser Estuary, German Bight)*. PhD thesis, Dissertation zur Erlangung des Doktorgrades der Naturwissenschaften, Fachebereich Geowissenschaften, Universität Bremen, 2003.

[47] P. L. Woodworth. A note on the nodal tide in sea level records. *Journal of Coastal Research*, 280:316–323, 2012. ISSN 0749-0208. doi: 10.2112/JCOASTRES-D-11A-00023.1.

[48] A. C. Zorndt. *Impacts of Climate Change on Hydrodynamic Conditions and Salinity of the Weser Estuary*. Dissertation, Leibniz Universität Hannover, Hannover, 2014.